

Heft 19

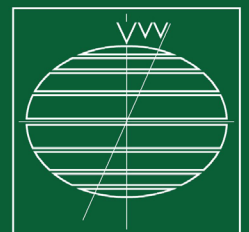
München, März 1986

GPS Research 1985
at the Institute of
Astronomical and Physical Geodesy

Herbert Landau
Bernd Eissfeller
Günter W. Hein

SCHRIFTENREIHE

Universitärer Studiengang Vermessungswesen
Universität der Bundeswehr München



Heft 19

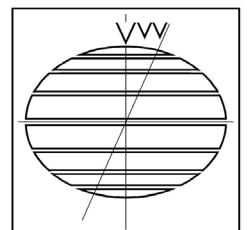
München, März 1986

**GPS Research 1985
at the Institute of
Astronomical and Physical Geodesy**

Herbert Landau
Bernd Eissfeller
Günter W. Hein

SCHRIFTENREIHE

Universitärer Studiengang Vermessungswesen
Universität der Bundeswehr München



Der Druck dieses Heftes wurde aus Haushaltsmitteln der Hochschule der Bundeswehr München gefördert.

Auflagenhöhe: 800 Exemplare

Verantwortlich für die Herausgabe der Schriftenreihe:

Der Prodekan des Universitären Studiengangs Vermessungswesen

Bezugsnachweis:

Universität der Bundeswehr München
Fakultät für Bauingenieur- und Vermessungswesen
Universitärer Studiengang Vermessungswesen
Werner-Heisenberg-Weg 39
8014 Neubiberg

ISSN 0173-1009

P R E F A C E

Although the availability of the Precise Positioning Service (PPS) of the Global Positioning System (GPS) in the future is still uncertain it seems to revolutionize geodesy and to replace classical surveying techniques even by only using the various other capabilities (Standard Positioning Service - SPS).

The Institute of Astronomical and Physical Geodesy (IAPG) of the University of the Federal Armed Forces Munich decided therefore mid of 1984 to concentrate its satellite research on the topic of GPS. The present report summarizes the investigations and achievements in 1985 in the form of seven papers.

Starting with basic physics and mathematics behind the analysis of GPS data the work covers aspects of GPS satellite selection in the field work, the incorporation of GPS baseline vectors in network adjustments with special emphasis of the determination of orthometric heights by combination with gravity data, and a description of one of the GPS analysis software products of IAPG, the phase-difference processing program. Finally, the required force-modelling for the orbit determination of GPS satellites is outlined, as it is used in our program system. Most of the theory written in the papers is accompanied by test computations.

The decision to publish the above mentioned papers in the green series of the University FAF Munich was mainly influenced by the fact, that knowledge and state-of-the-art in GPS research change very fast, and quick publication is therefore recommended in order to avoid duplication of work. Thus, it can happen, that described software is an "old hat" in one or two years. Nevertheless, let us hope, that some of the results reported here may be a small step towards the full use of the capability of GPS in geodesy and surveying, mainly in Germany.

We are indebted to Mrs. Grandl, Mrs. Grimm and Mrs. Zech for the patient and careful typing of the papers. We further acknowledge the Hessian Department of Surveys (Hessisches Landesvermessungsamt) in Wiesbaden, especially Dr.-Ing. Strauß, for making Macrometer field data available to us. Thanks also to the U.S. National Geodetic Survey, Rockville, Md., for providing data, and for assistance during the development of our own programs.

We further acknowledge the efforts of Miss Eggert who managed the editorial work.

Neubiberg, March 1986

Günter W. Hein

C O N T E N T S

	Page
<i>Hein, G.W. and B. Eissfeller</i>	
The Basic Observation Equations of Carrier Phase Measurements to the Global Positioning System Including General Orbit Modelling	7
 <i>Eissfeller, B.</i>	
A Taylor Series Expansion for the Transformation Problem of Cartesian Baseline Components Into Ellipsoidal Coordinate Differences	47
 <i>Landau, H. and B. Eissfeller</i>	
Optimization of GPS Satellite Selection for High Precision Differential Positioning	65
 <i>Eissfeller, B.</i>	
The Estimation of Orthometric Heights from GPS Baseline Vectors Using Gravity Field Information and Least-Squares Collocation	107
 <i>Landau, H.</i>	
GPS Baseline Vectors in a Threedimensional Inte- grated Adjustment Approach	127
 <i>Landau, H.</i>	
The IAPG Phase-Difference Processing Program - Modelling, Software Development and Results	161
 <i>Landau, H. and D. Hagmaier</i>	
Analysis of the Required Force-Modelling for NAVSTAR/GPS Satellites	193

THE BASIC OBSERVATION EQUATIONS OF CARRIER PHASE MEASUREMENTS
TO THE GLOBAL POSITIONING SYSTEM
INCLUDING GENERAL ORBIT MODELLING *)

Günter W. Hein and Bernd Eissfeller
University FAF Munich
Institute of Astronomical and Physical Geodesy
Werner-Heisenberg-Weg 39
8014 Neubiberg
Federal Republic of Germany

ABSTRACT. Starting with the physics of microwave propagation the non-linear observation equations of carrier phase (difference) observations to the Global Positioning System (GPS) are derived. A possible orbit model and its parameters are described for the GPS satellites and inserted in the observation equations following the principle of integrated geodesy. The treatment of tropospheric and ionospheric effect on the observations is presented as well as the complete linearization of the final observation equations. The general estimation model for multi-baseline vectors including orbit modelling is outlined.

The paper intends to present the mathematical background of the use of GPS phase observations for surveying in a general operational way. It does not discuss details of the numerical realization. Rather, it is devoted to show the different functional relationship of the basic parameters and assumptions inherent in any approach.

1. INTRODUCTION

Like the TRANSIT Doppler System, the GLOBAL POSITIONING SYSTEM (GPS) will replace classical surveying techniques in short time. GPS receivers and corresponding processing systems including implemented software can be bought already now. The surveyors will (and have to) trust on the given instrument.

This paper is concerned with the mathematical background of the use of GPS phase carrier measurements for baseline determination. Two goals we had in mind when writing it. First, aware of the fact that the numerical realization of GPS processing software is just in the beginning stage, showing not yet the ultimate way of analyzing those observations, we wanted to describe the mathematics and physics as general as possible in order to

*) A short summary of the paper was presented at the First International Symposium on Precise Positioning with the Global Positioning System, Rockville, Md., April 15-19, 1985, under the title "Integrated Modelling of GPS-Orbits and Multi-Baseline Components".

present the reader (in particular, students) a didactic way to this field. The second reason, following the tradition in geodesy to start from the large to the small, was the intention to imbed GPS observations in the model of integrated geodesy, taking advantage of such observations in a direct, operational way. Thereby the derived linear observation equations or corresponding systems can easily be combined with all other terrestrial geodetic observations (HEIN, 1982a, b).

It is obvious, that for the numerical realization of the presented mathematics, still more detailed investigations (in particular with respect to the ambiguities in the observations, gaps in the measurement series, etc.) are necessary.

Since the Global Positioning Systems appears to revolutionize surveying and geodesy in the near future, many colleagues and institutions are concerned with GPS research. As a consequence many papers are published. By writing the paper under consideration by far not all available papers could be considered. Therefore we like to refer the reader to a just published monograph by KING et al. (1985) and to the Proceedings of the First International Symposium on Precise Positioning with the Global Positioning (GOAD, 1985) which both can serve as sources for further literature.

2. THE OBSERVATION EQUATIONS OF CARRIER PHASE MEASUREMENTS

2.1 Basic relations

Every GPS satellite can be considered as a wave source transmitting electromagnetic waves near the microwave spectrum. The frequencies on the L-band are $L_1 := \nu_1 = 1575.42$ MHz and $L_2 := \nu_2 = 1227.6$ MHz corresponding to exactly 154 times and 120 times, respectively, the fundamental P-code chipping rate of 10.23 MHz.

The basic relations for the description of electromagnetic fields are the Maxwells equations (see e.g. LIVINGSTON, 1970)

$$\nabla \times \vec{H} = \frac{\partial \vec{D}}{\partial t} + \vec{I} \quad (2-1a)$$

$$\nabla \times \vec{E} = -\frac{\partial \vec{B}}{\partial t} \quad (2-1b)$$

$$\nabla \cdot \vec{D} = q \quad (2-1c)$$

$$\nabla \cdot \vec{B} = 0 \quad (2-1d)$$

The symbols in (2-1a) to (2-1d) are

- \vec{E} the electric field intensity in [V/m]
- \vec{H} the magnetic field intensity in [A/m]
- \vec{D} the electric displacement in [V/m²]
- \vec{B} the magnetic induction in [T] = [Wb/m²]
- \vec{I} the electric current density in [A/m²]
- q the electric charge density in [C/m³]
- t the time in seconds
- ∇ the nabla operator ($\nabla \cdot := \text{div}$, $\nabla \times := \text{rot}$)

For electromagnetic fields in the atmosphere the following assumptions are customary,

$$\vec{I} = \vec{0}, \vec{B} = \mu \vec{H}, \vec{D} = \epsilon \vec{E} \text{ and } q = 0$$

where μ is the magnetic permeability and ϵ the dielectric constant. Using these assumptions, (2-2a) and (2-2b) can be deduced.

$$\nabla^2 \vec{E} - \mu \epsilon \frac{\partial^2 \vec{E}}{\partial t^2} = \vec{0} \quad (2-2a)$$

$$\nabla^2 \vec{H} - \mu \epsilon \frac{\partial^2 \vec{H}}{\partial t^2} = \vec{0} \quad (2-2b)$$

where

$$\frac{1}{c^2} = \mu \cdot \epsilon \quad (2-2c)$$

(∇^2 is the Laplace operator).

These are the so-called wave equations. The simplest solutions of (2-2a, b) in one dimension are given by LIVINGSTON (1970)

$$E(\rho, t) = \hat{E}(t) \sin\left[2\pi \nu \left(\frac{\rho}{c} - t\right)\right] \quad (2-3a)$$

$$H(\rho, t) = \hat{H}(t) \sin\left[2\pi \nu \left(\frac{\rho}{c} - t\right)\right]. \quad (2-3b)$$

ρ is the length of the wave path, ν the frequency of the signal and the c the speed of light. By \hat{E} , \hat{H} , we denote the corresponding amplitudes. (2-3a) and (2-3b) imply, that the electric and the magnetic field have the same phase. The vectors \vec{E} and \vec{H} are orthogonal to the propagation direction and also orthogonal to each other ($\vec{E} \cdot \vec{H} = 0$).

$$\vec{P} = \vec{E} \times \vec{H} \quad (2-4)$$

\vec{P} is the so-called Poynting vector in the propagation direction.

From (2-3a,b) we find for the phase of the electromagnetic wave

$$\phi(\rho, t) = 2\pi\nu \left(\frac{\rho}{c} - t \right). \quad (2-5)$$

The phase (2-5) is the basic satellite observable in a GPS receiver.

Due to the sine term in (2-3a,b) the phase is not affected by a phase shift of $2\pi m$, where m is an integer. Thus

$$\sin \left[2\pi\nu \left(\frac{\rho}{c} - t \right) + 2\pi m \right] = \sin \left[2\pi\nu \left(\frac{\rho}{c} - t \right) \right]. \quad (2-6)$$

Consequently (2-5) can be written in a more general

$$\phi(\rho, t) = 2\pi\nu \left(\frac{\rho}{c} - t \right) + 2\pi m \quad (2-7)$$

which expresses the simple fact, that phase measurements are not unique. Inserting further in (2-7) $c = \lambda\nu$, where λ is the wavelength, one gets

$$\phi(\rho, t) = \frac{2\pi}{\lambda} (\rho - ct + m\lambda). \quad (2-8)$$

In order to derive the observation equations, we have to introduce two time instants for the signal propagation.

t_S is the transmission time of the satellite signal, and

$t_R = t_S + \frac{\rho}{c}$ is the time, when the signal is received.

We first note that the phase of the signal for $t = t_S$ and $t = t_R$ remains the same. Thus

$$\phi(0, t_S) = \phi(\rho, t_R). \quad (2-9)$$

Eq. (2-9) can be easily derived by inserting $t = t_S$, $\rho = 0$ and $t = t_R$, $\rho = \rho$ in (2-8).

From (2-9) follows the important fact, that we may describe the phase of the received signal either by $\phi(0, t_S)$ or $\phi(\rho, t_R)$.

Following REMONDI (1984) we define the phase of the satellite signal by

$$\phi_S(t_S) := \phi_S(0, t_S) \quad (2-10a)$$

or

$$\phi_S(t_S) := \frac{2\pi}{\lambda} (-ct_S + m\lambda). \quad (2-10b)$$

t_S and t_R are realized by precise oscillators in the satellite (S) and receiver (R). They are related to each other (as mentioned already above) by

$$t_S = t_R - \frac{\rho}{c} . \quad (2-11)$$

In (2-11) c is the mean value of the actual velocity of light in the considered medium. Thus, the following decomposition is reasonable,

$$c = c_0 - \delta c \quad (2-12)$$

where c_0 is the speed of light in the vacuum and δc is a small quantity expressing the mean variation of c_0 in the atmosphere. The minus sign is due to the relation $c < c_0$ for a medium with refraction coefficient $n > 1$. Using (2-12) in the expression ρ/c of (2-11) results in

$$\frac{\rho}{c} = \frac{\rho}{c_0 - \delta c} = \frac{\rho}{c_0 \left(1 - \frac{\delta c}{c_0}\right)} \doteq \frac{\rho}{c_0} \left(1 + \frac{\delta c}{c_0}\right) = \frac{\rho}{c_0} + \frac{\rho \delta c}{c_0^2} . \quad (2-13)$$

The last term on the right hand side of (2-13) may be considered as an propagation time delay Δt_a due to the atmosphere,

$$\Delta t_a = \frac{\rho}{c_0^2} \delta c .$$

The modelling of Δt_a is presented in section 4.

Inserting (2-13) in (2-11) yields

$$t_S = t_R - \frac{\rho}{c_0} - \Delta t_a . \quad (2-14)$$

Further, (2-14) in (2-10b) with $c = c_0$ results in

$$\phi_S(t_S) = \frac{2\pi}{\lambda} (\rho - c_0 t_R + c_0 \Delta t_a + m\lambda) . \quad (2-15)$$

$\phi_S(t_S)$ cannot directly be observed by a GPS receiver. Instead of that, the satellite signal phase $\phi_S(t_S)$ is compared with a reference oscillator $\phi_R(t_R)$ in the receiver, so that in reality the measurable quantity is the phase difference $\bar{\Psi}(t_R)$,

$$\bar{\Psi}_i(t_{R_i}) = \phi_{S_j}(t_{S_j}) - \phi_{R_i}(t_{R_i}) = \phi_{S_j}\left(t_{R_i} - \frac{\rho_{ij}}{c} - \Delta t_{a_{ij}}\right) - \phi_{R_i}(t_{R_i}) \quad (2-16)$$

R_i denotes the receiver i and S_j the satellite j .

Since the receiver oscillator may have a small error, we introduce a clock error term $\varepsilon_i(t)$.

$$t_{R_i} = t + \varepsilon_i(t) \quad (2-17)$$

which can be modelled by a polynomial (REMONDI, 1984)

$$\varepsilon(t) = \alpha_0 + \alpha_1 t + \alpha_2 t^2 + \dots \quad (2-18)$$

Assuming that the receiver frequency ν_{R_i} is constant ($\nu_{R_i} := \nu_i$) we write for ϕ_{R_i}

$$\phi_{R_i}(t_{R_i}) = 2\pi \nu_i t_{R_i} \quad (2-19)$$

Furthermore

$$\rho_{ij} = \rho_{ij}(t_{R_i})$$

$$\Delta t_a = \Delta t_a(t_{R_i}) \quad .$$

$\varepsilon_i(t)$ and Δt_a are already small quantities. Inserting (2-17) in (2-16), using (2-19) together with (2-15), and approximating $\rho_{ij}(t_{R_j})$ by a Taylor expansion, neglecting higher order terms,

$$\rho_{ij}(t_{R_i}) \doteq \rho_{ij}(t) + \dot{\rho}_{ij}(t) \varepsilon_i(t)$$

we get the basic phase comparison

$$\begin{aligned} \bar{\Psi}(t) = & 2\pi m + \frac{2\pi}{\lambda} [\rho_{ij}(t) + \dot{\rho}_{ij}(t) \varepsilon(t)] - \\ & - 2\pi (\nu_S + \nu_R) [t + \varepsilon_i(t)] + \\ & + 2\pi \nu_S \Delta t_{a_{ij}}(t) \end{aligned} \quad (2-20)$$

2.2 The observation equation for single-differences

In order to derive relative geometric information (baseline vectors) from phase observations of two receivers R_1, R_2 to one identical satellite S_j we subtract the corresponding equations (2-6) and obtain the observation equation of the so-called single-difference method.

$$\psi_{sd}(t) = \bar{\psi}_2(t) - \bar{\psi}_1(t) \quad (2-21)$$

$$\begin{aligned} \psi_{sd}(t) = & 2\pi(m_2 - m_1) + \frac{2\pi}{\lambda_s} [\rho_{2j}(t) - \rho_{1j}(t)] + \\ & + 2\pi(v_1 - v_2)t + 2\pi v_s [\Delta t_{a_{2j}}(t) - \Delta t_{a_{1j}}(t)] + \\ & + \psi_\varepsilon(t) \end{aligned} \quad (2-22a)$$

where the clock error term $\psi_\varepsilon(t)$ is of the form

$$\begin{aligned} \psi_\varepsilon(t) = & \frac{2\pi}{\lambda_s} [\dot{\rho}_{2j}(t) \varepsilon_2(t) - \dot{\rho}_{1j}(t) \varepsilon_1(t)] + \\ & + 2\pi[v_1 \varepsilon_1(t) - v_2 \varepsilon_2(t)] . \end{aligned} \quad (2-22b)$$

The single-difference observable (2-22a) does not contain the satellite phase value (no satellite clock error term), but now contains differences in clock values (or errors) between ground receivers 1 and 2, initial ambiguity differences $(m_2 - m_1)$ and distance differences $\rho_{2j}(t) - \rho_{1j}(t)$. Since the clock differences have not a known relationship from one epoch to the next, they must be eliminated epoch-wise. They remain, however, the same also for another satellite.

As long as only one baseline is processed, no phase observables appear more than once, thus the measurements (2-22) are uncorrelated.

2.3 The observation equation for double-differences

The double-differencing (BOSSLER, GOAD, BENDER 1980) was introduced in order to compensate for effects caused by the receiver oscillators (receiver clock errors).

The double-difference observables are computed on the base of two single-differences at epoch t using two different GPS satellites $S_j := (P, Q)$ are

$$\psi_d(t) = \psi_{sd,Q}(t) - \psi_{sd,P}(t) \quad (2-23)$$

$$\begin{aligned} \psi_d(t) = & 2\pi m_d + \\ & + \frac{2\pi}{\lambda_Q} [\rho_{2Q}(t) - \rho_{1Q}(t)] - \frac{2\pi}{\lambda_P} [\rho_{2P}(t) - \rho_{1P}(t)] + \\ & + 2\pi v_Q [\Delta t_{a_{2Q}}(t) - \Delta t_{a_{1Q}}(t)] - \\ & + 2\pi v_P [\Delta t_{a_{2P}}(t) - \Delta t_{a_{1P}}(t)] + \\ & + \psi_{\varepsilon,d}(t) \end{aligned} \quad (2-24a)$$

where

$$m_d = m_{2Q} - m_{1Q} + m_{1P} - m_{2P} \quad (2-24b)$$

$$\begin{aligned} \psi_{\varepsilon,d}(t) = & \frac{2\pi}{\lambda_Q} [\dot{\rho}_{2Q}(t) \varepsilon_2(t) - \dot{\rho}_{1Q}(t) \varepsilon_1(t)] - \\ & - \frac{2\pi}{\lambda_P} [\dot{\rho}_{2Q}(t) \varepsilon_2(t) - \dot{\rho}_{1P}(t) \varepsilon_1(t)] + \\ & + 2\pi(v_Q - v_P) [\varepsilon_1(t) - \varepsilon_2(t)] \end{aligned} \quad (2-24c)$$

If we assume that the transmitted signals of the two GPS satellites P, Q have (nearly) identical wavelength,

$$\lambda_P = \lambda_Q = \lambda_S$$

$$v_P = v_Q = v_S$$

then (2-24a,b,c) simplifies to

$$\begin{aligned} \psi_d(t) = & 2\pi m_d + \\ & + \frac{2\pi}{\lambda_S} [\rho_{2Q}(t) - \rho_{2P}(t) + \rho_{1P}(t) - \rho_{1Q}(t)] + \\ & + 2\pi v_S [\Delta t_{a_{2Q}}(t) - \Delta t_{a_{2P}}(t) + \Delta t_{a_{1P}}(t) - \Delta t_{a_{1Q}}(t)] + \\ & + \psi_{\varepsilon,d}(t) \end{aligned} \quad (2-25a)$$

where the integer ambiguity m_d consists of

$$m_d = m_{2Q} - m_{1Q} + m_{1P} - m_{2P} , \quad (2-25b)$$

and the clock-error term $\psi_{\varepsilon,d}(t)$ drops nearly out

$$\begin{aligned} \psi_{\varepsilon,d}(t) = & \frac{2\pi}{\lambda_S} \{ [\dot{\rho}_{2Q}(t) - \dot{\rho}_{2P}(t)] \varepsilon_2(t) + \\ & + [\dot{\rho}_{1P}(t) - \dot{\rho}_{1Q}(t)] \varepsilon_1(t) \} \end{aligned} \quad (2-25c)$$

In (2-25a) satellite and receiver clock differences are (nearly) removed. No epoch-to-epoch clock differences have to be modelled and estimated. Therefore double-differences are less complicated to process. However, data sets are correlated.

2.4 The observation equation for triple-differences

Following REMONDI (1984, 89 f.), the triple-difference observable $\Psi_t(t_1, t_2)$ is defined as the difference of two double-difference-observables each belonging to a successive epoch t_1, t_2 where the two satellites P, Q were observed

$$\Psi_t(t_1, t_2) = \Psi_d(t_2) - \Psi_d(t_1) \quad (2-26)$$

$$\begin{aligned} \Psi_t(t_1, t_2) = & 2\pi (m_{d2} - m_{d1}) + \\ & + \frac{2\pi}{\lambda_S} [\rho_{2Q}(t_2) - \rho_{2Q}(t_1) + \rho_{2P}(t_1) - \rho_{2P}(t_2) + \\ & + \rho_{1P}(t_2) - \rho_{1P}(t_1) + \rho_{1Q}(t_1) - \rho_{1Q}(t_2)] + \\ & + 2\pi v_S \{ \Delta t_{a_{2Q}}(t_2) - \Delta t_{a_{2Q}}(t_1) + \Delta t_{a_{2P}}(t_1) - \Delta t_{a_{2P}}(t_2) + \\ & + \Delta t_{a_{1P}}(t_2) - \Delta t_{a_{1P}}(t_1) + \Delta t_{a_{1Q}}(t_1) - \Delta t_{a_{1Q}}(t_2) \} + \\ & + \Psi_{\epsilon, t}(t_1, t_2) \end{aligned} \quad (2-26a)$$

where the remaining clock error term is given by

$$\begin{aligned} \Psi_{\epsilon, t}(t_1, t_2) = & \frac{2\pi}{\lambda_S} \{ [\dot{\rho}_{2Q}(t_2) - \dot{\rho}_{2P}(t_2)] \epsilon_2(t_2) + \\ & + [\dot{\rho}_{1P}(t_2) - \dot{\rho}_{1Q}(t_2)] \epsilon_1(t_2) - \\ & - [\dot{\rho}_{2Q}(t_1) - \dot{\rho}_{2P}(t_1)] \epsilon_2(t_1) - \\ & - [\dot{\rho}_{1P}(t_1) - \dot{\rho}_{1Q}(t_1)] \epsilon_1(t_1) \} \end{aligned} \quad (2-26b)$$

Triple-difference modelling has the effect of removing the bias by increasing the number of ranges ρ_{ij} . Losses of lock will therefore result in the form of spikes in the processing which can be easily removed even automatically. Thus, (2-26) is suited as a preprocessing algorithm to remove the "outliers".

3. ORBIT MODEL AND PARAMETERS

In the nonlinear observation equations for single-differences $\psi_{sd}(t)$, double-differences $\psi_d(t)$ and triple-differences $\psi_t(t)$ we find the distance (range) $\rho_{ij}(t)$ from the receiver to a GPS satellite and its first time-derivate $\dot{\rho}_{ij}(t)$.

The geometric information, to be derived from phase observations (e.g. baseline vectors), enter in the observation equations through $\rho_{ij}(t)$. $\dot{\rho}(t)$ is only a coefficient function for the clock error term.

In the following we will discuss the quantities $\rho(t)$ and $\dot{\rho}(t)$, which depend on both, the ground station and the satellite position. The last one is transmitted by the broadcast messages of the satellite in the form of estimates predicted by the control segment of the Global Positioning System. For many high-precision tasks, however, it might be preferable to model or to reprove the orbit. The following considerations have the intention to derive expressions for the orbit which can be inserted in the range ρ_{ij} , and subsequently substitute ρ_{ij} itself. Therefore a short summary of the necessary reference systems and the orbit motion is discussed first.

3.1 Reference systems

In satellite geodesy we need in principle two reference systems. On the one hand we need a reference frame for the orbit determination which is a close approximation to an inertial system within the measurement accuracy. Furthermore an earth fixed reference frame, usually the CIO-system, has to be considered to determine the station positions.

3.1.1 Inertial reference frame

The inertial system used in this paper is defined as the instantaneous astronomical system at epoch t_0 . We will deal with the motion of the satellite and the rotation of the earth for $t \geq t_0$ in the inertial reference frame.

We define the inertial system as follows:

$$\begin{array}{ll} \text{position} & \underline{x} = [x_1, x_2, x_3]^T \\ \text{base vectors} & \underline{e}_1^x, \underline{e}_2^x, \underline{e}_3^x \quad \text{with} \quad \left| \underline{e}_i^x \right| = 1 \end{array}$$

where

$$\begin{array}{ll} \underline{e}_1^x & \text{is the unit vector of the true equinox at } t=t_0, \\ \underline{e}_2^x = \underline{e}_3^x \times \underline{e}_1^x & , \text{ and} \end{array}$$

\underline{e}_3^x is the unit vector parallel to the true rotation axis $\underline{\omega}$ of the earth at epoch $t=t_0$,
 origin geocenter .

This system held fixed at $t=t_0$, is free of rotations for $t \geq t_0$ except its origin due to the movement of the earth. The apparent acceleration due to the translation of the earth is considered together with the attraction of sun and moon on the GPS satellites. (Here we consider always the acceleration of the satellite relative to the geocenter)

We neglect relativistic effects affecting the reference system.

3.1.2 Earth-fixed reference frame

The widely used earth-fixed reference frame is the CIO (Conventional International Origin) system. CIO is determined by the ILS (International Latitude Service). The second reference axis we need to define lies in the astronomical meridian plane of Greenwich.

The CIO-system is defined as follows:

position $\underline{y} = [y_1, y_2, y_3]^T$
 base vectors $\underline{e}_1^y, \underline{e}_2^y, \underline{e}_3^y$ with $|\underline{e}_i^y| = 1$

where

\underline{e}_1^y is the unit vector in the astronomical meridian plane of Greenwich, with $\underline{e}_1^{yT} \cdot \underline{e}_3^y = 0$
 $\underline{e}_2^y = \underline{e}_3^y \times \underline{e}_1^y$, and
 \underline{e}_3^y is the unit vector in the direction of the CIO-pole,
 origin geocenter .

3.1.3 Transformations

Using a matrix of rotations $\underline{R}(t)$, we find for the basic transformation between the inertial system and the earth-fixed system (see e.g. EISSFELLER and HEIN 1986)

$$\underline{x} = \underline{R}(t) \underline{y} \tag{3-1a}$$

$$\underline{y} = \underline{R}^T(t) \underline{x} \tag{3-1b}$$

where

$$\underline{R}(t) = \underline{N}(t_0) \underline{P}(t_0) \underline{P}^T(t) \underline{N}^T(t) \underline{R}_3(-\theta(t)) S(t) \quad (3-1c)$$

$$\underline{R}^T(t) = \underline{S}^T(t) \underline{R}_3^T(-\theta(t)) \underline{N}(t) \underline{P}(t) \underline{P}^T(t_0) \underline{N}^T(t_0) \quad (3-1d)$$

$$\underline{R}^{-1}(t) = \underline{R}^T(t) \quad (3-1e)$$

\underline{N} is the nutation matrix,

\underline{P} is the precession matrix,

\underline{R}_3 is the rotation matrix
(rotation around \underline{e}_3 -axis),

\underline{S} is the matrix of instantaneous polar coordinates,

θ is the sidereal time of Greenwich,

t is the instantaneous time, and

t_0 is the initial epoch of orbit integration.

3.2 Satellite motion

Although the satellites of the Global Positioning System are at altitudes of about 20 000 km, their orbit will not be a perfect Kepler ellipse.

This is caused by the presence of several disturbing accelerations, which have to be considered.

The basic vector differential equation of satellite motion in rectangular coordinates with respect to an inertial reference frame, treating the satellite as a point mass, is given by

$$\ddot{\underline{x}} = \underline{a}(\underline{x}, \dot{\underline{x}}, t) \quad (3-2)$$

where

$\ddot{\underline{x}} = \frac{d^2 \underline{x}}{dt^2}$ is the acceleration vector,

\underline{a} is the vector of resulting accelerations,

\underline{x} is the position vector, and

$\dot{\underline{x}} = \frac{d \underline{x}}{dt}$ is the velocity vector.

The usual way to solve (3-2) is to decompose \underline{a} into the dominant acceleration term \underline{g}_0 (radial symmetrical part of the earth's gravity field) and

in a vector \underline{f} of disturbing accelerations.

Thus,

$$\underline{a} = \underline{g}_0 + \underline{f} \quad (3-3a)$$

$$\text{with } \underline{g}_0 = -\frac{GM}{r^3} \underline{x} \quad \text{and} \quad r = |\underline{x}| \quad (3-3b)$$

$$\text{and } \underline{f} = \sum_i \underline{f}_i \quad (3-3c)$$

GM is the product consisting of the gravitational constant times the mass M of the earth. r is the norm of the radius vector of the satellite, $r = |\underline{x}|$.

$$\ddot{\underline{x}} = -\frac{GM}{r^3} \underline{x},$$

leads to the Kepler ellipse with six constants of integration.

The solution for the position and the velocity vector of a satellite is of the form

$$\underline{x} = \underline{x}(\underline{u}, t) \quad (3-4a)$$

$$\dot{\underline{x}} = \dot{\underline{x}}(\underline{u}, t) \quad (3-4b)$$

The vector \underline{u} is the vector of six integration constants, e.g. the six Kepler elements

$$\underline{u} = [\Omega, i, \omega, a, e, t_p]^T. \quad (3-5)$$

More details can be found, e.g., in ARNOLD (1970).

$$\underline{x}(t) = a \underline{R}_3(-\Omega) \underline{R}_1(-i) \underline{R}_3(-\omega) [\cos E - e, \sqrt{1-e^2} \sin E, 0]^T \quad (3-6a)$$

$$\dot{\underline{x}}(t) = \frac{a^2}{r} n \underline{R}_3(-\Omega) \underline{R}_1(-i) \underline{R}_3(-\omega) [-\sin E, \sqrt{1-e^2} \cos E, 0]^T \quad (3-6b)$$

$$\tilde{M} = n(t-t_p) = E - e \sin E \quad (3-6c)$$

$$n = \left(\frac{GM}{a^3} \right)^{1/2} \quad (3-6d)$$

$$r = a(1 - e \cos E) \quad (3-6e)$$

Ω is the right ascension of the ascending node,

i is the inclination of the orbital plane,

ω is the argument of the perigee,

a is the semimajor axis,

e is the eccentricity,

t_p is the time of perigee passage,

\tilde{M} is the mean anomaly,

V is the true anomaly,

E is the eccentric anomaly,

n is the angular velocity of the satellite, and

r is the radius of the orbit.

The entire problem (3-2) with respect to $\underline{a} = \underline{g}_0 + \underline{f}$ is solved, by the method of variation of constants.

Thus

$$\underline{u} = \underline{u}(t) . \quad (3-7)$$

Differentiating \underline{x} twice with respect to time results in

$$\dot{\underline{x}} = \frac{\partial \underline{x}}{\partial \underline{u}} \dot{\underline{u}} + \frac{\partial \underline{x}}{\partial t} \quad (3-8a)$$

$$\ddot{\underline{x}} = \frac{\partial \dot{\underline{x}}}{\partial \underline{u}} \dot{\underline{u}} + \frac{\partial^2 \underline{x}}{\partial t^2} \quad (3-8b)$$

$$\text{with } \underline{0} = \frac{\partial \underline{x}}{\partial \underline{u}} \dot{\underline{u}} . \quad (3-8c)$$

(3-8c) is a commonly used constraint on \underline{u} , because \underline{u} consists of six time functions but the problem (3-2) is uniquely determined already by three time functions.

Inserting $\ddot{\underline{x}}$ (3-8b) in the equation of motion of the satellite (3-2), we

get

$$\frac{\partial \underline{x}}{\partial \underline{u}} \dot{\underline{u}} = \underline{f} \quad (3-9)$$

because of

$$\frac{\partial^2 \underline{x}}{\partial t^2} - \underline{g}_0 = \underline{0} .$$

(3-8c) together with (3-9) forms a nonlinear vector differential equation for $\dot{\underline{u}}$.

Thus,

$$\frac{\partial \underline{x}}{\partial \underline{u}} \dot{\underline{u}} = \underline{0} \quad (3-10a)$$

$$\frac{\partial \dot{\underline{x}}}{\partial \underline{u}} \dot{\underline{u}} = \underline{f} \quad (3-10b)$$

In order to use analytical or numerical integration methods, it is usual to arrange the vector $\dot{\underline{u}}$ on one side.

Thus,

$$\dot{\underline{u}} = \begin{bmatrix} \frac{\partial \underline{x}}{\partial \underline{u}} \\ \frac{\partial \dot{\underline{x}}}{\partial \underline{u}} \end{bmatrix}^{-1} \begin{bmatrix} \underline{0} \\ \underline{f} \end{bmatrix} \quad (3-11)$$

The inverse on the right hand side of (3-11) can be computed analytically by inversion of the transformation relations $\underline{x} = \underline{x}(\underline{u})$ and $\dot{\underline{x}} = \dot{\underline{x}}(\underline{u})$ at $\underline{u} = \underline{u}(\underline{x}, \dot{\underline{x}})$ and using some differential identities (see, e.g. EISSFELLER (1985)).

The dimension of the inverse \underline{Y} in (3-11) is 6×3 . It can be shown to be

$$\underline{Y} = \frac{\partial \underline{u}}{\partial \dot{\underline{x}}} . \quad (3-12)$$

For the explicit form of $\frac{\partial \underline{u}}{\partial \underline{x}}$ see EISSFELLER (1985).

With (3-12) eq. (3-11) is reduced to

$$\dot{\underline{u}} = \underline{Y} \underline{f} \quad (3-13a)$$

or in integral form

$$\underline{u}(t) = \underline{u}(t_0) + \int_{t_0}^t \underline{Y}(t) \underline{f}(t) dt . \quad (3-13b)$$

Note, that $\underline{u}(t_0)$ is the initial state vector of Kepler elements at $t = t_0$.

If we introduce an acceleration model for $\underline{f}(t) = \sum_i \underline{f}_i(t)$ the integral in (3-13b) can be evaluated numerically.

By inserting the result of integration of (3-13b) in (3-4a,b), the position \underline{x} and the velocity vector $\dot{\underline{x}}$ of the satellite can be computed.

3.3 The range ρ_{ij} and its time derivative $\dot{\rho}_{ij}$

If we refer the quantities $\rho(t)$ and $\dot{\rho}(t)$ to the inertial system, the time variations of the receiver stations and of the satellite positions can be taken easily into consideration.

Denoting the vectors by index i , which refer to a satellite S_i , and those by index j , which refer to the receiver station R_j , we find for $\rho(t)$ and $\dot{\rho}(t)$,

$$\rho_{ij}(t) = \left| \underline{x}_i(t) - \underline{x}_j(t) \right| \quad (3-14a)$$

or

$$\rho_{ij}(t) = \left\{ \left[\underline{x}_i(t) - \underline{x}_j(t) \right]^T \left[\underline{x}_i(t) - \underline{x}_j(t) \right] \right\}^{0.5} \quad (3-14b)$$

$$\dot{\rho}_{ij}(t) = \frac{d\rho_{ij}(t)}{dt} \quad (3-14c)$$

or

$$\dot{\rho}_{ij}(t) = \frac{\left[\underline{x}_i(t) - \underline{x}_j(t) \right]^T \left[\dot{\underline{x}}_i(t) - \dot{\underline{x}}_j(t) \right]}{\rho_{ij}(t)} \quad (3-14d)$$

The vectors $\underline{x}_i(t)$ and $\dot{\underline{x}}_i(t)$ are given by

$$\underline{x}_i = \underline{x}_i(\underline{u}(t), t) \quad (3-15a)$$

$$\dot{\underline{x}}_i = \dot{\underline{x}}_i(\underline{u}(t), t) \quad (3-15b)$$

Using the transformation relation (3-1a), we find for $\underline{x}_j(t)$ and $\dot{\underline{x}}_j(t)$

$$\underline{x}_j(t) = \underline{R}(t) \underline{y}_j \quad (3-16a)$$

$$\dot{\underline{x}}_j(t) = \frac{d\underline{x}_j(t)}{dt} = \dot{\underline{R}}(t) \underline{y}_j \quad (3-16b)$$

where

$$\begin{aligned} \dot{\underline{R}}(t) = & \underline{N}(t_0) \underline{P}(t_0) \dot{\underline{P}}^T(t) \underline{N}^T(t) \underline{R}_3(-\underline{\theta}(t)) \underline{S}(t) + \\ & + \underline{N}(t_0) \underline{P}(t_0) \underline{P}^T(t) \dot{\underline{N}}^T(t) \underline{R}_3(-\underline{\theta}(t)) \underline{S}(t) + \\ & + \underline{N}(t_0) \underline{P}(t_0) \underline{P}^T(t) \underline{N}^T(t) \dot{\underline{R}}_3(-\underline{\theta}(t)) \underline{S}(t) + \\ & + \underline{N}(t_0) \underline{P}(t_0) \underline{P}^T(t) \underline{N}^T(t) \underline{R}_3(-\underline{\theta}(t)) \dot{\underline{S}}(t) \end{aligned} \quad (3-16c)$$

Evaluating the time derivative of $\underline{x}_j(t)$ (3-16b) we may set $\dot{\underline{y}}_j = \underline{0}$, because we want not to deal with geodynamics in this approach.

All the time derivatives of the matrices in (3-16c) can be computed analytically and/or numerically.

3.4 Acceleration model

In this paper the orbit model consists of four types of disturbing accelerations.

These are

- \underline{f}_1 the gravity acceleration of the earth's gravity field,
- \underline{f}_2 the solar radiations pressure,
- \underline{f}_3 the attractions of sun and moon, and
- \underline{f}_4 the remaining accelerations due to unmodelled effects.

Thus, the disturbing acceleration \underline{f} is of the form

$$\underline{f} = \sum_{i=1}^4 \underline{f}_i \quad (3-17)$$

Because of the altitude of the GPS satellites, we may assume, that air drag effects can be neglected.

We assume further, that the tidal deformation of the earth causes no significant effect on the satellite (< 1 m).

The vector \underline{f}_1 of the gravity acceleration will be smooth. Therefore the

modelling of \underline{f}_1 may be simplified in contrast to low orbiting satellites.

In opposite to this the accelerations $\underline{f}_2, \underline{f}_3$ have a greater impact on the satellite motion, because the GPS satellites are more closer to the sources of the forces (sun and moon).

Since the acceleration models used in satellite geodesy describe the physical reality only approximately, we have to consider some unmodelled residual accelerations.

In order to describe these residual effects, we use for \underline{f}_4 in this approach a trigonometric series with unknown amplitudes, frequency and phases. This approach can be found in POPINSKI (1984).

All accelerations depend on unknown dynamical parameters, which can be determined in principle from the observations ψ_{sd}, ψ_d and ψ_t .

3.4.1 Gravity acceleration \underline{f}_1

In deriving an expression for \underline{f}_1 we have to note, that the radial symmetrical term $\underline{g}_0 = -GM \frac{\underline{x}}{r^3}$ is already considered due to orbit integration, see (3-3a to c).

Thus, \underline{f}_1 represents the acceleration of the earth's disturbing gravity field. The gravity vector \underline{f}_1 can be computed as gradient of the spherical harmonic expansion of the gravity field.

$$\underline{f}_1 = \text{grad}_x (U - U_0) \quad (3-18a)$$

where

$$U_0 = \frac{GM}{r} \quad \text{and} \quad r = |\underline{x}| \quad (3-18b)$$

The operator grad_x in (3-18a) denotes partial differentiation of $(U - U_0)$ with respect to the inertial coordinates x_1, x_2, x_3 .

Since the spherical harmonic expansion of U refers to the earth-fixed system (earth-fixed spherical coordinates $\underline{q} = [r, \varphi, \lambda]^T$), we use the following transformation

$$\underline{f}_1 = \underline{R}(t) \frac{\partial \underline{q}^T}{\partial \underline{y}} \begin{bmatrix} \frac{\partial (U - U_0)}{\partial r} \\ \frac{\partial (U - U_0)}{\partial \varphi} \\ \frac{\partial (U - U_0)}{\partial \lambda} \end{bmatrix} \quad (3-19)$$

where

$$\frac{\partial \underline{q}}{\partial \underline{y}} = \begin{bmatrix} \cos \varphi \cos \lambda & \cos \varphi \sin \lambda & \sin \varphi \\ -\frac{\sin \varphi \cos \lambda}{r} & -\frac{\sin \varphi \sin \lambda}{r} & \frac{\cos \varphi}{r} \\ -\frac{\sin \lambda}{r \cos \varphi} & \frac{\cos \lambda}{r \cos \varphi} & 0 \end{bmatrix} \quad (3-20)$$

Using for $U - U_0$ the usual spherical harmonic expansion, see e.g. ARNOLD (1970), we can compute the partial derivatives with respect to r, φ, λ by

$$U - U_0 = GM \sum_{\mu=2}^n \sum_{\nu=0}^{\mu} \frac{R^{\mu}}{r^{\mu+1}} P_{\mu\nu}(\sin \varphi) \{c_{\mu\nu} \cos \nu \lambda + s_{\mu\nu} \sin \nu \lambda\} \quad (3-21)$$

$$\frac{\partial(U - U_0)}{\partial r} = GM \sum_{\mu=2}^n \sum_{\nu=0}^{\mu} \frac{R^{\mu}}{r^{\mu+2}} (\mu + 1) P_{\mu\nu}(\sin \varphi) \{c_{\mu\nu} \cos \nu \lambda + s_{\mu\nu} \sin \nu \lambda\} \quad (3-22a)$$

$$\frac{\partial(U - U_0)}{\partial \varphi} = GM \sum_{\mu=2}^n \sum_{\nu=0}^{\mu} \frac{R^{\mu}}{r^{\mu+1}} \frac{\partial P_{\mu\nu}(\sin \varphi)}{\partial \varphi} \{c_{\mu\nu} \cos \nu \lambda + s_{\mu\nu} \sin \nu \lambda\} \quad (3-22b)$$

$$\frac{\partial(U - U_0)}{\partial \lambda} = GM \sum_{\mu=2}^n \sum_{\nu=0}^{\mu} \frac{R^{\mu}}{r^{\mu+1}} \nu P_{\mu\nu}(\sin \varphi) \{s_{\mu\nu} \cos \nu \lambda - c_{\mu\nu} \sin \nu \lambda\} \quad (3-22c)$$

The functions $P_{\mu\nu}(\sin \varphi)$ are the associated Legendre polynomials of first kind,

$$P_{\mu\nu}(\sin \varphi) = \cos^{\nu} \varphi \sum_{\sigma=0}^{\kappa} a_{\mu\nu\sigma} \sin^{\mu-\nu-2\sigma} \varphi \quad (3-22d)$$

$$\frac{\partial P_{\mu\nu}(\sin \varphi)}{\partial \varphi} = \sum_{\sigma=0}^{\kappa} a_{\mu\nu\sigma} \{(\mu - \nu - 2) \cot \varphi - \nu \tan \varphi\} \cos^{\nu} \varphi \sin^{\mu-\nu-2\sigma} \varphi \quad (3-22e)$$

with

$$a_{\mu\nu\sigma} = \frac{(-1)^{\sigma} (2\mu - 2\sigma)!}{2^{\mu} \sigma! (\mu - \sigma)! (\mu - \nu - 2\sigma)!} \quad (3-22f)$$

and

$$\kappa = \begin{cases} \frac{\mu - \nu}{2} & , \text{ if } \mu - \nu \text{ is even} \\ \frac{\mu - \nu - 1}{2} & , \text{ if } \mu - \nu \text{ is odd.} \end{cases}$$

3.4.2 Solar radiation pressure \underline{f}_2

Following GSFC (1976, p. 4-60) we find for the direct solar radiation pressure the expression

$$\underline{f}_2 = \nu k a_S^2 \frac{\underline{x} - \underline{x}_S}{|\underline{x} - \underline{x}_S|^3} \quad (3-23)$$

with

$$k = P_S \left(\frac{A}{m} \right) c_R \quad (3-24a)$$

$$P_S = \frac{S}{c} \quad (3-24b)$$

$$c_R = 1 + c_j \quad (3-24c)$$

$$\underline{x}_S = r_S \begin{bmatrix} \cos \delta_S \cos \alpha_S \\ \cos \delta_S \sin \alpha_S \\ \sin \delta_S \end{bmatrix} \quad (3-24d)$$

$$r_S = a_S (1 - e_S \cos E_S) \quad (3-24e)$$

The variables have the following meaning:

k	...	unknown model parameter
ν	=	$\begin{cases} 1 & \text{if the satellite is in the sun light} \\ 0 & \text{if the satellite is in the earth-shadow} \end{cases}$
a_S	...	semimajor axis of the orbit of the earth
S	...	mean energy flux of the sun in Watt/m ²
c	...	velocity of light
c_j	...	quantity, which characterizes the optical properties of the surface material (e.g. for AL is $c_j = 0.95$)
$\frac{A}{m}$...	ratio of effective surface to mass of the satellite
r_S	...	radius sun - earth
δ_S	...	declination of the sun in the inertial system
α_S	...	right ascension of the sun in the inertial system
e_S	...	excentricity of the earth orbit
E_S	...	excentric anomaly of the sun
\underline{x}_S	...	position vector of the sun
\underline{x}	...	position vector of the satellite

(3-23) is only a rough model for the solar radiation effect. In a refined approach we would have to add the indirect solar radiation pressure (reflexion of solar radiation by the atmosphere), radiation pressure of the

earth and the Poynting - Robertson effect (relativistic corrections to (3-23)). In addition the true effective surface (solar paddles etc.) would have to be considered.

Because of the altitude of the GPS satellites and due to the relatively small velocity $(|\dot{\underline{x}}| \doteq 3,8 \frac{\text{km}}{\text{s}})$, it is justified to neglect these effects.

3.4.3 Attraction of sun and moon \underline{f}_3

Following GSFC (1976) the acceleration of the satellite due to a celestial body H relative to the geocenter is given by

$$\underline{f}_H = -GM_H \left[\frac{\underline{x} - \underline{x}_H}{|\underline{x} - \underline{x}_H|^3} + \frac{\underline{x}_H}{|\underline{x}_H|^3} \right] \quad (3-25)$$

where

- G ... is the constant of gravitation,
- M_H ... is the mass of the celestial body,
- \underline{x}_H ... is the position vector of the celestial body relative to the inertial system, and
- \underline{x} ... is the position vector of the satellite in the inertial system.

For the reason, why we take in (3-25) the relative acceleration of the satellite to the geocenter, see 3.1.1.

Adding the attraction effects of sun (S) and moon (M), we find for \underline{f}_3

$$\underline{f}_3 = -G \left[M_M \left(\frac{\underline{x} - \underline{x}_M}{|\underline{x} - \underline{x}_M|^3} + \frac{\underline{x}_M}{|\underline{x}_M|^3} \right) + M_S \left(\frac{\underline{x} - \underline{x}_S}{|\underline{x} - \underline{x}_S|^3} + \frac{\underline{x}_S}{|\underline{x}_S|^3} \right) \right] \quad (3-26)$$

where \underline{x}_S , \underline{x}_M are given by

$$\underline{x}_M = r_M \begin{bmatrix} \cos \delta_M \cos \alpha_M \\ \cos \delta_M \sin \alpha_M \\ \sin \delta_M \end{bmatrix} \quad (3-27a)$$

$$\underline{x}_S = r_S \begin{bmatrix} \cos \delta_S \cos \alpha_S \\ \cos \delta_S \sin \alpha_S \\ \sin \delta_S \end{bmatrix} \quad (3-27b)$$

$$r_M = a_M (1 - e_M \cos E_M) \quad (3-27c)$$

$$r_S = a_E (1 - e_E \cos E_S) \quad (3-27d)$$

δ_M, δ_S ... is the declination of moon and of sun, resp.,
 α_M, α_S ... is the rectascension of moon and of sun, resp.,
 r_M, r_S ... is the radial distance geocenter - moon,
 and geocenter - sun, resp.,
 e_M, e_E ... are the excentricities of the orbit of moon
 and of earth,
 a_M, a_E ... are the semimajor axes of the orbit of moon
 and of earth.

All quantities refer to the inertial system defined in 3.1.1.

3.4.4 Residual acceleration \underline{f}_4 due to unmodelled effects

Since all the acceleration models mentioned above are only approximations to the physical reality, we may consider some unmodelled effects acting on the satellite. The acceleration \underline{f}_4 shall be treated as the resulting acceleration of all unmodelled effects.

POPINSKI (1984) proposes a Fourier series approximation together with a secular variation for the orbital elements to take account for those effects. Using a series representation for the acceleration \underline{f}_4 has the advantage, that it would be possible to obtain an empirical acceleration model. If we have estimates of the amplitudes and frequencies in a series representation of \underline{f}_4 for many observation epochs, we are able to make a regression and correlation analysis, e.g. as a function of the epoch.

For later observation epochs we may use the results to extrapolate the vector \underline{f}_4 as a function of computed regression parameters.

A possible series expansion for \underline{f}_4 can be

$$\underline{f}_4 = \sum_{v=0}^k \{ \underline{a}_v \cos(v\omega t + \psi_v) + \underline{b}_v \sin(v\omega t + \psi_v) \} \quad (3-28)$$

where

$\underline{a}_v, \underline{b}_v$... are the unknown amplitude vectors,
 ω ... is the unknown basic frequency,
 ψ_v ... is the unknown phase,
 k ... is the upper summation index
 (which has to be determined by e.g.
 a trias and error method),

and

$$\underline{a}_v = [a_{1v}, a_{2v}, a_{3v}]^T \quad (3-29a)$$

$$\underline{b}_v = [b_{1v}, b_{2v}, b_{3v}]^T \quad (3-29b)$$

3.5 Dynamical parameters \underline{p}

The dynamical parameter \underline{p} entering the range ρ_{ij} and $\dot{\rho}_{ij}$ via the orbit integration (3-14), might be the following:

$$\underline{p} = [\Omega(t_0), i(t_0), \omega(t_0), a(t_0), e(t_0), t_p; \xi, \eta, \Theta; \\ c_{20}, c_{21}, \dots, c_{nn}, s_{20}, s_{21}, \dots, s_{nn}; k; \\ \dots a_{1v}, a_{2v}, a_{3v} \dots; \dots b_{1v}, b_{2v}, b_{3v} \dots; \omega; \dots \psi_v \dots] \quad (3-30)$$

where

$\Omega(t_0), i(t_0), \omega(t_0),$ $a(t_0), e(t_0), t_p$...	are the initial values of the Kepler elements for $t = t_0$ (see (3-13b)),
ξ, η	...	are the pole coordinates (instantaneous earth rotation axis - CIO),
Θ	...	is the sidereal time,
$c_{\mu\nu}, s_{\mu\nu}$...	are the parameters of the spherical harmonic expansion of the earth's gravity potential (3-21),
k	...	is the parameter of solar radiation pressure (3-23),
a_{1v}, a_{2v}, a_{3v} b_{1v}, b_{2v}, b_{3v} ω, ψ_v	...	are the parameters of the Fourier series representation for unmodelled effects (3-28).

It is obvious, that with respect to orbit integration of GPS satellites some of the above mentioned parameters can be considered as sufficiently known, as e.g. the gravity field parameters $c_{\mu\nu}, s_{\mu\nu}$ and the sidereal time Θ . The required minimal set of data for the orbit integration consists of the initial state elements, the polar motion coordinates ξ, η , the parameter of solar radiation pressure k and, eventually, the parameters for unmodelled accelerations.

3.6 Linearization procedure

We rewrite (3-13b), presenting the complete functional relations on \underline{p} , in form of

$$\underline{u}(\underline{p}, t) = \underline{u}_0(t_0) + \sum_{t_0}^t \underline{Y}(\underline{u}(\underline{p}, t), t) \cdot f(\underline{u}(\underline{p}, t), \underline{p}, t) dt \quad (3-31)$$

Using the common decomposition of \underline{p} into an approximate value \underline{p}^0 and into an unknown variation $\underline{\delta p}$,

$$\underline{p} = \underline{p}^0 + \underline{\delta p} \quad (3-32)$$

we find for the variation $\underline{\delta u}$ of the Kepler elements

$$\underline{\delta u}(\underline{p}^0, t) = \frac{\partial \underline{u}(\underline{p}^0, t)}{\partial \underline{p}} \underline{\delta p} \quad (3-33)$$

The Jacobi matrix $\frac{\partial \underline{u}}{\partial \underline{p}}$ is a solution of the following inhomogenous matrix differential equation

$$\begin{aligned} \frac{\partial \dot{\underline{u}}}{\partial \underline{p}} &= \left[\frac{\partial \underline{Y}}{\partial u_1} \underline{f}, \frac{\partial \underline{Y}}{\partial u_2} \underline{f}, \dots, \frac{\partial \underline{Y}}{\partial u_6} \underline{f} \right] + \\ &+ \underline{Y} \frac{\partial \underline{f}}{\partial \underline{u}} \frac{\partial \underline{u}}{\partial \underline{p}} + \underline{Y} \frac{\partial \underline{f}}{\partial \underline{p}} \end{aligned} \quad (3-34a)$$

or, in integral form

$$\begin{aligned} \frac{\partial \underline{u}}{\partial \underline{p}} &= \frac{\partial \underline{u}_0}{\partial \underline{p}} + \int_{t_0}^t \left[\frac{\partial \underline{Y}}{\partial u_1} \underline{f}, \frac{\partial \underline{Y}}{\partial u_2} \underline{f}, \dots, \frac{\partial \underline{Y}}{\partial u_6} \underline{f} \right] \frac{\partial \underline{u}}{\partial \underline{p}} + \\ &+ \int_{t_0}^0 \underline{Y} \frac{\partial \underline{f}}{\partial \underline{u}} \frac{\partial \underline{u}}{\partial \underline{p}} dt + \int_{t_0}^t \underline{Y} \frac{\partial \underline{f}}{\partial \underline{p}} dt \end{aligned} \quad (3-34b)$$

Since the Jacobi matrix $\frac{\partial \underline{u}}{\partial \underline{p}}$ is on both sides of (3-34b), an iterative method must be used to determine $\frac{\partial \underline{u}}{\partial \underline{p}}$.

Several numerical methods based on the approximation method of Picard can be found in numerical analysis to solve (3-34b) with sufficient accuracy, starting, e.g., with

$$\frac{\partial \underline{u}}{\partial \underline{p}} \doteq \frac{\partial \underline{u}_0}{\partial \underline{p}}$$

on the right hand side of (3-34b).

With $\underline{\delta u}(t)$ (3-33), we are able to determine the variation $\underline{\delta x}_i$ of the position vector of the satellite S_i . We find for $\underline{\delta x}_i(t)$ the expression by partial differentiation

$$\begin{aligned}
\delta \underline{x}_i(t) &= \frac{\partial \underline{x}_i(t)}{\partial \underline{u}(t)} \delta \underline{u}(t) \\
&= \frac{\partial \underline{x}_i(t)}{\partial \underline{u}(t)} \frac{\partial \underline{u}(t)}{\partial \underline{p}}
\end{aligned} \tag{3-35}$$

For the variation of the receiver position vector $\underline{x}_j(t)$ we can deduce from (3-16a)

$$\delta \underline{x}_j(t) = \frac{\partial \underline{x}_j(t)}{\partial \underline{p}} \delta \underline{p} + \underline{R}(t) \delta \underline{y}_j \tag{3-36}$$

The Jacobi matrix $\frac{\partial \underline{x}_i(t)}{\partial \underline{p}}$ consists only of the partial derivatives of the rotation matrix $\underline{R}(t)$ with respect to the earth rotation parameters ξ, η, θ in \underline{p} . All other partial derivatives with respect to p_i are zero.

The explicit forms of all partial derivatives in (3-33) to (3-36) can be found in EISSFELLER and HEIN (1986).

3.7 Linear variation $\delta \rho_{ij}(t)$

In order to linearize the nonlinear observation equations for single-differences, double-differences and triple-differences we need a linear variation $\delta \rho_{ij}(t)$ of the range between receiver $R_j := j$ and satellite $S_i := i$.

Starting with (3-14b), we obtain

$$\delta \rho_{ij}(t) = \frac{\partial \rho_{ij}(t)}{\partial \underline{x}_i(t)} \delta \underline{x}_i(t) + \frac{\partial \rho_{ij}(t)}{\partial \underline{x}_j(t)} \delta \underline{x}_j(t) . \tag{3-37}$$

The gradients $\frac{\partial \rho(t)}{\partial \underline{x}_i(t)}$ and $\frac{\partial \rho(t)}{\partial \underline{x}_j(t)}$ are of the following form

$$\frac{\partial \rho(t)}{\partial \underline{x}_i(t)} = \frac{[\underline{x}_i(t) - \underline{x}_j(t)]^T}{\rho(t)} \tag{3-38a}$$

$$\frac{\partial \rho(t)}{\partial \underline{x}_j(t)} = \frac{[\underline{x}_i(t) - \underline{x}_j(t)]^T}{\rho(t)} \tag{3-38b}$$

$$\frac{\partial \rho(t)}{\partial \underline{x}_j(t)} = - \frac{\partial \rho(t)}{\partial \underline{x}_i(t)} \quad (3-38c)$$

If we insert finally (3-35) and (3-36) in (3-37) considering (3-38c) we get

$$\delta \rho_{ij}(t) = \frac{\partial \rho_{ij}(t)}{\partial \underline{x}_i(t)} \left[\delta \underline{x}_i(t) - \delta \underline{x}_j(t) \right] \quad (3-39a)$$

$$\delta \rho_{ij}(t) = \frac{\partial \rho_{ij}(t)}{\partial \underline{x}_i(t)} \left[\frac{\partial \underline{x}_i(t)}{\partial \underline{u}(t)} \frac{\partial \underline{u}(t)}{\partial \underline{p}} - \frac{\partial \underline{x}_j(t)}{\partial \underline{p}} \right] \delta \underline{p} - \frac{\partial \rho_{ij}(t)}{\partial \underline{x}_i(t)} \underline{R}(t) \delta \underline{y}_j \quad (3-39b)$$

4. ATMOSPHERIC EFFECTS

In section 2 eq. (2-14) the propagation time delay Δt_a of the electromagnetic wave of the signal due to the atmosphere was already introduced. The physical reason for the delay Δt_a is the variation of the refraction index n in the atmosphere. Therefore the propagation speed of the signal is not equal to the speed of light in vacuum. Because of different physical properties the atmosphere has to be divided into the troposphere ($0 \text{ km} \leq H \leq 30 \text{ km}$) and into the ionosphere ($80 \text{ km} < H < 1000 \text{ km}$).

The basic relation between the actual speed of the light, c , and the speed in vacuum, c_0 , is given by

$$c = c_0/n . \quad (4-1)$$

Note, that n is in general frequency dependent, thus $n = n(\nu)$.

Because n differs only by a small quantity from 1 , the following decomposition is used,

$$n = 1 + N \quad (4-2)$$

where N is the refractivity.

For the signal speed c and the time differential dt along the range ρ we find

$$c = \frac{d\rho}{dt} \quad (4-3a)$$

or

$$dt = d\rho/c \quad (4-3b)$$

Using (4-1) and (4-2) we get from (4-3b) the propagation time

$$t = \frac{1}{c_0} \int_0^{\rho} n d\rho = \frac{1}{c_0} \int_0^{\rho} (1 + N) d\rho \quad (4-4a)$$

or

$$t = \frac{\rho}{c_0} + \frac{1}{c_0} \int_0^{\rho} N d\rho . \quad (4-4b)$$

The atmospheric time delay Δt_a is then

$$\Delta t_a = t - \frac{\rho}{c_0} = \frac{1}{c_0} \int_0^{\rho} N d\rho . \quad (4-5)$$

Expression (4-5) is conform with (2-14).

In order to consider the different effects of the troposphere and the ionosphere we have to do the decomposition

$$\Delta t_a = \frac{1}{c_0} \int_0^{\rho_T} N_T d\rho + \frac{1}{c_0} \int_{\rho_T}^{\rho_I} N_I d\rho \quad (4-6a)$$

where

N_T is the refractivity of the troposphere,

N_I is the refractivity of the ionosphere,

ρ_T, ρ_I is the range from the receiver to the upper bound of the troposphere, or, respectively, of the ionosphere.

Thus,

$$\Delta t_a = \Delta t_T + \Delta t_I . \quad (4-6b)$$

4.1 Tropospheric effects

The troposphere may be considered as a non-dispersive medium using the frequencies $L_1 (= \nu_1) = 1575.52$ MHz and $L_2 (= \nu_2) = 1227.6$ MHz . This means that the refractivity N_T is not a function of frequency. Since temperature and pressure data are not available along the range ρ_T , surface data must be used to predict N_T in the troposphere.

Following GSFC (1976, p. 7-43) N_T may be presented by

$$N_T = N_R \cdot e^{-\frac{(h-h_R)}{H_T}} \quad (4-7a)$$

where

$$H_T = \frac{1}{N_R} \int_{h_R}^{\infty} N_T(h) dh \quad (4-7b)$$

and

N_R is the surface refractivity, $N_R = N_R(T, p)$
(T temperature, p air pressure),

h is the altitude above sea-level,

h_R is the height of the receiver about sea-level, and

H_T is the tropospheric scale-height, defined by (4-7b).

If we consider H_T to be an unknown parameter, we may compute the time delay Δt_T (4-6a,b) in a first approximation.

Neglecting the curvature of the propagation path we use

$$\frac{dh}{d\rho} \doteq \cos z \doteq \frac{h}{\rho} \quad (4-8)$$

where z is the zenith distance of the GPS satellite in the receiver station R . We find for Δt_T

$$\Delta t_T = \frac{1}{c_0} \int_0^{\rho_T} N_T d\rho$$

$$\Delta t_T = \frac{N_R}{c_0 \cos z} \int_0^{\rho_T} \frac{h_T}{\cos z} e^{-\frac{(h-h_R)}{H_T}} dh . \quad (4-9)$$

If we perform the integration of the exponential function in (4-9), we get for Δt_T

$$\Delta t_T = \frac{N_R H_T e^{\frac{h_R}{H_T}}}{c_0 \cos z} \left(1 - e^{-\frac{h_T}{H_T \cos z}} \right) \quad (4-10)$$

Note in (4-10) that the zenith distance is a function of time due to the varying satellite position.

4.2 Ionospheric effects

In contrast to the troposphere, the ionosphere is a dispersive medium. This means, that the refractivity N_I is a function of frequency $N_I = N_I(\nu)$. Following again GSFC (1967, p. 7-44) N_I is given by

$$N_I = \pm \frac{40.3 N_e}{\nu^2} \quad (4-11)$$

where the "+" sign holds for the phase speed and the "-" sign for the group speed, and N_e are the number of electrons per volume.

In order to compute the time delay Δt_I similar to (4-10), a profile model $N_e = N_e(h)$ for the distribution of the electrons in the ionosphere is needed.

Using the modified Chapman profile we get for $N_e(h)$

$$N_e(h) = N_m e^{(1-x-e^{-x})} \quad (4-12a)$$

where

$$x = \frac{h - h_m}{H_I} \quad (4-12b)$$

and

$$H_I = \frac{5}{3} [30 + 0.2(h_m - 200)] \text{ [in km]}. \quad (4-12c)$$

The quantity N_m is an unknown scale factor, whereas the quantity h_m is an unknown reference height.

Using (4-11) together with (4-12a) and (4-8) we may compute the time delay Δt_I in first approximation.

$$\Delta t_I = \frac{1}{c_0} \int_{\rho_T}^{\rho_I} N_I d\rho \quad (4-13)$$

$$\Delta t_I = \frac{40.3 N_m}{c_0 v^2 \cos z} \int_{\frac{h_T}{\cos z}}^{\frac{h_I}{\cos z}} e^{(1-x-e^{-x})} dh \quad (4-13a)$$

Performing the integration in (4-13a) we find

$$\Delta t_I = \frac{40.3 N_m H_I}{c_0 v^2 \cos z} \left\{ e^{1-e^{-\left(\frac{h_I}{H_I \cos z} - \frac{h_m}{H_I}\right)}} - e^{1-e^{-\left(\frac{h_T}{H_I \cos z} - \frac{h_m}{H_I}\right)}} \right\} \quad (4-14)$$

4.3 Atmospheric parameters \underline{a}

For the total atmospheric phase delay Δt_a we find from (4-10) and (4-14)

$$\begin{aligned} \Delta t_a(t) = & \frac{N_R H_T e^{\frac{h_R}{H_T}}}{c_0 \cos z(t)} \left[1 - e^{-\frac{h_T}{H_T \cos z(t)}} \right] + \\ & + \frac{40.3 N_m H_I}{c_0 v^2 \cos z(t)} \left[e^{1-e^{-\frac{h_I}{H_I \cos z(t)}}} - e^{1-e^{-\left(\frac{h_T}{H_I \cos z(t)} - \frac{h_m}{H_I}\right)}} \right] \end{aligned} \quad (4-15)/11$$

It should be outlined that (4-15) is only a simple model. It is only used to show the fundamental dependence of Δt_a on some basic parameters. Of course, we may find some refined models, which can be introduced in the same way.

Since H_I is a function of h_m , we can introduce the following unknown atmospheric parameters \underline{a} .

$$\underline{a} = [H_T, h_T, N_m, h_m, h_I]^T \quad (4-16)$$

For the definition of H_T, h_T, N_m, h_m, h_I see the preceding chapters.

The second term in (4-15) is frequency-dependent. Thus, we might expect to get a good separation between tropospheric and ionospheric effects, if we work with two-frequency GPS receivers.

4.4 Linearizations of Δt_a

With the vector of atmospheric parameters \underline{a} (4-16) we have for Δt_a (4-15) the form

$$\Delta t_a = \Delta t_a(t, \underline{a}) . \quad (4-17)$$

Using the linearization

$$\underline{a} = \underline{a}^0 + \delta \underline{a} \quad (4-18)$$

we find by Taylor expansion

$$\Delta t_a = \Delta t_a(\underline{a}^0, t) + \frac{\partial \Delta t_a(\underline{a}^0, t)}{\partial \underline{a}} \delta \underline{a} \quad (4-19a)$$

$$\delta \Delta t_a = \frac{\partial \Delta t_a}{\partial \underline{a}} \delta \underline{a} \quad (4-19b)$$

The elements of the gradient $\partial \Delta t_a / \partial \underline{a}$ can be found by partial differentiation of (4-15). In principle, the parameters \underline{a} are functions of time.

There are two ways to solve this problem:

- (i) introduction of time-dependent base functions for the parameters \underline{a} (further parameterization), or
- (ii) introduction of different parameters $\underline{a}_i(t_i)$ for discrete times.

5. LINEAR OBSERVATION EQUATIONS FOR PHASE MEASUREMENTS

5.1 Linear observation equation for single-differences $\psi_{sd}(t)$

Using the decomposition

$$\psi_{sd}(t) = \psi_{sd}^0(t) + \delta\psi_{sd}(t) \quad (5-1)$$

we get for the approximate value $\psi_{sd}^0(t)$, see (2-22a),

$$\begin{aligned} \psi_{sd}^0(t) = & 2\pi (m_2^0 - m_1^0) + \frac{2\pi}{\lambda_s} [\rho_{2j}^0(t) - \rho_{1j}^0(t)] + \\ & + 2\pi (\mathbf{v}_1 - \mathbf{v}_2) t + 2\pi \mathbf{v}_s [\Delta t_{a_{2j}}^0(t) - \Delta t_{a_{1j}}^0(t)] \end{aligned} \quad (5-2a)$$

Thereby the clock-error term $\psi_\varepsilon(t)$ is already of first-order.

For the variation $\delta\psi_{sd}(t)$ in (5-1) we get

$$\begin{aligned} \delta\psi_{sd}(t) = & 2\pi \delta m + \frac{2\pi}{\lambda} [\delta\rho_{2j}(t) - \delta\rho_{1j}(t)] + \\ & + 2\pi \mathbf{v}_s [\delta\Delta t_{a_{2j}}(t) - \delta\Delta t_{a_{1j}}(t)] + \\ & + \psi_\varepsilon(t) \end{aligned} \quad (5-2b)$$

where $\psi_\varepsilon(t)$ is given already by (2-22b).

The quantity δm is the variation of $(m_2 - m_1)$, in order to get the true difference in integer wavelengths.

Using the expression for $\delta\rho_{ij}(t)$ (3-39b) and $\delta\Delta t_a$ (4-19b) we get the linear observation equation for single-differences in its final form

$$\begin{aligned} \delta\psi_{sd}(t) = & \frac{2\pi}{\lambda_s} \left\{ \left[\frac{\partial\rho_{2j}(t)}{\partial\underline{x}_s(t)} - \frac{\partial\rho_{1j}(t)}{\partial\underline{x}_s(t)} \right] \frac{\partial\underline{x}_s(t)}{\partial\underline{u}(t)} \frac{\partial\underline{u}(t)}{\partial\underline{p}} + \right. \\ & \left. + \frac{\partial\rho_{1j}(t)}{\partial\underline{x}_s(t)} \frac{\partial\underline{x}_{R_1}(t)}{\partial\underline{p}} - \frac{\partial\rho_{2j}(t)}{\partial\underline{x}_s(t)} \frac{\partial\underline{x}_{R_2}(t)}{\partial\underline{p}} \right\} \delta\underline{p} + \\ & + \frac{2\pi}{\lambda_s} \left[\frac{\partial\rho_{1j}(t)}{\partial\underline{x}_s(t)} \underline{R}(t) \delta\underline{y}_1 - \frac{\partial\rho_{2j}(t)}{\partial\underline{x}_s(t)} \underline{R}(t) \delta\underline{y}_2 \right] + \\ & + 2\pi \delta m + \underline{\varepsilon}_0^\top \delta\underline{\varepsilon} \quad . \end{aligned} \quad (5-3)$$

The clock-error term in (5-3) is of the form

$$\underline{\varepsilon}_0 = \left[-\frac{2\pi}{\lambda} \dot{\rho}_1^0(t) + 2\pi \mathbf{v}_S + 2\pi \mathbf{v}_1, \frac{2\pi}{\lambda} \dot{\rho}_2^0(t) - 2\pi \mathbf{v}_S - 2\pi \mathbf{v}_2 \right]^T \quad (5-4a)$$

$$\underline{\delta \varepsilon} = [\varepsilon_1(t), \varepsilon_2(t)]^T \quad (5-4b)$$

It is obvious, that a further parameterization for $\varepsilon_i(t)$ like in (2-18) can be done straightforward.

5.2 Linear observation equation for double-differences

The nonlinear observation equation for double differences was given by (2-25a,b,c). In order to obtain the linear observation equation we decompose again

$$\psi_d(t) = \psi_d^0(t) + \delta\psi_d(t) \quad (5-5)$$

where the approximate value $\psi_d^0(t)$ is given by

$$\begin{aligned} \psi_d^0(t) = & 2\pi m_d^0 + \\ & + \frac{2\pi}{\lambda_S} [\rho_{2Q}^0(t) - \rho_{2P}^0(t) + \rho_{1P}^0(t) - \rho_{1Q}^0(t)] + \\ & + 2\pi \mathbf{v}_S [\Delta t_{a_{2Q}}^0(t) - \Delta t_{a_{2P}}^0(t) + \Delta t_{a_{1P}}^0(t) - \Delta t_{a_{1Q}}^0(t)] \end{aligned} \quad (5-6a)$$

and

$$\begin{aligned} \delta\psi_d(t) = & \frac{2\pi}{\lambda_S} [\delta\rho_{2Q}(t) - \delta\rho_{2P}(t) + \delta\rho_{1P}(t) - \delta\rho_{1Q}(t)] + \\ & + 2\pi \delta m_d + \\ & + 2\pi \mathbf{v}_S [\delta\Delta t_{a_{2Q}}(t) - \delta\Delta t_{a_{2P}}(t) + \delta\Delta t_{a_{1P}}(t) - \delta\Delta t_{a_{1Q}}(t)] + \\ & + \psi_{\varepsilon,d}(t) \end{aligned} \quad (5-6b)$$

The clock-error term $\psi_{\varepsilon,d}(t)$ (already of first order) was given by (2-25c),

$$\psi_{\varepsilon,d}(t) = \frac{2\pi}{\lambda_S} \{ [\dot{\rho}_{2Q}(t) - \dot{\rho}_{2P}(t)] \varepsilon_2(t) + [\dot{\rho}_{1P}(t) - \dot{\rho}_{1Q}(t)] \varepsilon_1(t) \} .$$

Note, that P and Q are two different GPS satellites.

Using again the formulas for $\delta\rho_{ij}(t)$, Eq. (3-39b) and for $\delta\Delta t_{a_2}$ (4-19b), we find the linear observation equation for double differences

$$\begin{aligned}
\delta\psi_d(t) = & \frac{2\pi}{\lambda_s} \left\{ \left[\frac{\partial\rho_{2Q}(t)}{\partial\underline{x}_Q(t)} - \frac{\partial\rho_{1Q}(t)}{\partial\underline{x}_Q(t)} \right] \frac{\partial\underline{x}_Q(t)}{\partial\underline{u}_Q(t)} \frac{\partial\underline{u}_Q(t)}{\partial\underline{p}_Q} + \right. \\
& \left. + \frac{\partial\rho_{1Q}(t)}{\partial\underline{x}_Q(t)} \frac{\partial\underline{x}_1(t)}{\partial\underline{p}_Q} - \frac{\partial\rho_{2Q}(t)}{\partial\underline{x}_Q(t)} \frac{\partial\underline{x}_2(t)}{\partial\underline{p}_Q} \right\} \delta\underline{p}_Q - \\
& - \frac{2\pi}{\lambda_s} \left\{ \left[\frac{\partial\rho_{2P}(t)}{\partial\underline{x}_P(t)} - \frac{\partial\rho_{1P}(t)}{\partial\underline{x}_P(t)} \right] \frac{\partial\underline{x}_P(t)}{\partial\underline{u}_P(t)} \frac{\partial\underline{u}_P(t)}{\partial\underline{p}_P} + \right. \\
& \left. + \frac{\partial\rho_{1P}(t)}{\partial\underline{x}_P(t)} \frac{\partial\underline{x}_1(t)}{\partial\underline{p}_P} - \frac{\partial\rho_{2P}(t)}{\partial\underline{x}_P(t)} \frac{\partial\underline{x}_2(t)}{\partial\underline{p}_P} \right\} \delta\underline{p}_P + \\
& + \frac{2\pi}{\lambda_s} \left[\frac{\partial\rho_{1Q}(t)}{\partial\underline{x}_Q(t)} - \frac{\partial\rho_{1P}(t)}{\partial\underline{x}_P(t)} \right] \underline{R}(t) \delta\underline{y}_1 + \\
& + \frac{2\pi}{\lambda_s} \left[\frac{\partial\rho_{2P}(t)}{\partial\underline{x}_P(t)} - \frac{\partial\rho_{2Q}(t)}{\partial\underline{x}_Q(t)} \right] \underline{R}(t) \delta\underline{y}_2 + \\
& + 2\pi v_s \left\{ \frac{\partial\Delta t_{a_{2Q}}(t)}{\partial\underline{a}_{2Q}} \delta\underline{a}_{2Q} - \frac{\partial\Delta t_{a_{1Q}}(t)}{\partial\underline{a}_{1Q}} \delta\underline{a}_{1Q} - \right. \\
& \left. - \frac{\partial\Delta t_{a_{2P}}(t)}{\partial\underline{a}_{2P}} \delta\underline{a}_{2P} + \frac{\partial\Delta t_{a_{1P}}(t)}{\partial\underline{a}_{1P}} \delta\underline{a}_{1P} \right\} + \\
& + 2\pi \delta m_d + \underline{\varepsilon}_d^T \delta\underline{\varepsilon}
\end{aligned} \tag{5-7}$$

The clock-error term is here of the form

$$\underline{\varepsilon}_d = \left[\frac{2\pi}{\lambda_s} (\dot{\rho}_{1P}(t) - \dot{\rho}_{1Q}(t)), \frac{2\pi}{\lambda_s} (\dot{\rho}_{2P}(t) - \dot{\rho}_{2Q}(t)) \right]^T \tag{5-8a}$$

$$\delta\underline{\varepsilon} = [\varepsilon_1(t), \varepsilon_2(t)]^T \tag{5-8b}$$

For further parameterization of $\varepsilon_i(t)$ see eq. (2-18).

In (5-7) we observe two satellites P , Q having different orbital elements $\underline{u}_P(t)$ and $\underline{u}_Q(t)$.

5.3 Linear observation equation for triple-differences

The nonlinear observation equation for triple-differences was given by (2-26). We decompose again by

$$\psi_t(t_1, t_2) = \psi_t^0(t_1, t_2) + \delta\psi_t(t_1, t_2) \quad (5-9a)$$

or

$$\psi_t(t_1, t_2) = \psi_d^0(t_2) - \psi_d^0(t_1) + \delta\psi_d(t_2) - \delta\psi_d(t_1) \quad (5-9b)$$

where the approximate value ψ_t^0 is given by

$$\begin{aligned} \psi_t^0(t_1, t_2) = & \frac{2\pi}{\lambda_S} [\rho_{2Q}^0(t_2) - \rho_{2Q}^0(t_1) + \rho_{2P}^0(t_1) - \rho_{2P}^0(t_2) + \\ & + \rho_{1P}^0(t_2) - \rho_{1P}^0(t_1) + \rho_{1Q}^0(t_1) - \rho_{1Q}^0(t_2)] + \\ & + 2\pi (m_{d_2}^0 - m_{d_1}^0) + \\ & + 2\pi v_S [\Delta t_{a_{2Q}}^0(t_2) - \Delta t_{a_{2Q}}^0(t_1) + \Delta t_{a_{2P}}^0(t_1) - \\ & - \Delta t_{a_{2P}}^0(t_2) + \Delta t_{a_{1P}}^0(t_1) - \Delta t_{a_{1P}}^0(t_1) + \\ & + \Delta t_{a_{1Q}}^0(t_1) - \Delta t_{a_{1Q}}^0(t_2)] \end{aligned} \quad (5-10a)$$

and the variation $\delta\psi_t(t_1, t_2)$ is

$$\begin{aligned} \delta\psi_t(t_1, t_2) = & \frac{2\pi}{\lambda_S} [\delta\rho_{2Q}(t_2) - \delta\rho_{2Q}(t_1) + \delta\rho_{2P}(t_1) - \delta\rho_{2P}(t_2) + \\ & + \delta\rho_{1P}(t_2) - \delta\rho_{1P}(t_1) + \delta\rho_{1Q}(t_1) - \delta\rho_{1Q}(t_2)] + \\ & + 2\pi \delta m_t + \\ & + 2\pi v_S [\delta\Delta t_{a_{2Q}}(t_2) - \delta\Delta t_{a_{2Q}}(t_1) + \delta\Delta t_{a_{2P}}(t_1) - \\ & - \delta\Delta t_{a_{2P}}(t_2) + \delta\Delta t_{a_{1P}}(t_2) - \delta\Delta t_{a_{1P}}(t_1) + \\ & + \delta\Delta t_{a_{1Q}}(t_1) - \delta\Delta t_{a_{1Q}}(t_2)] + \\ & + \psi_{\varepsilon, t}(t_1, t_2) \end{aligned} \quad (5-10b)$$

where the clock-error term is already given by (2-27b) and

$$\delta m_t = \delta m_{d_2} - \delta m_{d_1} . \quad (5-10c)$$

Using the expressions for $\delta \rho_{ij}(t)$, see (3-39b), and those for $\delta \Delta t_a$, see (4-19b), we get the final form for the linear observation equation for triple-differences

$$\begin{aligned} \delta \psi_t(t_1, t_2) = & \frac{2\pi}{\lambda_s} \left\{ \left[\frac{\partial \rho_{10}(t_2)}{\partial \underline{x}_0(t_2)} - \frac{\partial \rho_{20}(t_2)}{\partial \underline{x}_0(t_2)} \right] \frac{\partial \underline{x}_0(t_2)}{\partial \underline{u}_0(t_2)} \frac{\partial \underline{u}_0(t_2)}{\partial \underline{p}_0} + \right. \\ & + \left[\frac{\partial \rho_{10}(t_1)}{\partial \underline{x}_0(t_1)} - \frac{\partial \rho_{20}(t_1)}{\partial \underline{x}_0(t_1)} \right] \frac{\partial \underline{x}_0(t_1)}{\partial \underline{u}_0(t_1)} \frac{\partial \underline{u}_0(t_1)}{\partial \underline{p}_0} + \\ & + \frac{\partial \rho_{10}(t_2)}{\partial \underline{x}_0(t_2)} \frac{\partial \underline{x}_1(t_2)}{\partial \underline{p}_0} - \frac{\partial \rho_{20}(t_2)}{\partial \underline{x}_0(t_2)} \frac{\partial \underline{x}_2(t_2)}{\partial \underline{p}_0} + \\ & \left. + \frac{\partial \rho_{20}(t_1)}{\partial \underline{x}_0(t_1)} \frac{\partial \underline{x}_2(t_1)}{\partial \underline{p}_0} - \frac{\partial \rho_{10}(t_1)}{\partial \underline{x}_0(t_1)} \frac{\partial \underline{x}_1(t_1)}{\partial \underline{p}_0} \right\} \delta \underline{p}_0 - \\ & + \frac{2\pi}{\lambda_s} \left\{ \left[\frac{\partial \rho_{2p}(t_2)}{\partial \underline{x}_p(t_2)} - \frac{\partial \rho_{1p}(t_2)}{\partial \underline{x}_p(t_2)} \right] \frac{\partial \underline{x}_p(t_2)}{\partial \underline{u}_p(t_2)} \frac{\partial \underline{u}_p(t_2)}{\partial \underline{p}_p} + \right. \\ & + \left[\frac{\partial \rho_{1p}(t_1)}{\partial \underline{x}_p(t_1)} - \frac{\partial \rho_{2p}(t_1)}{\partial \underline{x}_p(t_1)} \right] \frac{\partial \underline{x}_p(t_1)}{\partial \underline{u}_p(t_1)} \frac{\partial \underline{u}_p(t_1)}{\partial \underline{p}_p} + \\ & + \frac{\partial \rho_{1p}(t_2)}{\partial \underline{x}_p(t_2)} \frac{\partial \underline{x}_1(t_2)}{\partial \underline{p}_p} - \frac{\partial \rho_{2p}(t_2)}{\partial \underline{x}_p(t_2)} \frac{\partial \underline{x}_2(t_2)}{\partial \underline{p}_p} + \\ & \left. + \frac{\partial \rho_{2p}(t_1)}{\partial \underline{x}_p(t_1)} \frac{\partial \underline{x}_2(t_1)}{\partial \underline{p}_p} - \frac{\partial \rho_{1p}(t_1)}{\partial \underline{x}_p(t_1)} \frac{\partial \underline{x}_1(t_1)}{\partial \underline{p}_p} \right\} \delta \underline{p}_p + \\ & + \frac{2\pi}{\lambda_s} \left\{ \left[\frac{\partial \rho_{10}(t_2)}{\partial \underline{x}_0(t_2)} - \frac{\partial \rho_{1p}(t_2)}{\partial \underline{x}_p(t_2)} \right] \underline{R}(t_2) + \right. \\ & \left. + \left[\frac{\partial \rho_{1p}(t_1)}{\partial \underline{x}_p(t_1)} - \frac{\partial \rho_{10}(t_1)}{\partial \underline{x}_0(t_1)} \right] \underline{R}(t_1) \right\} \delta y_{-1} + \\ & + \frac{2\pi}{\lambda_s} \left\{ \left[\frac{\partial \rho_{2p}(t_2)}{\partial \underline{x}_p(t_2)} - \frac{\partial \rho_{20}(t_2)}{\partial \underline{x}_0(t_2)} \right] \underline{R}(t_2) + \right. \\ & \left. + \left[\frac{\partial \rho_{20}(t_1)}{\partial \underline{x}_0(t_1)} - \frac{\partial \rho_{2p}(t_1)}{\partial \underline{x}_p(t_1)} \right] \underline{R}(t_1) \right\} \delta y_{-2} + \end{aligned}$$

$$\begin{aligned}
& + 2\pi v_s \left\{ \left[\frac{\partial \Delta t_{a_{2Q}}(t_2)}{\partial \underline{a}_{2Q}} - \frac{\partial \Delta t_{a_{2Q}}(t_1)}{\partial \underline{a}_{2Q}} \right] \delta \underline{a}_{2Q} + \right. \\
& \quad + \left[\frac{\partial \Delta t_{a_{1Q}}(t_1)}{\partial \underline{a}_{1Q}} - \frac{\partial \Delta t_{a_{1Q}}(t_2)}{\partial \underline{a}_{1Q}} \right] \delta \underline{a}_{1Q} + \\
& \quad + \left[\frac{\partial \Delta t_{a_{1P}}(t_2)}{\partial \underline{a}_{1P}} - \frac{\partial \Delta t_{a_{1P}}(t_1)}{\partial \underline{a}_{1P}} \right] \delta \underline{a}_{1P} + \\
& \quad \left. + \left[\frac{\partial \Delta t_{a_{2P}}(t_1)}{\partial \underline{a}_{2P}} - \frac{\partial \Delta t_{a_{2P}}(t_2)}{\partial \underline{a}_{2P}} \right] \delta \underline{a}_{2P} \right\} + \\
& + 2\pi \delta m_t + \underline{\varepsilon}_t^T \delta \underline{\varepsilon}
\end{aligned} \tag{5-11}$$

where the clock-error term $\underline{\varepsilon}_t^T \delta \underline{\varepsilon}$ is of the following form

$$\begin{aligned}
\underline{\varepsilon}_t = \frac{2\pi}{\lambda_s} \{ & [\dot{\rho}_{1P}(t_2) - \dot{\rho}_{1Q}(t_2) - \dot{\rho}_{1P}(t_1) + \dot{\rho}_{1Q}(t_1)] , \\
& [\dot{\rho}_{2Q}(t_2) - \dot{\rho}_{2P}(t_2) - \dot{\rho}_{2Q}(t_1) + \dot{\rho}_{2P}(t_1)] \}^T
\end{aligned} \tag{5-12a}$$

$$\underline{\delta \varepsilon} = [\varepsilon_1(t), \varepsilon_2(t)]^T \tag{5-12b}$$

For the parameters $\varepsilon_i(t)$, $i = \{1, 2\}$, see (2-18).

6. GENERAL ESTIMATION MODEL

The linearized observation equations for GPS phase (difference) measurements form the following linear system of equations

$$\underline{l} = \underline{A}_1 \underline{p} + \underline{A}_2 \underline{y} + \underline{A}_3 \underline{x}_a + \underline{A}_4 \underline{\varepsilon} + \underline{n} \tag{6-1}$$

where

- \underline{l} is the vector of phase (difference) observations,
- \underline{A}_i ($i = 1, \dots, 4$) are the corresponding design matrices of \underline{p} , \underline{y} , \underline{x}_a , and $\underline{\varepsilon}$,
- \underline{p} is the vector of unknown dynamical parameters of the orbit, see (3-30),
- \underline{y} is the vector of unknown 3d-station coordinates in an earth-fixed reference frame,

\underline{x}_a is the vector of unknown atmospheric parameters,

$\underline{\varepsilon}$ is the vector of unknown clock-errors and of the unknown integer number of wavelengths, and

\underline{n} is the vector of observational noise.

In general, one does not solve for all unknowns in (6-1), at least not in one step. For most routine applications the orbit information transmitted by the broadcast ephemerides of the GPS satellites can be considered as sufficiently known, so that the term $\underline{A}_1 \underline{p}$ in (6-1) is determined. The same holds for the integer number of wavelengths in $\underline{\varepsilon}$ derived from a pre-processing and applied at the raw observations, or the treatment of atmospheric parameters, if at all considered. Thus, the general model may e.g. reduce to

$$\underline{l} = \underline{A}_2 \underline{y} + \underline{A}_4 \underline{\varepsilon} + \underline{n} \quad (6-2)$$

where the usual least-squares minimum norm $\underline{n}^T \underline{C}_{nn}^{-1} \underline{n}$ can be used to solve (6-2). Possible correlations between the observations due to differencing are expressed in the variance-covariance matrix \underline{C}_{nn} . For the defect inherent in (6-1) or (6-2) station coordinates (and/or other parameters) have to be fixed.

The functional relationship of GPS observations with regard to all possible parameters in the general form of (6-1) should, however, show the user the assumptions made in the available algorithms for GPS-processing. Moreover it might serve as the basis for improvements in the available processing software. If, for example, a given orbit has to be improved, then the given elements $\underline{u}(t)$ can be used as appropriate values $\underline{u}^{\hat{0}}(t) := \underline{u}(t)$, and the orbit integration (3-31) can be omitted.

Present algorithms are developed for single baselines. One of the improvements in the future must concern the extension to multi-baseline determination of networks in one step. The theoretical model (6-1) is already defined without restrictions.

A variety of solutions to (6-1) in more or less sequential form is possible. Numerical realizations have to show the best way to get the desired accuracy of the baseline vectors.

7. REFERENCES

- Arnold, K. (1970): *Methoden der Satellitengeodäsie*. Akademie Verlag, Berlin
- Bossler, J.D., C.C. Goad, P.L. Bender (1980): *Using the Global Positioning System (GPS) for geodetic surveying*. Bulletin Géodésique 54, 553-563
- Eissfeller, B. (1985): *Orbit improvement using local gravity field information and least-squares prediction*. Manuscripta geodaetica 10, 91-101

- Eissfeller, B. and G.W. Hein (1984): *The observation equations of satellite techniques in the model of integrated geodesy*. In: Proc. of the International Symposium on Space Techniques for Geodynamics, Sopron, Hungary, July 9-13, 1984, (2) 119-129
- Eissfeller, B. and G.W. Hein (1984): *A contribution to 3D-operational geodesy. Part 4: The observation equations of satellite geodesy in the model of integrated geodesy*. Heft 17 der Schriftenreihe des univ. Studiengangs Vermessungswesen der Universität der Bundeswehr München
- Goad, C.C. -convenor- (1985): *Proceedings of the First International Symposium on Precise Positioning with the Global Positioning System - Positioning with GPS - 1985*. U.S. Department of Commerce, NOAA, Rockville, Md., May 1985, 946 pp.
- GSFC (1976): (Cappelari, J.O., C.E. Velez, and A.J. Fuchs) *Mathematical theory of the goddard trajectory determination system*. Doc. X-582-76-77, Goddard Space Flight Center, Greenbelt, Md.
- Hein, G.W. (1982a): *A contribution to 3D-operational geodesy. Part 1: Principle and observational equations of terrestrial type*. In: Deutsche Geodätische Kommission, Reihe B, Nr. 258/VII, 31-64, München
- Hein, G.W. (1982b): *A contribution to 3D-operational geodesy. Part 2: Concepts of solution*. In: Deutsche Geodätische Kommission, Reihe B, Nr. 256/VII, 65-85, München
- King, R.W., E.G. Masters, C. Rizos, A. Stolz and J. Collins (1986): *Surveying with GPS*. Monograph No. 9, School of Surveying. The University of New South Wales, Kensington, NSW, Australia 2033
- Livingston, D.C. (1970): *The Physics of Microwave Propagation*. Microwave and Field Series, Prentice-Hill, Englewood Cliffs, New Jersey
- Popinski, W. (1984): *The unmodelled effects in the motion of artificial satellites*. Planetary Geodesy 19(1), 17-40, Warsaw, Poland
- Remondi, B.W. (1984): *Using the Global Positioning System (GPS) Phase Observable for Relative Geodesy: Modelling, Processing and Results*. Dissertation, The University of Texas at Austin

A TAYLOR SERIES EXPANSION FOR THE TRANSFORMATION
PROBLEM OF CARTESIAN BASELINE COMPONENTS INTO
ELLIPSOIDAL COORDINATE DIFFERENCES

Bernd Eissfeller
University FAF Munich
Institute of Astronomical and Physical Geodesy
Werner-Heisenberg-Weg 39
8014 Neubiberg
Federal Republic of Germany

ABSTRACT. This paper deals with the problem of transforming Cartesian baseline vectors (derived from the GPS) into differences in ellipsoidal coordinates (B,L,h).

In opposite to iterative solutions of this problem (HEISKANEN and MORITZ 1967, SCHÖDLBAUER 1984), a direct solution, based on a Taylor series expansion up to the complete third order terms, is presented.

Numerical investigations show, that the approximation error, neglecting higher order terms, is about 2.0 cm/60 km in ellipsoidal latitude and about 1.0 cm/80 km in ellipsoidal height (per baseline length).

Finally an application field for this method is discussed, in particular GPS moving baseline applications.

1. INTRODUCTION

The adjustment of differential GPS observations (single, double, triple differences) in stationary and non-stationary (moving baseline) applications results in Cartesian baseline vectors which refer to the World Geodetic System 1972 (WGS 72) or in future to WGS 1984 (Block II NAVSTAR/GPS Satellites).

Using this new type of data for geodetic purpose the following computational problem arises:

- (i) transformation of the baseline vectors to a national reference frame
- (ii) conversion of the so transformed baseline vectors into differences in ellipsoidal coordinates (B,L,h)

For other curvilinear coordinate systems besides of (B,L,h) which are of interest in geometrical geodesy, see SCHÖDLBAUER (1985).

Besides these two more or less geometrical problems we are in addition concerned with the problem of converting differences in ellipsoidal heights into differences in orthometric heights. For more detail on this height problem see e.g. ENGELIS, TSCHERNING and RAPP (1984), HEIN (1985) and EISSFELLER (1985).

The problem (i) is easily solved by applying an appropriate rotation matrix on the baseline components referring to WGS 72, e.g. EISSFELLER (1985).

The standard solution for problem (ii) is first to add the transformed Cartesian baseline vector $\Delta \underline{x}_{ij}$ (between two stations i,j) to the position vector $\underline{x}_i(B_i, L_i, h_i)$ in order to obtain the position vector $\underline{x}_j(B_j, L_j, h_j)$. In a second step the ellipsoidal coordinates B_j, L_j, h_j are derived by inverting the three nonlinear component functions of the vector \underline{x}_j .

From a geometrical point of view this inversion problem consists in finding the intersection point at the ellipsoid of reference by orthogonal projection of a space point to the ellipsoid. Numerically this problem is solved iteratively by Newtons iteration method, see e.g. HEISKANEN and MORITZ (1967), BARTELME and MEISSL (1975) and SCHÖDLBAUER (1984).

However a direct solution is discussed in BENNING (1974). It is shown in BENNING (1974), that the intersection problem described above is equivalent to the problem of finding the roots of a fourth order algebraic equation. Because these roots have a rather complicated structure, the method proposed by BENNING (1974) is not widely used in geometrical geodesy. GPS baseline vectors in practice hardly exceed 100 km of baseline length. Therefore baseline components are in principle small quantities relative to the dimensions of earth.

For that reason it is very straightforward to construct a Taylor series expansion of the ellipsoidal coordinates B, h as a function of the baseline components $\Delta x, \Delta y, \Delta z$. The left or right baseline station may be used as Taylor point in this expansion. Note, that because of the symmetry of the problem (rotational ellipsoid), the difference in longitude L can always be computed directly with the aid of elementary trigonometric relations. Let f be the geodetic function to be expanded, the basic concept of geometrical geodesy may be summarized as follows, see also HEITZ (1985, p. 181)

$$f(\underline{x}) = f(\underline{x}^0) + \sum_{k=1}^{\infty} \frac{1}{k!} \left(\frac{\partial}{\partial x_1} \Delta x_1 + \frac{\partial}{\partial x_2} \Delta x_2 + \dots + \frac{\partial}{\partial x_m} \Delta x_m \right)^k f(\underline{x}^0) \quad (1-1)$$

- f function to be expanded
- \underline{x} vector of m independent variables
- \underline{x}^0 Taylor point
- Δx_i variations of components of \underline{x}

Thus, eq. (1-1) is a polynomial function of k 'th order in the variations \underline{x}_i . The topic of this paper is to derive a Taylor series expansion for ellipsoidal latitude B and ellipsoidal height h as a function of baseline components $\Delta x, \Delta y, \Delta z$ including complete third order terms, based on (1-1). The necessary partial derivatives are computed with the aid of implicit differentiation techniques.

A similar approach, but presenting only approximate third order terms and using tensor calculus together with direct differentiation techniques, is

given in HEITZ (1985, p. 215).

2. BASIC RELATIONS

The starting point of the derivations is the functional relationship of the position vector $\underline{x}=[x,y,z]^T$ (given in a national reference frame) with ellipsoidal coordinates (HEISKANEN and MORITZ 1967, p. 184)

$$\begin{bmatrix} x \\ y \\ z \end{bmatrix} = \begin{bmatrix} (N+h) \cos B \cos L \\ (N+h) \cos B \sin L \\ \left(\frac{b^2}{a^2} N+h\right) \sin B \end{bmatrix} \quad (2-1)$$

with

B , L , h ellipsoidal latitude, longitude, height
a , b semimajor and semiminor axis of reference
 ellipsoid
N east-west radius of curvature.

Following GROSSMANN (1976, p. 12) the quantity N is defined as follows

$$N = \frac{c}{V} \quad (2-2a)$$

$$c = \frac{a^2}{b} \quad (2-2b)$$

$$V = (1 + e'^2 \cos^2 B)^{1/2} \quad (2-2c)$$

$$e'^2 = \frac{a^2 - b^2}{b^2} \quad (2-2d)$$

Let in addition be $\underline{\Delta x}$ the vector of GPS baseline components

$$\underline{\Delta x} = [\Delta x, \Delta y, \Delta z]^T . \quad (2-3)$$

Based on (2-1), (2-2) and (2-3) the topic of this paper is to present the following Taylor series expansions

$$t = \tan B \quad (2-4a)$$

$$t = t_0 + \sum_{k=1}^n \frac{1}{k!} \left(\frac{\partial}{\partial x} \Delta x + \frac{\partial}{\partial y} \Delta y + \frac{\partial}{\partial z} \Delta z \right)^k t_0 + R_{\mu_n} \quad (2-4b)$$

$$h = h_0 + \sum_{k=1}^n \frac{1}{k!} \left(\frac{\partial}{\partial x} \Delta x + \frac{\partial}{\partial y} \Delta y + \frac{\partial}{\partial z} \Delta z \right)^k h_0 + R_{h_n} \quad (2-4c)$$

The quantities t_0 and h_0 are the corresponding values of t and h at the Taylor point.

Notice, that instead of B itself the tangens of B is used as the basic function in the series expansion.

This has some computational advantages and is allowed, because $\tan B$ is a unique function of B in the interval $[-\frac{\pi}{2}, \frac{\pi}{2}]$. The only problem, we are in the following discussions concerned with, is to compute the partial derivatives of t and h in (2-4b,c).

In order to do these differentiations efficiently, we need the functional relations of h with respect to rectangular coordinates (x,y,z) .

2.1 Basic expression of t

Let p be the radial distance in the equatorial (x,y) -plane to the projection point of the position vector \underline{x} (projection parallel to z -axis). Thus,

$$p = (x^2 + y^2)^{1/2}. \quad (2-5)$$

If we square and sum the first two components of (2-1), we find for p in curvilinear coordinates

$$p = \left(\frac{c}{V} + h \right) \cos B. \quad (2-6a)$$

Using (2-2a,b) the third component of (2-1) is of the form

$$z = \left(\frac{b}{V} + h \right) \sin B. \quad (2-6b)$$

Elimination of h in (2-6a,b) and using the trigonometric identities

$$\sin^2 B = \frac{t^2}{1+t^2} \quad (2-7a)$$

$$\cos^2 B = \frac{1}{1+t^2} \quad (2-7b)$$

leads to a fundamental expression of t

$$(\alpha^2 + t^2)(pt - z)^2 = \beta^2 t^2 \quad (2-8)$$

$$\alpha^2 = \frac{a^2}{b^2} \quad (2-8a)$$

$$\beta^2 = b^2 e'^4. \quad (2-8b)$$

Eq. (2-8) is again an algebraic equation of fourth order (see the introduction).

It should be mentioned, that in the special case $a = b$ (spherical approximation of ellipsoid) eq. (2-8) degenerates to

$$(1+t^2)(pt-z)^2 = 0 \quad (2-9)$$

The roots of (2-9) are easily computed as

$$t_{1,2} = \pm i ; \quad i = \sqrt{-1} \quad (2-9a)$$

$$t_{3,4} = \frac{z}{p} . \quad (2-9b)$$

Equation (2-9b) is nothing else than $\tan\varphi$, where φ is the spherical latitude.

Equation (2-8) shows, that

$$t = t(p,z) \quad (2-10)$$

which is the basic function, we need. In order to compute the partial derivatives of t with respect to (x,y,z) it is not necessary to find the explicit form of t (2-10) by solving (2-8), because (2-8) can be used directly for this purpose by implicit differentiation.

2.2 Basic expression of h

Considering (2-6a) we find for the ellipsoidal height h

$$h = \frac{p}{\cos B} - \frac{c}{V} . \quad (2-11)$$

Using again (2-7b) and α^2 (2-8a) the final expression of h is to be

$$h = p \cdot (1+t^2)^{1/2} - c \left(\frac{1+t^2}{\alpha^2+t^2} \right)^{1/2} \quad (2-12)$$

because $t = t(p,z)$ (2-10) and $p = p(x,y)$ (2-5), equation (2-12) is in principle a function of (x,y,z)

2.3 Basic expression of L

As already mentioned in the introduction the problem of determination of L is simplified, when using a rotational ellipsoid of reference.

Considering the quotient $y:x$ from (2-1) one finds for ΔL

$$\Delta L = L - L_0 = \arctan \frac{y+\Delta y}{x+\Delta x} - \arctan \frac{y}{x} . \quad (2-13)$$

Because of the simple structure of (2-13) the latitude L is left out of consideration from now on.

3. SERIES EXPANSIONS

In this chapter the Taylor series expansions of t and h as functions of baseline components $(\Delta x, \Delta y, \Delta z)$ are presented, including third order terms.

3.1 Series expansion of $t = \tan B$

Considering only third order terms the series of t is of the following form

$$t = t_0 + t_1 + t_2 + t_3 + O_4 \quad (3-1)$$

with

$$t_0 = \tan B_0 \quad (3-2a)$$

$$t_1 = t_x \Delta x + t_y \Delta y + t_z \Delta z \quad (3-2b)$$

$$\begin{aligned} t_2 = & \frac{1}{2} t_{xx} \Delta x^2 + t_{xy} \Delta x \Delta y + \frac{1}{2} t_{yy} \Delta y^2 \\ & + t_{xz} \Delta x \Delta z + t_{yz} \Delta y \Delta z + \frac{1}{2} t_{zz} \Delta z^2 \end{aligned} \quad (3-2c)$$

$$\begin{aligned} t_3 = & \frac{1}{6} t_{xxx} \Delta x^3 + \frac{1}{2} t_{xxy} \Delta x^2 \Delta y + \frac{1}{2} t_{xyy} \Delta x \Delta y^2 \\ & + \frac{1}{6} t_{yyy} \Delta y^3 + \frac{1}{2} t_{xxz} \Delta x^2 \Delta z + t_{xyz} \Delta x \Delta y \Delta z \\ & + \frac{1}{2} t_{yyz} \Delta y^2 \Delta z + \frac{1}{2} t_{xzz} \Delta x \Delta z^2 + \frac{1}{2} t_{yzz} \Delta y \Delta z^2 \\ & + \frac{1}{6} t_{zzz} \Delta z^3 \end{aligned} \quad (3-2d)$$

3.1.1 Transformation of partial derivatives

Because $t = t(p, z)$ (2-10) and $p = (x^2 + y^2)^{1/2}$ (2-5) it is reasonable to differentiate t first with respect to p and afterwards p with respect to (x, y) by applying the chain rule of differentiation.

Thus, we are concerned with the following differential transformations

1st order derivatives

$$t_x = t_p p_x \quad (3-3a)$$

$$t_y = t_p p_y \quad (3-3b)$$

$$t_z = t_z \quad (3-3c)$$

2nd order derivatives

$$t_{xx} = t_{pp} p_x^2 + t_p p_{xx} \quad (3-3d)$$

$$t_{xy} = t_{pp} p_x p_y + t_p p_{xy} \quad (3-3e)$$

$$t_{yy} = t_{pp} p_y^2 + t_p p_{yy} \quad (3-3f)$$

$$t_{xz} = t_{pz} p_x \quad (3-3g)$$

$$t_{yz} = t_{pz} p_y \quad (3-3h)$$

$$t_{zz} = t_{zz} \quad (3-3i)$$

3rd order derivatives

$$t_{xxx} = t_{ppp} p_x^3 + 3t_{pp} p_x p_{xx} + t_p p_{xxx} \quad (3-3j)$$

$$t_{xxy} = t_{ppp} p_y p_x^2 + t_{pp} (2p_x p_{xy} + p_y p_{xx}) + t_p p_{xxy} \quad (3-3k)$$

$$t_{xyy} = t_{ppp} p_x p_y^2 + t_{pp} (2p_y p_{xy} + p_x p_{yy}) + t_p p_{xyy} \quad (3-3l)$$

$$t_{yyy} = t_{ppp} p_y^3 + 3t_{pp} p_y p_{yy} + t_p p_{yyy} \quad (3-3m)$$

$$t_{xxz} = t_{ppz} p_x^2 + t_{pz} p_{xx} \quad (3-3n)$$

$$t_{xyz} = t_{ppz} p_x p_y + t_{pz} p_{xy} \quad (3-3o)$$

$$t_{yyz} = t_{ppz} p_y^2 + t_{pz} p_{yy} \quad (3-3p)$$

$$t_{xzz} = t_{pzz} p_x \quad (3-3q)$$

$$t_{yzz} = t_{pzz} p_y \quad (3-3r)$$

$$t_{zzz} = t_{zzz} \quad (3-3s)$$

3.1.2 Partial derivatives of t with respect to p and z

As mentioned already before the partial derivatives of t with respect to (p, z) may be obtained by implicit differentiation of (2-8). Therefore we define the following auxiliary function

$$\Phi\{p, z, t(p, z)\} = (\alpha^2 + t^2)(pt - z)^2 - \beta^2 t^2 = 0 \quad (3-4)$$

With (3-4) we find for the partial derivatives of t

1st order derivatives

$$t_p = - \frac{\Phi_p}{\Phi_t} \quad (3-5a)$$

$$t_z = - \frac{\Phi_z}{\Phi_t} \quad (3-5b)$$

2nd order derivatives

$$t_{pp} = -(\phi_{pp} + 2\phi_{pt}t_p + \phi_{tt}t_p^2) : \phi_t \quad (3-5c)$$

$$t_{pz} = -(\phi_{pz} + \phi_{pt}t_z + \phi_{tt}t_p t_z + \phi_{tz}t_p) : \phi_t \quad (3-5d)$$

$$t_{zz} = -(\phi_{zz} + 2\phi_{tz}t_z + \phi_{tt}t_z^2) : \phi_t \quad (3-5e)$$

3rd order derivatives

$$t_{ppp} = -(\phi_{ppp} + 3\phi_{ppt}t_p + 3\phi_{ptt}t_p^2 + 3\phi_{pt}t_{pp} + \phi_{ttt}t_p^3 + 3\phi_{tt}t_p t_{pp}) : \phi_t \quad (3-5f)$$

$$t_{ppz} = -(\phi_{ppz} + \phi_{ppt}t_z + 2\phi_{ptz}t_p + 2\phi_{ptt}t_p t_z + \phi_{ttz}t_p^2 + \phi_{ttt}t_z t_p^2 + 2\phi_{pt}t_{pz} + \phi_{tt}(2t_p t_{pz} + t_z t_{pp}) + \phi_{tz}t_{pp}) : \phi_t \quad (3-5g)$$

$$t_{pzz} = -(\phi_{zpp} + \phi_{zzt}t_p + 2\phi_{ptz}t_z + 2\phi_{ztt}t_p t_z + 2\phi_{tz}t_{pz} + \phi_{ttt}t_z^2 + \phi_{ttt}t_p t_z^2 + \phi_{tt}(2t_z t_{pz} + t_p t_{zz}) + \phi_{pt}t_{zz}) : \phi_t \quad (3-5h)$$

$$t_{zzz} = -(\phi_{zzz} + 3\phi_{zzt}t_z + 3\phi_{ttz}t_z^2 + 3\phi_{tz}t_{zz} + \phi_{ttt}t_z^3 + 3\phi_{tt}t_z t_{zz}) : \phi_t \quad (3-5i)$$

In order to evaluate the expressions (3-5) the explicit partial derivatives of ϕ with respect to (p, t, z) are necessary.

By differentiation of (3-4) we find

$$\phi_p = 2t(p t - z)(\alpha^2 + t^2) \quad (3-6a)$$

$$\phi_t = -2\{\beta^2 t - p(p t - z)(\alpha^2 + t^2) - t(p t - z)^2\} \quad (3-6b)$$

$$\phi_z = -2(p t - z)(\alpha^2 + t^2) \quad (3-6c)$$

$$\phi_{pp} = 2t^2(\alpha^2 + t^2) \quad (3-6d)$$

$$\phi_{pt} = 2(2\alpha^2 p t - \alpha^2 z + 4p t^3 - 3t^2 z) \quad (3-6e)$$

$$\phi_{pz} = -2t(\alpha^2 + t^2) \quad (3-6f)$$

$$\phi_{tt} = 2(\alpha^2 p^2 - \beta^2 + 6p^2 t^2 - 6p t z + z^2) \quad (3-6g)$$

$$\phi_{tz} = -2\{p(\alpha^2 + t^2) + 2t(p t - z)\} \quad (3-6h)$$

$$\phi_{zz} = 2(\alpha^2 + t^2) \quad (3-6i)$$

$$\phi_{ppp} = 0 \quad (3-6j)$$

$$\phi_{ppz} = 0 \quad (3-6k)$$

$$\phi_{ppt} = 4t(\alpha^2 + 2t^2) \quad (3-6l)$$

$$\phi_{ptz} = -2(\alpha^2 + 3t^2) \quad (3-6m)$$

$$\phi_{zzp} = 0 \quad (3-6n)$$

$$\phi_{zzt} = 4t \quad (3-6o)$$

$$\phi_{zzz} = 0 \quad (3-6p)$$

$$\phi_{ttp} = 4(\alpha^2 p + 6pt^2 - 3tz) \quad (3-6q)$$

$$\phi_{ttz} = -4(3pt - z) \quad (3-6r)$$

$$\phi_{ttt} = 12p(2pt - z) \quad (3-6s)$$

3.2 Series expansion of h

Considering only 3rd order terms the series of h is of the following form

$$h = h_0 + h_1 + h_2 + h_3 + O_4 \quad (3-7)$$

with

h_0 height in the Taylor point

$$h_1 = h_x \Delta x + h_y \Delta y + h_z \Delta z \quad (3-8a)$$

$$\begin{aligned} h_2 = & \frac{1}{2} h_{xx} \Delta x^2 + h_{xy} \Delta x \Delta y + \frac{1}{2} h_{yy} \Delta y^2 \\ & + h_{xz} \Delta x \Delta z + h_{yz} \Delta y \Delta z + \frac{1}{2} h_{zz} \Delta z^2 \end{aligned} \quad (3-8b)$$

$$\begin{aligned} h_3 = & \frac{1}{6} h_{xxx} \Delta x^3 + \frac{1}{2} h_{xxy} \Delta x^2 \Delta y + \frac{1}{2} h_{xyy} \Delta x \Delta y^2 \\ & + \frac{1}{6} h_{yyy} \Delta y^3 + \frac{1}{2} h_{xxz} \Delta x^2 \Delta z + h_{xyz} \Delta x \Delta y \Delta z \\ & + \frac{1}{2} h_{yyz} \Delta y^2 \Delta z + \frac{1}{2} h_{xzz} \Delta x \Delta z^2 + \frac{1}{2} h_{yzz} \Delta y \Delta z^2 \\ & + \frac{1}{6} h_{zzz} \Delta z^3 \end{aligned} \quad (3-8c)$$

3.2.1 Transformation of partial derivatives

Because of (2-12) $h = h(p,t)$, (2-10) $t = t(p,z)$ and (2-5) $p = p(x,y)$ it is reasonable to differentiate h first with respect to p and z , and second to transform the so obtained partial derivatives in those with respect to (x,y,z) . The following transformation expressions are quite analogous to the expressions (3-3a to s).

1st order derivatives

$$h_x = h_p p_x \quad (3-9a)$$

$$h_y = h_p p_y \quad (3-9b)$$

$$h_z = h_z \quad (3-9c)$$

2nd order derivatives

$$h_{xx} = h_{pp} p_x^2 + h_p p_{xx} \quad (3-9d)$$

$$h_{xy} = h_{pp} p_x p_y + h_p p_{xy} \quad (3-9e)$$

$$h_{yy} = h_{pp} p_y^2 + h_p p_{yy} \quad (3-9f)$$

$$h_{xz} = h_{pz} p_x \quad (3-9g)$$

$$h_{yz} = h_{pz} p_y \quad (3-9h)$$

$$h_{zz} = h_{zz} \quad (3-9i)$$

3rd order derivatives

$$h_{xxx} = h_{ppp} p_x^3 + 3h_{pp} p_x p_{xx} + h_p p_{xxx} \quad (3-9j)$$

$$h_{xxy} = h_{ppp} p_y p_x^2 + h_{pp} (2p_x p_{xy} + p_y p_{xx}) + h_p p_{xxy} \quad (3-9k)$$

$$h_{xyy} = h_{ppp} p_x p_y^2 + h_{pp} (2p_y p_{xy} + p_x p_{yy}) + h_p p_{xyy} \quad (3-9l)$$

$$h_{yyy} = h_{ppp} p_y^3 + 3h_{pp} p_y p_{yy} + h_p p_{yyy} \quad (3-9m)$$

$$h_{xxz} = h_{ppz} p_x^2 + h_{pz} p_{xx} \quad (3-9n)$$

$$h_{xyz} = h_{ppz} p_x p_y + h_{pz} p_{xy} \quad (3-9o)$$

$$h_{yyz} = h_{ppz} p_y^2 + h_{pz} p_{yy} \quad (3-9p)$$

$$h_{xzz} = h_{pzz} p_x \quad (3-9q)$$

$$h_{yzz} = h_{pzz} p_y \quad (3-9r)$$

$$h_{zzz} = h_{zzz} \quad (3-9s)$$

3.2.2 Partial derivatives of h with respect to p and z

In order to compute the partial derivatives of h with respect to p and z a second auxiliary function Θ is defined.

$$h = \Theta\{p, t(p, z)\} = p(1+t^2)^{1/2} - c\left(\frac{1+t^2}{\alpha^2+t^2}\right)^{1/2} \quad (3-10)$$

With the aid of Θ the partial derivatives of h are of the following form. Note, that Θ does not explicitly depend on z

1st order derivatives

$$h_p = \Theta_p + \Theta_t t_p \quad (3-11a)$$

$$h_z = \Theta_t t_z \quad (3-11b)$$

2nd order derivatives

$$h_{pp} = \Theta_{pp} + 2\Theta_{pt}t_p + \Theta_{tt}t_p^2 + \Theta_t t_{pp} \quad (3-11c)$$

$$h_{pz} = \Theta_{pt}t_z + \Theta_{tt}t_p t_z + \Theta_t t_{pz} \quad (3-11d)$$

$$h_{zz} = \Theta_{tt}t_z^2 + \Theta_t t_{zz} \quad (3-11e)$$

3rd order derivatives

$$h_{ppp} = \Theta_{ppp} + 3\Theta_{ppt}t_p + 3\Theta_{ptt}t_p^2 + \Theta_{ttt}t_p^3 + 3\Theta_{pt}t_{pp} + 3\Theta_{tt}t_p t_{pp} + \Theta_t t_{ppp} \quad (3-11f)$$

$$h_{ppz} = \Theta_{ppt}t_z + 2\Theta_{ptt}t_p t_z + \Theta_{ttt}t_z t_p^2 + 2\Theta_{pt}t_{pz} + \Theta_{tt}(2t_p t_{pz} + t_z t_{pp}) + \Theta_t t_{ppz} \quad (3-11g)$$

$$h_{pzz} = \Theta_{ptt}t_z^2 + \Theta_{ttt}t_p t_z^2 + \Theta_{tt}(2t_z t_{pz} + t_p t_{zz}) + \Theta_{pt}t_{zz} + \Theta_t t_{pzz} \quad (3-11h)$$

$$h_{zzz} = \Theta_{ttt}t_z^3 + 3\Theta_{tt}t_z t_{zz} + \Theta_t t_{zzz} \quad (3-11i)$$

The partial derivatives of t with respect to p and z are already given in (3-5). In order to evaluate the expressions (3-11) the partial derivatives of Θ have to be additionally known. With the definition (3-10) of Θ , we find the following formulas.

$$\Theta_p = (1+t^2)^{1/2} \quad (3-12a)$$

$$\Theta_t = \frac{t\left\{p(\alpha^2+t^2)^{3/2} + c(1-\alpha^2)\right\}}{(1+t^2)^{1/2}(\alpha^2+t^2)^{3/2}} \quad (3-12b)$$

$$\Theta_{pp} = 0 \quad (3-12c)$$

$$\Theta_{pt} = \frac{t}{(1+t^2)^{1/2}} \quad (3-12d)$$

$$\Theta_{tt} = \frac{p(\alpha^2+t^2)^{5/2} - c(1-\alpha^2)(3t^4+2t^2-\alpha^2)}{(1+t^2)^{3/2}(\alpha^2+t^2)^{5/2}} \quad (3-12e)$$

$$\Theta_{ppp} = 0 \quad (3-12f)$$

$$\Theta_{ppt} = 0 \quad (3-12g)$$

$$\Theta_{ptt} = \frac{1}{(1+t^2)^{3/2}} \quad (3-12h)$$

$$\Theta_{ttt} = -\frac{t}{(1+t^2)^{5/2}(\alpha^2+t^2)^{7/5}} \left\{ (1+t^2)(\alpha^2+t^2) \left[4c(1-\alpha^2)(1-3t^2) - 5p(\alpha^2+t^2)^{3/2} \right] + (8t^2+3\alpha^2+5) \left[c(1-\alpha^2)(\alpha^2-3t^4-2t^2) + p(\alpha^2+t^2)^{5/2} \right] \right\} \quad (3-12i)$$

3.3 Partial derivatives of p with respect to x and y

In order to evaluate the transformation relations (3-3) and (3-9), finally the partial derivatives of p (2-5) with respect to x and y are given.

1st order derivatives

$$p_x = \frac{x}{p} \quad (3-13a)$$

$$p_y = \frac{y}{p} \quad (3-13b)$$

2nd order derivatives

$$p_{xx} = \frac{y^2}{p^3} \quad (3-13c)$$

$$p_{xy} = -\frac{xy}{p^3} \quad (3-13d)$$

$$p_{yy} = \frac{x^2}{p^3} \quad (3-13e)$$

3rd order derivatives

$$p_{xxx} = -\frac{3xy^2}{p^5} \quad (3-13f)$$

$$p_{xxy} = \frac{y(2x^2 - y^2)}{p^5} \quad (3-13g)$$

$$p_{xyy} = -\frac{x(x^2 - 2y^2)}{p^5} \quad (3-13h)$$

$$p_{yyy} = -\frac{3x^2y}{p^5} \quad (3-13i)$$

4. NUMERICAL INVESTIGATIONS

In the following two basic problems concerning the series expansions of t (3-1) and h (3-7) are discussed numerically:

- (i) approximation errors of the complete third order expansions
- (ii) magnitude of the third order terms

The problems (i) and (ii) are discussed at a Taylor point (left baseline point) with

$$\begin{aligned} B_0 &= 50^\circ 00' 00'' .00 \\ L_0 &= 8^\circ 00' 00'' .00 \\ h_0 &= 500 \text{ m} \end{aligned} \quad (4-1)$$

4.1 Approximation error of series expansions

In principle it is possible to find analytic expressions for higher-order neglect terms in Taylor expansions. In order to do this, the fourth order derivatives of t and h with respect to (x,y,z) are required. A numerical study is preferred here, in order to avoid the computation of the higher order (>3) partial derivatives. Obviously the O_4 -terms, which are the approximation errors in (3-1) and (3-7), are a function of baseline length b . For this reason the approximation errors are analysed with respect to b .

$$b = (\Delta x^2 + \Delta y^2 + \Delta z^2)^{1/2} \quad (4-2)$$

The accuracy of the third order expansions of h and t was investigated in two steps:

- (i) a set of baseline components $(\Delta x_i, \Delta y_i, \Delta z_i)$ was generated by use of eq. (2-1) vice

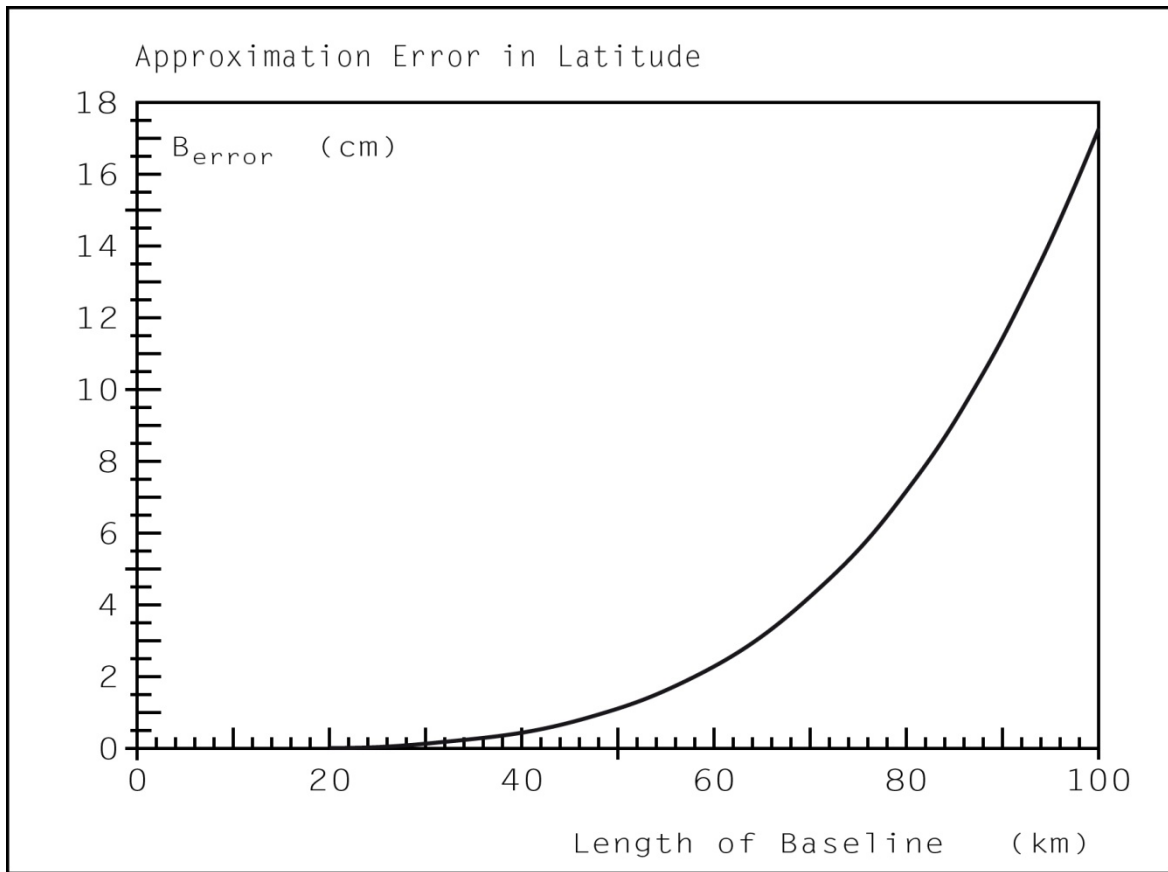


Figure 1 Approximation Error in Latitude

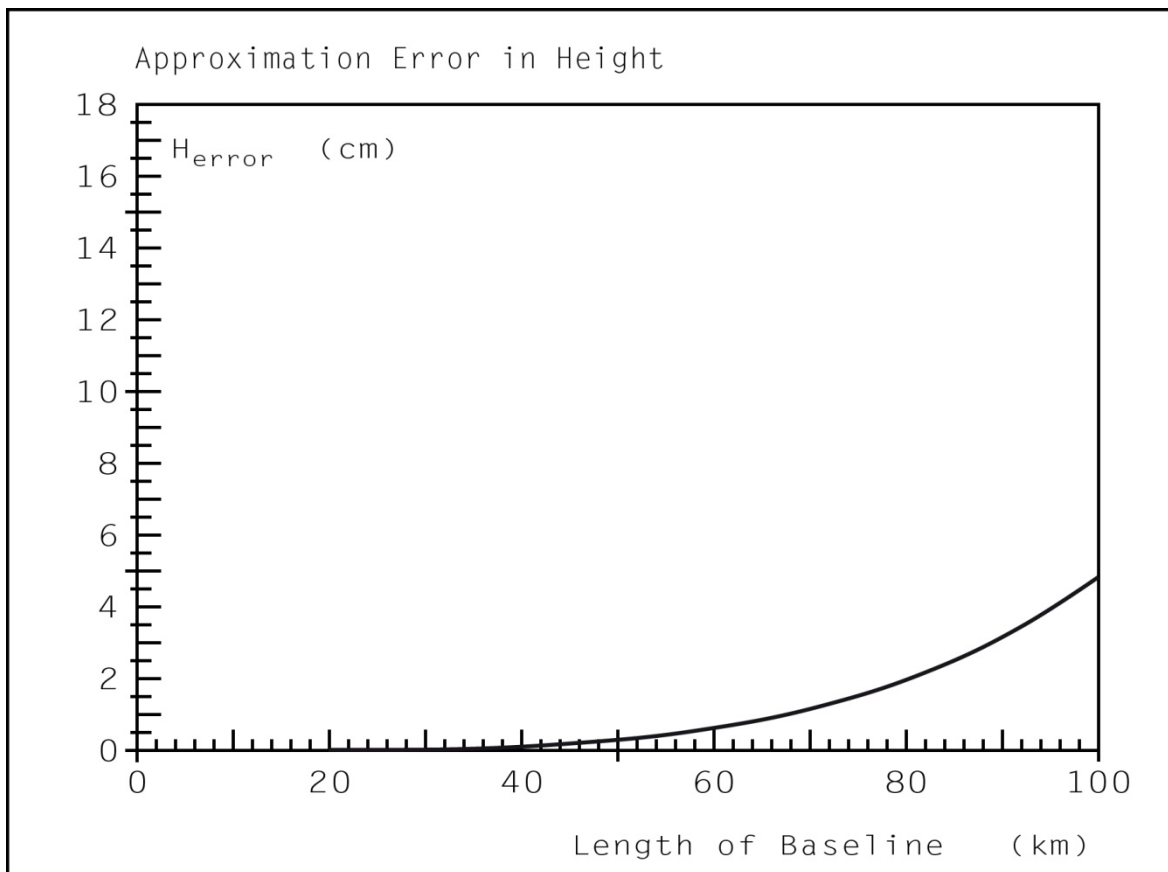


Figure 2 Approximation Error in Height

$$\begin{bmatrix} \Delta x_i \\ \Delta y_i \\ \Delta z_i \end{bmatrix} = \begin{bmatrix} (N(B_i) + h_i) \cos B_i \cos L_i - (N(B_0) + h_0) \cos B_0 \cos L_0 \\ (N(B_i) + h_i) \cos B_i \sin L_i - (N(B_0) + h_0) \cos B_0 \sin L_0 \\ \left(\frac{b^2}{a^2} N(B_i) + h_i\right) \sin B_i - \left(\frac{b^2}{a^2} N(B_0) + h_0\right) \sin B_0 \end{bmatrix} \quad (4-3)$$

with

$$B_i = B_0 + i' \frac{\pi}{180 \cdot 60'}$$

$$L_i = L_0 + i' \frac{\pi}{180 \cdot 60'} \quad (4-4)$$

$$h_i = h_0 + 500.00 \text{ m} = \text{const.}$$

Based on (4-4) the latitude B_i and the longitude L_i are computed with 1' increments ($\cong 2.2$ km) from 1' to 50' or 2.2 km up to 110.0 km.

(ii) The series expansions (3-1) and (3-7) for t and h were programmed in FORTRAN.

With the generated baseline components (4-3) the series expansions were evaluated based on (ii). The so computed values (\hat{B}_i, \hat{h}_i) are compared with the true values (B_i, h_i) (4-4) which have been previously used to compute the baseline components (4-3) as input for (ii). The results of this comparison, $B(\text{error}) = B_i - \hat{B}_i$ and $h(\text{error}) = h_i - \hat{h}_i$ as a function of baseline length b are presented in figures 1 and 2.

It can be seen, that the approximation errors increase exponentially with b . If we allow an approximation error of 1 cm as upper limit for geodetic applications the Taylor expansions (3-1) and (3-7) are sufficiently accurate up to 50 km in latitude and 80 km in height.

4.2 Magnitude of third order terms

Because the third order terms t_3 (3-2d) and h_3 (3-8c) have a rather complicated structure in comparison to the first and second order terms, we have to ask the question, if these terms may be neglected up to a fixed baseline length b .

The following tables 1 and 2 show the magnitudes of t_3 and h_3 as a function of b . The baseline components used for the computation of t_3 and h_3 are again computed with the aid of (4-3) and (4-4) in 2' increments ($\cong 4.4$ km).

We learn from table 1 and 2, that it is possible to neglect h with an approximation error of 2 cm for baseline length up to 110.0 km.

For precise computations in latitude the t_3 -term has to be considered even for short baselines.

b [km]	t ₃ [m]	b [km]	h ₃ [m]
4.4	0.000	4.4	0.000
8.8	0.003	8.8	0.000
13.2	0.013	13.2	0.001
17.6	0.034	17.6	0.002
22.1	0.070	22.1	0.003
26.5	0.125	26.5	0.004
30.9	0.205	30.9	0.006
35.3	0.313	35.3	0.008
39.7	0.455	39.7	0.009
44.1	0.634	44.1	0.011
48.5	0.857	48.5	0.013
52.9	1.129	52.9	0.015
57.3	1.454	57.3	0.016
61.7	1.838	61.7	0.017
66.1	2.287	66.1	0.018
70.5	2.806	70.5	0.019
74.9	3.401	74.9	0.019
79.3	4.077	79.3	0.018
83.7	4.842	83.7	0.016
88.0	5.701	88.0	0.013
92.4	6.660	92.4	0.009
96.8	7.726	96.8	0.004
101.2	8.905	101.2	0.003
105.6	10.205	105.6	0.011
110.0	11.631	110.0	0.021

Table 1 Magnitude of t₃

Table 2 Magnitude of h₃

5. PRACTICAL APPLICATIONS

The solution presented has a rather complicated structure in comparison to the iterative procedures discussed in BARTELME and MEISSEL (1975), HEISKANEN and MORITZ (1967) and SCHÖDLBAUER (1984).

Therefore the critical reader might ask the question: What is the practical use of these series expansions?

To answer this question beforehand, one has to consider the following facts:

- (i) The coefficients in the series (3-1) and (3-7) depend only on the Taylor point or on one baseline point (reference station). If these coefficients are once evaluated, every arbitrary set of baseline components ($\Delta x, \Delta y, \Delta z$) can be transformed by a simple third order polynomial in geodetic coordinates.
- (ii) The iterative procedures mentioned above and in the introduction require for every GPS station (B, L, h) the evaluation of many trigonometric (inversion of (2-1)) functions which is computer time consuming.

Whereas in the series expansion proposed, only trigonometric

functions in the reference station (B_0, L_0, h_0) are needed.

Considering (i) and (ii) we have to state, that the iterative solutions are of course favourable, if we have only to transform a few baseline vectors with respect to one reference station.

But e.g. in moving baseline applications, where we work with one fixed master station and with one moving GPS receiver, perhaps hundreds or thousands of different baseline vectors referring all to the same reference station are to be transformed.

In this application field the method discussed in this paper would be superior to the iterative solutions because of (i) and (ii).

Concerning moving baseline applications we have also to think of GPS aided inertial navigation systems (INS). In order to update the INS online by baseline vectors one consistent geodetic coordinate system is required. The transformation of baseline vectors to geodetic coordinates can be computed very fast by the polynomial approximations (3-1) and (3-7) with constant coefficients. Thus, an operational approach would be:

- (a) Compute all the coefficients in (3-1) and (3-7) for the master station premission.
- (b) Solve the online transformation problem of baseline vectors and the polynomials (3-1) and (3-7) on the navigation computer.

For (b) we have to notice, that polynomials may be evaluated numerically very advanced by use of the Horner scheme.

The Horner decomposition of a third order polynomial f in $(\Delta x, \Delta y, \Delta z)$ like (3-1) or (3-7) is e.g. of the following form.

$$\begin{aligned}
 f(\Delta x, \Delta y, \Delta z) = & \alpha_{000} \\
 & + \Delta x \{ \alpha_{100} + \alpha_{120} \Delta y + \Delta z (\alpha_{130} + \alpha_{123} \Delta y) \\
 & \quad + \Delta x (\alpha_{110} + \alpha_{111} \Delta x + \alpha_{112} \Delta y + \alpha_{113} \Delta z) \} \\
 & + \Delta y \{ \alpha_{200} + \alpha_{230} \Delta z + \Delta y (\alpha_{220} + \alpha_{122} \Delta x + \alpha_{222} \Delta y + \alpha_{223} \Delta z) \} \\
 & + \Delta z \{ \alpha_{300} + \Delta z (\alpha_{330} + \alpha_{133} \Delta x + \alpha_{233} \Delta y + \alpha_{333} \Delta z) \}
 \end{aligned} \tag{5-1}$$

with

α_{ijk} coefficients associated with the partial derivatives

$$\frac{\partial^{i+k+j} f}{\partial x^i \partial y^k \partial z^j}$$

REFERENCES

- BARTELME, N., MEISSL, P. (1975): *Ein einfaches, rasches und numerisch stabiles Verfahren zur Bestimmung des kürzesten Abstandes eines Punktes von einem sphäroidischen Rotationsellipsoid*. Allgemeine Vermessungsnachrichten, Heft 12, p. 436-439. Wichmann-Verlag, Karlsruhe.
- BENNING, W. (1974): *Der kürzeste Abstand eines in rechtwinkligen Koordinaten gegebenen Außenpunktes vom Ellipsoid*. Allgemeine Vermessungsnachrichten, Heft 11, p. 429-433, Wichmann-Verlag, Karlsruhe.
- EISSFELLER, B. (1985): *The estimation of orthometric heights from GPS baseline vectors using gravity field information and least-squares collocation*. In: GPS Research at the Institute of Astronomical and Physical Geodesy, Report No. 19, University FAF Munich.
- ENGELIS, T., TSCHERNING, C.C., RAPP, R.H. (1984): *The precise computation of geoid undulation differences with comparison to results obtained from GPS*. Geophysical Research Letters 11-9, p. 821-824.
- GROSSMANN, W. (1976): *Geodätische Rechnungen und Abbildungen in der Landesvermessung*. Verlag Konrad Wittwer, Stuttgart.
- HEIN, G. (1985): *Orthometric height determination using GPS observations and the integrated geodesy adjustment model*. NOAA Technical Report NOS 110 NGS 32, U.S. Department of Commerce, National Oceanic and Atmospheric Administration, Rockville, Md.
- HEISKANEN, W.A., MORITZ, H. (1967): *Physical Geodesy*. W.H. Freeman & Co., San Francisco and London, Library of Congress Catalogue Card Number: 66-24950.
- HEITZ, S. (1985): *Koordinaten auf geodätischen Bezugsflächen*. Ferd. Dümmler Verlag, Bonn. ISBN 3-427-78981-0.
- SCHÖDLBAUER, A. (1984): *Bezugssysteme der Landesvermessung unter Berücksichtigung terrestrischer und satelliten-geodätischer Meß- und Auswerteverfahren*. In: Schödlbauer, A. and W. Welsch (Eds.): Satelliten-Doppler-Messungen, Heft 15 der Schriftenreihe des Wissenschaftlichen Studiengangs der Universität der Bundeswehr München, p. 63-153.
- SCHÖDLBAUER, A. (1985): *Local reference systems in geodetic survey under consideration of terrestrial and satellite positioning methods*. Proceedings of First International Symposium on Precise Positioning with the Global Positioning System. Rockville, Md., April 15-19, 1985, p. 713-721.

OPTIMIZATION OF GPS SATELLITE SELECTION FOR HIGH PRECISION DIFFERENTIAL POSITIONING

H. Landau, B. Eissfeller
University FAF Munich
Institute of Astronomical and Physical Geodesy
Werner-Heisenberg-Weg 39
8014 Neubiberg
Federal Republic of Germany

ABSTRACT. When reaching the full operational capability of the NAVSTAR/GPS system with 18 satellites in 6 orbital planes an optimal selection of satellites becomes more and more of importance. GPS then provides 4 to 8 visible satellites above the horizon to any user in the world at any time, however, most of the receivers are able to track only four satellites. Therefore it will be necessary to select 4 satellites at any time of the tracking interval. This selection has a great influence on accuracy of the processing results and is usually based on the so-called geometric dilution of precision (GDOP). Up to now selection algorithms are implemented in the receivers, which try to approximate the smallest GDOP with smallest computational requirements.

Since geodesists are interested in the highest possible accuracy, the applied selection method should be based on the special geodetic observation and computation techniques using phase differences, which have a quite different error behaviour than pseudo-range measurements. The paper discusses an optimum selection method for different observation types and visibility. Various error sources like atmospheric propagation delays and ephemeris errors are considered in the discussion.

1. INTRODUCTION

The NAVSTAR/GPS satellite system was primarily designed for military and civil navigation applications using the pseudo-ranging technique. Geodesists make use of the system for high-precise differential positioning using instantaneous carrier phase difference measurements. In contrast to the users of the navigation mode of NAVSTAR, the group of geodetic users is very small. Therefore the development of GPS receivers by firms is primarily directed toward the requirements of online navigation processing and not to geodetic postprocessing. According to the authors information the only pure geodetic receivers are the models Macrometer V-1000 and Macrometer II, which are codeless receivers. This means, that they are not able to process pseudo-ranges.

In the late 1980s 4 to 8 satellites will be visible above the horizon as soon as GPS a reaching the full 18-satellite configuration. Most of the

receivers are able to track up to 4 satellites only. Therefore the question of an optimum selection arises.

The satellite selection method in GPS receivers is based on the geometric configuration of satellites which is very well represented by the so-called geometric dilution of precision (GDOP). Selection algorithms were developed which allow a good and fast fitting to the smallest obtainable GDOP (KIHARA and OKADA, 1984).

In the following we want to discuss

- the influence of a more physical orientated model on satellite selection, describing the optimal satellite configuration and taking atmospheric models into account,
- the different error behaviour of the different observation types, like pseudo-ranging, single, double and triple differences,
- the influence of different error sources on geodetic positioning,
- the optimal observation time for different observation types.

Other authors have already treated the optimization of GPS observations and networks. VANÍČEK et al. (1984) have analysed the geometrical properties of different observation types. The publication of GRAFAREND et al. (1985) deals with the second order design of the Global Positioning Systems.

2. A SHORT DESCRIPTION OF PSEUDO-RANGING AND THE GEOMETRIC DILUTION OF PRECISION

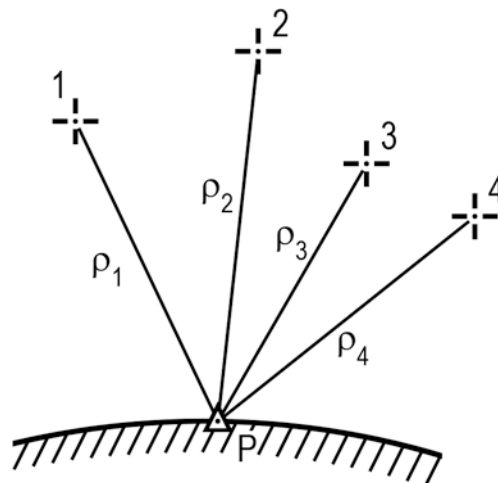


Fig. 1: Pseudo-ranging constellation

By use of pseudo-range measurements to 4 satellites we are able to determine the position of P in three dimensions and an unknown receiver clock offset

$$\rho_i = c(\tau_i + \tau_0) = \sqrt{(x_p - x_i)^2 + (y_p - y_i)^2 + (z_p - z_i)^2} \quad (2-1)$$

with $i = 1, 2, 3, 4$

where

ρ_i ... is the distance from the receiver point P to the satellite i

τ_i ... is the transmission time of the satellite signal from satellite i to receiver P

τ_0 ... is the unknown receiver clock offset

Differentiating with respect to x_p , y_p , z_p and τ_0 we get the following design matrix

$$\underline{B} = \begin{bmatrix} -\frac{x_p - x_1}{\rho_1} & -\frac{y_p - y_1}{\rho_1} & -\frac{z_p - z_1}{\rho_1} & -1 \\ \vdots & \vdots & \vdots & \vdots \\ -\frac{x_p - x_4}{\rho_4} & -\frac{y_p - y_4}{\rho_4} & -\frac{z_p - z_4}{\rho_4} & -1 \end{bmatrix} \quad (2-2)$$

The matrix $(\underline{B}^T \underline{B})^{-1}$ then represents the covariance matrix of the errors determining the users position. The geometric dilution of precision is defined as the square-root of the trace of this matrix.

$$\text{GDOP} = \left(\text{tr} \left((\underline{B}^T \underline{B})^{-1} \right) \right)^{1/2} = (\sigma_{11}^2 + \sigma_{22}^2 + \sigma_{33}^2 + \sigma_{44}^2)^{1/2} \quad (2-3)$$

The radial component (position dilution of precision) is defined by

$$\text{PDOP} = (\sigma_{11}^2 + \sigma_{22}^2 + \sigma_{33}^2)^{1/2} \quad (2-4)$$

The time dilution of precision is

$$\text{TDOP} = (\sigma_{44}^2)^{1/2} \quad (2-5)$$

3. PHASE DIFFERENCE OBSERVATIONS

In the following we want to discuss the modelling of the phase difference observations as considered in our numerical investigations, which will be described later. Carrier phase measurements are much more precise than pseudo-ranges. In the following we will assume, that the phase can be measured with an accuracy of 1 degree (STANSELL et al., 1985). That corresponds to a range error of 0.5 mm. The precision of the measurements is limited by an insufficient knowledge of the satellite orbit, atmospheric propagation delays and the clock uncertainty. Accuracies of 1 ppm are already achieved in practice.

3.1 Single differences

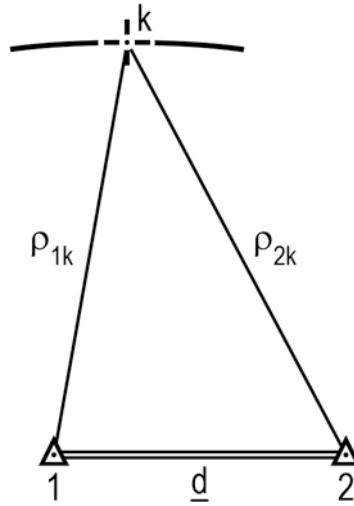


Fig. 2: Single difference constellation

Consider the baseline \underline{d} between the points 1 and 2. Carrier phase differences are measured in both end points and the differences of these carrier phases are known as "single differences".

The single phase difference is given by REMONDI (1984), HEIN and EISSFELLER (1985).

$$\begin{aligned} \psi_S = & \frac{2\pi}{\lambda} \{ \rho_{2k}(t) - \rho_{1k}(t) \} + 2\pi (m_2 - m_1) + 2\pi (v_{R_2} - v_{R_1}) t + \\ & + \psi_\varepsilon(t) + \psi_a(t) \end{aligned} \quad (3-1)$$

with

$$\begin{aligned} \psi_\varepsilon(t) = & \frac{2\pi}{\lambda} \{ \dot{\rho}_{2k}(t) \varepsilon_2 - \dot{\rho}_{1k}(t) \varepsilon_1 \} + \\ & + 2\pi v_S \{ \varepsilon_2 - \varepsilon_1 \} + \\ & + 2\pi \{ v_{R_1} \varepsilon_2 - v_{R_2} \varepsilon_1 \} \end{aligned} \quad (3-2)$$

In our simulation computations we will assume, that

$$v_S \doteq v_{R_1} \doteq v_{R_2} = \text{const}$$

$$\varepsilon_1 \doteq \varepsilon_2 = \text{const}$$

and that the ambiguities m_1 and m_2 are known quantities, so that they cannot cause any bias to the observed quantity ψ_S . The first term of ψ_ε in (3-2) is a very small quantity and will therefore be neglected.

$\psi_a(t)$ describes the atmospheric correction term and is given by

$$\psi_a(t) = \frac{2\pi}{\lambda} \cdot \{ \Delta\rho_{2k_I} - \Delta\rho_{1k_I} \} + \frac{2\pi}{\lambda} \cdot \{ \Delta\rho_{2k_T} - \Delta\rho_{1k_T} \} \quad (3-3)$$

where

$\Delta\rho_{ik_I}$... is the ionospheric range correction for point i to satellite k,

and

$\Delta\rho_{ik_T}$... is the tropospheric range correction for point i to satellite k.

Using these considerations and assumptions, equation (3-1) becomes

$$\psi_S = \frac{2\pi}{\lambda} \{ \rho_{2k}(t) - \rho_{1k}(t) \} + 2\pi v \{ \varepsilon_2 - \varepsilon_1 \} + \psi_a(t) \quad (3-4)$$

Differentiating with respect to satellite and receiver positions we obtain

$$\delta\rho_{2k} = \frac{\partial\rho_{2k}}{\partial\underline{x}_k} \delta\underline{x}_k + \frac{\partial\rho_{2k}}{\partial\underline{x}_2} \delta\underline{x}_2 \quad (3-5)$$

$$\delta\rho_{1k} = \frac{\partial\rho_{1k}}{\partial\underline{x}_k} \delta\underline{x}_k + \frac{\partial\rho_{1k}}{\partial\underline{x}_1} \delta\underline{x}_1 \quad (3-6)$$

with the partial derivatives

$$\begin{aligned} \frac{\partial\rho_{2k}}{\partial\underline{x}_k} &= \frac{(\underline{x}_k - \underline{x}_2)^T}{\rho_{2k}} ; & \frac{\partial\rho_{2k}}{\partial\underline{x}_2} &= -\frac{(\underline{x}_k - \underline{x}_2)^T}{\rho_{2k}} \\ \frac{\partial\rho_{1k}}{\partial\underline{x}_k} &= \frac{(\underline{x}_k - \underline{x}_1)^T}{\rho_{1k}} ; & \frac{\partial\rho_{1k}}{\partial\underline{x}_1} &= -\frac{(\underline{x}_k - \underline{x}_1)^T}{\rho_{1k}} \end{aligned} \quad (3-7)$$

Finally we get the linear observation equation of ψ_S

$$\begin{aligned} \delta\psi_S &= \frac{2\pi}{\lambda} \left\{ \frac{(\underline{x}_k - \underline{x}_2)^T}{\rho_{2k}} - \frac{(\underline{x}_k - \underline{x}_1)^T}{\rho_{1k}} \right\} \delta\underline{x}_k + \\ &+ \frac{2\pi}{\lambda} \left\{ \frac{(\underline{x}_k - \underline{x}_1)^T}{\rho_{1k}} \delta\underline{x}_1 + \frac{(\underline{x}_k - \underline{x}_2)^T}{\rho_{2k}} \delta\underline{x}_2 \right\} + \\ &+ 2\pi v \{ \delta\varepsilon_2 - \delta\varepsilon_1 \} + \frac{2\pi}{\lambda} \{ \delta\Delta\rho_{2k_I} - \delta\Delta\rho_{1k_I} \} + \\ &+ \frac{2\pi}{\lambda} \{ \delta\Delta\rho_{2k_T} - \delta\Delta\rho_{1k_T} \} \end{aligned} \quad (3-8)$$

The typical procedure is to fix station 1 and adjust station 2 relative to 1. Any error in the approximate coordinates of station 1 would then be propagated into station 2.

A more advanced solution is to solve for the mean vector \underline{a} and difference vector \underline{d} of the station coordinates (REMONDI, 1984) with

$$\begin{aligned} \underline{a} &= (\underline{x}_1 + \underline{x}_2) / 2 \\ \text{and} \quad \underline{d} &= (\underline{x}_2 - \underline{x}_1) \end{aligned} \tag{3-9}$$

The above partial derivatives must then be replaced by

$$\frac{\partial \underline{x}_2}{\partial \underline{a}} = \frac{\partial \underline{x}_1}{\partial \underline{a}} = 1 \quad \text{and} \quad \frac{\partial \underline{x}_2}{\partial \underline{d}} = \frac{1}{2} \frac{\partial \underline{x}_1}{\partial \underline{d}} = -\frac{1}{2} \tag{3-10}$$

The partial derivatives with respect to \underline{a} and \underline{d} are

$$\begin{aligned} \frac{\partial \psi_s}{\partial \underline{d}} &= \frac{2\pi}{\lambda} \left\{ -\frac{\partial \rho_{1k}}{\partial \underline{x}_1} \frac{\partial \underline{x}_1}{\partial \underline{d}} + \frac{\partial \rho_{2k}}{\partial \underline{x}_2} \frac{\partial \underline{x}_2}{\partial \underline{d}} \right\} \\ &= \frac{\pi}{\lambda} \left\{ \frac{(\underline{x}_k - \underline{x}_1)^T}{\rho_{1k}} + \frac{(\underline{x}_k - \underline{x}_2)^T}{\rho_{2k}} \right\} \end{aligned} \tag{3-11}$$

$$\begin{aligned} \frac{\partial \psi_s}{\partial \underline{a}} &= \frac{2\pi}{\lambda} \left\{ -\frac{\partial \rho_{1k}}{\partial \underline{x}_1} \frac{\partial \underline{x}_1}{\partial \underline{a}} + \frac{\partial \rho_{2k}}{\partial \underline{x}_2} \frac{\partial \underline{x}_2}{\partial \underline{a}} \right\} \\ &= \frac{2\pi}{\lambda} \left\{ -\frac{\partial \rho_{1k}}{\partial \underline{x}_1} + \frac{\partial \rho_{2k}}{\partial \underline{x}_2} \right\} \end{aligned} \tag{3-12}$$

Involving (3-11) and (3-12) in (3-8) results in the following equation:

$$\begin{aligned} \delta \psi_s &= \frac{2\pi}{\lambda} \left\{ \frac{(\underline{x}_k - \underline{x}_1)^T}{\rho_{1k}} - \frac{(\underline{x}_k - \underline{x}_2)^T}{\rho_{2k}} \right\} \delta \underline{a} + \\ &+ \frac{\pi}{\lambda} \left\{ \frac{(\underline{x}_k - \underline{x}_1)^T}{\rho_{1k}} + \frac{(\underline{x}_k - \underline{x}_2)^T}{\rho_{2k}} \right\} \delta \underline{d} + \\ &+ \frac{2\pi}{\lambda} \left\{ \frac{(\underline{x}_k - \underline{x}_2)^T}{\rho_{2k}} - \frac{(\underline{x}_k - \underline{x}_1)^T}{\rho_{1k}} \right\} \delta \underline{x}_k + \dots \end{aligned} \tag{3-13}$$

In practical applications the station average vector \underline{a} will be held fixed and we will solve for the coordinate difference vector \underline{d} .

3.2 Double differences

The double difference is the difference of two single differences to different satellites m and k .

$$\psi_D = \frac{2\pi}{\lambda} \{(\rho_{2k} - \rho_{1k}) - (\rho_{2m} - \rho_{1m})\} + \psi_\varepsilon + \psi_a \quad (3-14)$$

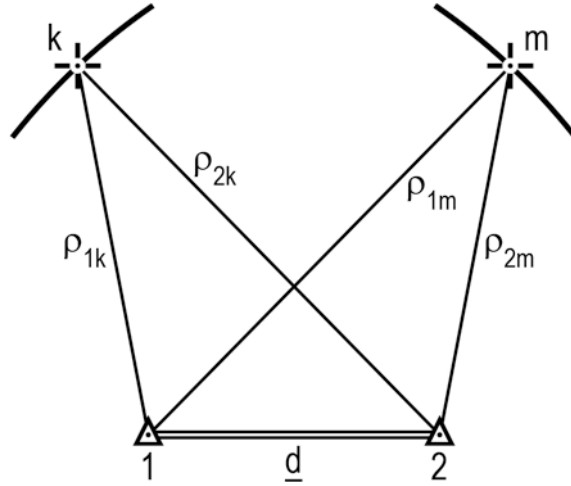


Fig. 3: Double difference constellation

For the linear observation equation one finds REMONDI (1984),

$$\begin{aligned} \delta\psi_D = \frac{2\pi}{\lambda} \left\{ \left(-\frac{\partial\rho_{1k}}{\partial x_1} + \frac{\partial\rho_{1m}}{\partial x_1} \right) \delta x_1 + \left(-\frac{\partial\rho_{2m}}{\partial x_2} + \frac{\partial\rho_{2k}}{\partial x_2} \right) \delta x_2 + \right. \\ \left. + \left(\frac{\partial\rho_{2k}}{\partial x_k} - \frac{\partial\rho_{1k}}{\partial x_k} \right) \delta x_k + \left(\frac{\partial\rho_{2m}}{\partial x_m} - \frac{\partial\rho_{1m}}{\partial x_m} \right) \delta x_m \right\} \end{aligned} \quad (3-15)$$

The partial derivatives are of the form

$$\begin{aligned} \frac{\partial\rho_{1k}}{\partial x_1} = -\frac{(x_k - x_1)^T}{\rho_{1k}} \quad ; \quad \frac{\partial\rho_{1m}}{\partial x_1} = -\frac{(x_m - x_1)^T}{\rho_{1m}} \\ \frac{\partial\rho_{2m}}{\partial x_2} = -\frac{(x_m - x_2)^T}{\rho_{2m}} \quad ; \quad \frac{\partial\rho_{2k}}{\partial x_2} = -\frac{(x_k - x_2)^T}{\rho_{2k}} \end{aligned} \quad (3-16)$$

$$\frac{\partial \rho_{1k}}{\partial x_k} = -\frac{\partial \rho_{1k}}{\partial x_1} ; \quad \frac{\partial \rho_{2k}}{\partial x_k} = -\frac{\partial \rho_{2k}}{\partial x_2} ; \quad \frac{\partial \rho_{2m}}{\partial x_m} = -\frac{\partial \rho_{2m}}{\partial x_2} ; \quad \frac{\partial \rho_{1m}}{\partial x_m} = -\frac{\partial \rho_{1m}}{\partial x_1}$$

Introducing again coordinate averages and differences, we finally arrive at

$$\begin{aligned} \delta\psi_D = & \frac{2\pi}{\lambda} \left\{ \frac{(x_m - x_1)^T}{\rho_{1m}} - \frac{(x_k - x_1)^T}{\rho_{1k}} + \frac{(x_k - x_2)^T}{\rho_{2k}} - \frac{(x_m - x_2)^T}{\rho_{2m}} \right\} \delta\bar{a} + \\ & + \frac{\pi}{\lambda} \left\{ \frac{(x_k - x_2)^T}{\rho_{2k}} - \frac{(x_m - x_2)^T}{\rho_{2m}} + \frac{(x_k - x_1)^T}{\rho_{1k}} - \frac{(x_m - x_1)^T}{\rho_{1m}} \right\} \delta\bar{d} + \quad (3-17) \\ & + \frac{2\pi}{\lambda} \left\{ \left(\frac{(x_k - x_1)^T}{\rho_{1k}} - \frac{(x_k - x_2)^T}{\rho_{2k}} \right) \delta x_k + \left(\frac{(x_m - x_2)^T}{\rho_{2m}} - \frac{(x_m - x_1)^T}{\rho_{1m}} \right) \delta x_m \right\} + \\ & + \dots \end{aligned}$$

Since for double difference processing the main part of the receiver clock error cancels out, the influence of the receiver clock error will be neglected.

3.3 Triple differences

The triple difference is the difference of two double differences for two epochs (REMONDI, 1984).

$$\begin{aligned} \psi_T = & \frac{2\pi}{\lambda} \left\{ \left((\rho_{2k}^2 - \rho_{1k}^2) - (\rho_{2m}^2 - \rho_{1m}^2) \right) - \left((\rho_{2k}^1 - \rho_{1k}^1) - (\rho_{2m}^1 - \rho_{1m}^1) \right) \right\} + \\ & + \psi_\varepsilon + \psi_a \quad (3-18) \end{aligned}$$

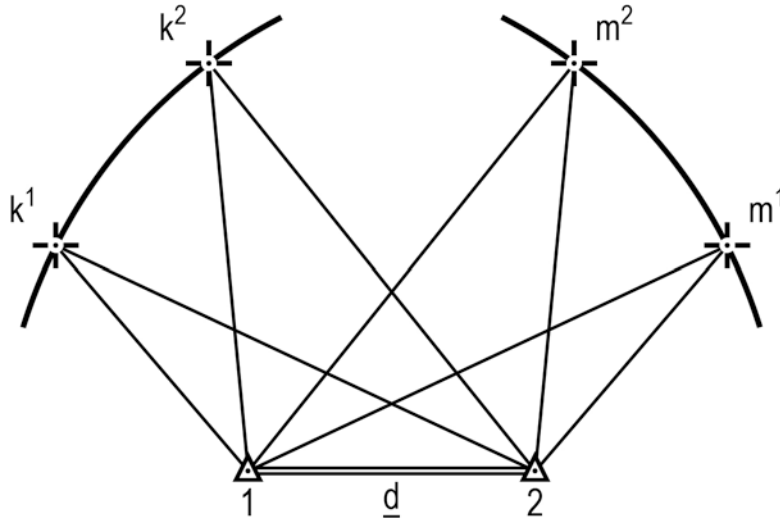


Fig. 4: Triple difference constellation

The linear observation equation

$$\begin{aligned}
\delta\psi_T = & \frac{2\pi}{\lambda} \left\{ \left(\left(\frac{\partial \rho_{1m}^2}{\partial x_1} - \frac{\partial \rho_{1k}^2}{\partial x_1} \right) + \left(\frac{\partial \rho_{1k}^1}{\partial x_1} - \frac{\partial \rho_{1m}^1}{\partial x_1} \right) \right) \delta x_1 + \right. \\
& + \left(\left(\frac{\partial \rho_{2k}^2}{\partial x_2} - \frac{\partial \rho_{2m}^2}{\partial x_2} \right) + \left(\frac{\partial \rho_{2m}^1}{\partial x_2} - \frac{\partial \rho_{2k}^1}{\partial x_2} \right) \right) \delta x_2 + \\
& + \left(\frac{\partial \rho_{2k}^2}{\partial x_k} - \frac{\partial \rho_{1k}^2}{\partial x_k} + \frac{\partial \rho_{1k}^1}{\partial x_k} - \frac{\partial \rho_{2k}^1}{\partial x_k} \right) \delta x_k + \\
& + \left. \left(\frac{\partial \rho_{2m}^2}{\partial x_m} - \frac{\partial \rho_{1m}^2}{\partial x_m} + \frac{\partial \rho_{1m}^1}{\partial x_m} - \frac{\partial \rho_{2m}^1}{\partial x_m} \right) \delta x_m \right\} + \\
& + \psi_\varepsilon + \psi_a
\end{aligned} \tag{3-19}$$

Introducing coordinate averages and differences as above, we get

$$\begin{aligned}
\delta\psi_T = & \frac{2\pi}{\lambda} \left\{ \frac{(x_k - x_1)^{T_2}}{\rho_{1k}} - \frac{(x_m - x_1)^{T_2}}{\rho_{1m}} + \frac{(x_m - x_1)^{T_1}}{\rho_{1m}} - \frac{(x_k - x_1)^{T_1}}{\rho_{1k}} + \right. \\
& + \left. \frac{(x_m - x_2)^{T_2}}{\rho_{2m}} - \frac{(x_k - x_2)^{T_2}}{\rho_{2k}} + \frac{(x_k - x_2)^{T_1}}{\rho_{2k}} - \frac{(x_m - x_2)^{T_1}}{\rho_{2m}} \right\} \delta \underline{a} + \\
& + \frac{\pi}{\lambda} \left\{ \left(\frac{(x_k - x_1)^{T_2}}{\rho_{1k}} - \frac{(x_m - x_1)^{T_2}}{\rho_{1m}} + \frac{(x_m - x_1)^{T_1}}{\rho_{1m}} - \frac{(x_k - x_1)^{T_1}}{\rho_{1k}} \right) - \right. \\
& - \left. \left(\frac{(x_m - x_2)^{T_2}}{\rho_{2m}} - \frac{(x_k - x_2)^{T_2}}{\rho_{2k}} + \frac{(x_k - x_2)^{T_1}}{\rho_{2k}} - \frac{(x_m - x_2)^{T_1}}{\rho_{2m}} \right) \right\} \delta \underline{d} + \\
& + \frac{2\pi}{\lambda} \left\{ \frac{(x_k - x_2)^{T_2}}{\rho_{2k}} - \frac{(x_k - x_1)^{T_2}}{\rho_{1k}} + \frac{(x_m - x_1)^{T_1}}{\rho_{1k}} - \frac{(x_k - x_2)^{T_1}}{\rho_{2k}} \right\} \delta x_k + \\
& + \frac{2\pi}{\lambda} \left\{ \frac{(x_m - x_1)^{T_2}}{\rho_{1m}} - \frac{(x_m - x_2)^{T_2}}{\rho_{2m}} + \frac{(x_m - x_2)^{T_1}}{\rho_{2m}} - \frac{(x_k - x_1)^{T_1}}{\rho_{1m}} \right\} \delta x_m + \\
& + \psi_\varepsilon + \psi_a
\end{aligned} \tag{3-20}$$

Note, that again in (3-21) the receiver clock error virtually cancels out.

3.4 Error propagation analysis

Our aim is to describe the influence of different error sources like orbit, clock and atmospheric influences on differential positioning.

All linear observation equations are of the general form

$$\underline{l} = \underline{A}\underline{x} + \underline{B}\underline{d} + \underline{C}\underline{\varepsilon} + \underline{D}\underline{a} + \underline{n} \quad (3-21)$$

where

\underline{l} ... is the observational vector with
 $\underline{l} = [\delta\psi_1, \delta\psi_2, \dots]$,

\underline{A} ... is a matrix containing partial derivatives with respect to the satellite position coordinates,

\underline{x} ... is the satellite position vector,

\underline{B} ... is the design matrix containing partial derivatives with respect to the baseline vector \underline{d} ,

\underline{d} ... is the unknown baseline vector,

\underline{C} ... contains partial derivatives with respect to unknown clock errors,

$\underline{\varepsilon}$... is the vector of unknown clock parameters,

\underline{D} ... contains partial derivatives with respect to atmospheric corrections,

\underline{a} ... is the vector of atmospheric correction parameters,

and \underline{n} ... is a noise vector.

The error covariance matrix \underline{Q}_{dd} of the baseline vector \underline{d} is derived by the law of error propagation as

$$\underline{Q}_{dd} = \left(\underline{B}^T \left(\underline{Q}_{ll} + \underline{A}\underline{Q}_{xx}\underline{A}^T + \underline{C}\underline{Q}_{\varepsilon\varepsilon}\underline{C}^T + \underline{D}\underline{Q}_{aa}\underline{D}^T \right)^{-1} \underline{B} \right)^{-1} \quad (3-22)$$

In the following the square-root of the trace of this matrix is used as a basic error criterion for the discussion of optimum satellite configurations.

4. ATMOSPHERIC EFFECTS

The atmosphere causes propagation delays of the electromagnetic wave of the satellites and the required corrections depend mainly on the elevation angle above the horizon. The range correction due to ionospheric effects varies between 10 and 60 m and the correction due to tropospheric effects between 2 and 15 m.

Figure 5 shows the different behaviour of the ionospheric and tropospheric time delays. Considering the frequencies used in GPS the two effects have nearly the same magnitude.

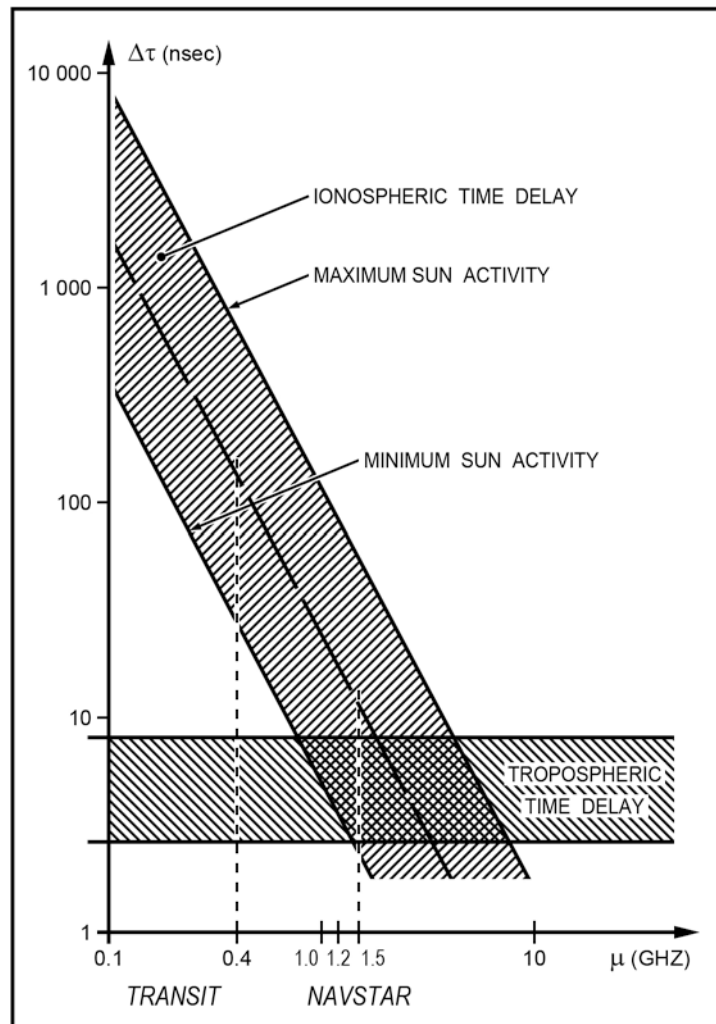


Fig. 5: Different behaviour of ionospheric and tropospheric delays

4.1 Ionospheric propagation delay

The ionosphere is that part of the atmosphere located approximately 80 km to 1000 km above the earth's surface. The delay in electromagnetic wave propagation caused by the ionosphere depends on the electron content, which is the integral of the electron density over the signal path. The time delay is related to the number of electrons along the slant path from satellite to receiver by

$$\Delta t = \frac{40.3}{c f^2} N_c \quad (4-1)$$

where

N_c is the total electron content
(total number of electrons along the path from satellite to receiver in units of electrons per square meter column)

c is the speed of light in m/s

f is the system operating frequency in Hertz

The total electron content N_c depends on several parameters, upon which the sun plays a major role. This dependency leads to diurnal and seasonal variations of the electron density. Furthermore N_c depends on oscillations due to solar flux, on the geographical location of the observation point and on the magnetic activity. The maximum electron density is expected at 2 pm local time.

A lot of models have been developed for describing the ionospheric propagation delays. They differ very much in complexity and in attainable accuracy. Table 1 shows the expected accuracy of several models and in comparison the accuracy expected from two-frequency ionospheric corrections.

In the following we want to use only the most simple model to derive ionospheric propagation delays for our simulations. The model developed by KLOBUCHAR has an accuracy of about 50 % and is used in connection with the Global Positioning System. The polynomial coefficients of the model described later are part of the navigation message of GPS satellites. Because of its small computational requirements it can be used by GPS receivers for operational correction of the ionospheric propagation delay.

Let us briefly describe the algorithm developed by KLOBUCHAR. The diurnal behaviour of the time delay is approximated by a simple cosine function

$$T_g = DC + A \cos \left\{ \frac{(t - \phi) 2\pi}{P} \right\} \quad (4-2)$$

where

t ... is the local time at the ionospheric point in seconds,

ϕ ... is the local time of maximum ionospheric correction
(We have used $\phi = 50400$ s),

DC... is the base ionospheric time delay
(We have used $DC = 5 \cdot 10^{-9}$ s),

A ... is the amplitude of the ionospheric delay function in seconds,

and P ... is the period of the ionospheric delay function in seconds.

A and P are computed from the broadcast data α_i and β_i by the following relations

$$A = \sum_{i=1}^4 \alpha_{i-1} \varphi_m^{i-1} \quad (4-3)$$

$$P = \sum_{i=1}^4 \beta_{i-1} \varphi_m^{i-1} \quad (4-4)$$

where φ_m is the geomagnetic latitude of the ionospheric subpoint in semi-cycles. If $|(t-\phi)2\pi/P|$ exceeds $\frac{\pi}{2}$ the time delay is represented by the DC term only.

The elevation angle is considered by introducing an obliquity factor SF defined by

$$SF = \sec \left[\sin^{-1} \left(\frac{r_0}{r_0+h} \cos \alpha \right) \right] \quad (4-5)$$

where

α ... is the elevation angle,

r_0 ... is the mean earth radius,

and h ... is the point height.

Figure 6 shows the dependency of ionospheric correction on the elevation angle computed from the KLOBUCHAR model.

In our simulation program we have used this model to describe the influence of the ionosphere on the differential point positioning. We distinguish here between different cases. At first we assume that we have a one frequency receiver and we are not able to correct for ionospheric time delay by use of a special model. Then for single difference positioning the difference

$$(\Delta\rho_{2I} - \Delta\rho_{1I}) \frac{2\pi}{\lambda} \quad (4-6)$$

affects our measurement where $\Delta\rho_{2I}$ and $\Delta\rho_{1I}$ are the ionospheric range delays. In our case we will derive these quantities from our ionospheric model.

Because the measurements are made simultaneously, the corrections depend on the elevation angle and slightly on the azimuth. For short baselines and elevation angles greater than 10° degrees the ionospheric influence will cancel out. In order to describe the ionospheric influence in our least squares model we assume that the quantity given in (4-6) is a mean value and introduce the square of it as variance in the \underline{Q}_{aa} matrix already mentioned above. This is only an approximation and is mathematically not completely correct.

In the second case we try to model the ionospheric error expected from two-frequency measurements.

The frequency dependency of the ionospheric delay can be used to determine the correction by using both L-Band frequencies of the NAVSTAR system ($L_1 = 1575$ MHz and $L_2 = 1227$ MHz).

The differential time delay of the two signals is given by

$$\Delta t_{L_1} - \Delta t_{L_2} = \frac{40.3 N_c}{c} \left[\frac{1}{f_{L_1}^2} - \frac{1}{f_{L_2}^2} \right] \quad (4-7)$$

Solving for the electron content we get

$$N_c = \frac{c (\Delta t_{L_1} - \Delta t_{L_2})}{40.3} \left[\frac{f_{L_1}^2 f_{L_2}^2}{f_{L_2}^2 - f_{L_1}^2} \right] \quad (4-8)$$

According to KLOBUCHAR et al. (1980) the two frequency ionospheric correction technique has a r.m.s. of about 2 meters for range measurements, which corresponds to a time delay of about 6.7 nanoseconds.

Therefore we assume that the relative error of such observations caused by ionospheric delay is about 5 %. The variance of such an ionospheric residual error is

$$\left(0.05 (\Delta\rho_{2I} - \Delta\rho_{1I}) \frac{2\pi}{\lambda} \right)^2 \quad (4-9)$$

Note, that we neglect the difference in wave length of the two signals in order to simplify the simulation.

4.2 Tropospheric effects

The troposphere is that part of the atmosphere which is located between the earth's surface and a height of about 70 km. It can be treated as a nondispersive medium. That means that the tropospheric propagation delay is not a function of the signal frequency (see Fig. 5). The propagation delay depends on the refractivity of the medium and the refractivity depends on the temperature T and the air pressure p. The formulas of SMITH and WEINTRAUB (1953) define the atmospheric refractivity as the sum of a wet and a dry term.

The dry term is defined by

$$N_D = 77.6 \frac{p}{T} \quad (4-10)$$

and the wet term by

$$N_W = 3.73 \cdot 10^5 \left(\frac{e}{T^2} \right) \quad (4-11)$$

where N ... is the refractivity,

p ... is the air pressure in millibars,

T ... is the temperature in Kelvin,

and e ... is the pressure of the water vapour in millibars.

Since pressure and temperature are not available along the signal path, the surface measurements are used to predict the refractivity along the path of the electromagnetic wave. For the prediction of the refractivity usually exponential profiles are used. In our simulation program we use a tropospheric range correction algorithm developed by BLACK (1978).

The range correction is defined by the sum of the dry and wet part

$$\Delta\rho_T = \Delta\rho_{T_D} + \Delta\rho_{T_W} \quad (4-12)$$

The dry part is given by

$$\Delta\rho_{T_D} = 2.343 p \left(\frac{T - 4.12}{T} \right) \cdot I(h=h_D, \alpha) \quad (4-13)$$

and the wet part is

$$\Delta\rho_{T_W} = K_W I(h=h_W, \alpha) \quad (4-14)$$

with

$$I(h, \alpha) = \left\{ 1 - \left[(\cos \alpha) / (1 + (1 - l_c) h / r_s) \right]^2 \right\}^{-1/2} \quad (4-15)$$

where

$h_D \dots$ 148.98 (T - 4.12) m above the station,
 $h_W \dots$ 13000 m,
 $l_c \dots$ 0.85,
 $K_W \dots$ 0.28 for summer,
 0.36 for spring or fall in midlatitudes,
 0.12 for winter in maritime latitudes,
 0.06 for winter in continental latitudes,
 0.05 for polar regions,
 $r_s \dots$ distance from earth center to the station,
 $p \dots$ surface pressure in standard atmospheres,
 $T \dots$ surface temperature in degrees Kelvin.

In figure 7 the dry and the wet part of the tropospheric correction are shown as a function of the elevation angle. Note that the wet part is only a small quantity in comparison to the dry part.

According to REMONDI (1984) the tropospheric correction can be modelled within 2 - 5 % for the dry part which is about 80 % of the correction. The modelling of the wet part is a bit more complicated. For simplicity we assume a relative error of 3 % for the complete correction and introduce similar to (4-9) a variance of

$$\left(0.03 (\Delta \rho_{2T} - \Delta \rho_{1T}) \frac{2\pi}{\lambda} \right)^2 \quad (4-16)$$

5. NUMERICAL INVESTIGATIONS

Software was developed for the analysis described in chapter 3. Based on an 18 - satellite constellation we have derived satellite positions in an earth fixed reference frame at epoch intervals of 1 minute. For these preliminary computations the orbital elements of table 2 were used.

All following simulation computations were done for a baseline of about 64.8 km length, which is located in West-Germany and has really been observed in 1983 during a Macrometer V-1000 campaign of the "Hessisches Landesvermessungsamt" (LANDAU, 1986) (see figure 8). We are aware of the fact, that we have chosen a baseline with an average length.

The computations are done for a fictitious day July 1, 1990. Figure 9 shows the satellite traces for one day in the horizon system of point Ronneburg, located in West-Germany. The "hole" in the northern part of the figure is conspicuous. It has a diameter of 70° degrees and is caused by the fact that the inclination is put equal to 55° for all satellites. The missing satellites in that part of the sky are a little unfavourable for geodetic applications.

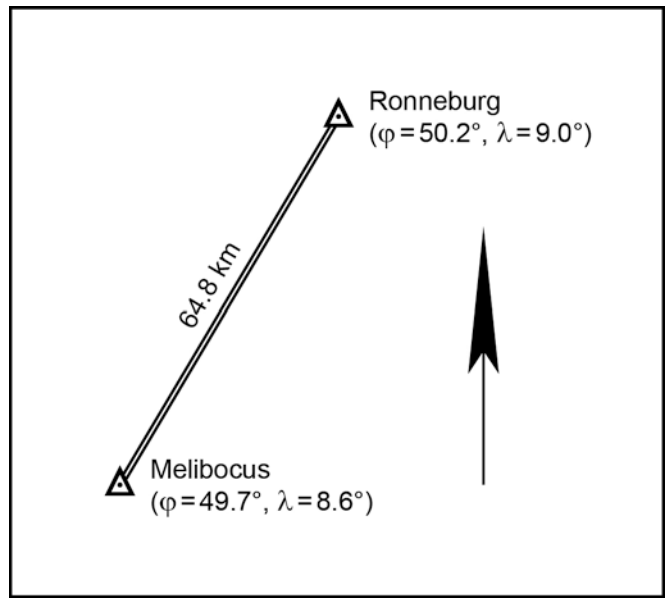


Fig. 8: Geographical location of the considered baseline

Figure 10 shows the distribution of satellites throughout the day and the number of visible satellites. There are 5 to 8 satellites always visible at station Ronneburg. The geometric dilution of precision is given in figure 11. It varies between 1.8 and 5.5.

Because most of the available GPS receivers are able to track only 4 satellites, we assume in our considerations, that 4 satellites have to be collected from the number of all visible satellites. All satellites which have an elevation angle of more than 5° degrees above the horizon are visible. In all figures presented in this paper the smallest available error was plotted which was found by checking all possible satellite combinations. The number of possible combinations can easily be computed by the relation

$$m = \binom{n}{p} = \frac{n \cdot (n-1) \cdot \dots \cdot (n-p+1)}{1 \cdot 2 \cdot 3 \cdot \dots \cdot (p-1) p} \tag{5-1}$$

where n is the number of visible satellites and p is the maximum number of satellites which can be tracked (here p = 4).

n	m
4	1
5	5
6	15
7	35
8	70

5.1 Consideration of different error sources

5.1.1 Influence of receiver clock errors on phase difference measurements

According to DAVIDSON et al. (1983) the r.m.s. error of a receiver clock offset is about 10^{-10} seconds. The variance of a single receiver clock offset converted to carrier phase is given by $(2\pi\nu)^2 m_{\epsilon}^2$. With $\nu = 1575.42$ MHz (L_1 -frequency) we finally get $(0.98986558)^2$. Considering the receiver clock errors of both receivers we get for a single difference observation

$$(2\pi\nu)^2 m_{\epsilon 1}^2 + (2\pi\nu)^2 m_{\epsilon 2}^2 \quad (5-2)$$

This corresponds to a range error of ± 0.042 m.

For double and triple difference processing the receiver clock offset cancels out. In our simulations we assume that no clock errors effect the baseline determination in that case.

5.1.2 Orbit errors

We further assume, that the satellite positions are given with a r.m.s. error of ± 10 m, which seems to be a realistic assumption of the orbit accuracy (see LANDAU and HAGMAIER, 1986).

5.2 Discussion of results

Phase difference measurements have a completely different error behaviour than pseudo-range measurements. Phase difference measurements have geometric strength in the direction of the satellites motion, whereas pseudo-range measurements have geometric strength in the direction of the satellite receiver connection. This behaviour must be reflected in the optimal satellite selection. The computations described in the following are done to prove this assumption. They are always carried out in the same manner: Simulating different observation types the algorithm looks for the best satellite combination which minimizes the trace of the \underline{Q}_{dd} matrix. All possible satellite combinations are computed for a whole day and compared to the trace achieved for the satellite combination proposed by the GDOP computations. This accuracy difference is always drawn in the lower part of the figures in the appendix and reflects the difference in expected accuracy for different satellite combinations. It is self-evident, that this quantity does not give the obtainable r.m.s. error for baseline components from one epoch measurements, but it describes the error behaviour very well and helps us to get an impression of the effects of different error sources on accuracy.

As already mentioned above, we made computations with single, double and triple differences and compared results to GDOP computations. We distinguish between different atmosphere modelling:

Ionosphere	
error flag	
0	no ionospheric delay considered
1	considered but not corrected (see 4-6)
2	two-frequency correction (see 4-9)
3	KLOBUCHAR correction applied.

Troposphere		
error flag		
0	no tropospheric delay considered	
1	considered and corrected	(see 4-16)

We handle troposphere and ionosphere in different ways because up to now (as far as we know) in present post-processing software only the tropospheric error is corrected but not the ionospheric. So the ionospheric error (flag 1) allows to get an idea of the error induced by neglecting the ionospheric refraction.

5.2.1 Results of single difference processing

The error behaviour of single difference processing is very similar to the behaviour of pseudo-ranging. Figure 12 shows the accuracy profile with a difference profile caused by different satellite combination selections. Note that the selected satellites are the same as those proposed by the geometric dilution of precision except for a few epochs. The maximum accuracy difference is small: about 1 cm. The differences appear more frequently, if we consider atmospheric modelling. These influences will be discussed in greater detail for the double difference processing.

5.2.2 Results of double difference processing

Double difference processing will be discussed in greater detail because it is the most frequently used processing technique.

Figure 13 (a-f) and table 4 describe the obtainable accuracy derived from double difference processing in comparison to the accuracy which can be achieved using the GDOP proposal. Figure 13a shows that the accuracy differences appear more frequently and becomes larger than for single difference processing. The error behaviour is slightly different. Whereas in single difference processing the largest discrepancy appears at about 8 pm the largest one in double difference processing appears with 4 cm at about 3 pm. The profile of the obtainable accuracy in the upper part of the figure looks very similar to the profile in figure 12.

Introducing the error model described in chapter 3 for two-frequency measurements the profile does not change very much. The maximum baseline error increases from ± 17 cm to ± 20 cm (fig. 13b).

Considering atmospheric effects in case of one-frequency measurements, but not correcting them, leads to a maximum error of ± 1.63 m and a maximum accuracy difference of 0.83 m (fig. 13c). The largest errors occur in the time span between 7 am and 7 pm. The errors for the other periods of the day are smaller than ± 30 cm. An observation with one-frequency receivers should therefore be carried out between 7 pm in the evening and 7 am in the morning. Using a simple ionospheric correction model like that of KLOBUCHAR the error can be reduced to a maximum of ± 97 cm (fig. 13d).

Figure 13e shows the error caused by consideration of tropospheric effects and correcting them with an accuracy of 3 %. The tropospheric effects influence the satellite selection more than the ionospheric ones corrected by two-frequency measurements. This is caused by the different properties of the correction formulas. Please note, that the curve in figure 7 has a much

larger gradient than the curve in figure 6 for elevation angles between 5° and 15° degrees. The difference in atmospheric correction influences the differential positioning. This difference is caused by differences in elevation angles from the two end points. For low elevation angles the troposphere will therefore effect the measurement much more than the ionosphere.

Figure 13f gives an impression of the influence on baseline determination when combining two-frequency measurements with tropospheric correction.

In table 4 the expected accuracies for 35 different satellite combinations are presented corresponding to the different figures described above. The satellite combination study is given for a single epoch $5^h 40^m$ UTC. The proposal of 4 different satellite combinations demonstrates the difference in error behaviour of the models. Figure 15 shows the satellite configuration at that epoch. 7 satellites are visible: 3, 6, 9, 12, 14, 15, 17. 6, 9 and 15 are below an elevation angle of 15° degrees, at positions where large atmospheric effects can be expected. Double difference processing without consideration of atmospheric effects (a) proposes to use sats 6, 9, 15, 17 where 6 and 9 are satellites with low elevation angle. This combination gives the best results when considering only geometrical aspects. In column (e) we have considered tropospheric effect.

Satellite 9, which has the lowest altitude and therefore causes the largest atmospheric error, drops out. Columns (c) and (d) demonstrate the influence of atmospheric effects in addition. In these cases satellite combinations were chosen which have only one satellite with low altitude, although that causes a change for the worse in geometry of tracked satellites.

A comparison of the combination 33 proposed by GDOP for different atmospheric modelling shows that the received accuracy is in most cases not the smallest attainable one.

5.2.3 Results of triple difference processing

The triple difference processing technique has a completely different error behaviour than single or double difference processing. In the above mentioned processing techniques the position of satellites and their configurations plays the major role. Yet, in triple difference processing the relative motion of the satellites with respect to the baseline is considered. In our simulation we considered an epoch interval of ten minutes. During that time the space vehicle flies about 2400 km. The baseline determination using triple differences is therefore weaker and has a completely different error behaviour. The accuracy profile for the fictitious day in 1990 is given in figure 14. It is evident that the difference in proposed satellite combinations is much larger than for single or double difference processing.

Figure 18 describes the different accuracies obtained by use of an optimal selection algorithm and of a conventional one. It shows the superiority of the improved algorithm which results during the whole observation span in smaller r.m.s. errors. The advantage of an improved algorithm is the fact that the gradient becomes greater and therefore the accuracy increases rapidly with the observation time.

5.3 Final comparison of different phase difference measurements

In order to compare the phase difference observation types the obtained accuracies are given in table 3 and in figure 16. Note that the error behaviour of single difference processing and pseudo-ranging is similar because of the limited combination possibilities. (The orbits of the satellites are fixed. The satellite position optimization is therefore strongly limited.) In case of double difference processing the different error behaviour is more fully expressed. The selected satellite combination changes. The behaviour of triple difference processing is completely different which is also shown in figure 14.

The effect of satellite selection on the accuracy of baseline determination is described in table 5. Different accuracy estimates are compared for conventional and improved satellite selection methods. Whereas the difference is large for one-frequency receivers (neglecting ionospheric effects), the difference is small in case of two-frequency ionospheric correction. This is especially valid for single and double difference methods. The triple difference method is improved significantly, which could be expected due to the completely different error behaviour (compare figures 11 and 14).

We could state that it is possible to avoid satellite selection if we have a receiver with a sufficient number of channels to track all visible satellites. The question is whether or not a receiver with 6 channels (like the Macrometer) is superior to a 4 channel receiver. Figure 16 shows the trace of the variance-covariance matrix \underline{Q}_{dd} with respect to daytime for double difference processing with a maximum of 6 satellites. The improvement seems to be very small. In order to get an idea about the influence of 6-channel processing on the received baseline accuracy, we compared in figure 17 the accuracies of 4- and 6-channel observation with respect to the observation time span. We see that the improvement is in the range of millimeters.

6. CONCLUSIONS

High precision geodetic differential positioning using GPS carrier phase difference measurements requires an optimal satellite selection algorithm. The algorithms currently in use do not always result in an optimum selection, which depends highly on the post-processing algorithm. The highest precision is received if all possible error sources are modelled before satellite selection. This is especially true for processing techniques using satellite positions at different epochs for forming the observations like delta- or triple-differences. These types of algorithms are applied frequently in dynamic positioning. The improved algorithm cannot be run on a computer in online processing mode during observation time due to the large computational requirements. Therefore we recommend the following procedure:

1. Choose the post-processing algorithm
2. Compute optimal satellite configurations for the desired observation time span under considerations of all error sources like clock and orbit errors and atmospheric effects on a large scale computer and store the selection on tape.

3. Use the selection information by co-operation of a magtape-recorder with the receiver in the field.

7. REFERENCES

- Black, H.D. (1978): *An easily implemented algorithm for the tropospheric range correction*. Journal of Geophysical Research, Vol. 83, April 1978
- Davidson, D., D. Delikaraoglou, R. Langley, B. Nickerson, P. Vaníček and D. Wells (1983): *Global Positioning System differential positioning simulations*. Dept. Surv. Eng. Tech. Rep. No. 90, UNB, Fredericton
- Grafarend, E.W., W. Lindlohr, A. Stomma (1985): *Improved second order design of the Global Positioning System, Ephemerides, clocks and atmospheric influence*. In: Proc. of the First International Symposium on Precise Positioning with the Global Positioning System, April 15-19, 1985
- Hein, G.W., B. Eissfeller (1985): *Integrated modelling of GPS - orbits and multi-baseline components*. In: Proc. of the First International Symposium on Precise Positioning with the Global Positioning System, April 15-19, 1985
- Kihara, M., T. Okada (1984): *A satellite selection method and accuracy for the Global Positioning System*. Navigation, Vol. 31, Spring 1984
- Klobuchar, J.A., H. Soicher, J.A. Pearson (1980): *A preliminary evaluation of the two-frequency ionospheric correction for the NAVSTAR-Global positioning System*. In: AGARD-CP-284: Propagation effects in space/earth paths
- Klobuchar, J.A. (1976): *Ionospheric time delay corrections for advanced satellite ranging systems*. AGARD-CP-209
- Landau, H. (1986): *GPS baseline vectors in a three-dimensional integrated adjustment approach*. In: GPS-research at the Institute of Astronomical and Physical Geodesy, Report No. 19, University FAF Munich
- Landau, H., D. Hagmaier (1986): *Analysis of the required force modelling for NAVSTAR/GPS satellites*. In: GPS-research at the Institute of Astronomical and Physical Geodesy, Report No. 19, University FAF Munich
- Nakiboglu, S.M., E.J. Krakiwsky, K.P. Schwarz, B. Buffet, B. Wanless (1985): *A multi-station, multi-pass approach to Global Positioning System improvement and precise positioning*. Contract Report No. OST83-00340, submitted to Geodetic Survey of Canada, Department of Energy, Mines and Resources
- Remondi, B. (1984): *Using the Global Positioning System (GPS) phase observable for relative geodesy: modelling, processing and results*. Ph.D. Dissertation, University for Space Research, The University of Texas in Austin
- Smith, E.K., S. Weintraub (1953): *The constants in the equation for atmospheric refraction index at radio frequencies*. In: Proc. IRE 41, 1035-1037

- Stansell, T.A., S.M. Chamberlain, F.K. Brunner (1985): *The first WILD-Magnavox GPS satellite surveying equipment: WM 101*. In: Proc. of the First International Symposium on Precise Positioning with the Global Positioning System, April 15-19, 1985
- Stein, V. (1982): *Modelle der ionosphärischen Elektronendichteverteilung zur Korrektur von Ausbreitungsfehlern elektromagnetischer Wellen*. DFVLR-Mitt. 82-03
- Vaníček, P., R.B. Langley, D.E. Wells (1984): *Geometrical aspects of differential GPS positioning*. In: Technical Report No. 108, Department of Surveying Engineering, University of New Brunswick, Canada

Appendix: Figures and Tables

	ionospheric range error
without correction	20 - 60 m
Klobuchar model	10 - 30 m
Bent model	4 - 12 m
Bent model + updating	2 - 6 m
two-frequency observation	3 m

Table 1: Expected residual error for different ionospheric correction methods (elevation > 5°) (from STEIN, 1982)

Sat. No.	a (m)	e	ω (deg)	i (deg)	Ω (deg)	M (deg)
1	26 560 001.	0.003	0.0	55.0	0	0
2	26 560 002.	0.003	0.0	55.0	0	120
3	26 560 003.	0.003	0.0	55.0	0	240
4	26 560 004.	0.003	0.0	55.0	60	40
5	26 560 005.	0.003	0.0	55.0	60	160
6	26 560 006.	0.003	0.0	55.0	60	280
7	26 560 007.	0.003	0.0	55.0	120	80
8	26 560 008.	0.003	0.0	55.0	120	200
9	26 560 009.	0.003	0.0	55.0	120	320
10	26 560 010.	0.003	0.0	55.0	180	120
11	26 560 011.	0.003	0.0	55.0	180	240
12	26 560 012.	0.003	0.0	55.0	180	0
13	26 560 013.	0.003	0.0	55.0	240	160
14	26 560 014.	0.003	0.0	55.0	240	280
15	26 560 015.	0.003	0.0	55.0	240	40
16	26 560 016.	0.003	0.0	55.0	300	200
17	26 560 017.	0.003	0.0	55.0	300	320
18	26 560 018.	0.003	0.0	55.0	300	80

Table 2: GPS 18 satellite constellations (from Nakiboglu et al., 1985)

No.	SINGLE	DOUBLE	TRIPLE	PDOP	SATS
1	0.652	0.403	0.141	13.364	3 6 9 12
2	0.493	0.381	0.520	10.012	3 6 9 14
3	0.113	0.073	0.104	2.342	3 6 9 15
4	0.293	0.204	0.104	5.867	3 6 9 17
5	0.311	0.210	0.088	6.285	3 6 12 14
6	0.135	0.070	0.163	2.687	3 6 12 15
7	0.353	0.222	0.123	6.942	3 6 12 17
8	0.124	0.075	0.083	2.485	3 6 14 15
9	0.276	0.189	0.057	5.478	3 6 14 17
10	0.325	0.215	0.634	6.427	3 6 15 17
11	0.299	0.237	0.084	5.991	3 9 12 14
12	0.139	0.078	0.120	2.758	3 9 12 15
13	0.683	0.379	0.515	13.331	3 9 12 17
14	0.298	0.215	0.082	5.899	3 9 14 15
15	0.290	0.204	0.055	5.716	3 9 14 17
16	0.155	0.096	0.125	3.018	3 9 15 17
17	0.152	0.094	0.471	3.018	3 12 14 15
18	121,193	71.243	0.079	2470,487	3 12 14 17
19	0.209	0.104	0.122	4.058	3 12 15 17
20	0.155	0.093	0.064	3.019	3 14 15 17
21	0.324	0.174	0.080	6.530	6 9 12 14
22	0.150	0.065	0.160	3.206	6 9 12 15
23	0.258	0.118	0.224	5.439	6 9 12 17
24	0.192	0.096	0.061	3.952	6 9 14 15
25	6.607	3.326	0.048	135.675	6 9 14 17
26	0.115	0.053	0.078	2.426	6 9 15 17
27	0.303	0.153	0.222	6.236	6 12 14 15
28	0.198	0.099	0.052	4.079	6 12 14 17
29	0.124	0.062	0.112	2.540	6 12 15 17
30	0.115	0.058	0.054	2.354	6 14 15 17
31	0.591	0.367	0.084	11.847	9 12 14 15
32	0.274	0.168	0.074	5.493	9 12 14 17
33	0.101	0.065	0.090	2.028	9 12 15 17
34	0.157	0.093	0.670	3.138	9 14 15 17
35	0.132	0.080	0.082	2.635	12 14 15 17
	0.101	0.053	0.048	2.028	smallest error
	9 12 15 17	6 9 15 17	6 9 14 17	9 12 15 17	corresp. sats

Table 3: Phase difference accuracy at 5^h 40^m UTC for different satellite combinations (Atmospheric effects are neglected)

DOUBLE DIFFERENCES														
Iono flag:	0			1			2			SATS				
	0	1	2	0	1	2	0	1	2					
Trop flag:	0			0			1			PDOP				
	0	1	2	0	1	2	0	1	2					
1	0.403	0.405	0.403	0.814	0.651	0.558	0.558	0.651	0.559	13.364	3	6	9	12
2	0.381	0.383	0.381	0.718	0.583	0.510	0.510	0.583	0.511	10.012	3	6	9	14
3	0.073	0.079	0.073	0.625	0.330	0.102	0.102	0.330	0.107	2.342	3	6	9	15
4	0.204	0.204	0.204	0.386	0.311	0.272	0.272	0.311	0.272	5.867	3	6	9	17
5	0.210	0.211	0.210	0.394	0.279	0.228	0.228	0.279	0.229	6.285	3	6	12	14
6	0.070	0.076	0.070	0.577	0.299	0.077	0.077	0.299	0.082	2.687	3	6	12	15
7	0.222	0.222	0.222	0.408	0.290	0.239	0.239	0.290	0.240	6.942	3	6	12	17
8	0.075	0.081	0.075	0.608	0.316	0.082	0.082	0.316	0.088	2.485	3	6	14	15
9	0.189	0.189	0.189	0.343	0.243	0.203	0.203	0.243	0.204	5.478	3	6	14	17
10	0.215	0.230	0.215	1.669	0.867	0.234	0.234	0.867	0.248	6.427	3	6	15	17
11	0.237	0.237	0.237	0.279	0.308	0.299	0.299	0.308	0.299	5.991	3	9	12	14
12	0.078	0.084	0.078	0.614	0.324	0.100	0.100	0.324	0.105	2.758	3	9	12	15
13	0.379	0.379	0.379	0.459	0.493	0.477	0.477	0.493	0.477	13.331	3	9	12	17
14	0.215	0.230	0.215	1.630	0.862	0.273	0.273	0.862	0.285	5.899	3	9	14	15
15	0.204	0.204	0.204	0.238	0.262	0.257	0.257	0.262	0.257	5.716	3	9	14	17
16	0.096	0.102	0.096	0.717	0.379	0.121	0.121	0.379	0.126	3.018	3	9	15	17
17	0.094	0.100	0.094	0.726	0.377	0.095	0.095	0.377	0.102	3.018	3	12	14	15
18	71.243	71.268	71.243	79.656	73.745	71.285	71.285	73.745	71.310	2470.487	3	12	14	17
19	0.104	0.111	0.104	0.785	0.408	0.105	0.105	0.408	0.112	4.058	3	12	15	17
20	0.093	0.100	0.093	0.693	0.360	0.095	0.095	0.360	0.101	3.019	3	14	15	17
21	0.174	0.177	0.174	0.665	0.454	0.322	0.322	0.454	0.323	6.530	6	9	12	14
22	0.065	0.078	0.065	0.988	0.447	0.130	0.130	0.447	0.136	3.206	6	9	12	15
23	0.118	0.120	0.118	0.437	0.310	0.219	0.219	0.310	0.220	5.439	6	9	12	17
24	0.096	0.112	0.096	1.353	0.617	0.182	0.182	0.617	0.191	3.952	6	9	14	15
25	3.326	3.381	3.326	10.586	8.656	6.159	6.159	8.656	6.289	135.675	6	9	14	17
26	0.053	0.062	0.053	0.717	0.328	0.098	0.098	0.328	0.103	2.426	6	9	15	17
27	0.153	0.178	0.153	2.147	0.950	0.225	0.225	0.950	0.243	6.236	6	12	14	15
28	0.099	0.100	0.099	0.379	0.226	0.141	0.141	0.226	0.142	4.079	6	12	14	17
29	0.062	0.072	0.062	0.834	0.370	0.089	0.089	0.370	0.096	2.540	6	12	15	17
30	0.058	0.067	0.058	0.755	0.338	0.082	0.082	0.338	0.089	2.354	6	14	15	17
31	0.367	0.400	0.367	3.379	1.728	0.667	0.667	1.728	0.686	11.847	9	12	14	15
32	0.168	0.168	0.168	0.245	0.314	0.303	0.303	0.314	0.303	5.493	9	12	14	17
33	0.065	0.071	0.065	0.608	0.311	0.119	0.119	0.311	0.123	2.028	9	12	15	17
34	0.093	0.102	0.093	0.843	0.433	0.168	0.168	0.433	0.173	3.138	9	14	15	17
35	0.080	0.087	0.080	0.652	0.353	0.081	0.081	0.353	0.088	2.635	12	14	15	17
	0.053	0.062	0.053	0.238	0.226	0.077	0.077	0.226	0.082	2.028				smallest error
	6.9,15,17	6.9,15,17	6.9,15,17	3.9,14,17	6.12,14,17	3.6,12,15	3.6,12,15	6.12,14,17	3.6,12,15	9.12,15,17				corresp. sats

Table 4: Double differences accuracy at 5^h 40^m UTC for different satellite combinations

SINGLE		DOUBLE		TRIPLE	
CONVENTIONAL	IMPROVED	CONVENTIONAL	IMPROVED	CONVENTIONAL	IMPROVED
0.076	0.052	0.105	0.088	0.119	0.084
0.053	0.053	0.076	0.050	0.127	0.079
0.073	0.054	0.126	0.063	0.080	0.052
Ionospheric Effects Neglected					
Two-frequency Ionospheric Correction					
0.011	0.010	0.010	0.010	0.016	0.006
0.010	0.009	0.007	0.006	0.017	0.007
0.010	0.010	0.013	0.011	0.011	0.006

Table 5: Comparison of obtained accuracies after a 4 hour observation interval
(Derived from measurements from 14 : 00 to 18 : 00 UTC)

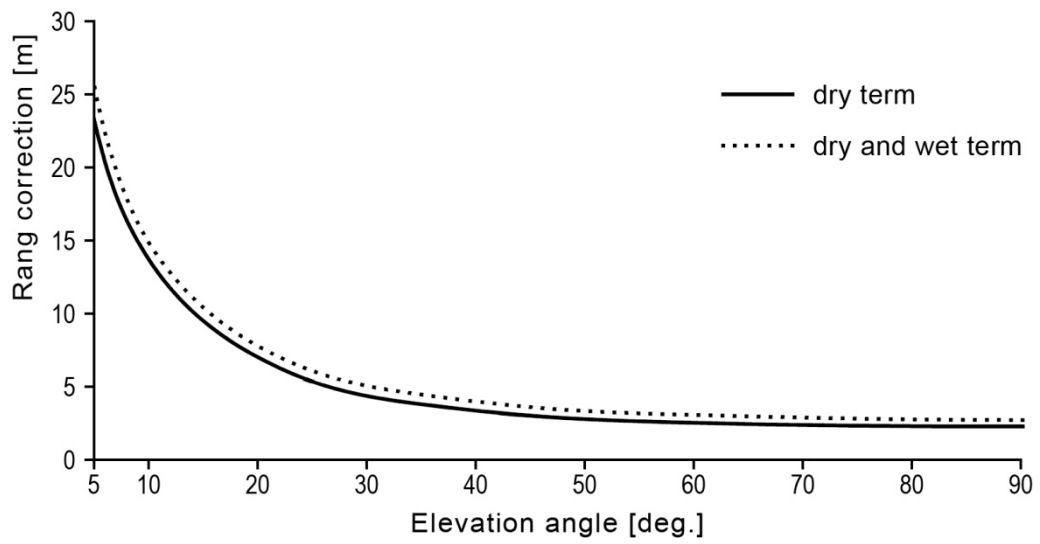


Fig. 7: Tropospheric range correction computed from the Black model

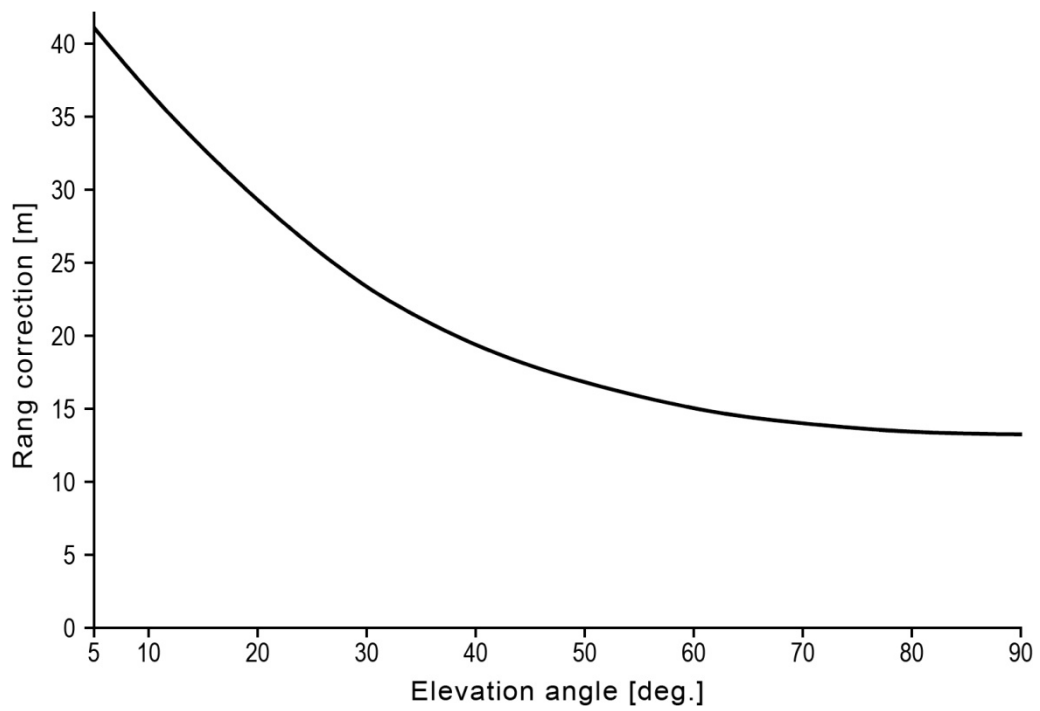


Fig. 6: Ionospheric range correction computed from the Klobuchar model for 2 pm local time

SATELLITE PASSES OF THE NAVSTAR-GPS SYSTEM

STATION : RONNEBURG

DATE : 1.7.90

Latitude : 50.240 degrees

Longitude : 9.068 degrees

Height : 236 meter

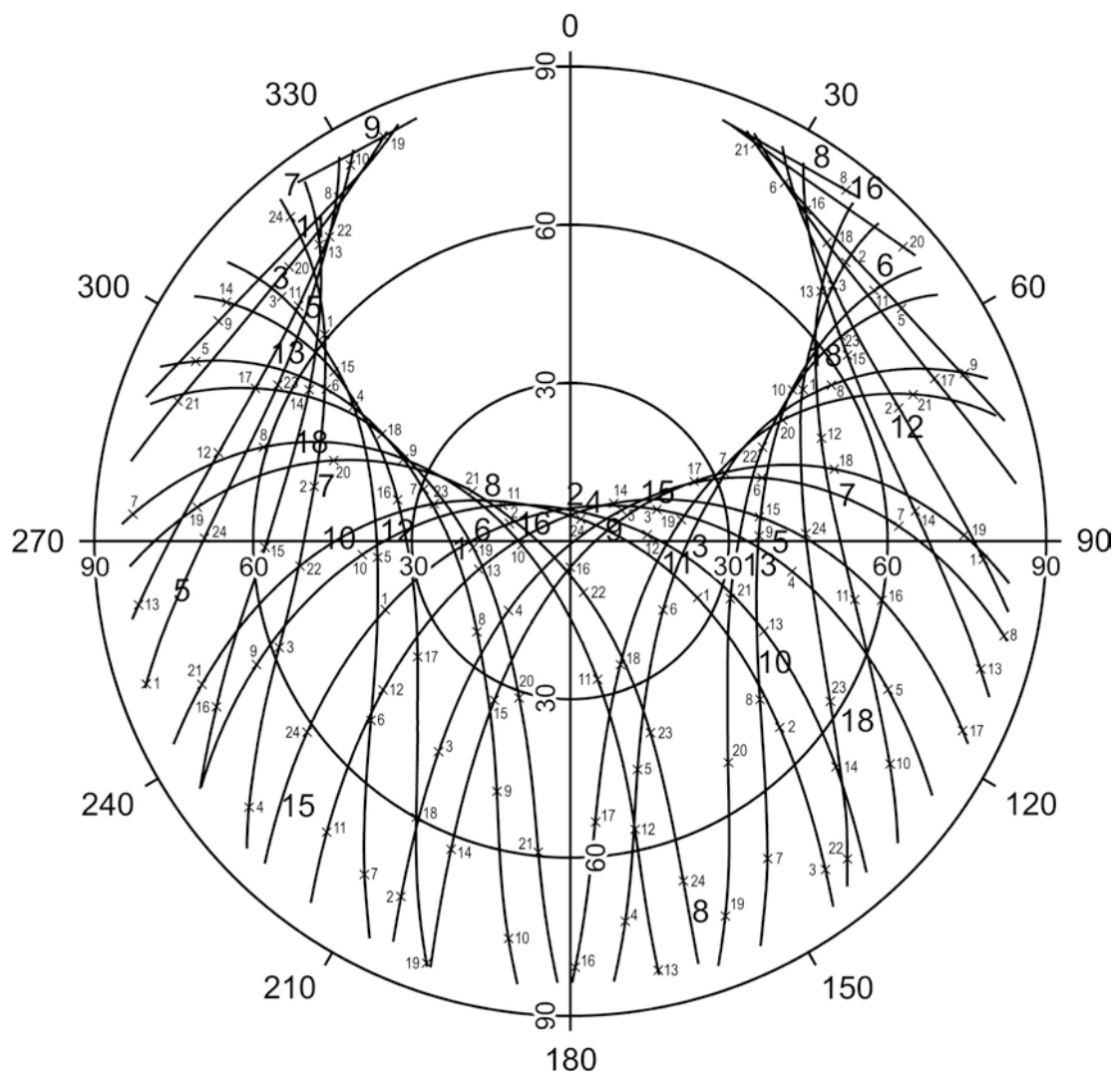


Fig. 9: Satellite traces for the simulation day and location

SATELLITE VISIBILITY OF NAVSTAR-GPS SYSTEM

STATION : RONNEBURG

DATE : 1.7.90

Latitude : 50.240 degrees

Longitude : 9.068 degrees

Height : 236 meter

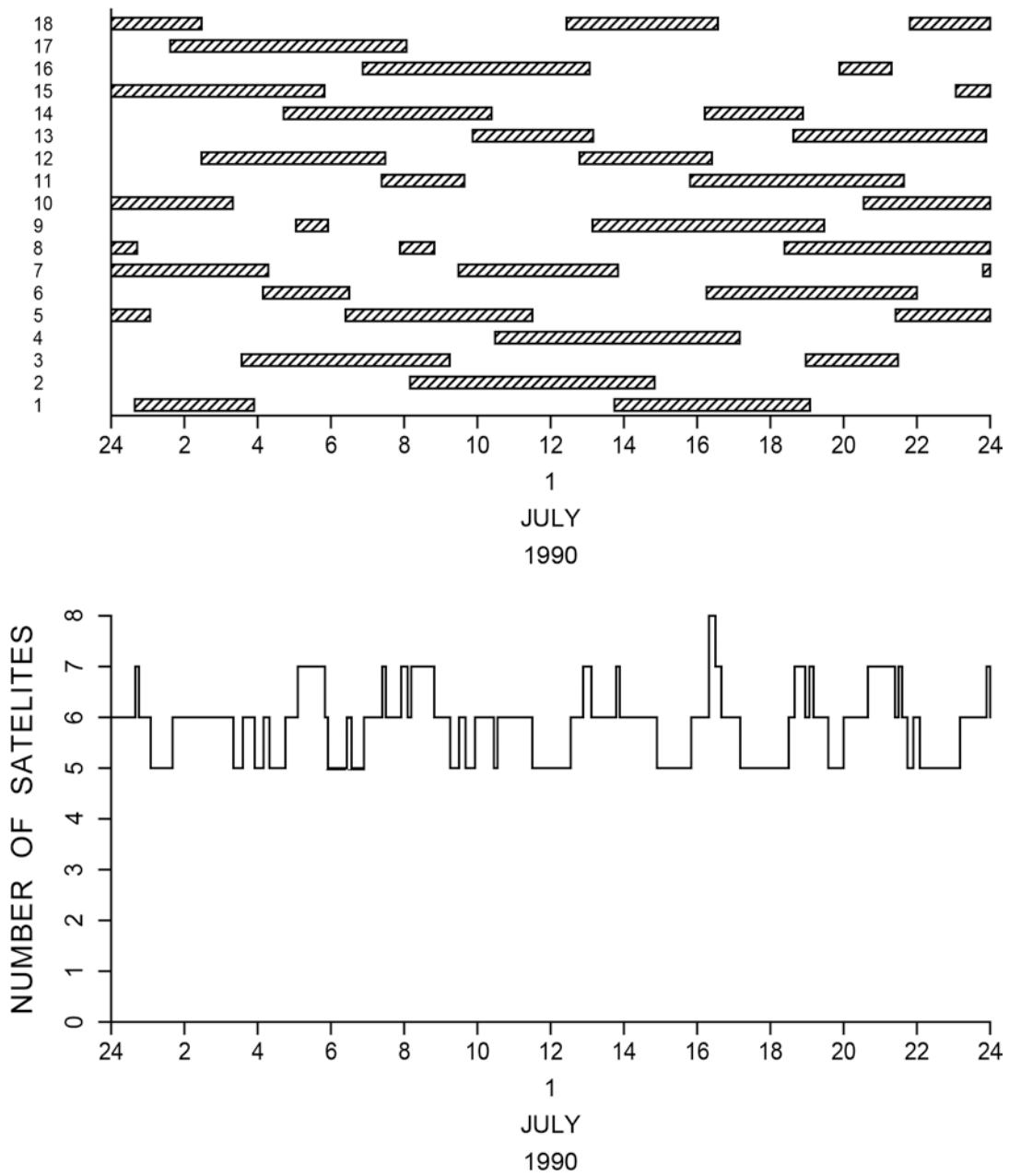


Fig. 10: Satellite visibility

GEOMETRIC DILUTION OF PRECISION - NAVSTAR

STATION : RONNEBURG

DATE : 1.7.90

Latitude : 50.240 degrees

Longitude : 9.068 degrees

Height : 236 meter

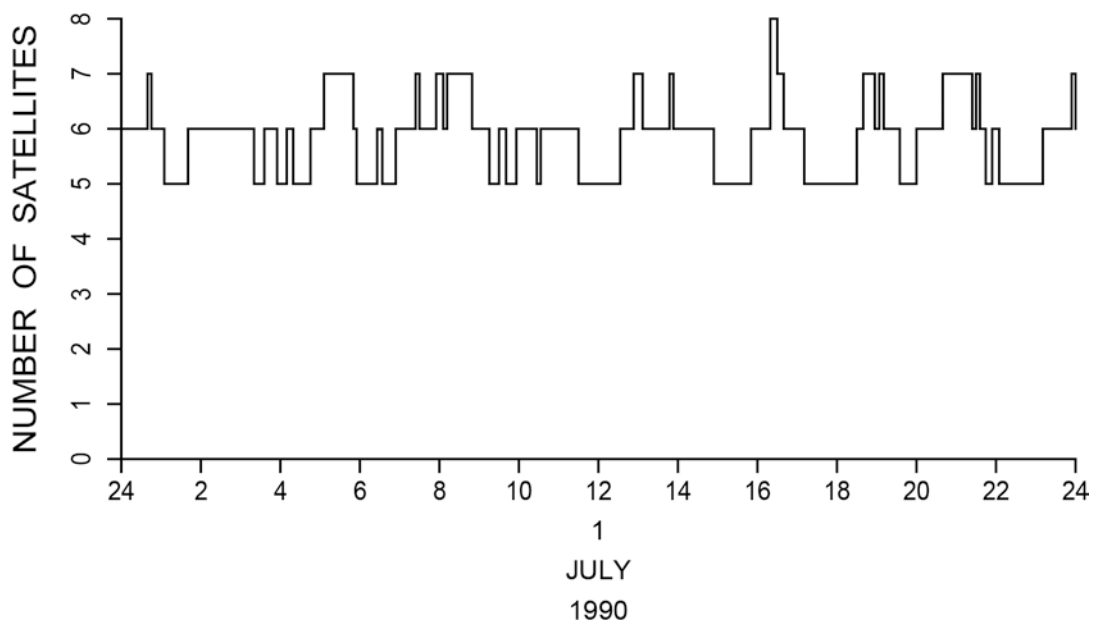
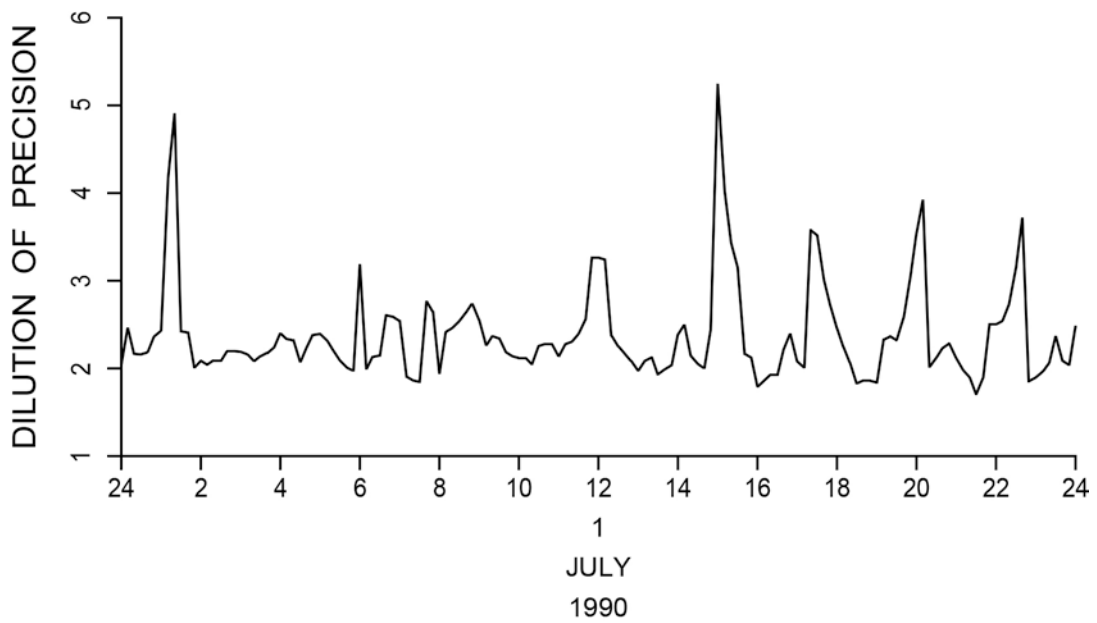


Fig. 11: Geometric dilution of precision

ACCURACY OF SINGLE DIFFERENCE PROCESSING

STATION 1 : RONNEBURG

STATION 2 : MELIBOCUS

Latitude : 50.240 degrees

Latitude : 49.726 degrees

Longitude : 9.064 degrees

Longitude : 8.637 degrees

Height : 228 meter

Height : 515 meter

Baseline Length : 64806.1 (m)

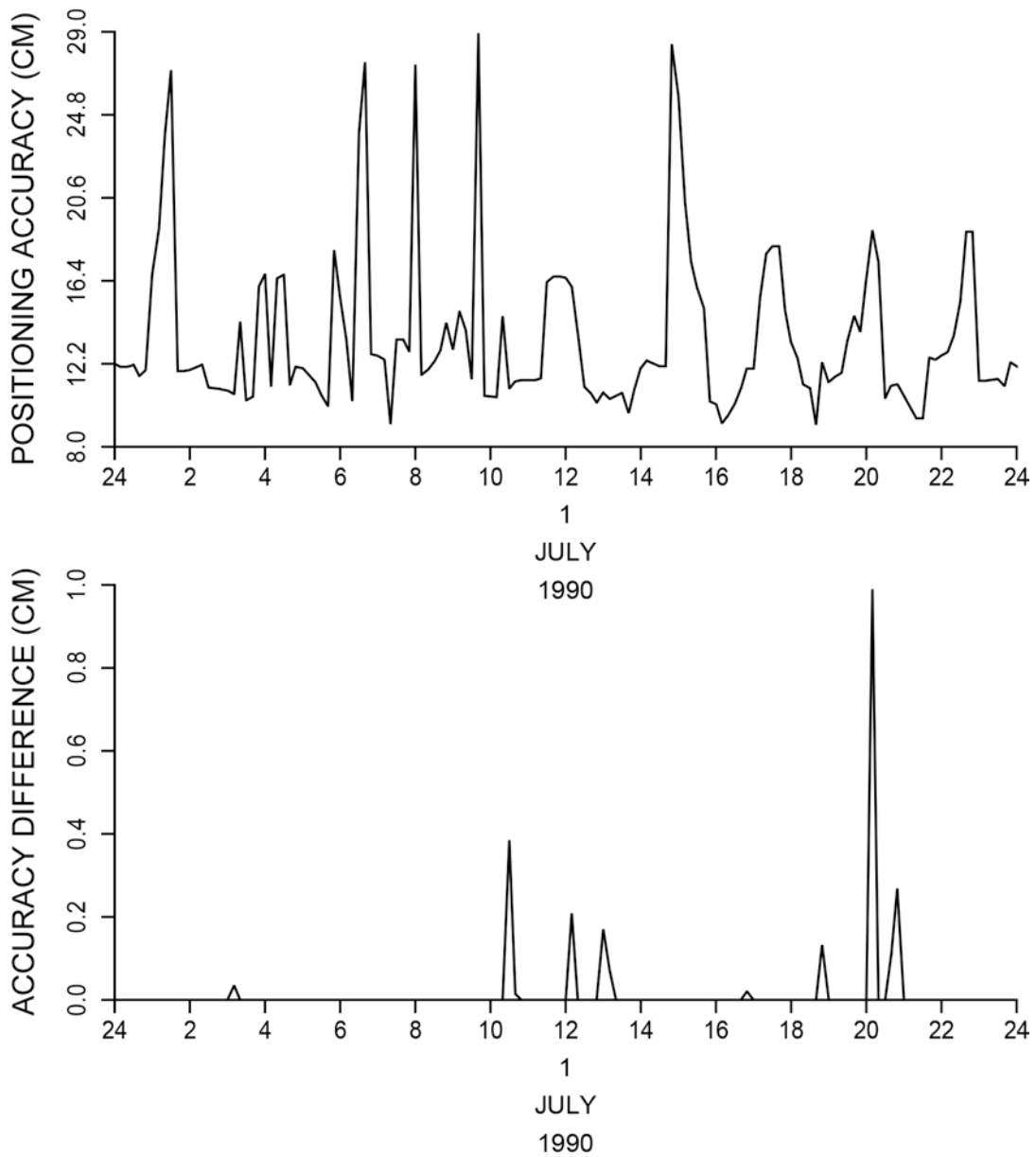


Fig. 12: Single difference processing

ACCURACY OF DOUBLE DIFFERENCE PROCESSING

STATION 1 : RONNEBURG

STATION 2 : MELIBOCUS

Latitude : 50.240 degrees

Latitude : 49.726 degrees

Longitude : 9.064 degrees

Longitude : 8.637 degrees

Height : 228 meter

Height : 515 meter

Baseline Length : 64806.1 (m)

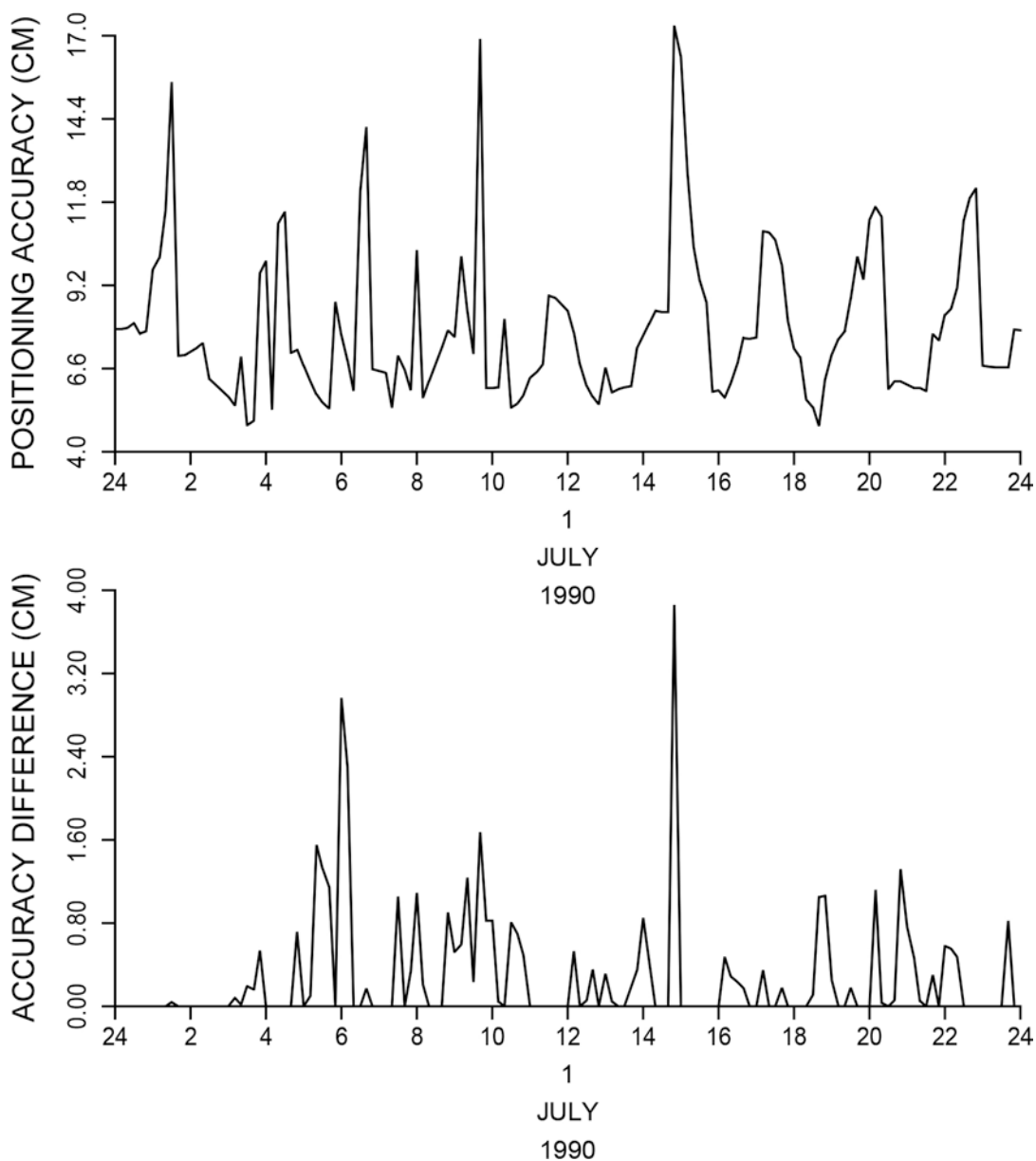


Fig. 13a: Double difference processing (case 0:0)

ACCURACY OF DOUBLE DIFFERENCE PROCESSING

STATION 1 : RONNEBURG

STATION 2 : MELIBOCUS

Latitude : 50.240 degrees

Latitude : 49.726 degrees

Longitude : 9.064 degrees

Longitude : 8.637 degrees

Height : 228 meter

Height : 515 meter

Baseline Length : 64806.1 (m)

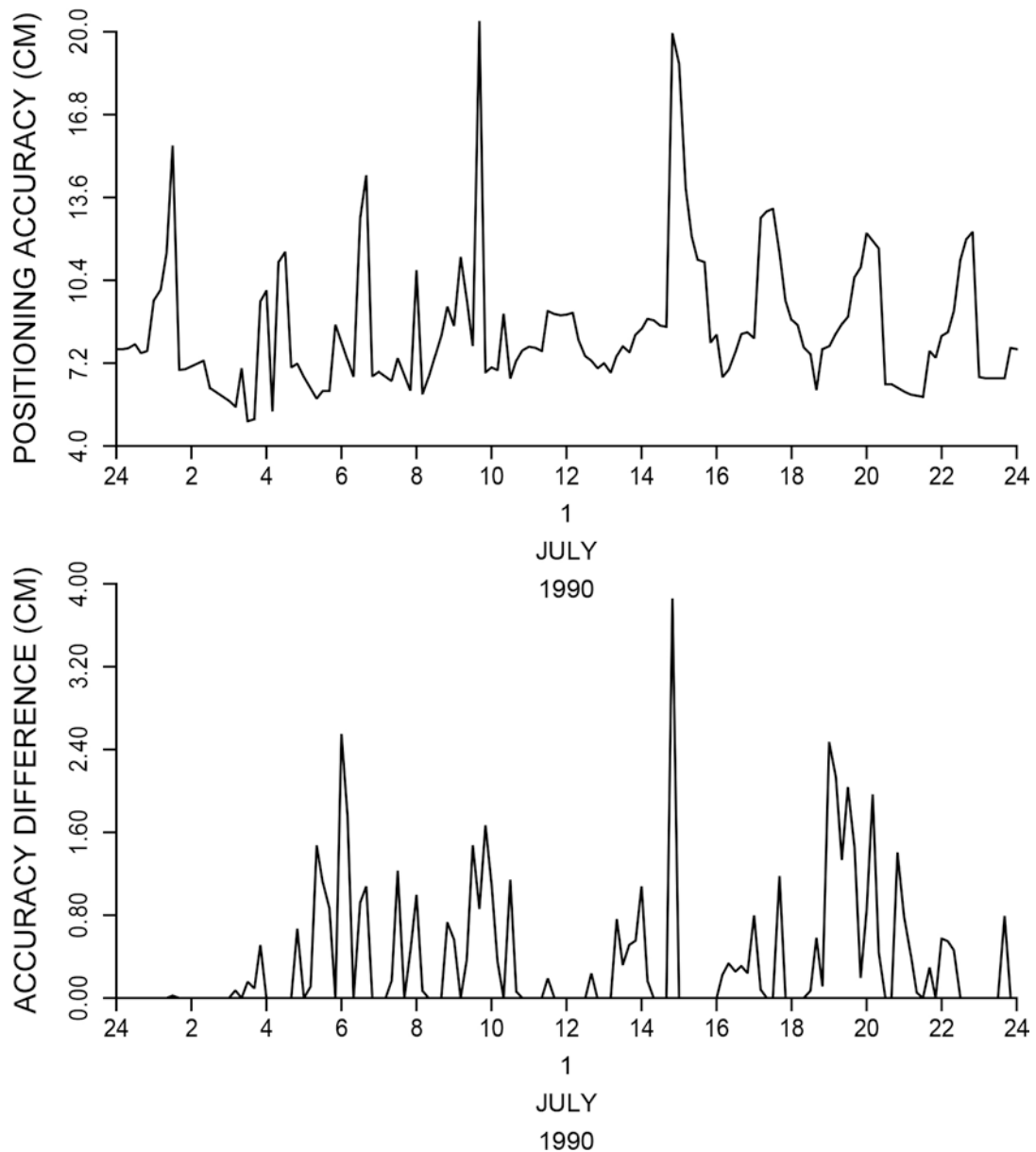


Fig. 13b: Double difference processing (case 2:0)

ACCURACY OF DOUBLE DIFFERENCE PROCESSING

STATION 1 : RONNEBURG

STATION 2 : MELIBOCUS

Latitude : 50.240 degrees

Latitude : 49.726 degrees

Longitude : 9.064 degrees

Longitude : 8.637 degrees

Height : 228 meter

Height : 515 meter

Baseline Length : 64806.1 (m)

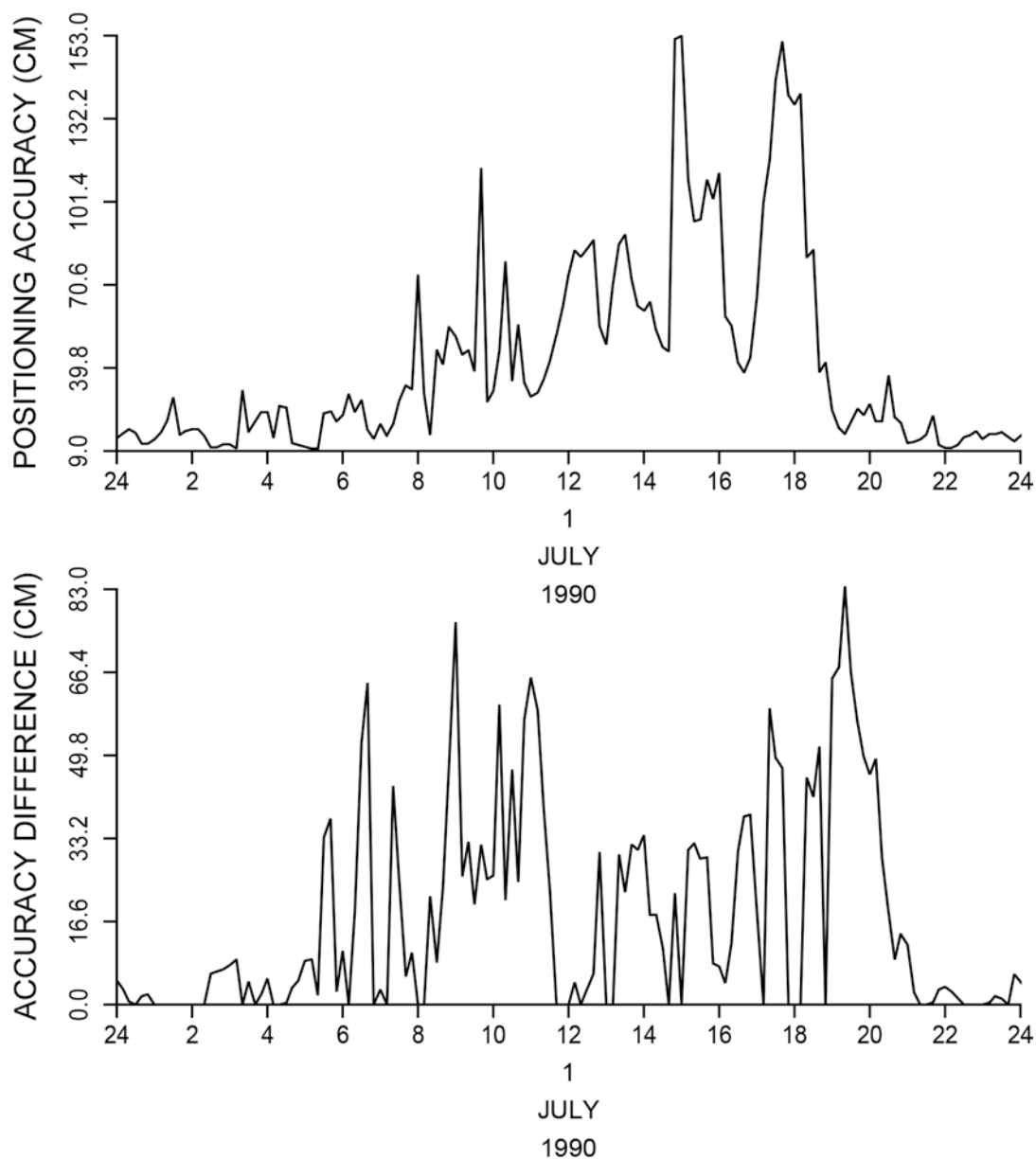


Fig. 13c: Double difference processing (case 1:0)

ACCURACY OF DOUBLE DIFFERENCE PROCESSING

STATION 1 : RONNEBURG

STATION 2 : MELIBOCUS

Latitude : 50.240 degrees

Latitude : 49.726 degrees

Longitude : 9.064 degrees

Longitude : 8.637 degrees

Height : 228 meter

Height : 515 meter

Baseline Length : 64806.1 (m)

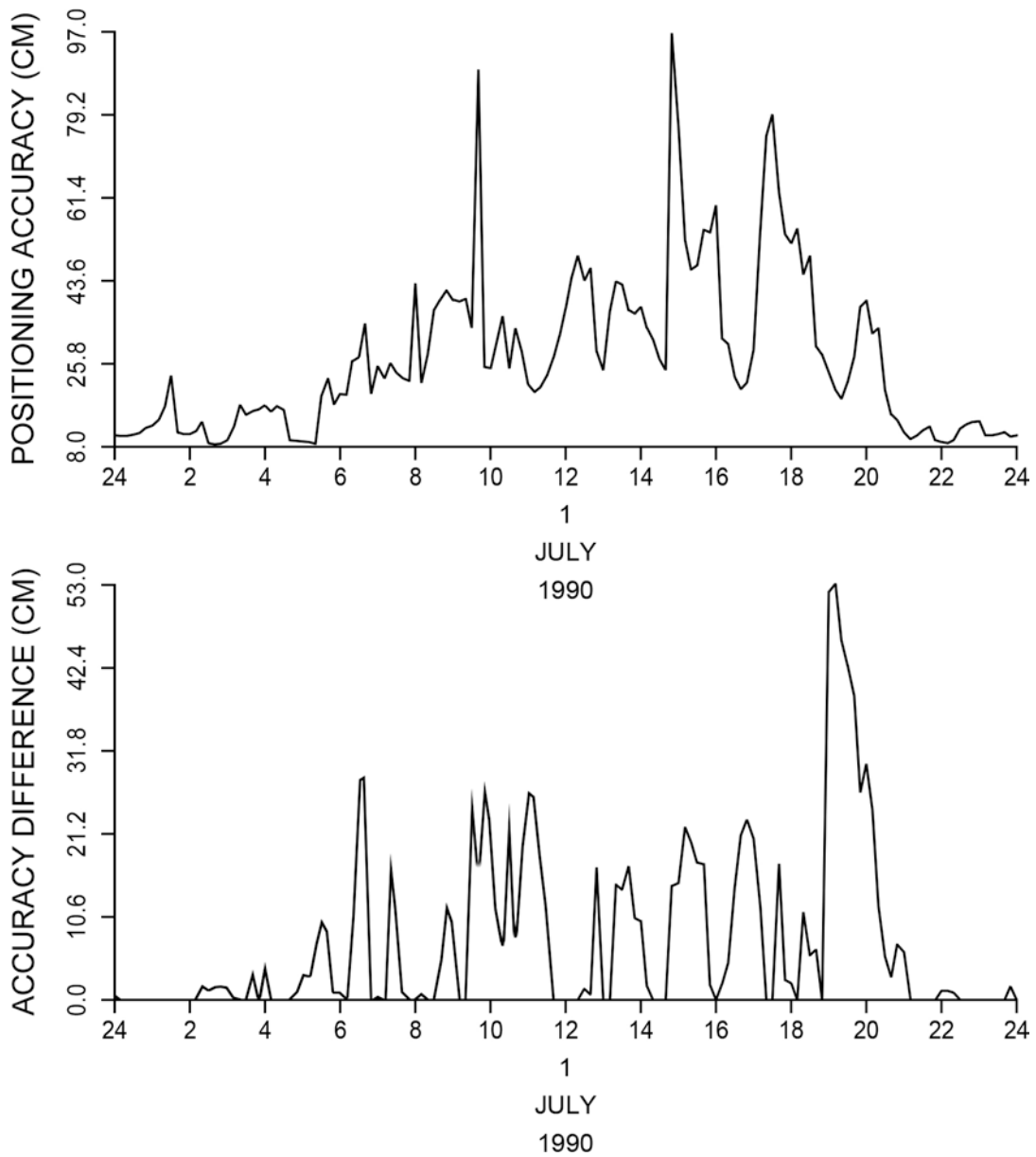


Fig. 13d: Double difference processing (case 3:1)

ACCURACY OF DOUBLE DIFFERENCE PROCESSING

STATION 1 : RONNEBURG

STATION 2 : MELIBOCUS

Latitude : 50.240 degrees

Latitude : 49.726 degrees

Longitude : 9.064 degrees

Longitude : 8.637 degrees

Height : 228 meter

Height : 515 meter

Baseline Length : 64806.1 (m)

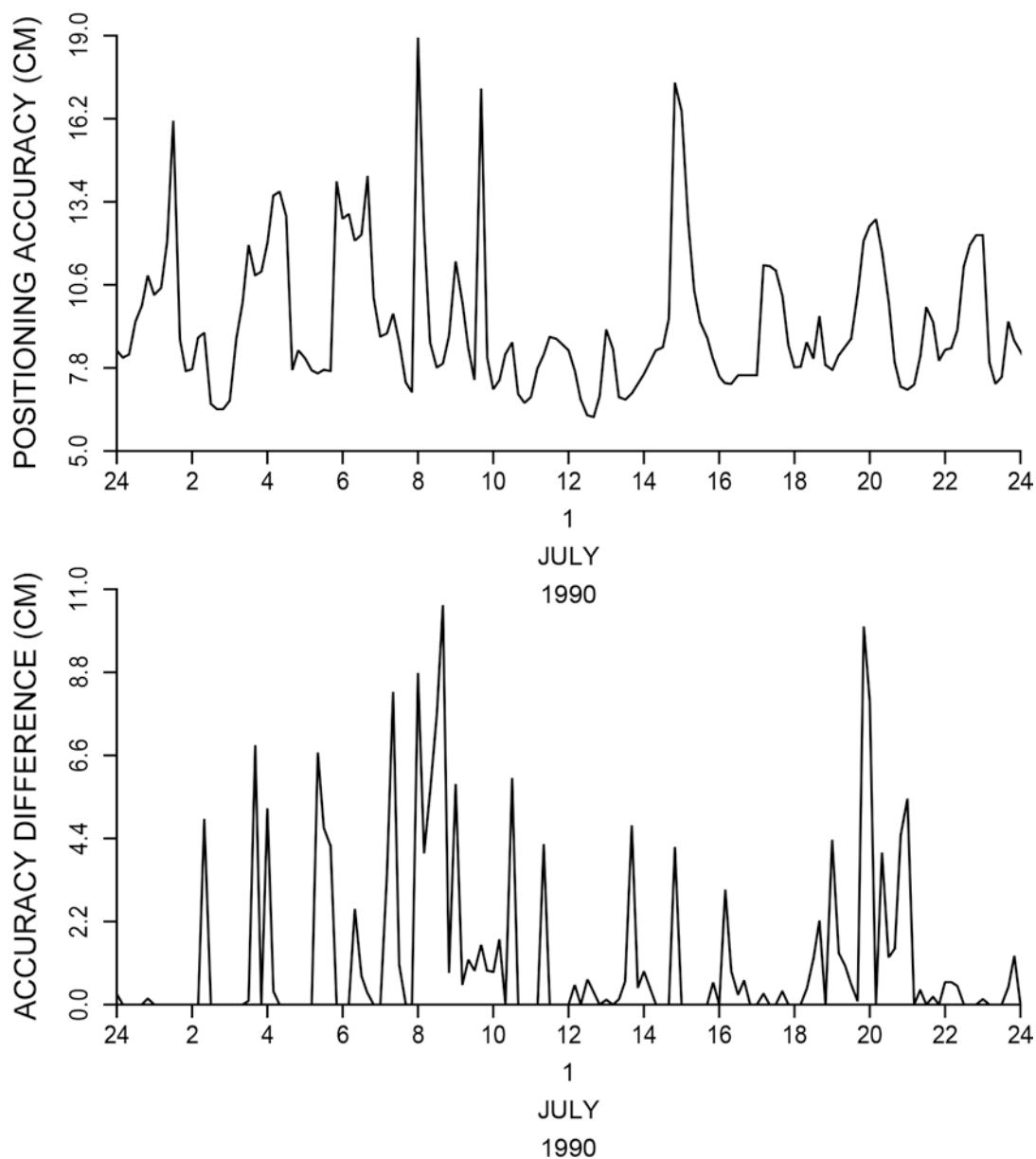


Fig. 13e: Double difference processing (case 0:1)

ACCURACY OF DOUBLE DIFFERENCE PROCESSING

STATION 1 : RONNEBURG

STATION 2 : MELIBOCUS

Latitude : 50.240 degrees

Latitude : 49.726 degrees

Longitude : 9.064 degrees

Longitude : 8.637 degrees

Height : 228 meter

Height : 515 meter

Baseline Length : 64806.1 (m)

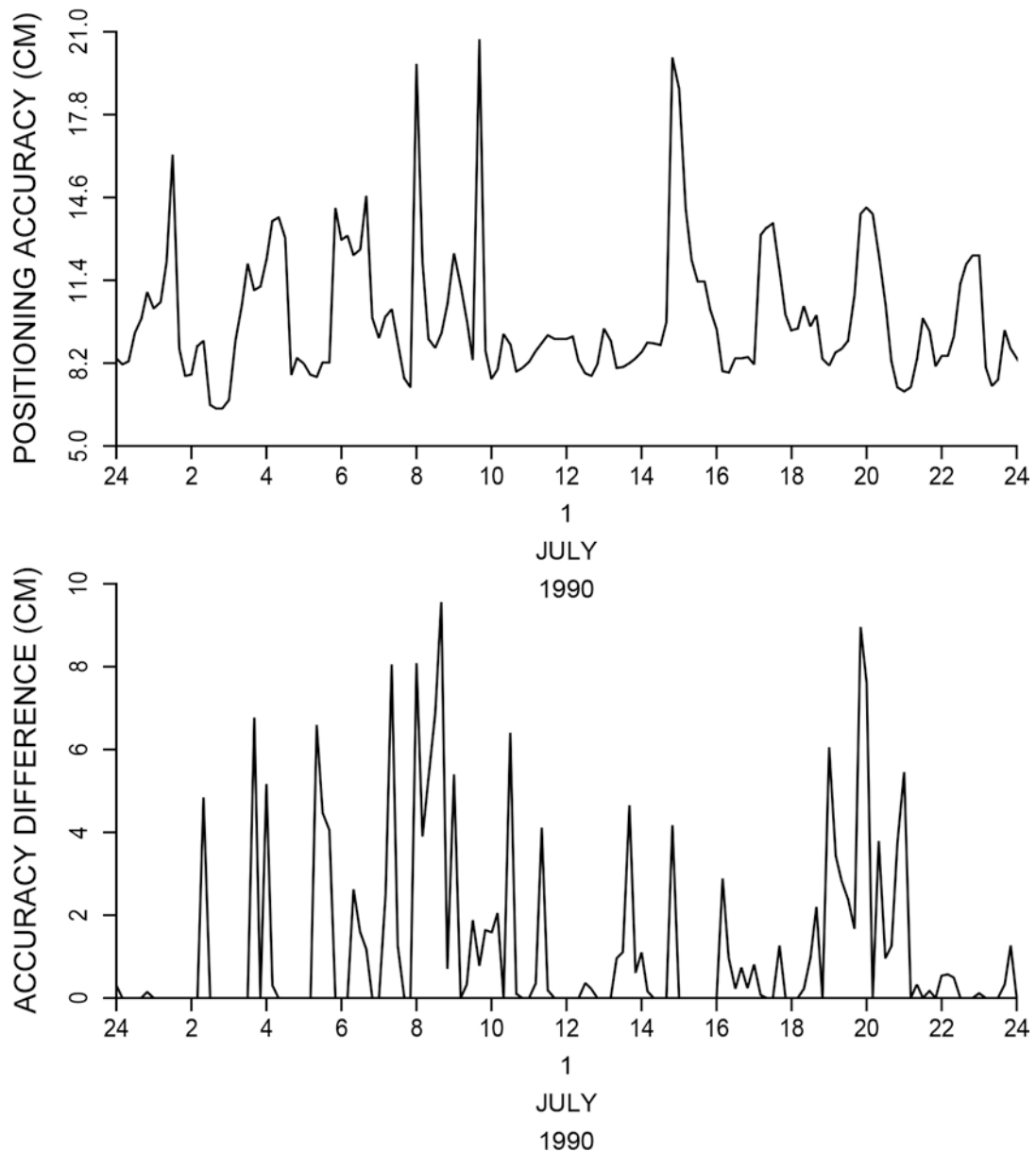


Fig. 13f: Double difference processing (case 2:1)

ACCURACY OF DOUBLE DIFFERENCE PROCESSING

STATION 1 : RONNEBURG

STATION 2 : MELIBOCUS

Latitude : 50.240 degrees

Latitude : 49.726 degrees

Longitude : 9.064 degrees

Longitude : 8.637 degrees

Height : 228 meter

Height : 515 meter

Baseline Length : 64806.1 (m)

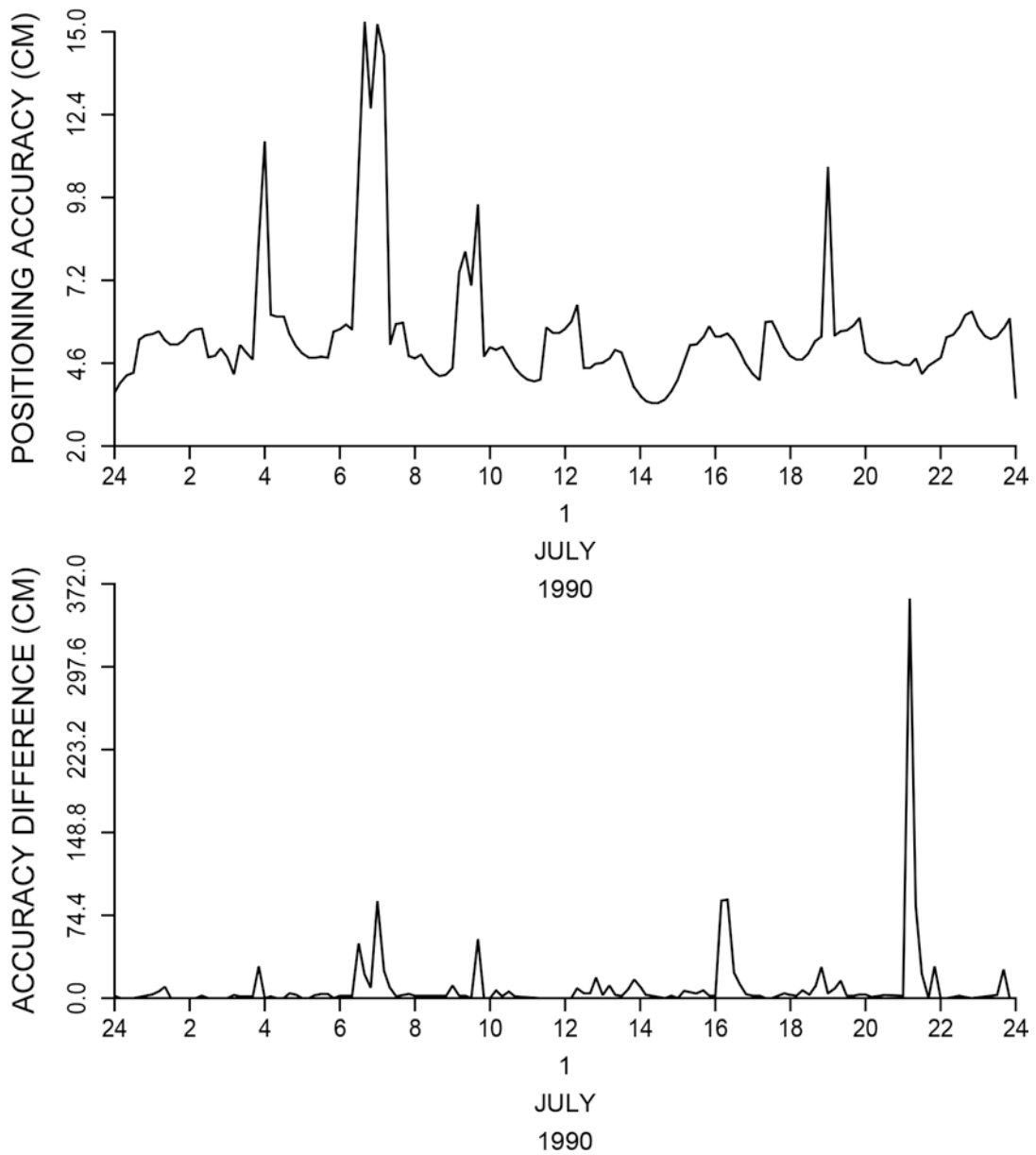


Fig. 14: Triple difference processing

SATELLITE PASSES OF THE NAVSTAR-GPS SYSTEM

STATION : RONNEBURG

Latitude : 50.240 degrees

Longitude : 9.064 degrees

Height : 228 meter

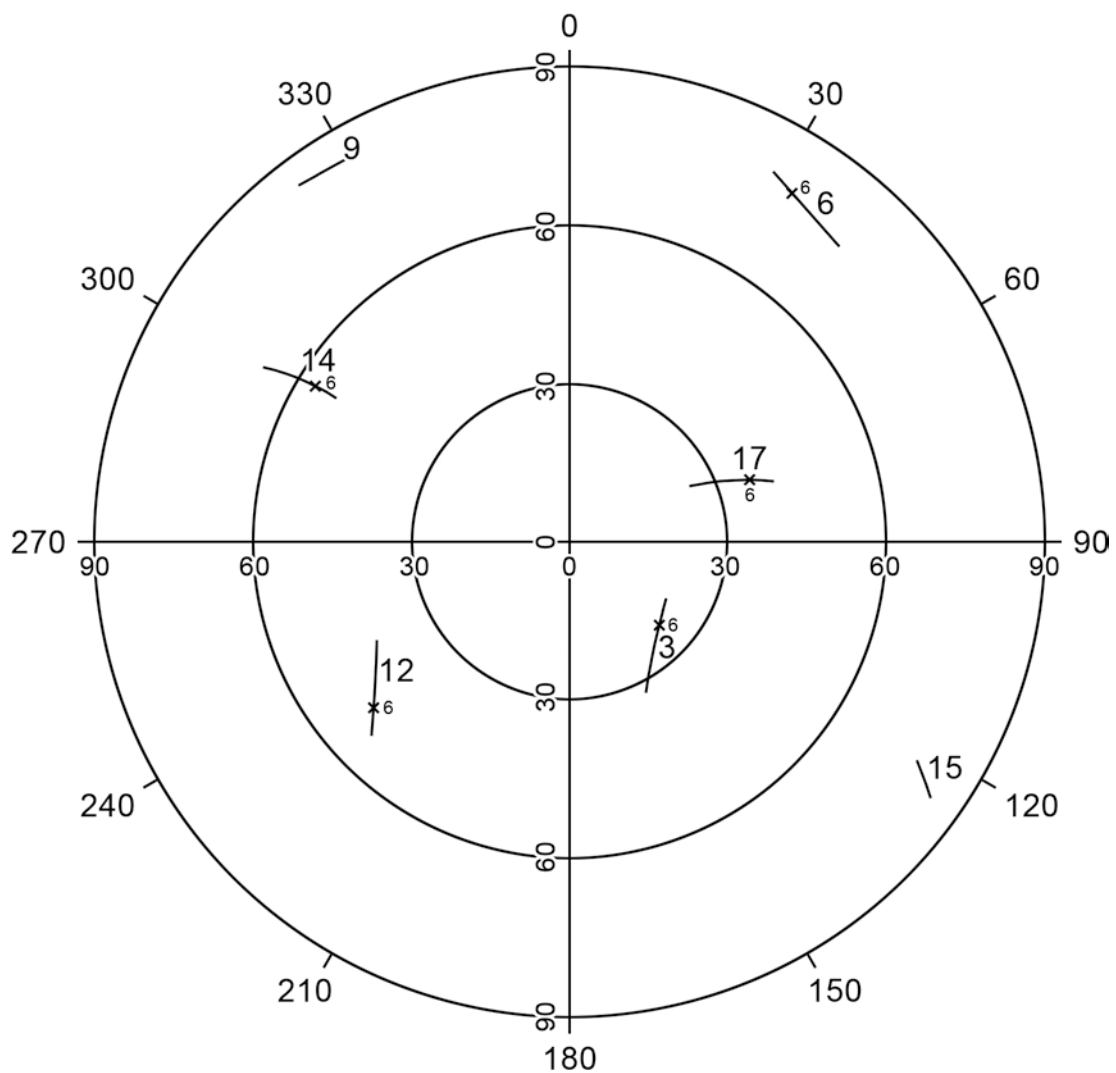


Fig. 15: Satellite configuration at about 6 am

ACCURACY OF DIFFERENCE PROCESSING

STATION 1 : RONNEBURG

STATION 2 : MELIBOCUS

Latitude : 50.240 degrees

Latitude : 49.726 degrees

Longitude : 9.064 degrees

Longitude : 8.637 degrees

Height : 228 meter

Height : 515 meter

Baseline Length : 64806.1 (m)

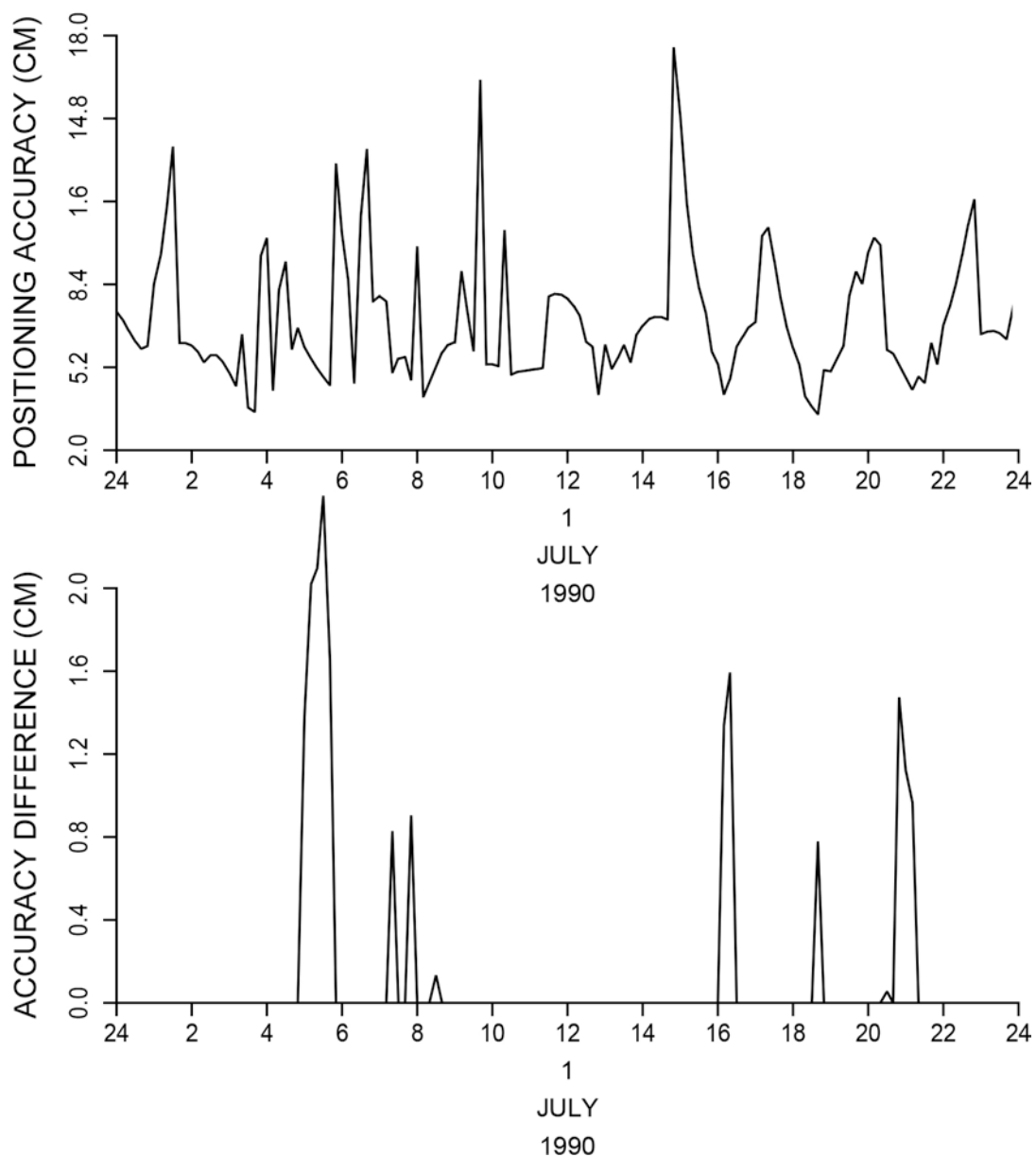


Fig. 16: Double difference processing (6-channel receiver)

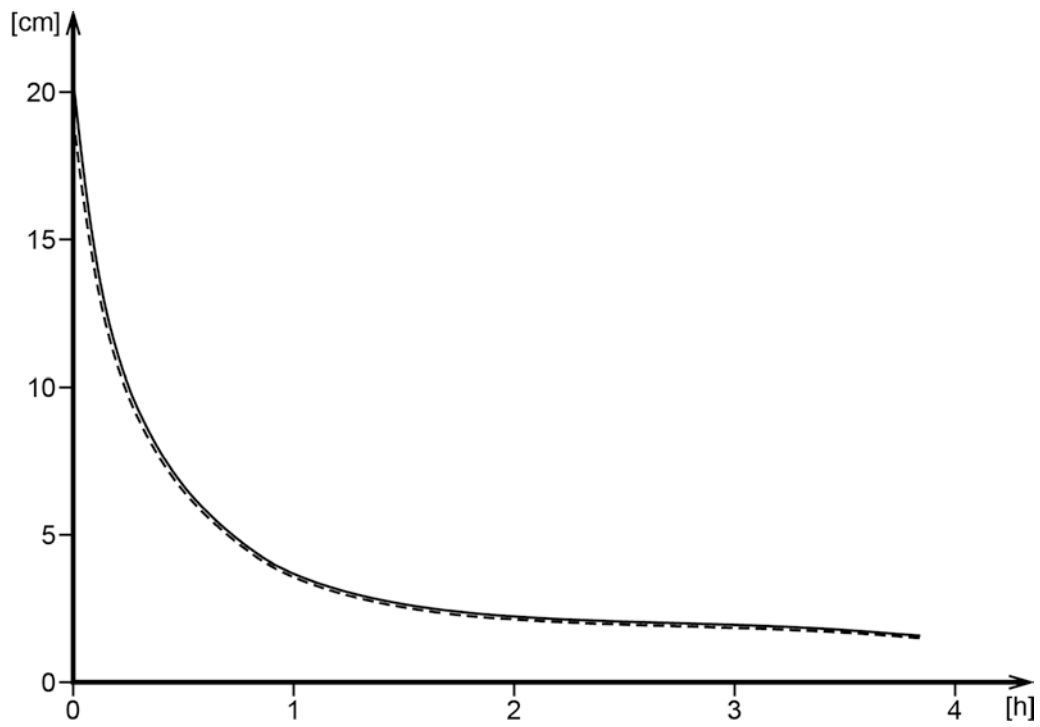


Fig. 17: Comparison of achieved accuracies with double difference processing. 1) 4-channel receiver (—) 2) 6-channel receiver (---)

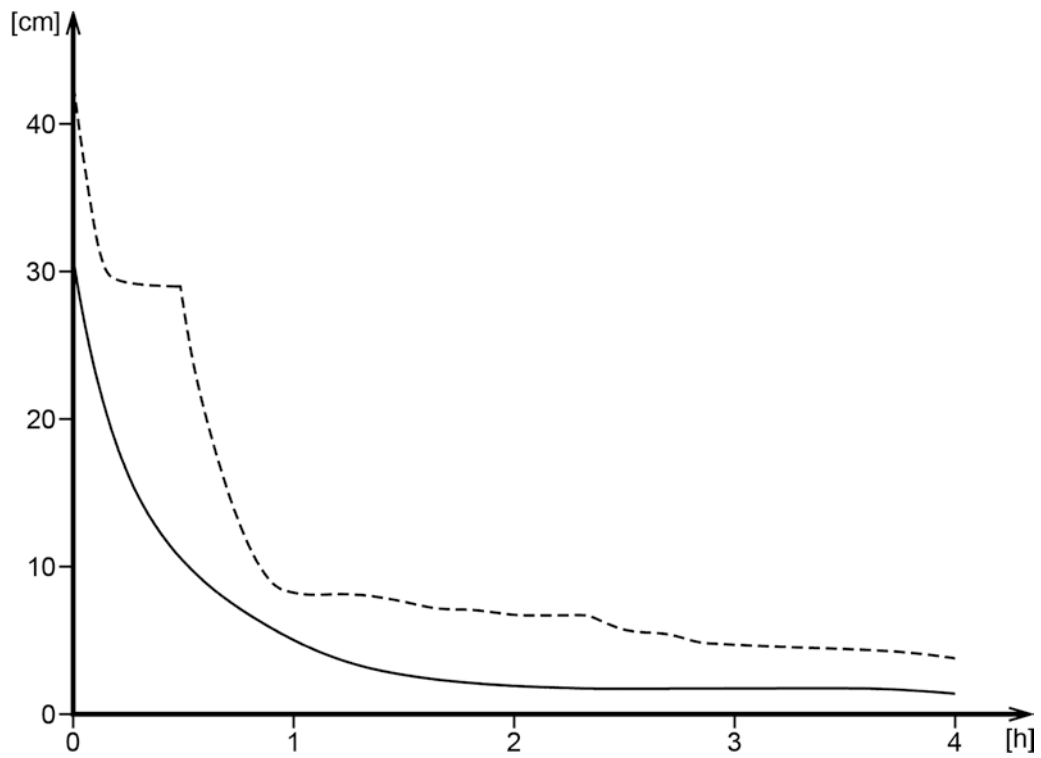


Fig. 18: Comparison of achieved accuracies with triple difference processing. 1) optimal selection method (—) 2) conventional selected method (---)

THE ESTIMATION OF ORTHOMETRIC HEIGHTS FROM GPS BASELINE VECTORS USING GRAVITY FIELD INFORMATION AND LEAST-SQUARES COLLOCATION

Bernd Eissfeller
University FAF Munich
Institute of Astronomical and Physical Geodesy
Werner-Heisenberg-Weg 39
8014 Neubiberg, F.R. Germany

ABSTRACT. The adjustment of GPS baseline vectors in geodetic networks yields (among other quantities) very precise ellipsoidal height differences. Due to the fact that the (orthometric) heights in classical geodetic networks are defined physically referring to the geoid as vertical reference surface, heights above the ellipsoid are in principle of no use for geodetic and surveying applications.

The topic of this paper is to discuss a solution strategy for the separation of orthometric heights and relative geoidal heights, which can be done only by taking into account additional gravity field data in such an approach.

Starting with the basic observation of cartesian baseline vectors, a least-squares collocation solution strategy is presented. Minimizing the hybrid quadratic norm of observational noise and the functionals of the gravity disturbing potential (signals), ellipsoidal coordinates B , L , orthometric heights H , and geoidal undulations N can be estimated in a unified model approach.

1. INTRODUCTION

Although the basic observables of interferometric satellite geodesy are phase-measurements, the user of the GPS is mostly concerned with cartesian baseline vectors between the network stations.

The baseline components are derived by a preprocessing adjustment from single, double and triple differences (see e.g. REMONDI (1984), BOSSLER et al. (1980), HEIN and EISSFELLER (1985)) and are handed over to the user together with their variance-covariance matrix.

Referring to BOCK et al. (1984) the today obtainable accuracy of all three baseline components is about 1.6 ppm of baseline length (Macrometer Model V - 1000).

In consideration of this remarkable accuracy it is obvious to use GPS-baseline vectors not only for the improvement or estimation of horizontal coordinates, but also for the estimation of heights.

Cartesian baseline vectors are in principle purely geometrical quantities, which are determined a priori in WGS 72 (geocentric, GPS based earth-fixed reference frame).

It follows out of this, that if we transform the baseline components to a national (local) reference frame (three rotations and scale), it is easily possible to convert them into differences of ellipsoidal latitude B , longitude L and into differences of ellipsoidal heights h (EISSFELLER (1986), in this volume).

On the other hand the heights in national geodetic networks are physically defined orthometric heights H , referring to the geoid as reference surface.

In order to relate the precise differences in ellipsoidal heights, computed with the aid of GPS-baseline vectors to the national height systems, precise geoidal undulations or gravity field data are necessary.

It is well known, that the geoid has a very irregular geometry. Therefore relative large variations in geoidal heights even over short distances are to be expected. For example in mountainous regions a variation of the geoid about 1.5 m to 2.5 m/50 km is no rarity (SÜNKEL (1983)). Even in plain regions the variations of the geoid are larger than the r.m.s. error of ellipsoidal height-differences derived from the GPS.

Thus the topic of this paper is to discuss a solution strategy for the estimation of orthometric heights from GPS-baseline vectors only in combination with gravity field data.

The basic starting-point in this approach is to set the ellipsoidal heights h equal to the sum of geoidal heights N and orthometric heights H .

When doing so, we arrive finally at the general linear model of least-squares collocation with parameters (MORITZ (1980)). This model is usually solved by minimizing the hybrid norm of observational noise and gravity field functionals (signals). In particular this model approach implicitly comprises various possibilities of interpolation and improvement of geoidal heights.

2. OBSERVATION EQUATIONS

The observational data, considered in this paper, are cartesian baseline vectors, already adjusted coordinates and orthometric heights (e.g. the results of a national survey), geoidal undulations, gravity anomalies and deflections of the vertical.

The use of already adjusted coordinates is optional.

Concerning the gravity field data the user has the option to use all possible combinations of the data types mentioned above.

2.1 Observation equation of cartesian baseline components

Let $\underline{\tilde{x}}$ be the position vector of a network station in WGS 72 and \underline{x} the corresponding position vector in the national reference frame. The basic transformation relation between $\underline{\tilde{x}}$ and \underline{x} for two stations i, j is then given as

$$\underline{\tilde{x}}_i = \underline{\tilde{x}}_0 + \lambda \underline{R}(\underline{\epsilon}) \underline{x}_i \quad (2-1a)$$

$$\underline{\tilde{x}}_j = \underline{\tilde{x}}_0 + \lambda \underline{R}(\underline{\epsilon}) \underline{x}_j \quad (2-1b)$$

where

λ scale factor

$\underline{\epsilon}$ vector of Eulerian angles $\underline{\epsilon} = [\epsilon_1, \epsilon_2, \epsilon_3]^T$

$\underline{R}(\underline{\epsilon})$ matrix of rotations (WGS 72 to national datum)

$\underline{\tilde{x}}_0$ displacement vector of national reference frame (origin) in WGS 72

Using (2-1a,b) the baseline vector \underline{b}_{ij} in WGS 72 is obtained as the difference

$$\underline{b}_{ij} = \underline{\tilde{x}}_j - \underline{\tilde{x}}_i = \lambda \underline{R}(\underline{\epsilon}) (\underline{x}_j - \underline{x}_i) \quad (2-2)$$

Note, that the displacement vector $\underline{\tilde{x}}_0$ drops out (due to the difference in (2-2)) and is therefore an unestimable quantity.

The rotation angles $\underline{\epsilon}$ may be considered as small quantities, hardly exceeding 10" of arc. Therefore the matrix of Eulerian rotations $\underline{R}(\underline{\epsilon})$, which can be found e.g. in WOLF (1975), including the second order terms (approximation error ≤ 1.0 mm), is approximately given as

$$\underline{R}(\underline{\epsilon}) \doteq \begin{bmatrix} 1 - \frac{\epsilon_2^2}{2} - \frac{\epsilon_3^2}{2} & \epsilon_3 + \epsilon_1 \epsilon_2 & \epsilon_1 \epsilon_3 - \epsilon_2 \\ \epsilon_3 & 1 - \frac{\epsilon_1^2}{2} - \frac{\epsilon_3^2}{2} & \epsilon_2 \epsilon_3 + \epsilon_1 \\ \epsilon_2 & -\epsilon_1 & 1 - \frac{\epsilon_1^2}{2} - \frac{\epsilon_2^2}{2} \end{bmatrix} \quad (2-3)$$

Because the GPS user is primarily interested in ellipsoidal coordinates B, L and in heights, it is quite natural to involve in (2-2) the well-known relationship of \underline{x} on B, L, h .

Following HEISKANEN and MORITZ (1967) the transformation relation can be found to be

$$\underline{x}(\underline{u}, h) = \begin{bmatrix} (N(B)+h) & \cos B \cos L \\ (N(B)+h) & \cos B \sin L \\ \left(\frac{b^2}{a^2} N(B)+h\right) & \sin B \end{bmatrix} \quad (2-4a)$$

with

$$N(B) = \frac{c}{V(B)} = \frac{c}{(1+e'^2 \cos^2 B)^{1/2}} \quad (2-4b)$$

$$c = \frac{a^2}{b}, \quad e'^2 = \frac{a^2 - b^2}{b^2} \quad (2-4c), (2-4d)$$

and

$$\underline{u} = [B, L]^T \quad (2-4e)$$

$N(B)$ east-west radius of curvature of reference ellipsoid

B, L ellipsoidal latitude, longitude

h ellipsoidal heights

a, b semimajor, semiminor axis of reference ellipsoid

The decomposition of B, L, h in \underline{u} and h is due to the separation in horizontal coordinates and in heights.

The basic starting-point of the further discussion is to approximate the ellipsoidal height h by the sum of orthometric height H and geoidal height N . In addition to this N is replaced by Bruns formula, that is $N = T/j$.

Thus,

$$h \doteq H + \frac{T}{j} \quad (2-5)$$

where

T gravity disturbing potential

j normal gravity

Concerning eq. (2-5) it is assumed, that the neglect of the curvature and the torsion of the plumbline will cause only a small model error within centimeter level. In order to get the linear observation equation of \underline{b}_{ij} (2-2), we do the usual Taylor expansion near some approximate values $\lambda^0, \epsilon^0, \underline{u}^0, H^0$ and T^0 .

This yields

$$\delta \underline{b}_{ij} = \underline{b}_{ij} - \underline{b}_{ij}^0 \quad \text{or} \quad (2-6a)$$

$$\begin{aligned} \delta \underline{b}_{ij} = & \frac{\partial \underline{b}_{ij}}{\partial \lambda} \delta \lambda + \frac{\partial \underline{b}_{ij}}{\partial \underline{\epsilon}} \delta \underline{\epsilon} + \frac{\partial \underline{b}_{ij}}{\partial \underline{u}_j} \delta \underline{u}_j - \frac{\partial \underline{b}_{ij}}{\partial \underline{u}_i} \delta \underline{u}_i + \\ & + \frac{\partial \underline{b}_{ij}}{\partial H_j} \delta H_j - \frac{\partial \underline{b}_{ij}}{\partial H_i} \delta H_i + \frac{1}{j} \frac{\partial \underline{b}_{ij}}{\partial H_j} \delta T_j - \frac{1}{j} \frac{\partial \underline{b}_{ij}}{\partial H_i} \delta T_i \end{aligned} \quad (2-6b)$$

The partial derivatives in eq. (2-6b), stored in Jacobi matrices and vectors, are defined as follows

$$\frac{\partial \underline{b}_{ij}}{\partial \lambda} = \underline{R}(\underline{\epsilon}) (\underline{x}_j - \underline{x}_i) \quad (2-7a)$$

$$\frac{\partial \underline{b}_{ij}}{\partial \underline{\epsilon}} = \lambda \begin{bmatrix} \epsilon_2 \Delta x_2 + \epsilon_3 \Delta x_3 & \epsilon_1 \Delta x_2 - \epsilon_2 \Delta x_1 - \Delta x_3 & \Delta x_2 - \epsilon_3 \Delta x_1 + \epsilon_1 \Delta x_3 \\ \Delta x_3 - \epsilon_1 \Delta x_2 & \epsilon_3 \Delta x_3 & \epsilon_2 \Delta x_3 - \epsilon_3 \Delta x_2 - \Delta x_1 \\ -\Delta x_2 - \epsilon_1 \Delta x_3 & \Delta x_1 - \epsilon_2 \Delta x_3 & 0 \end{bmatrix} \quad (2-7b)$$

with

$$\Delta x_1 = x_{1,j} - x_{1,i} \quad , \quad \Delta x_2 = x_{2,j} - x_{2,i} \quad \text{and} \quad \Delta x_3 = x_{3,j} - x_{3,i}$$

$$\frac{\partial \underline{b}_{ij}}{\partial \underline{u}_{i,j}} = \begin{bmatrix} \frac{\partial x_1}{\partial B} & \frac{\partial x_1}{\partial L} \\ \frac{\partial x_2}{\partial B} & \frac{\partial x_2}{\partial L} \\ \frac{\partial x_3}{\partial B} & \frac{\partial x_3}{\partial L} \end{bmatrix}_{i,j} \quad (2-7c) \quad \text{and} \quad \frac{\partial \underline{b}_{ij}}{\partial H_{i,j}} = \begin{bmatrix} \frac{\partial x_1}{\partial H} \\ \frac{\partial x_2}{\partial H} \\ \frac{\partial x_3}{\partial H} \end{bmatrix}_{i,j} \quad (2-7d)$$

For the elements of (2-7c,d) we find in particular with the north-south radius of curvature $M(B)$.

$$M(B) = \frac{c}{V(B)^3} = \frac{c}{(1 + e^2 \cos^2 B)^{3/2}} \quad (2-8)$$

$$\frac{\partial x_1}{\partial B} = -\left(M + H + \frac{T}{j}\right) \sin B \cos L \quad (2-9a)$$

$$\frac{\partial x_2}{\partial B} = -\left(M + H + \frac{T}{j}\right) \sin B \sin L \quad (2-9b)$$

$$\frac{\partial x_3}{\partial B} = -\left(M + H + \frac{T}{j}\right) \cos B \quad (2-9c)$$

$$\frac{\partial x_1}{\partial L} = -\left(N + H + \frac{T}{j}\right) \cos B \sin L \quad (2-10a)$$

$$\frac{\partial x_2}{\partial L} = -\left(N + H + \frac{T}{j}\right) \cos B \cos L \quad (2-10b)$$

$$\frac{\partial x_3}{\partial L} = 0 \quad (2-10c)$$

$$\frac{\partial x_1}{\partial H} = \cos B \cos L \quad (2-11a)$$

$$\frac{\partial x_2}{\partial H} = \cos B \sin L \quad (2-11b)$$

$$\frac{\partial x_3}{\partial H} = \sin B \quad (2-11c)$$

2.2 Observation equation for already adjusted coordinates

For at least some of the network stations of national control networks, where we perform GPS observations, results of former adjustments for B, L and orthometric heights H are available. The adjustment of these stations was usually done by conventional least-squares methods, based on terrestrial observations.

Because the original observations are often no more available, we propose to introduce the adjusted coordinates together with their variance-covariance matrix (as derived observations) in the adjustment of GPS-baseline

vectors as follows

$$\underline{u}_i = \underline{u}_i^0 + \delta \underline{u}_i \quad (2-12a)$$

or

$$\begin{bmatrix} B_i \\ L_i \end{bmatrix} = \begin{bmatrix} B_i^0 \\ L_i^0 \end{bmatrix} + \begin{bmatrix} \delta B_i \\ \delta L_i \end{bmatrix} \quad (2-12b)$$

and

$$H_i = H_i^0 + \delta H_i \quad (2-12c)$$

2.3 Observation equation of gravity field data

Because the variations δH and $\delta T/j$ in eq. (2-6b) are linear dependent (due to the same partial derivatives) the separation problem of ellipsoidal heights in orthometric and geoidal heights can only be solved with additional gravity field information.

As gravity field information, introduced in this context, we want to discuss geoidal undulations, gravity anomalies and deflections of the vertical.

With respect to the approximate value T^0 for the gravity disturbing potential (chapter 3) we are in the following only concerned with residual gravity field functionals. Following MORITZ (1980) the linear observation equations for residual geoidal heights, gravity anomalies and deflections of the vertical in a station i are given as

$$\delta N_i = \frac{\delta T_i}{j} \quad (2-13a)$$

$$\delta \Delta g_i = -\frac{\partial \delta T}{\partial R_i} - \frac{2\delta T_i}{R_i} \quad (2-13b)$$

$$\delta \xi_i = \frac{1}{j R_i} \frac{\partial \delta T_i}{\partial \varphi} \quad (2-13c)$$

$$\delta \eta_i = \frac{1}{j R_i \cos \varphi_i} \frac{\partial \delta T_i}{\partial \lambda} \quad (2-13d)$$

where R mean earth radius.

The approximate values for all the above residuals are found in applying the same linear operators to T^0 as to δT in (2-13a to d).

3. APPROXIMATE VALUE FOR THE GRAVITY DISTURBING POTENTIAL

In the chapter before we have already introduced an approximate value T^0 for the gravity disturbing potential.

If we know, such a T^0 , an approximate value for the orthometric height may be computed via $H^0 = h^0 - T^0/j$, where h^0 is the ellipsoidal height derived from baseline components.

This is relevant for the combination of baseline components with already adjusted or observed orthometric heights (2-12c).

Besides of this T^0 serves as a consistent reference value for the observation equation of baseline components and for the observed or computed gravity field functionals.

One might evidently assume, that in most countries no precise geoid is available. Similar to SÜNKEL (1983), we therefore propose to compose the approximate value T^0 by three different components.

Thus,

$$T^0 = T_{180} + T_{\text{trend}} + T_{\text{terrain}} , \quad (3-1)$$

where

T^0	approximate value
T_{180}	global trend based on earth-model (e.g. GEM-10C, $n = 180$)
T_{trend}	empirical (local) trend function
T_{terrain}	terrain correction

When introducing an approximate function T^0 for the disturbing potential itself, we have to reduce all the gravity field data too in applying the respective linear operators (SÜNKEL (1983)) on T^0 .

Thus,

$$N^0 = \frac{T^0}{j} \quad (3-2a)$$

$$\Delta g^0 = -\frac{\partial T^0}{\partial R} - \frac{2 T^0}{R} \quad (3-2b)$$

$$\xi^0 = \frac{1}{j R} \frac{\partial T^0}{\partial \varphi} \quad (3-2c)$$

$$\eta^0 = \frac{1}{j R \cos \varphi} \frac{\partial T^0}{\partial \lambda} \quad (3-2d)$$

In addition to the three components in (3-1) it might be reasonable in mountainous regions to introduce an isostatic reduction term as a fourth component (SÜNKEL (1983)).

3.1 Global trend T_{180}

The global trend of the disturbing potential T may be modeled with a spherical harmonic expansion of the geopotential, e.g. with the earth-model GEM-10 C of order and degree $n = 180$.

$$T_{180} = \frac{kM}{r} \sum_{\mu=1}^{180} \sum_{\nu=0}^{\mu} \left(\frac{R}{r}\right)^{\mu} P_{\mu\nu}(\sin \varphi) (C_{\mu\nu} \cos \nu\lambda + S_{\mu\nu} \sin \nu\lambda) \quad (3-3)$$

Note the presence of the term $\mu = 1$ in (3-3) (relative potential!). For the notation (3-3) see e.g. MORITZ (1980).

3.2 Local (empirical) trend T_{trend}

As already mentioned in the introduction the solution of the linear observational model, we are concerned with, is based on least-squares collocation, treating the residual disturbing potential δT and its functionals $\delta\Delta g$, $\delta\xi$ and $\delta\eta$ as signals.

Concerning the signals, we have at least approximately to fulfill the conditions (MORITZ (1980)) in the region of interest

$$E\{\delta T\} \doteq 0 \quad (3-4a)$$

$$E\{\delta\Delta g\} \doteq 0 \quad (3-4b)$$

$$E\{\delta\xi\} \doteq 0 \quad (3-4c)$$

$$E\{\delta\eta\} \doteq 0 \quad (3-4d)$$

where

$E\{\cdot\}$ is the expectation operator.

However, it cannot be expected, that the conditions (3-4a to d) are fulfilled, if we consider a local network and take only the global trend T_{180} into account.

3.2.1 Trend polynomial

The most simple expression for T_{trend} is a linear trend function with additional unknowns a_0 , a_1 , a_2 and a_3 .

$$T_{\text{trend}} = a_0 + a_1(h - h_0) + a_2(\varphi - \varphi_0) + a_3(\lambda - \lambda_0) \quad (3-5)$$

where

$(h_0)h$ (mean) height

$(\varphi_0)\varphi$ (mean) latitude

$(\lambda_0)\lambda$ (mean) longitude

The mean values h_0 , φ_0 , λ_0 are the mean values of the region under consideration.

If we apply the respective linear operators to (3-5) (with the approximation $\frac{\partial}{\partial r} \doteq \frac{\partial}{\partial h}$), the corresponding trend functions for all the gravity field functionals can be found.

$$\Delta g_{\text{trend}} = 2 \frac{a_0}{R} - a_1 \left(1 + 2 \frac{(h-h_0)}{R} \right) - 2 \frac{a_2}{R} (\varphi - \varphi_0) - 2 \frac{a_3}{R} (\lambda - \lambda_0) \quad (3-6a)$$

$$\xi_{\text{trend}} = \frac{a_2}{j R} \quad (3-6b)$$

$$\eta_{\text{trend}} = \frac{a_3}{j R \cos \varphi} \quad (3-6c)$$

Note, that all trend functions have to observe the Laplace equation $\Delta T = 0$.

Concerning (3-5), the Laplace equation causes a linear relation between a_1 and a_2 .

$$a_2 = \frac{2 R}{\tan \varphi} a_1 \quad (3-7)$$

In practice trend elimination with polynomials (3-5) will be restricted to the case, where information on the disturbing potential is already available (existing geoid!). Only in this case a significant estimation of a_0 can be expected.

3.2.2 Trend elimination based on Stokes integral

In general we may assume, that completely no geoidal information is available, or if such information is available, the accuracy of geoidal heights is not sufficient.

Usually we start here with observed gravity anomalies in order to improve the geoid, because gravity anomalies are the only gravity field data, which is available densely spaced over large regions of a nation.

If we consider a local GPS network, the condition $E\{\delta \Delta g\} \doteq 0$ (3-4b) will be normally violated, because Δg_{180} does not represent a sufficient mean value.

Again one may fit an empirical polynomial to the remaining gravity anomalies $(\Delta g - \Delta g_{180})$ by a preprocessing adjustment, e.g.

$$\Delta g_{\text{trend}} = \Delta g - \Delta g_{180} = b_0 + b_1 (h - h_0) + b_2 (\varphi - \varphi_0) + b_3 (\lambda - \lambda_0) . \quad (3-8)$$

For the notation see eq. (3-5).

The basic problem is now to convert Δg_{trend} into a respective trend in the disturbing potential T_{trend} , because least-squares collocation will result only in residual disturbing potentials, when using trend corrected Δg values as input data.

A very simple approach to this conversion problem is to apply the Stokes operator on Δg_{trend} .

Thus,

$$T_{\text{trend}} = \frac{R}{4\pi} \iint_{\sigma} \Delta g_{\text{trend}} S(\psi) d\sigma . \quad (3-9)$$

With

$S(\psi)$ Stokes function

$\sigma, d\sigma$ surface and surface element of unit sphere.

The integration of all the polynomial terms in (3-8) via (3-9) may be performed by numerical methods.

3.3 Terrain correction T_{terrain}

According to SÜNKEL (1983) and to FORSBERG and TSCHERNING (1981) it is quite useful to remove the short wavelength gravity field from the disturbing potential and its functionals. The short wavelength gravity field is strongly correlated with the topography and can be removed by terrain corrections, based on Newton's integral.

The correction expressions T_{terrain} , $\Delta g_{\text{terrain}}$, ξ_{terrain} and η_{terrain} are given as follows

$$T_{\text{terrain}} = k \int_v \frac{\rho}{l} dv \quad (3-10a)$$

$$\Delta g_{\text{terrain}} = k \int_v \frac{(r^2 - R r \cos \psi - 2 l)^2}{r l^3} \rho dv \quad (3-10b)$$

$$\xi_{\text{terrain}} = -\frac{k R}{j} \int_v \frac{\sin \psi \cos \alpha}{l^3} \rho dv \quad (3-10c)$$

$$\eta_{\text{terrain}} = -\frac{k R}{j} \int_v \frac{\sin \psi \sin \alpha}{l^3} \rho dv \quad (3-10d)$$

with

$$l = (r^2 + R^2 - 2 r R \cos \psi)^{1/2} \quad (3-11)$$

ψ spherical distance between space point and integration point

r radial distance of space point

R mean earth radius

α azimuth of integration point relative to space point on the unit sphere

ρ density

v volume of integration.

The evaluation of the integrals (3-10a to d) provides a digital terrain model and a density hypothesis.

E.g. a digital terrain model is available in the FRG with a resolution of 100 m × 100 m.

Applying the terrain corrections, we may expect to get a smooth (homogeneous and isotropic) residual field for δT , $\delta \Delta g$, $\delta \xi$, $\delta \eta$. Besides of this the correction length of the covariance functions, e.g. $\text{cov}[\delta \Delta g, \delta \Delta g]$, $\text{cov}[\delta \Delta g, \delta T]$ and $\text{cov}[\delta T, \delta T]$ will increase.

4. LINEAR MODEL AND SOLUTION STRATEGY

If we rewrite the observation equations of GPS-baseline components (2-6b), of already adjusted coordinates (2-12a,b,c) and of gravity field functionals (2-13a to d) in vector-matrix notation, we arrive at the following linear model

$$\underline{l}_1 = \underline{A}_1 \underline{z}_1 + \underline{A}_2 \underline{z}_2 + \underline{R}_1 \underline{t} + \underline{n}_1 \quad (4-1a)$$

$$\underline{l}_2 = \underline{z}_1 + \underline{n}_2 \quad (4-1b)$$

$$\underline{l}_3 = \underline{R}_2 \underline{s} + \underline{n}_3 \quad (4-1c)$$

with

- \underline{l}_1 vector of observed baseline components
- \underline{l}_2 vector of already adjusted coordinates
- \underline{l}_3 vector of observed or computed gravity field data
- \underline{z}_1 unknown transformation parameters and unknown coordinates of old stations
- \underline{z}_2 unknown coordinates of new stations
- \underline{n}_i observational noise
- \underline{A}_i coefficient-matrices of parameters
- \underline{R}_i coefficient-matrices of gravity field signals, containing the respective linear operators
- \underline{t} disturbing potentials in the GPS stations
- \underline{s} disturbing potentials in the gravity field data stations

or more explicitly

$$\underline{l}_1 = [\dots \delta b_{ij} \dots]^T \quad (4-2a)$$

$$\underline{l}_2 = [\dots \delta B_i, \delta L_i, \delta H_i \dots]^T \quad (4-2b)$$

$$\underline{l}_3 = [\dots \delta T_i, \delta \Delta g_i, \delta \xi_i, \delta \eta_i \dots]^T \quad (4-2c)$$

$$\underline{z}_1 = [\delta\lambda, \delta\underline{\varepsilon}, \dots, \delta B_i, \delta L_i, \delta H_i, \dots]^T \quad (4-2d)$$

$$\underline{z}_2 = [\dots \delta B_i, \delta L_i, \delta H_i, \dots]^T \quad (4-2e)$$

$$\underline{t} = [\dots \delta T_i \dots]^T \quad (4-2f)$$

$$\underline{s} = [\dots \delta T_j \dots]^T \quad (4-2g)$$

As a priori statistics of noise and signals in the linear model (4-1) the following variance-covariance matrices are given.

$$\underline{C}_{11} = E \{ \underline{n}_1 \underline{n}_1^T \} \quad (4-3a)$$

$$\underline{C}_{22} = E \{ \underline{n}_2 \underline{n}_2^T \} \quad (4-3b)$$

$$\underline{C}_{33} = E \{ \underline{n}_3 \underline{n}_3^T \} \quad (4-3c)$$

$$\underline{C}_{tt} = E \{ \underline{t} \underline{t}^T \} \quad (4-3d)$$

$$\underline{C}_{ss} = E \{ \underline{s} \underline{s}^T \} \quad (4-3e)$$

$$\underline{C}_{st} = E \{ \underline{s} \underline{t}^T \} = \underline{C}_{ts}^T \quad (4-3f)$$

Because the vectors \underline{l}_1 , \underline{l}_2 and \underline{l}_3 are fairly different types of observations, the corresponding noise vectors \underline{n}_1 , \underline{n}_2 and \underline{n}_3 are assumed to be uncorrelated. This means for all i, j ($i \neq j$) that $\underline{C}_{ij} = \underline{0}$.

For the computation of the autocovariance matrices \underline{C}_{ss} , \underline{C}_{tt} and the cross-covariance matrix \underline{C}_{st} of the gravity field functionals see e.g. MORITZ (1980).

The linear model (4-1) is the general model of least-squares collocation with parameters.

Minimizing the hybrid norm (MORITZ (1980))

$$\begin{aligned} & \underline{n}_1^T \underline{C}_{11}^{-1} \underline{n}_1 + \underline{n}_2^T \underline{C}_{22}^{-1} \underline{n}_2 + \underline{n}_3^T \underline{C}_{33}^{-1} \underline{n}_3 + \\ & + [\underline{t}^T \underline{s}^T] \begin{bmatrix} \underline{C}_{tt} & \underline{C}_{ts} \\ \underline{C}_{ts}^T & \underline{C}_{ss} \end{bmatrix}^{-1} \begin{bmatrix} \underline{t} \\ \underline{s} \end{bmatrix} = \min \end{aligned} \quad (4-4)$$

estimates for the unknown parameters and the signals are found as

$$\underline{z}^* = \begin{bmatrix} \underline{z}_1 \\ \underline{z}_2 \end{bmatrix} = (\underline{A}^T \underline{D}^{-1} \underline{A})^{-1} \underline{A}^T \underline{D}^{-1} \underline{l} \quad (4-5a)$$

$$\underline{s}^* = \begin{bmatrix} \underline{t} \\ \underline{s} \end{bmatrix} = \begin{bmatrix} \underline{C}_{tt} & \underline{C}_{ts} \\ \underline{C}_{ts}^T & \underline{C}_{ss} \end{bmatrix} \underline{R}^T \underline{D}^{-1} (\underline{I} - \underline{A} \underline{z}^*) \quad (4-5b)$$

with

$$\underline{A} = \begin{bmatrix} \underline{A}_1 & \underline{A}_2 \\ \underline{0} & \underline{I} \\ \underline{0} & \underline{0} \end{bmatrix} \quad (4-6a), \quad \underline{R} = \begin{bmatrix} \underline{R}_1 \\ \underline{0} \\ \underline{R}_2 \end{bmatrix} \quad (4-6b)$$

$$\underline{C} = \begin{bmatrix} \underline{C}_{11} & \underline{0} & \underline{0} \\ \underline{0} & \underline{C}_{22} & \underline{0} \\ \underline{0} & \underline{0} & \underline{C}_{33} \end{bmatrix} \quad (4-6c), \quad \underline{l} = \begin{bmatrix} \underline{l}_1 \\ \underline{l}_2 \\ \underline{l}_3 \end{bmatrix} \quad (4-6d)$$

$$\text{and } \underline{D} = \begin{bmatrix} \underline{C}_{11} + \underline{R}_1 \underline{C}_{tt} \underline{R}_1^T & \underline{0} & \underline{R}_1 \underline{C}_{ts} \underline{R}_2^T \\ \underline{0} & \underline{C}_{22} & \underline{0} \\ \underline{R}_2 \underline{C}_{ts}^T \underline{R}_1^T & \underline{0} & \underline{C}_{33} + \underline{R}_2 \underline{C}_{ss} \underline{R}_2^T \end{bmatrix} \quad (4-6e)$$

The error statistics are given in MORITZ (1980) as

$$\underline{E}_{z^* z^*} = (\underline{A}^T \underline{D}^{-1} \underline{A})^{-1} \quad (4-7a)$$

$$\underline{E}_{s^* s^*} = \underline{C}_{s^* s^*} - \underline{C}_{s^* z^*} \underline{R}^T \underline{D}^{-1} (\underline{I} - \underline{A} \underline{E}_{z^* z^*} \underline{A}^T \underline{D}^{-1}) \underline{R} \underline{C}_{s^* s^*} . \quad (4-7b)$$

Equations (4-5a,b) may be written in a more direct form, if we use the block-matrix inversion formulas of the Appendix. Marking the elements of the inverses \underline{D}^{-1} with an asterisk and considering its symmetry, thus

$$\underline{D}^{-1} = \begin{bmatrix} \underline{D}_{11}^* & \underline{D}_{12}^* & \underline{D}_{13}^* \\ \underline{D}_{12}^{*T} & \underline{D}_{22}^* & \underline{D}_{23}^* \\ \underline{D}_{13}^{*T} & \underline{D}_{23}^{*T} & \underline{D}_{33}^* \end{bmatrix}, \quad (4-8)$$

we find for the six independent elements in (4-8) with the aid of Appendix B

$$\begin{aligned} \underline{D}_{11}^* = & \left\{ \underline{C}_{11} + \underline{R}_1 \underline{C}_{tt} \underline{R}_1^T - \underline{R}_2 \underline{C}_{ts} \underline{R}_2^T \left(\underline{C}_{33} + \underline{R}_2 \underline{C}_{ss} \underline{R}_2^T - \right. \right. \\ & \left. \left. - \underline{R}_2 \underline{C}_{ts} \underline{R}_1^T \left(\underline{C}_{11} + \underline{R}_1 \underline{C}_{tt} \underline{R}_1^T \right) \underline{R}_1 \underline{C}_{ts} \underline{R}_2^T \right)^{-1} \cdot \right. \\ & \left. \cdot \underline{R}_2 \underline{C}_{ts}^T \underline{R}_1 \right\}^{-1} \end{aligned} \quad (4-9a)$$

$$\underline{D}_{12}^* = \underline{0} \quad (4-9b)$$

$$\underline{D}_{13}^* = - \left(\underline{C}_{11} + \underline{R}_1 \underline{C}_{tt} \underline{R}_1^T \right)^{-1} \underline{R}_1 \underline{C}_{ts} \underline{R}_2^T \underline{D}_{33}^* \quad (4-9c)$$

$$\underline{D}_{22}^* = \underline{C}_{22}^{-1} \quad (4-9d)$$

$$\underline{D}_{23}^* = \underline{0} \quad (4-9e)$$

$$\begin{aligned} \underline{D}_{33}^* = & \left\{ \underline{C}_{33} + \underline{R}_2 \underline{C}_{ss} \underline{R}_2^T - \underline{R}_2 \underline{C}_{ts}^T \underline{R}_1^T \cdot \right. \\ & \left. \cdot \left(\underline{C}_{11} + \underline{R}_1 \underline{C}_{tt} \underline{R}_1^T \right) \underline{R}_1 \underline{C}_{ts} \underline{R}_2^T \right\}^{-1} \end{aligned} \quad (4-9f)$$

Denoting $\underline{A}^T \underline{D}^{-1}$ with \underline{N} , the block-matrix elements of \underline{N} are found as

$$\underline{N}_{11} = \underline{A}_1^T \underline{D}_{11}^* \underline{A}_1 + \underline{D}_{22}^* \quad (4-10a)$$

$$\underline{N}_{12} = \underline{A}_1^T \underline{D}_{11}^* \underline{A}_2 \quad (4-10b)$$

$$\underline{N}_{22} = \underline{A}_2^T \underline{D}_{11}^* \underline{A}_2 \quad (4-10c)$$

$$\underline{N}_{21} = \underline{N}_{12}^T \quad (4-10d)$$

With the four input blocks (4-10a up to d) it is easily possible to compute the blocks of $\underline{Q} = \underline{N}^{-1}$. For the relationship of \underline{Q}_{11} , \underline{Q}_{12} , \underline{Q}_{22} and \underline{Q}_{21} on \underline{N}_{11} , \underline{N}_{12} , \underline{N}_{22} and \underline{N}_{21} see the Appendix A.

With the so partitioned matrix expressions we find for the unknowns and signals

$$\begin{aligned} \underline{z}_1 = & \left(\underline{Q}_{11} \underline{A}_1^T + \underline{Q}_{12} \underline{A}_2^T \right) \underline{D}_{11}^* \underline{l}_1 + \underline{Q}_{11} \underline{D}_{22}^* \underline{l}_2 + \\ & + \left(\underline{Q}_{11} \underline{A}_1^T + \underline{Q}_{12} \underline{A}_2^T \right) \underline{D}_{13}^* \underline{l}_3 \end{aligned} \quad (4-11a)$$

$$\begin{aligned} \underline{z}_2 = & \left(\underline{Q}_{12}^T \underline{A}_1^T + \underline{Q}_{22} \underline{A}_2^T \right) \underline{D}_{11}^* \underline{l}_1 + \underline{Q}_{12}^T \underline{D}_{22}^* \underline{l}_2 + \\ & + \left(\underline{Q}_{12}^T \underline{A}_1^T + \underline{Q}_{22} \underline{A}_2^T \right) \underline{D}_{13}^* \underline{l}_3 \end{aligned} \quad (4-11b)$$

$$\begin{aligned} \underline{t} = & \left(\underline{C}_{tt} \underline{R}_1^T \underline{D}_{11}^* + \underline{C}_{ts} \underline{R}_2^T \underline{D}_{13}^* \right) \left(\underline{l}_1 - \underline{A}_1 \underline{z}_1 - \underline{A}_2 \underline{z}_2 \right) + \\ & + \left(\underline{C}_{tt} \underline{R}_1^T \underline{D}_{13}^* + \underline{C}_{ts} \underline{R}_2^T \underline{D}_{33}^* \right) \underline{l}_3 \end{aligned} \quad (4-11c)$$

$$\begin{aligned} \underline{s} = & \left(\underline{C}_{ts}^T \underline{R}_1^T \underline{D}_{11}^* + \underline{C}_{ss} \underline{R}_2^T \underline{D}_{13}^* \right) \left(\underline{l}_1 - \underline{A}_1 \underline{z}_1 - \underline{A}_2 \underline{z}_2 \right) + \\ & + \left(\underline{C}_{ts}^T \underline{R}_1^T \underline{D}_{13}^* + \underline{C}_{ss} \underline{R}_2^T \underline{D}_{33}^* \right) \underline{l}_3 \end{aligned} \quad (4-11d)$$

It can be seen from (4-11a up to d) how the observation groups \underline{l}_1 , \underline{l}_2 , \underline{l}_3 and the variance-covariance structure of noise and signals enter in the estimation procedure.

Besides of this, equations (4-11a to d) are also of practically significance.

In practice the vector \underline{l}_3 of gravity field data will be of much larger dimension as the observation vectors \underline{l}_1 and \underline{l}_2 together. Therefore it is quite reasonable to detach the matrix inversions concerned with \underline{l}_3 from those matrix inversions concerned with \underline{l}_1 and \underline{l}_2 .

Note again, that the vectors of unknowns \underline{z}_1 and \underline{z}_2 contain besides ellipsoidal coordinates B, L and transformation parameters the wanted orthometric heights H.

5. SUMMARY AND CONCLUSIONS

Geodetic positioning with the GPS is because on its high accuracy a very potential future surveying technique. It will certainly replace the today customary terrestrial surveying techniques in near future.

This statement should only be understood in the sense of national surveys.

If using the GPS only, e.g. without spirit levelling, the basic problem is the problem of deriving orthometric heights, which refer to the geoid.

We have clearly to state the fact, that ellipsoidal heights without further geoidal information are of no use for the surveyor (especially in mountain-regions).

In this paper a solution strategy for the estimation of orthometric heights and horizontal ellipsoidal coordinates from cartesian baseline components only in combination with gravity field data was proposed.

The underlying estimation procedure is the method of least-squares collocation with parameters.

Thus, additionally the proposed method will result in geoidal heights at all the GPS stations, making use of the interpolation properties of least-squares collocation.

The cost, which is to pay for this approach, is the requirement of a dense gravity field covering and of a digital terrain model in the whole area of a nation.

From a more practical point of view the concept of solution is the following:

- (i) use all the gravity field data available in the region of interested in order to compute a high precision geoid on a regular grid,
- (ii) arrange the geoidal data with the appropriate corrections or reductions (chapter 3) in a database,
- (iii) observe or reobserve the national geodetic networks with use of the GPS,
- (iv) use the method proposed to adjust the baseline components together with the geoidal heights stored in the vector \underline{l}_3 (4-1c).

If the data required is once arranged, the estimation of orthometric heights is reduced to a numerical problem.

And if in addition the geoidal heights and the digital heights are referred to a regular grid, like mentioned in (i), very powerful algorithms for the computation of terrain-corrections and the inversion of the variance-covariance matrix \underline{D} (4-6c) may be applied via the FFT (Fast Fourier Transformation).

The method proposed here starts with the basic decomposition $h = H + N$.

In contrast to the approach of ENGELIS, TSCHERNING and RAPP (1984), where orthometric heights are derived in a two step solution via $H = h - N$, where step one consists of the adjustment of baseline components (B, L, h) and step two of the computation of the geoid (N), the linear model (4-1) combines all the observations in a unique model approach.

Thus we may expect, that our approach will give the most realistic estimates of parameters and error statistics, because the variance-covariance structure of all the observations and of the gravity field functionals enter into the estimation procedure. Note, that the observed or computed gravity field functionals are not longer treated as errorless corrections.

Of course it would be possible to replace the orthometric heights in (2-5) by the corresponding mapping equation of potential differences into metric values, e.g. $H(P) = \frac{W_0 - W(P)}{g(P) + \alpha H(P)}$ (here Helmert's definition).

This approach can be found in HEIN (1985).

The linearization of the mapping equation, using the usual decomposition $W = U + T$, will result in the context of eq. (2-6b) in a more complex gravity disturbing potential signal structure.

This is, because via the linearization procedure the disturbing potential is introduced in the material station at earth-surface and in the projection point at the geoid too.

Appendix A

Inversion of a (2,2) symmetrical block-matrix

Let the matrix to be inverted be given as

$$\underline{N} = \begin{bmatrix} \underline{N}_{11} & \underline{N}_{12} \\ \underline{N}_{12}^T & \underline{N}_{22} \end{bmatrix} \quad (\text{A1})$$

Using the relations of Schur and Frobenius (WOLF (1975)), we find for the block elements of $\underline{Q} = \underline{N}^{-1}$ the following expressions

$$\underline{Q}_{11} = \left(\underline{N}_{11} - \underline{N}_{12} \underline{N}_{22}^{-1} \underline{N}_{12}^T \right)^{-1} \quad (\text{A2})$$

$$\underline{Q}_{12} = -\underline{N}_{11}^{-1} \underline{N}_{12} \underline{Q}_{22} \quad (\text{A3})$$

$$\underline{Q}_{22} = \left(\underline{N}_{22} - \underline{N}_{12}^T \underline{N}_{11}^{-1} \underline{N}_{12} \right)^{-1} \quad (\text{A4})$$

$$\underline{Q}_{21} = \underline{Q}_{12}^T \quad (\text{A5})$$

Appendix B

Inversion of a (3,3) symmetrical block-matrix

The matrix to be inverted is thus given as

$$\underline{N} = \begin{bmatrix} \underline{N}_{11} & \underline{N}_{12} & \underline{N}_{13} \\ \underline{N}_{12}^T & \underline{N}_{22} & \underline{N}_{23} \\ \underline{N}_{13}^T & \underline{N}_{23}^T & \underline{N}_{33} \end{bmatrix} \quad (\text{B1})$$

Similar to Appendix A the inverse block-matrix $\underline{Q} = \underline{N}^{-1}$ can be derived. For reasons of clearness it is useful to introduce some auxiliary matrices \underline{P}_{ij} .

$$\underline{P}_{11} = \underline{N}_{11} - \underline{N}_{12} \underline{N}_{22}^{-1} \underline{N}_{12}^T = \underline{P}_{11}^T \quad (\text{B2})$$

$$\underline{P}_{22} = \underline{N}_{22} - \underline{N}_{12}^T \underline{N}_{11}^{-1} \underline{N}_{12} = \underline{P}_{22}^T \quad (\text{B3})$$

$$\underline{P}_{33} = \underline{N}_{33} - \underline{N}_{13}^T \underline{N}_{11}^{-1} \underline{N}_{13} = \underline{P}_{33}^T \quad (\text{B4})$$

$$\underline{P}_{13} = \underline{N}_{13} - \underline{N}_{12}^T \underline{N}_{22}^{-1} \underline{N}_{23} = \underline{P}_{31}^T \quad (\text{B5})$$

$$\underline{P}_{23} = \underline{N}_{23} - \underline{N}_{12}^T \underline{N}_{11}^{-1} \underline{N}_{13} = \underline{P}_{32}^T \quad (\text{B6})$$

With the aid of the matrices \underline{P}_{ij} the block elements \underline{Q}_{ij} of \underline{Q} can be derived.

$$\underline{Q}_{11} = \left(\underline{P}_{11} - \underline{P}_{13} \underline{P}_{33}^{-1} \underline{P}_{13}^T \right)^{-1} \quad (\text{B7})$$

$$\underline{Q}_{22} = \left(\underline{P}_{22} - \underline{P}_{23} \underline{P}_{33}^{-1} \underline{P}_{23}^T \right)^{-1} \quad (\text{B8})$$

$$\underline{Q}_{33} = \left(\underline{P}_{33} - \underline{P}_{23}^T \underline{P}_{22}^{-1} \underline{P}_{23} \right)^{-1} \quad (\text{B9})$$

$$\underline{Q}_{12} = \underline{N}_{11}^{-1} \left(\underline{N}_{13} \underline{P}_{33}^{-1} \underline{P}_{23}^T - \underline{N}_{12} \right) \underline{Q}_{22} \quad (\text{B10})$$

$$\underline{Q}_{13} = \underline{N}_{11}^{-1} \left(\underline{N}_{12} \underline{P}_{22}^{-1} \underline{P}_{23} - \underline{N}_{13} \right) \underline{Q}_{33} \quad (\text{B11})$$

$$\underline{Q}_{23} = - \underline{P}_{22}^{-1} \underline{P}_{23} \underline{Q}_{33} \quad (\text{B12})$$

$$\underline{Q}_{21} = \underline{Q}_{12}^T \quad (\text{B13})$$

$$\underline{Q}_{31} = \underline{Q}_{13}^T \quad (\text{B14})$$

$$\underline{Q}_{32} = \underline{Q}_{23}^T \quad (\text{B15})$$

REFERENCES

- Bock, Y., Abbot, R.I., Counselman, C.C., Gourevitch, S.A., King, R.W., Paradis, A.R. (1984): *Geodetic accuracy of the Macrometer model V-1000*. Bulletin Géodésique 58-2, 211-221
- Bosser, I.D., Goad, C.C., Bender, P.L. (1980): *Using the global positioning system (GPS) for geodetic positioning*. Bulletin Géodésique 54, 553-563
- Eissfeller, B. (1986): *A Taylor series expansion for the transformation problem of cartesian baseline components into ellipsoidal coordinate differences*. In: GPS-research at the Institute of Astronomical and Physical Geodesy, Report No. 19, University FAF Munich
- Engelis, T., Tscherning, C.C., Rapp, R.H. (1984): *The precise computation of geoid undulation differences with comparison of results obtained from GPS*. Geophysical Research Letters 11-9, 821-824
- Forsberg, R., Tscherning, C.C. (1981): *The use of height data in gravity field approximation by collocation*. Journal of Geophysical Research, Vol. 86, B9, 7843-7854
- Hein, G.W., Eissfeller, B. (1985): *Integrated modelling of GPS-orbits and multi-baseline components*. Proceedings of First International Symposium on Precise Positioning with the Global Positioning System, April 15-19, Rockville, Maryland
- Hein, G.W. (1985): *Orthometric heights determination using GPS observations and the Integrated Adjustment Model*. NOAA Technical Report NOS 110 NGS 32, U.S. Department of Commerce, Rockville, MD
- Heiskanen, W.A., Moritz, H. (1967): *Physical Geodesy*. W.H. Freeman and Company, San Francisco and London, Library of Congress Catalogue Card Number: 66-24950
- Moritz, H. (1980): *Advanced Physical Geodesy*. Herbert Wichmann Verlag, Karlsruhe, Abacus Press, Tunbridge Wells, Kent, ISBN 3-87907-106-3
- Remondi, B.W. (1984): *Using the Global Positioning System (GPS) phase observable for relative geodesy: modelling, processing, and results*. Dissertation, The University of Texas
- Sünkel, H. (1983): *Geoidbestimmung, Berechnungen an der TU Graz, 2. Teil*. In: Das Geoid in Österreich. Geodätische Arbeiten Österreichs für die Internationale Erdmessung, Neue Folge, Band III, Graz
- Wolf, H. (1975): *Ausgleichsrechnung, Formeln zur praktischen Anwendung*. Ferd. Dummlers Verlag, Bonn, Dümmlerbuch 7835, ISBN 3-427-78351-0

GPS BASELINE VECTORS IN A THREEDIMENSIONAL
INTEGRATED ADJUSTMENT APPROACH

Herbert Landau
Institute of Astronomical and
Physical Geodesy
University FAF Munich
Werner-Heisenberg-Weg 39
D-8014 Neubiberg, F.R. Germany

ABSTRACT. The Global Positioning System (GPS) offers the possibility to determine coordinate differences in a three-dimensional coordinate system with high accuracy. In geodesy GPS will be able to replace (nearly) all surveying techniques currently used for observations between points separated by more than a few tens of kilometers. Therefore it is necessary to derive models for the integration of GPS-vectors in classical networks and coordinate systems.

GPS baseline vectors are pure geometrical values providing a coordinate determination in a 3D-Euclidian space.

In order to use the full potential of GPS it is necessary to solve the following problems:

- (i) The transformation problem
- (ii) The determination of orthometric heights

For that purpose the knowledge of high-precision geoid heights is required.

Integrated geodesy allows by combination of GPS baseline vectors with other geodetic observations the determination of both, pure geometric positions and dynamical parameters as orthometric and geoidal heights.

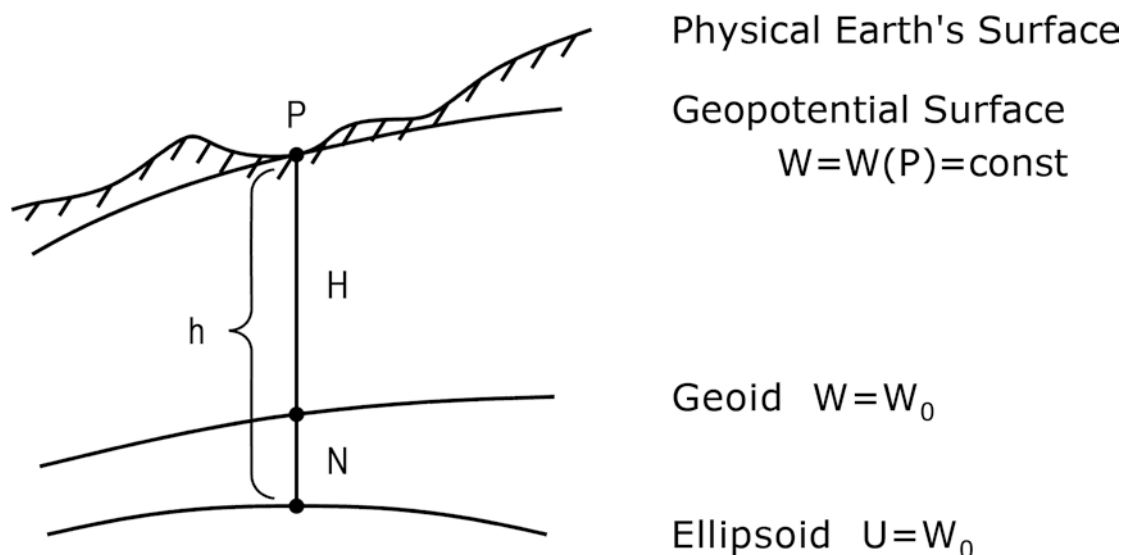
The results of numerical investigations are presented to show the efficiency of the integrated geodesy model in network adjustments using GPS baseline vectors.

1. INTRODUCTION

With the advent of the Global Positioning System (GPS) it is now possible to derive coordinate differences in an earth-fixed coordinate system with cm - accuracy. This extraterrestrial method for relative point positioning seems to be already fully accepted by the geodetic community. With the necessary integration of GPS baseline vectors derived from phase (difference) observations two major problems arise. This is the transformation problem between the different reference frames and the determination of the dynamical height component for geodetic purposes.

Although these extraterrestrial methods allow a (geometrical) height determination with cm - accuracy the derived ellipsoidal height alone is not sufficient for surveying applications.

In surveying and engineering the orthometric height above the geoid is preferred which differs from the ellipsoidal height by the geoidal undulation.



where h ... ellipsoidal height
 H ... orthometric height
 N ... geoid height

Figure 1

The knowledge of geoidal undulations is necessary (at least) for two purposes:

- (1) For all network points with fixed vertical components the geoidal height has to be known for the derivation of ellipsoidal heights. These (geometric) ellipsoidal heights are absolutely necessary for the determination of transformation parameters between the satellite reference frame and the local geodetic system.
- (2) For all stations with "free" vertical components it is necessary to know the geoidal height for the derivation of orthometric heights.

The geoidal height is a dynamic quantity which can be computed by applying integral formulas or collocation. Non-consideration of geoidal heights will lead to a decrease in horizontal positioning accuracy especially in mountainous areas. For example in the GPS-network of Hessen, which will be described later, the geoidal heights of the six network points differ up to two meters. In the following considerations the influence of neglecting of geoidal heights will be estimated more in detail.

The integration of GPS baseline vectors in the integrated geodesy model will allow a combination with "dynamical" parameters like potential differences, gravity and astronomical observations. Such an integrated approach will provide both, horizontal coordinates and orthometric heights, as well as geoidal undulations within one three-dimensional network adjustment.

2. A CONVENTIONAL APPROACH USING LEAST SQUARES ADJUSTMENT

The ephemeris data for the satellites of the NAVSTAR-system are given in the World Geodetic System 1972 (WGS 72). The derived baseline vectors are therefore defined in that system, too. For applications in surveying and engineering those coordinate differences have to be integrated in classical geodetic networks with a local datum definition like the German "Bessel" ellipsoid with the "Rauenberger Datum".

Different strategies have already been developed to solve this problem (WOLF 1985, SWIATEK 1984).

2.1 The mathematical model

Let us shortly describe a model using common least-squares adjustment following in principle STEEVES (1984).

A relation between two reference systems is given by the seven-parameter similarity transformation

$$\underline{\Delta x} = (1+K) \underline{R}_\omega \underline{\Delta x}_{OBS} \quad (2-1)$$

where

$\underline{\Delta x}_{OBS}$... is the vector of "observed" differences
in WGS 72

$\underline{\Delta x}$... is the vector of transformed coordinate differences
in the local reference system

K ... is a scale factor

and \underline{R}_ω ... is a rotation matrix of the following form

$$\begin{aligned} \underline{R}_\omega &= \begin{bmatrix} 1 & \omega_z & -\omega_y \\ -\omega_z & 1 & \omega_x \\ \omega_y & -\omega_x & 1 \end{bmatrix} \\ &= \begin{bmatrix} 1 & 0 & 0 \\ 0 & 1 & 0 \\ 0 & 0 & 1 \end{bmatrix} + \begin{bmatrix} 0 & \omega_z & -\omega_y \\ -\omega_z & 0 & \omega_x \\ \omega_y & -\omega_x & 0 \end{bmatrix} \end{aligned} \quad (2-2)$$

$$\underline{R}_\omega = \underline{I} + \underline{U}_\omega$$

Considering differential rotations

$$\underline{\Delta X} = \underline{R}_\omega \underline{\Delta X}_{OBS} = (\underline{I} + \underline{U}_\omega) \underline{\Delta X}_{OBS} = \underline{\Delta X}_{OBS} + \underline{U}_\omega \underline{\Delta X}_{OBS} \quad (2-3)$$

or

$$\underline{\Delta X} - \underline{\Delta X}_{OBS} = \underline{U}_\omega \underline{\Delta X}_{OBS} = \underline{\Delta U}_r \cdot \begin{bmatrix} \omega_x \\ \omega_y \\ \omega_z \end{bmatrix} \quad (2-4)$$

with

$$\underline{\Delta U}_r = \begin{bmatrix} 0 & -\Delta Z_{OBS} & \Delta Y_{OBS} \\ \Delta Z_{OBS} & 0 & -\Delta X_{OBS} \\ -\Delta Y_{OBS} & \Delta X_{OBS} & 0 \end{bmatrix} \quad (2-5)$$

and differential scale change we get

$$\underline{\Delta X} = (1 + K) \underline{\Delta X}_{OBS} = \underline{\Delta X}_{OBS} + K \underline{\Delta X}_{OBS} \quad (2-6)$$

or

$$\underline{\Delta X} - \underline{\Delta X}_{OBS} = K \cdot \underline{\Delta X}_{OBS} \quad (2-7)$$

By combination of both parts we get finally

$$\underline{\Delta X} - \underline{\Delta X}_{OBS} = \underline{\Delta U}_r \begin{bmatrix} \omega_x \\ \omega_y \\ \omega_z \end{bmatrix} + K \cdot \underline{\Delta X}_{OBS} \quad (2-8)$$

The observational equation is given by

$$d\underline{\Delta X}_{ij} = -d\underline{x}_i + d\underline{x}_j + \underline{\Delta U}_r \begin{bmatrix} \omega_x \\ \omega_y \\ \omega_z \end{bmatrix} + K \cdot \underline{\Delta X}_{OBS} + \underline{f}_{\Delta x \Delta y \Delta z} \quad (2-9)$$

with the "observation vector"

$$\underline{f}_{\Delta x \Delta y \Delta z} = \underline{\Delta X}_{OBS} - \underline{\Delta X}_0 \quad (2-10)$$

where $\Delta \underline{x}_0$ is a coordinate difference vector computed from the approximate coordinates of the network points.

The formulas above are given for an adjustment procedure in a cartesian coordinate system. Since we want to work in an ellipsoidal coordinate system the coefficients of the design matrix have to be transformed by the following relations

$$\frac{\partial l}{\partial \varphi} = \frac{\partial l}{\partial x} \cdot \frac{\partial x}{\partial \varphi} + \frac{\partial l}{\partial y} \cdot \frac{\partial y}{\partial \varphi} + \frac{\partial l}{\partial z} \cdot \frac{\partial z}{\partial \varphi}$$

$$\frac{\partial l}{\partial \lambda} = \frac{\partial l}{\partial x} \cdot \frac{\partial x}{\partial \lambda} + \frac{\partial l}{\partial y} \cdot \frac{\partial y}{\partial \lambda} + \frac{\partial l}{\partial z} \cdot \frac{\partial z}{\partial \lambda} \quad (2-11)$$

$$\frac{\partial l}{\partial h} = \frac{\partial l}{\partial x} \cdot \frac{\partial x}{\partial h} + \frac{\partial l}{\partial y} \cdot \frac{\partial y}{\partial h} + \frac{\partial l}{\partial z} \cdot \frac{\partial z}{\partial h}$$

The partial derivatives with respect to the ellipsoidal coordinates are defined in EISSFELLER et al. (1985).

$$\frac{\partial x}{\partial \varphi} = \left[\frac{a^2 - b^2}{a^4} N^3 \cos^2 \varphi - N - h \right] \sin \varphi \cos \lambda \quad (2-12a)$$

$$\frac{\partial y}{\partial \varphi} = \left[\frac{a^2 - b^2}{a^4} N^3 \cos^2 \varphi - N - h \right] \sin \varphi \sin \lambda \quad (2-12b)$$

$$\frac{\partial z}{\partial \varphi} = \left[\frac{b^2}{a^2} \cdot \frac{a^2 - b^2}{a^4} N^3 \sin^2 \varphi + \frac{b^2}{a^2} N + h \right] \cos \varphi \quad (2-12c)$$

$$\frac{\partial x}{\partial \lambda} = -(N + h) \cos \varphi \sin \lambda \quad (2-12d)$$

$$\frac{\partial y}{\partial \lambda} = (N + h) \cos \varphi \cos \lambda \quad (2-12e)$$

$$\frac{\partial z}{\partial \lambda} = 0 \quad (2-12f)$$

$$\frac{\partial x}{\partial h} = \cos \varphi \cos \lambda \quad (2-12g)$$

$$\frac{\partial y}{\partial h} = \cos \varphi \sin \lambda \quad (2-12h)$$

$$\frac{\partial z}{\partial h} = \sin \varphi \quad (2-12i)$$

The final observation equations are given by

$$\begin{bmatrix} d\Delta x_{ij} \\ d\Delta y_{ij} \\ d\Delta z_{ij} \end{bmatrix} = -\underline{I}_i \cdot \begin{bmatrix} d\varphi_i \\ d\lambda_i \\ dh_i \end{bmatrix} + \underline{I}_j \cdot \begin{bmatrix} d\varphi_j \\ d\lambda_j \\ dh_j \end{bmatrix} + \Delta \underline{U}_r \cdot \begin{bmatrix} \omega_x \\ \omega_y \\ \omega_z \end{bmatrix} + K \Delta x_{OBS} + \underline{f}_{\Delta x \Delta y \Delta z} \quad (2-13)$$

where \underline{I} is a matrix of the following structure

$$\underline{I} = \begin{bmatrix} \frac{\partial \Delta x}{\partial \varphi} & \frac{\partial \Delta x}{\partial \lambda} & \frac{\partial \Delta x}{\partial h} \\ \frac{\partial \Delta y}{\partial \varphi} & \frac{\partial \Delta y}{\partial \lambda} & \frac{\partial \Delta y}{\partial h} \\ \frac{\partial \Delta z}{\partial \varphi} & \frac{\partial \Delta z}{\partial \lambda} & \frac{\partial \Delta z}{\partial h} \end{bmatrix} \quad (2-14)$$

Writing the observation equation (2-13) in matrix equation we get

$$\underline{l} = \underline{A} \underline{x} + \underline{n} \quad (2-15)$$

where

\underline{l} ... is the observational vector

\underline{x} ... is the unknown vector $\underline{x} = \underline{x}(\varphi, \lambda, h, \omega_x, \omega_y, \omega_z, K)$

\underline{A} ... is the design matrix

and \underline{n} ... is the white noise vector

The system can be solved by applying the L_2 -norm

$$\underline{n}^T \underline{C}_{nn}^{-1} \underline{n} = \text{Min} \quad (2-16)$$

where \underline{C}_{nn} is the variance-covariance matrix of observations.

2.2 Practical computations with the conventional least-squares model

Using the least-squares adjustment model we made several computations in a GPS-network in Hessen (West-Germany).

A six station three-dimensional geodetic control network was observed with MACROMETER model V-1000 field units. For a detailed description see SCHWINTZER et al. (1985), LANDAU (1985). The network was surveyed by GPS interferometry under the commission of the department of surveys Landesvermessungsamt Hessen (LVA). The purpose of this campaign was to densify the German first and second order geodetic triangulation network. The derived baseline components were kindly provided by the LVA.

In our considerations three of the six network points were held fixed in space by attaching a high weight to their coordinates. These were the points Taufstein, Feldberg and Melibocus. This procedure was chosen since it allowed a comparison with a classical triangulation adjustment. The ellipsoidal coordinates were derived from a terrestrial network adjustment and were supplied to us by the LVA. In addition orthometric heights of the network points were available. Geoidal heights were derived from a geoid computation of LELGEMANN et al. (1981).

The network consists of 12 baselines (one baseline was observed twice) with a maximum length of 96 km. The largest misclosures after the adjustment procedure are received for coordinate differences between fixed points. They appear for the difference dX between Feldberg and Melibocus with -0.10 m and for dX between Melibocus and Taufstein with +0.22 m. All values of the noise vector after the adjustment are lower than 0.10 m. The greatest standardized misclosure is +1.1 for the dZ - component of the baseline vector Kloppenheim - Melibocus. All other are less than 1.0. Gross errors in the observations can therefore be excluded.

Figure 3 shows an output print of the program using least-squares adjustment. The received mean standard errors are

± 0.092 m in latitude direction
± 0.073 m in longitude direction
± 0.094 m in orthometric height

The decrease in accuracy from point Kloppenheim to point Geiersberg is caused by the unfavorable network structure. (There is no connection between the points Ronneburg, Geiersberg and Taufstein).

ADJUSTED POSITIONS

SSN NAME	LATITUDE	LONGITUDE	M.S.L.	G. HT.	E. HT.	AZ=	HOR=	TOT=
1 001 TAUFSTEIN (5421)1/21W SHIFTS (M.) UNSCALED SIGMAS (M.) GOOGES	50 30 37.30745N 0.000S 0.001 1.0D+00	9 13 32.18997E 0.000W 0.001 1.0D+00	744.907	0.100	745.007	0.000	0	0.0
2 002 FELDBERG (5716)1/02 SHIFTS (M.) UNSCALED SIGMAS (M.) GOOGES	50 14 4.38396N 0.000N 0.001 1.0D+00	8 27 31.25703E 0.000W 0.001 1.0D+00	873.327	-0.400	872.927	0.000	0	0.0
3 003 KLOPPENHEIM (5718)1/01 SHIFTS (M.) UNSCALED SIGMAS (M.) GOOGES	50 13 14.58034N 0.010N 0.050 8.0D-02	8 43 55.16804E 0.080W 0.041 6.2D-01	173.582	-0.750	172.832	-0.088	AZ=278	0.1
4 004 RONNEBURG (5720)1/21W SHIFTS (M.) UNSCALED SIGMAS (M.) GOOGES	50 14 24.02187N 0.005S 0.091 5.1D-02	9 3 50.70836E 0.159E 0.071 3.3D-01	228.875	-0.750	228.125	-0.045	AZ= 92	0.2
5 005 GEIERSBERG (6022)1/21W SHIFTS (M.) UNSCALED SIGMAS (M.) GOOGES	49 54 10.25316N 0.002S 0.120 6.4D-02	9 25 42.60173E 0.129E 0.096 3.8D-01	581.151	-1.300	579.851	-0.051	AZ= 91	0.1
6 006 MELIBOCUS (6217)1/01W SHIFTS (M.) UNSCALED SIGMAS (M.) GOOGES	49 43 33.13970N 0.000S 0.001 1.0D+00	8 38 14.38112E 0.000E 0.001 1.0D+00	517.380	-1.900	515.480	-0.000	AZ= 0	0.0

Figure 3: Adjustment program output using conventional least-squares adjustment
 (modified version of a program kindly provided by the NGS)

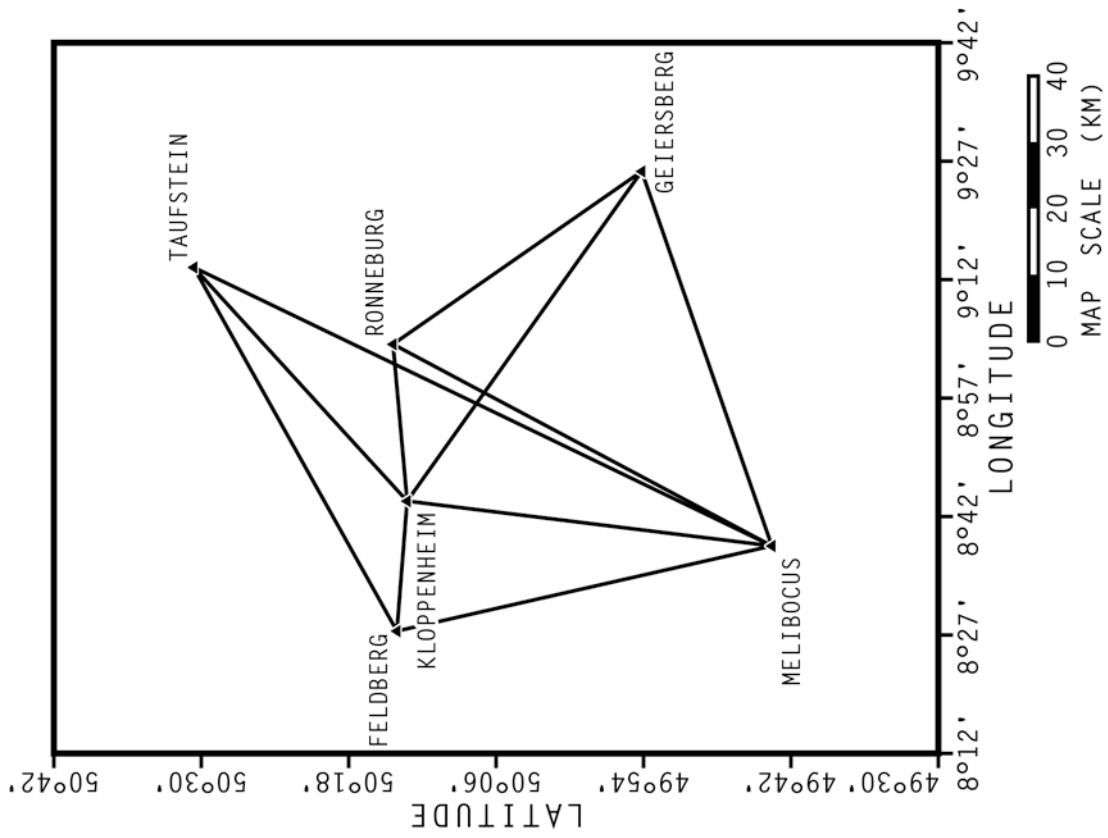


Figure 2: GPS - network Hessen

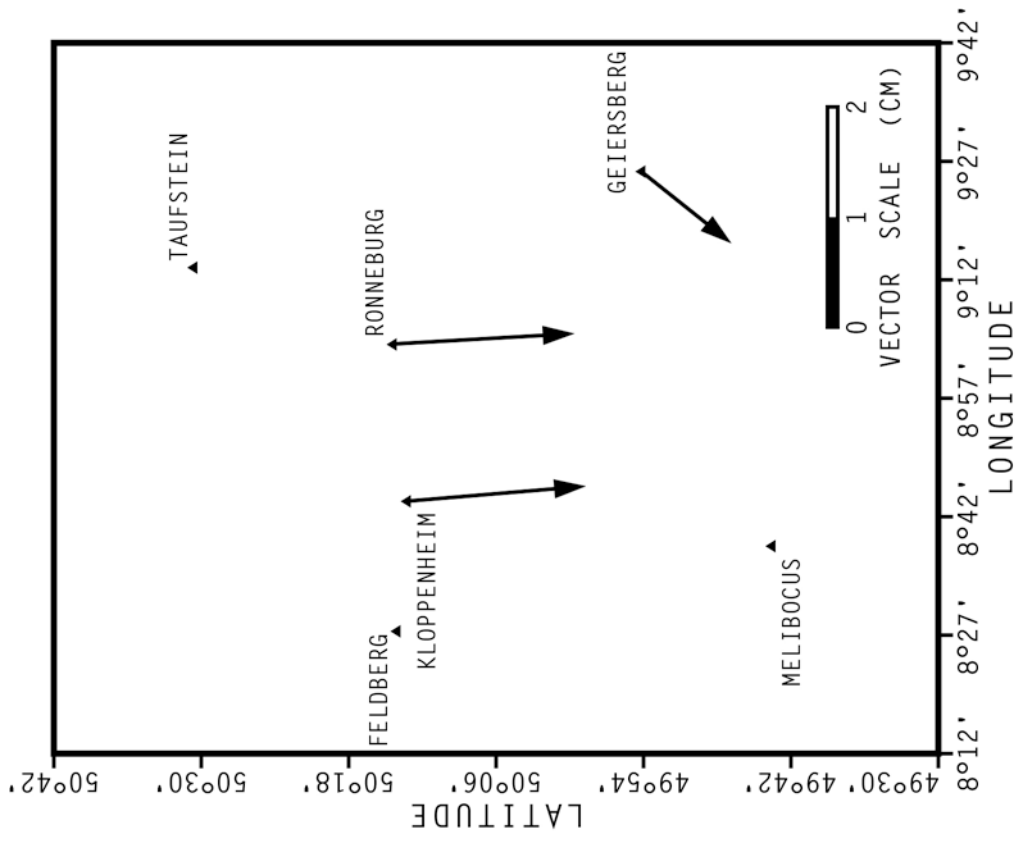


Figure 4: Location differences caused by neglecting geoidal heights

3. THE NEED FOR AN INTEGRATED APPROACH

In principle a geodetic network built up by GPS baseline component vectors is a purely geometrical figure, which is independent of the gravity field (as far as the orbit of the satellites is not considered). The need for an integrated model is obvious, if orthometric height determination is desired in connection with GPS-measurements. Merely the ellipsoidal heights of points on the earth's surface can be derived from GPS baseline vectors by known transformation parameters and without knowledge of orthometric heights which are preferred in surveying applications. As already discussed above, the knowledge of the geoidal height is in particular necessary for the integration of GPS derived coordinates into classical geodetic networks. Geoid heights can be computed using integral formulas and/or collocation procedures.

3.1 The influence of geoidal heights on the determination of horizontal coordinates

Let us shortly discuss the influence of geoidal heights on the location of new points in order to proof the proposition that neglecting of geoidal heights at fixed stations does not influence the coordinates of new points significantly. For that purpose we made some computations in the already mentioned GPS network in Hessen. We neglected the geoidal heights and introduced orthometric instead of ellipsoidal heights at fixed network stations. The location changes for all 3 new points were less than 2 cm, consequently within the computed error estimates of coordinates. However, with increasing accuracy of coordinate differences derived from GPS interferometry or for larger geoidal height differences the error might be significant and no more neglectable.

3.2 Estimation of the approximation error when neglecting geoidal heights

The usual least-squares adjustment model is

$$\hat{\underline{x}}_1 = \left(\underline{A}^T \underline{C}_{nn}^{-1} \underline{A} \right)^{-1} \underline{A}^T \underline{C}_{nn}^{-1} \underline{l}_1 \quad (3-1)$$

where

$\hat{\underline{x}}_1$... is the unknown vector of coordinates

and $\underline{l}_1 \dots$ is the observational vector (observed values minus the reference value derived from approximate coordinates)

An error in the approximate height component will cause an error in the observational vector $\Delta \underline{l} = \underline{l}_2 - \underline{l}_1$ where \underline{l}_2 is the observational vector computed from approximate coordinates with unknown geoidal heights. Thereby the ellipsoidal height was approximated by the orthometric height.

The error in the coordinate unknowns can then be estimated by the relation

$$\Delta \underline{x} = \hat{\underline{x}}_2 - \hat{\underline{x}}_1 = \left(\underline{A}^T \underline{C}_{nn}^{-1} \underline{A} \right)^{-1} \underline{A}^T \underline{C}_{nn}^{-1} \Delta \underline{l} \quad (3-2)$$

The vector $\Delta \underline{l}$ is defined

$$\begin{bmatrix} d\Delta x_{ij} \\ d\Delta y_{ij} \\ d\Delta z_{ij} \end{bmatrix} = \begin{bmatrix} -\frac{\partial \Delta x}{\partial h_i} & \frac{\partial \Delta x}{\partial h_j} \\ -\frac{\partial \Delta y}{\partial h_i} & \frac{\partial \Delta y}{\partial h_j} \\ -\frac{\partial \Delta z}{\partial h_i} & \frac{\partial \Delta z}{\partial h_j} \end{bmatrix} \cdot \begin{bmatrix} N_i \\ N_j \end{bmatrix} \quad (3-3)$$

where N_i, N_j are the geoidal heights at the stations i and j ,

where

$$\frac{\partial \Delta x}{\partial h} = \cos \varphi \cos \lambda \quad (3-4a)$$

$$\frac{\partial \Delta y}{\partial h} = \cos \varphi \sin \lambda \quad (3-4b)$$

$$\frac{\partial \Delta z}{\partial h} = \sin \varphi \quad (3-4c)$$

Let us assume that the rotational parameters and the scale factor are known. Considering a single baseline the following relations express the influence of geoidal heights on the location of network points (Point 1 is assumed to be fixed in the coordinate system).

$$\begin{aligned}
dx_2 = & -\sin \varphi_2 \cos \lambda_2 \cdot (-\cos \varphi_1 \cos \lambda_1 \cdot N_1 + \cos \varphi_2 \cos \lambda_2 \cdot N_2) - \\
& -\sin \varphi_2 \sin \lambda_2 \cdot (-\cos \varphi_1 \sin \lambda_1 \cdot N_1 + \cos \varphi_2 \sin \lambda_2 \cdot N_2) + \\
& + \cos \varphi_2 \cdot (-\sin \varphi_1 \cdot N_1 + \sin \varphi_2 \cdot N_2)
\end{aligned} \tag{3-5}$$

$$\begin{aligned}
dy_2 = & -\cos \varphi_2 \sin \lambda_2 \cdot (-\cos \varphi_1 \cos \lambda_1 \cdot N_1 + \cos \varphi_2 \cos \lambda_2 \cdot N_2) - \\
& -\cos \varphi_2 \cos \lambda_2 \cdot (-\cos \varphi_1 \sin \lambda_1 \cdot N_1 + \cos \varphi_2 \sin \lambda_2 \cdot N_2) + \\
& + 0 \cdot (-\sin \varphi_1 \cdot N_1 + \sin \varphi_2 \cdot N_2)
\end{aligned} \tag{3-6}$$

where dx_2, dy_2 are metric quantities in latitude and longitude direction, respectively. It can be shown that the influence of the geoidal undulation at point 2 cancels out. We finally get

$$\begin{aligned}
dx_2 = & (\sin \varphi_2 \cos \lambda_2 \cos \varphi_1 \cos \lambda_1 + \sin \varphi_2 \sin \lambda_2 \cos \varphi_1 \sin \lambda_1 - \\
& - \cos \varphi_2 \sin \varphi_1) \cdot N_1
\end{aligned} \tag{3-7}$$

$$dy_2 = (\cos \varphi_2 \sin \lambda_2 \cos \varphi_1 \cos \lambda_1 + \cos \varphi_2 \cos \lambda_2 \cos \varphi_1 \sin \lambda_1) \cdot N_1 \tag{3-8}$$

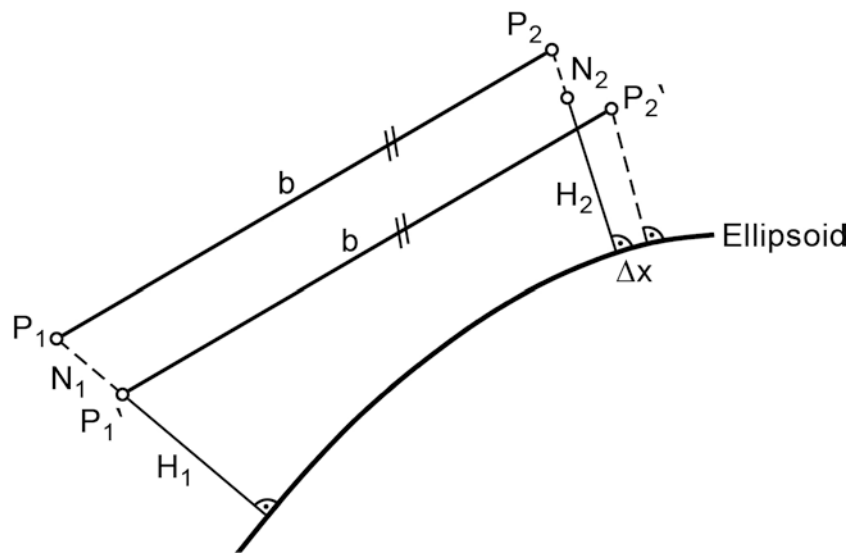


Figure 5: Location error at point P_2 caused by neglecting the geoidal height at point P_1

Let us now use these relations to estimate the horizontal location error for a baseline. We define two points $P_1 (\varphi_1 = 50^\circ, \lambda_1 = 0^\circ)$ and $P_2 (\varphi_2 = 50^\circ.1 - 60^\circ.6, \lambda_2 = 0^\circ)$. Now we are varying both, the geoidal height at the fixed station P_1 and the latitude of P_2 and estimate an approximation error for "true" baseline components, between points P_1 and P_2 .

We are only interested in the resulting latitude error of point 2. The results of the computations are presented in figure 6.

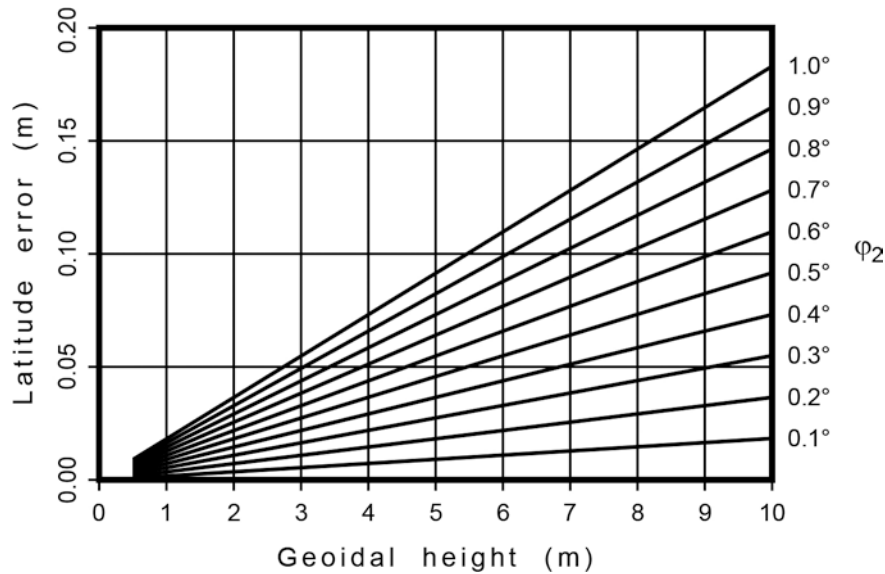


Figure 6: Horizontal location error for single baselines

It can be seen that the location error increases with increasing baseline length and geoidal height.

3.3 The influence of geoidal heights on the determination of transformation parameters

The geoidal heights at fixed network stations influence the determination of rotational angles and scale factor of the transformation between WGS 72 and the local reference system (here the Bessel ellipsoid with the "Rauenberger Datum"). In order to examine the magnitude of the influence two adjustments were performed, one with, the other without considering geoidal heights.

1. Computation of transformation parameters without consideration of geoidal heights

$$\begin{aligned}
 K &= -8.46 \cdot 10^{-6} \pm 4.46 \cdot 10^{-7} \\
 \omega_x &= -1''.11 \quad \pm 0''.17 \\
 \omega_y &= 5''.73 \quad \pm 0''.16 \\
 \omega_z &= -2''.48 \quad \pm 0''.23
 \end{aligned}$$

2. Computation of transformation with geoidal heights taken into account

$$\begin{aligned}K &= -8.53 \cdot 10^{-6} \pm 4.45 \cdot 10^{-7} \\ \omega_x &= 0".50 \quad \pm 0".17 \\ \omega_y &= 0".69 \quad \pm 0".16 \\ \omega_z &= -3".16 \quad \pm 0".23\end{aligned}$$

This demonstrates that for the derivation of transformation parameters the knowledge of geoidal heights is absolutely necessary. In particular, the rotational angles are sensitive for geoidal height differences. The scale factor is influenced mainly by a constant shift in height information.

4. THE INTEGRATED MODEL APPROACH

As mentioned above a good knowledge of the geoid is necessary for the integration of GPS-derived coordinate differences into existing networks. The influence of geoidal heights on horizontal locations has already been discussed in detail. Future investigations in the refinement of phase modelling will lead to an increase in accuracy for the derived coordinate differences. Therefore the knowledge of the geoidal height will become more and more of interest. Furthermore the question arises how precise orthometric height information can be used in such a procedure. The derivation of precise orthometric height information was discussed by ENGELIS et al. (1984, 1985).

We want to present a model which allows the combination of GPS baseline components with classical geodetic measurements like horizontal and vertical angles, distances, azimuths as well as "dynamical" observations like potential differences, gravity and astronomical observations. Such a model is an application of the integrated geodesy philosophy and the collocation theory (HEIN 1982). A similar method was described by HEIN (1985) which allows a combined adjustment of orthometric height observation with GPS baseline components in the integrated model. EISSFELLER et al. (1985) discussed the combination of gravity data with GPS baseline vectors in detail.

The functional model can be described by the matrix equation

$$\underline{l} = \underline{A} \underline{x} + \underline{R} \underline{t} + \underline{n} \quad (4-1)$$

where

- \underline{l} ... is the observational vector,
- \underline{A} ... the design matrix,
- \underline{x} ... the unknown vector,
- \underline{R} ... the coefficient matrix for the gravity disturbing potential and derivatives of it,
- \underline{t} ... the signal vector,
- and \underline{n} ... is the noise vector.

The vector \underline{x} consists of the following types of unknowns

$$\underline{x} = \underline{x}(\varphi, \lambda, H, \omega_x, \omega_y, \omega_z, K, o, r) \quad (4-2)$$

where

φ, λ ... are ellipsoidal latitudes and longitudes,
 H ... are orthometric heights,
 $\omega_x, \omega_y, \omega_z$... are rotational unknowns,
 K ... is the scale factor,
 o ... are orientation unknowns (for direction),
and r ... are refraction unknowns (for zenith distances).

The vector \underline{t} consists of

$$\underline{t} = \underline{t}(T(N \cdot \gamma), \xi, \eta, \delta g) \quad (4-3)$$

where

T ... is the gravity disturbing potential,
 N ... the geoidal height,
 ξ ... the deflection component in latitude direction,
 η ... the deflection component in longitude direction,
 δg ... is the gravity disturbance.

Note that the ellipsoidal height h was split up into the orthometric height H in the deterministic part and the geoid height N in the pseudostochastic part. In the linearized equation system (4-1) both parts have similar coefficients (the orthometric height H in the \underline{A} -matrix and the geoid height N in the \underline{R} -matrix).

In common least-squares approaches this split up will cause a rank defect. In collocation the system can be solved applying the hybrid norm

$$\underline{n}^T \underline{C}_{nn}^{-1} \underline{n} + \underline{t}^T \underline{K}_{tt}^{-1} \underline{t} = \text{Min} \quad (4-4)$$

where \underline{C}_{nn} is the variance-covariance matrix of observations and \underline{K}_{tt} is that one of the signal quantities.

By including dynamical observations it will be possible to compute optimal estimates for the geoidal height. An efficient solution for combination of geodetic observations with gravity data is discussed in LANDAU et al. (1985).

4.1 The observation equations

The observation equations of GPS-derived coordinates in the integrated geodesy model are given similar as in the conventional approach by

$$\begin{aligned}
 \begin{bmatrix} d\Delta X_{ij} \\ d\Delta Y_{ij} \\ d\Delta Z_{ij} \end{bmatrix} &= -\underline{I}_i^* \begin{bmatrix} d\varphi_i \\ d\lambda_i \\ dH_i \end{bmatrix} + \underline{I}_j^* \begin{bmatrix} d\varphi_j \\ d\lambda_j \\ dH_j \end{bmatrix} + \Delta U_r \begin{bmatrix} \omega_x \\ \omega_y \\ \omega_z \end{bmatrix} + K \cdot \Delta X_{OBS} - \\
 &- \begin{bmatrix} \frac{\partial \Delta x_{ij}}{\partial N_i} \\ \frac{\partial \Delta y_{ij}}{\partial N_i} \\ \frac{\partial \Delta z_{ij}}{\partial N_i} \end{bmatrix} \cdot N_i + \begin{bmatrix} \frac{\partial \Delta x_{ij}}{\partial N_j} \\ \frac{\partial \Delta y_{ij}}{\partial N_j} \\ \frac{\partial \Delta z_{ij}}{\partial N_j} \end{bmatrix} \cdot N_j + \underline{f}_{\Delta x \Delta y \Delta z} \quad (4-5)
 \end{aligned}$$

where

$$\underline{I}^* = \begin{bmatrix} \frac{\partial \Delta X}{\partial \varphi} & \frac{\partial \Delta X}{\partial \lambda} & \frac{\partial \Delta X}{\partial H} \\ \frac{\partial \Delta Y}{\partial \varphi} & \frac{\partial \Delta Y}{\partial \lambda} & \frac{\partial \Delta Y}{\partial H} \\ \frac{\partial \Delta Z}{\partial \varphi} & \frac{\partial \Delta Z}{\partial \lambda} & \frac{\partial \Delta Z}{\partial H} \end{bmatrix} \quad (4-6)$$

4.2 Properties of the integrated approach

The inclusion of GPS-baseline vectors into the integrated model approach has several advantages.

- The internal consideration of geoidal heights results in precise horizontal coordinates and transformation parameters. The highest obtainable point accuracy is therefore achieved.
- The combination with orthometric heights, gravity field data and potential differences results in high-precision orthometric and geoidal heights at all network points. The high-precision GPS ellipsoidal height information combined with orthometric heights enables the user to improve the modelling of the gravity field and therefore supports the correction for the deflection of the vertical, e.g., for zenith distances.
- The internal prediction allows the determination of geoidal heights or other functionals of the gravity disturbing potential at non-network points.
- The combination with all types of geodetic measurements leads to an optimal network adjustment.

4.3 The GPS-network Summit County

Some numerical investigations were made in a GPS control network located in Ohio (U.S.A.). The network consists of 38 network points and has a size of about $35 \times 50 \text{ km}^2$. The height differences in that area are less than 100 m. Therefore we may expect that the geoid will be a rather smooth surface allowing excellent interpolation. Besides the 66 determined GPS baselines, information about already determined triangulation stations and orthometric heights were available. All information was kindly provided by the U.S. National Geodetic Survey, Rockville, Md.

In addition to the geometric information 199 gravity measurements were available, see Fig. 8.

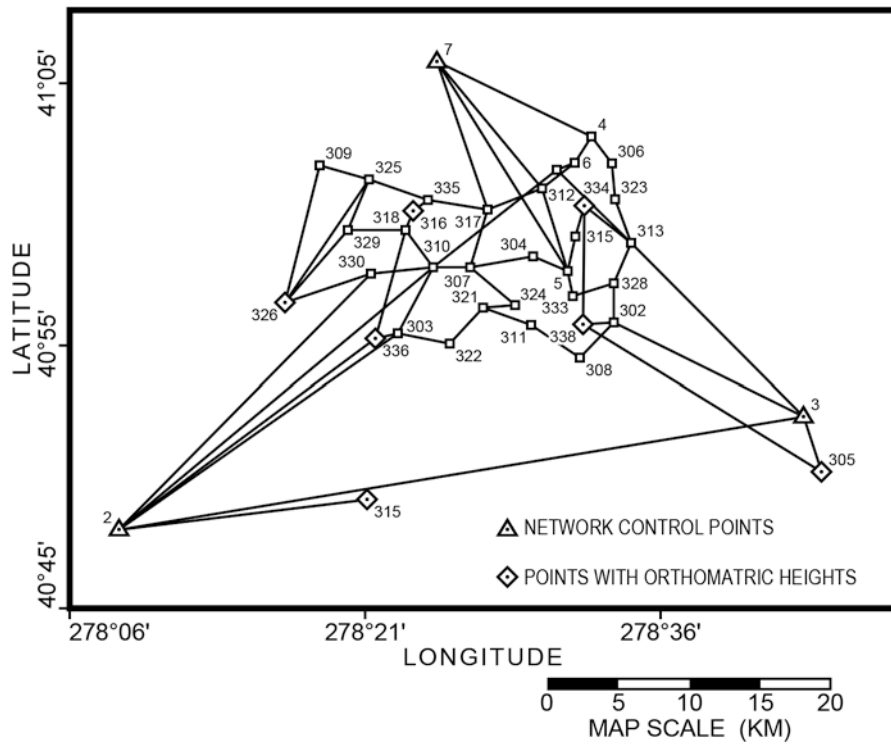


Figure 7: Network configuration - Summit County, Ohio

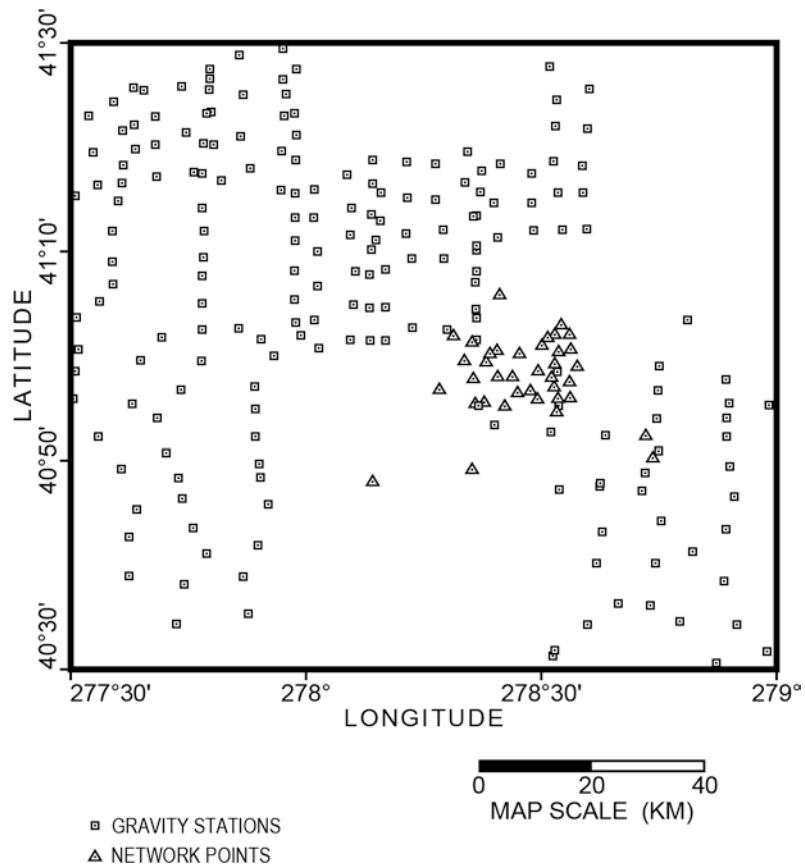


Figure 8: Gravity measurements and network points in Summit County

Approximation errors may be caused by unfavorable distribution of the gravity data. Therefore a computation of more or less absolute geoidal heights using integral techniques seems to be impossible without additional interpolations. For such techniques a 2° cap with dense gravity data around the computation points is required. The following computations are therefore restricted to the determination of a relative geoid. They will show in which way the gravity data are able to improve geoidal height determination and by that the derivation of orthometric heights.

4.4 The gravity anomaly covariance function

From the available 199 gravity anomalies we computed an empirical covariance function characterized by the following parameters:

Variance of gravity anomalies	$C_0 = 123.78 \text{ mgal}^2$
Variance of horizontal gradients	$G_0 = 112.74 \text{ E}^2$
Correlation length	$\xi = 22.14 \text{ km}$

Using these parameters we defined the chosen analytic covariance model of TSCHERNING and RAPP (1974), by an iterative procedure. The results are:

Squared ratio of Bjerhammer's sphere to earth radius	$s = 0.999153$
Order of local covariance function	$n = 102$

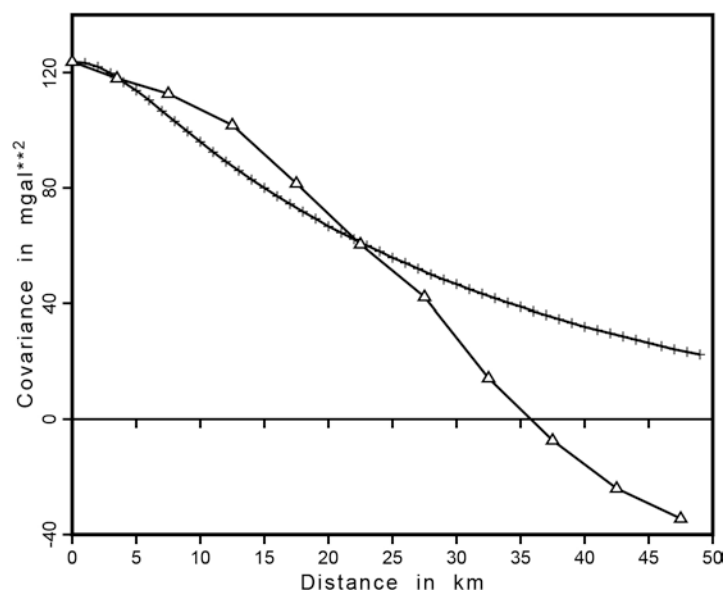


Figure 9: Empirical and analytical covariance function of gravity anomalies (Δ = empirical, + = analytical)

The order of the local covariance function and the variance of horizontal gradients reflect the smoothness of the gravity field.

4.5 Practical computations

In the following we want to discuss three different variants of adjustment solutions and will analyze their properties. In all variants we hold point 7 in all three directions and points 2 and 3 with their horizontal coordinates fixed in space. From the computed ellipsoidal heights orthometric heights were derived at all possible stations.

Solution 1: Conventional least-squares adjustment using the model discussed in chapter 2

Solution 2: Integrated adjustment using the same information as in solution 1

Solution 3: Integrated adjustment similar to solution 2 plus 199 gravity observations

The results of the three adjustment strategies are listed in table 1.

4.5.1 Solution 1

Solution 1 is an adjustment solution using the conventional least-squares adjustment model described in chapter 2. The received mean standard errors are ± 0.79 cm in latitude, ± 0.95 cm in longitude and ± 3.78 cm in ellipsoidal height. Figure 10 shows error ellipsoids for the network adjustment. The results reflect the high precision of the coordinates derived from GPS-baseline component vectors.

From the adjusted ellipsoidal heights and the given orthometric heights at the 11 network stations we were able to determine relative geoidal heights. They are listed in table 2.

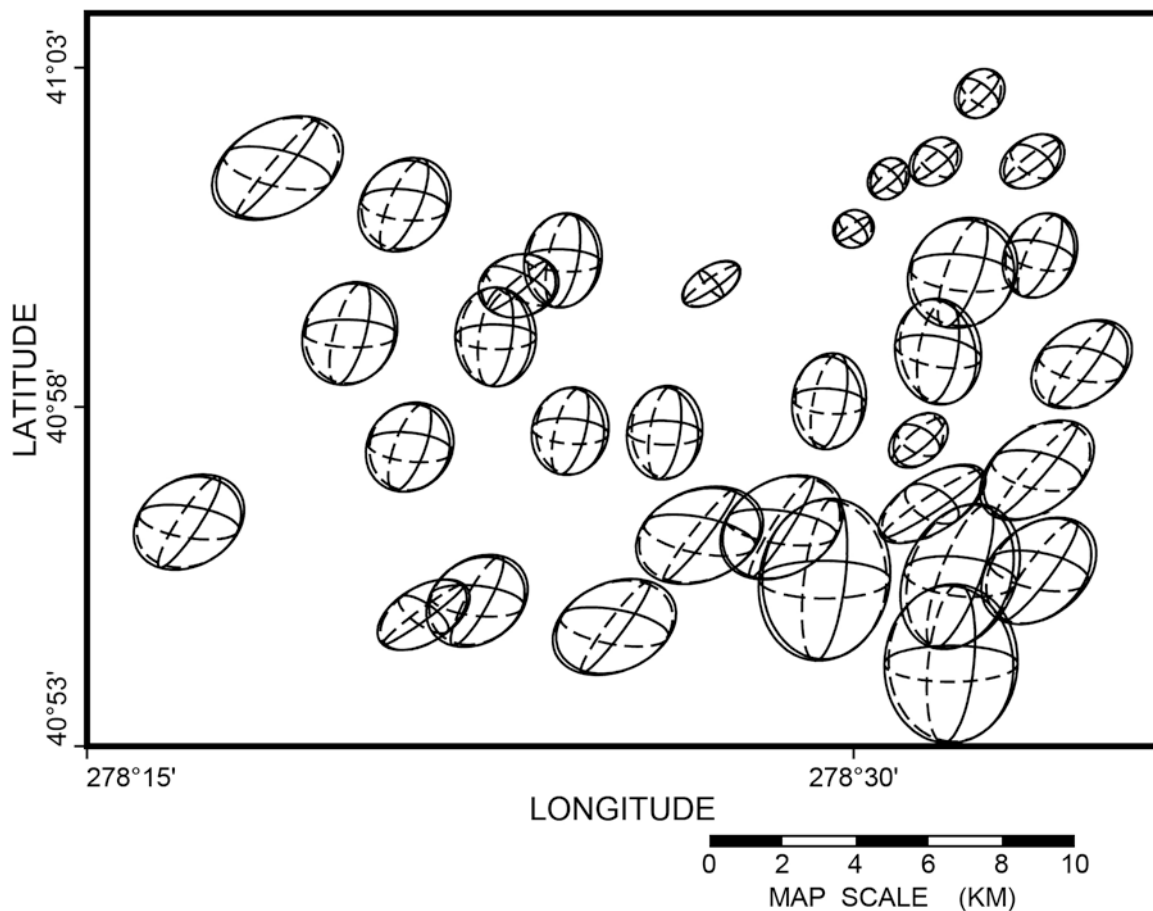


Figure 10: Error ellipsoids of the network points.

(Note that the points 2, 3, 305 and 315 were excluded)

4.5.2 Solution 2

In solution 2 we applied the integrated geodesy model approach and splitted the ellipsoidal height into the orthometric and the geoidal part as described above. We used the same data as in solution 1 plus the eleven orthometric heights which were held fixed and get finally the mean coordinate standard error of ± 0.8 cm in latitude, ± 0.9 cm in longitude and ± 1.9 cm in orthometric height. In contrast to solution 1 we determined directly orthometric and not ellipsoidal heights. Note that the integrated geodesy model allows by the internal interpolation properties the determination of orthometric and geoidal heights at stations without any a priori knowledge of orthometric or geoidal heights.

Table 2 presents therefore not only geoidal heights for eleven points as in solution 1 but at all network points. The mean standard error of the geoidal heights was computed to ± 1.9 cm.

Figure 14 shows the standard errors of geoidal heights in form of an iso-line plot. It demonstrated that the standard errors in the outer network part increase rapidly. This is due to the extrapolation of the collocation algorithm.

The results look very promising. We state, that it is possible to determine precise orthometric and geoidal heights with cm-accuracy using few orthometric height information and GPS-baseline components by applying the integrated approach. However, the reader has to be reminded that the covariance function was derived from given gravity anomalies, and the geoid in the area under consideration is very smooth.

Otherwise additional gravity field information is necessary to support the internal interpolation and prediction properties.

4.5.3 Solution 3

In solution 3 we introduced 199 gravity observations in order to improve the geoid height determination. This results in mean coordinate standard errors of ± 0.7 cm in latitude, ± 0.9 cm in longitude and ± 1.4 cm in height. It shows an improvement in both, horizontal and vertical coordinate components. The improvement in horizontal location is small, but the improvement in height is remarkable. The determined geoidal heights are listed in table 2. They were determined with a mean standard error of ± 1.4 cm. Comparing the geoidal heights of the solution 2 and 3 we get a mean absolute difference of 3.9 cm. The improvement of the geoidal heights by inclusion of gravity data is of the order of 20 cm for point 2 which is located in the southwestern part of the network area.

The geoid height differences are plotted in figure 13. One can see that the largest differences are at points in the western part of the network area, where only few gravity data are given, see figure 7. With a more dense distribution of gravity observations in that area the determination of the height component might improve significantly.

Determined standard errors for coordinates derived from different adjustment solutions (all quantities given in centimeter) :

Name	SOLUTION 1			SOLUTION 2			SOLUTION 3		
	mB	mL	mh	mB	mL	mH	mB	mL	mH
1	0.36	0.63	2.00	0.33	0.61	0.00	0.33	0.61	0.00
2	0.00	0.00	2.29	0.00	0.00	8.20	0.00	0.00	5.57
3	0.00	0.00	2.04	0.00	0.00	2.51	0.00	0.00	1.78
5	0.42	0.69	2.15	0.41	0.69	1.38	0.41	0.69	0.97
4	0.38	0.60	1.99	0.36	0.59	0.00	0.36	0.59	0.00
6	0.29	0.51	1.73	0.25	0.48	0.00	0.25	0.47	0.00
7	0.00	0.00	0.00	0.00	0.00	0.00	0.00	0.00	0.00
302	0.85	1.23	4.23	0.83	1.18	1.18	0.80	1.14	1.33
303	0.75	0.99	3.78	0.73	0.98	1.02	0.71	0.95	0.92
304	0.84	0.82	3.83	0.84	0.81	1.70	0.83	0.81	1.47
305	1.62	0.91	7.32	1.57	0.90	0.00	1.48	0.88	0.00
306	0.40	0.75	2.17	0.38	0.74	0.74	0.38	0.74	0.71
307	0.83	0.80	3.75	0.82	0.79	1.73	0.82	0.79	1.56
308	1.50	1.38	6.42	1.48	1.34	2.36	1.47	1.30	1.85
309	0.80	1.28	4.14	0.77	1.27	2.42	0.75	1.26	1.31
310	0.75	0.80	3.56	0.73	0.80	1.39	0.70	0.79	1.25
311	1.49	1.39	6.47	1.48	1.37	2.53	1.47	1.37	2.13
312	0.25	0.48	1.56	0.24	0.47	0.44	0.24	0.47	0.42
313	0.75	1.06	3.53	0.74	1.01	1.59	0.73	1.00	1.57
315	0.33	1.04	3.23	0.33	1.04	0.00	0.33	1.03	0.00
316	0.40	0.81	2.57	0.39	0.80	0.00	0.38	0.80	0.00
317	0.24	0.66	1.77	0.24	0.65	1.05	0.23	0.65	0.96
318	0.87	0.84	4.02	0.87	0.83	1.03	0.86	0.83	1.01
319	1.00	0.98	4.24	0.80	0.96	0.76	0.75	0.96	0.61
321	0.79	1.19	3.94	0.75	1.17	2.04	0.73	1.16	1.74
322	0.78	1.15	3.86	0.74	1.16	1.90	0.71	1.14	1.53
323	0.75	0.87	3.35	0.74	0.86	1.24	0.73	0.85	1.21
324	0.84	1.18	4.13	0.84	1.17	2.11	0.83	1.17	1.76
325	0.79	0.95	3.80	0.76	0.94	1.45	0.74	0.93	0.97
326	0.77	1.08	3.84	0.74	1.07	0.00	0.71	1.05	0.00
328	0.76	1.20	3.81	0.75	1.17	1.39	0.75	1.13	1.43
329	0.88	0.95	4.12	0.87	0.95	1.46	0.86	0.94	1.28
330	0.76	0.90	3.61	0.74	0.89	1.15	0.71	0.88	1.10
333	0.48	1.21	2.95	0.47	1.19	1.43	0.47	1.16	1.07
334	1.00	1.13	4.38	0.79	1.08	0.00	0.74	1.06	0.00
335	0.82	0.82	3.89	0.82	0.82	1.04	0.82	0.81	1.03
336	0.34	0.98	2.86	0.33	0.97	0.00	0.33	0.91	0.00
338	1.28	1.38	5.83	1.14	1.27	0.00	0.95	1.19	0.00
Mean standard errors	0.79	0.95	3.78	0.76	0.93	1.88	0.73	0.92	1.42

where B = ellipsoidal latitude
 L = ellipsoidal longitude
 h = ellipsoidal height
and H = orthometric height

Table 1: Coordinate accuracies derived from different solution strategies

STATION	SOLUTION 1	SOLUTION 2		SOLUTION 3		
	N_1	N_2	m_{N_2}	N_3	m_{N_3}	$N_3 - N_2$
1	35.3	35.7	0.5	35.5	0.5	-0.2
2		86.0	8.2	107.2	5.6	21.1
3		46.9	2.6	47.1	1.8	0.2
5		54.4	1.3	48.8	0.9	-5.6
4	31.2	31.5	0.5	31.2	0.5	-0.3
6	33.8	34.4	0.5	33.6	0.5	-0.8
7	0.0	0.0	0.1	0.0	0.1	0.0
302		57.8	1.7	56.0	1.4	-1.8
303		70.0	0.9	63.2	0.8	-6.8
304		49.7	1.4	44.3	1.2	-5.4
305	43.0	44.1	2.0	47.1	1.8	3.0
306		40.5	0.9	40.6	0.9	0.2
307		48.0	1.5	42.2	1.4	-5.9
308		59.6	1.8	59.2	1.1	-0.5
309		23.4	2.5	38.5	1.1	15.1
310		47.8	1.2	42.2	1.2	-5.6
311		59.1	1.7	56.3	1.4	-2.7
312		37.0	0.6	35.0	0.6	-2.0
313		55.0	1.8	52.2	1.6	-2.8
315	80.0	81.4	0.9	81.8	0.9	0.4
316	28.9	29.5	0.7	29.2	0.7	-0.4
317		33.9	1.1	28.9	1.1	-5.0
318		36.3	0.8	35.0	0.8	-1.2
319		51.2	1.1	46.4	0.8	-4.8
321		57.5	1.7	52.9	1.6	-4.5
322		66.8	1.6	61.0	1.4	-5.7
323		48.7	1.2	47.6	1.1	-1.1
324		56.7	1.7	52.7	1.5	-4.0
325		22.5	1.4	35.0	0.8	12.4
326	68.7	68.6	1.0	71.6	1.0	3.0
328		57.0	1.7	53.1	1.4	-4.0
329		40.2	1.4	46.0	1.2	5.8
330		43.7	1.1	52.8	1.1	-0.9
333		56.6	1.4	52.1	1.0	-4.5
334	52.5	47.2	0.9	45.0	0.8	-2.2
335		26.7	0.8	25.0	0.7	-1.7
336	73.1	73.1	0.8	68.3	0.7	-4.8
338	57.1	58.1	1.5	55.7	1.0	-2.4
Mean values			+/- 1.9		+/- 1.4	3.9

Table 2: Geoid heights (all quantities given in cm)

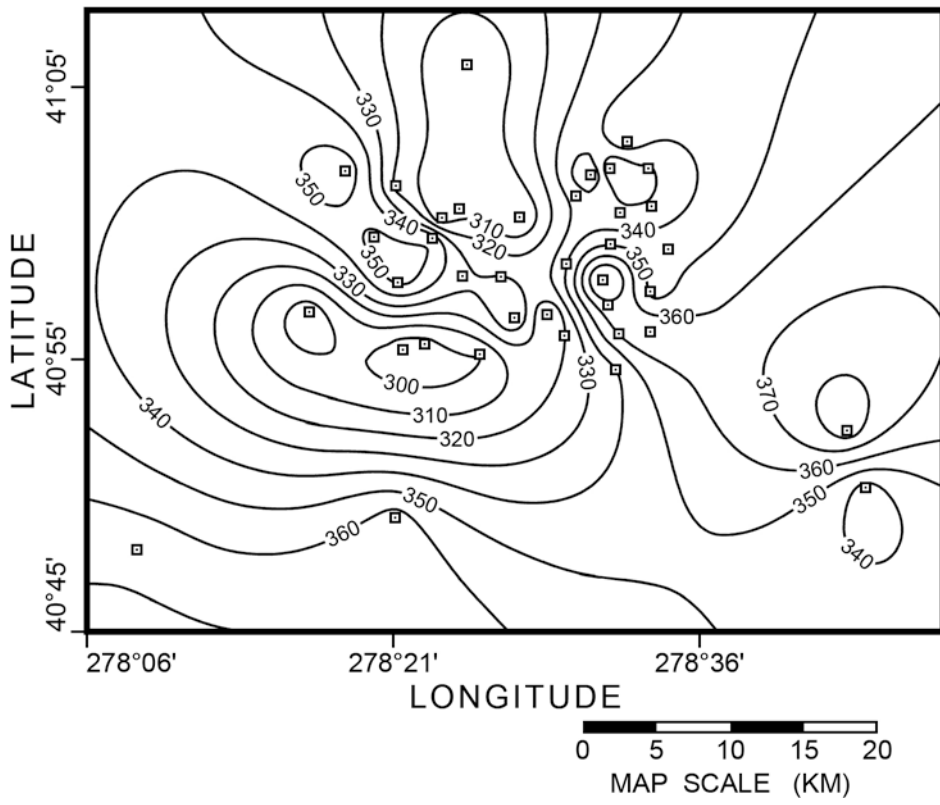


Figure 11: Heights in the network area given in meter

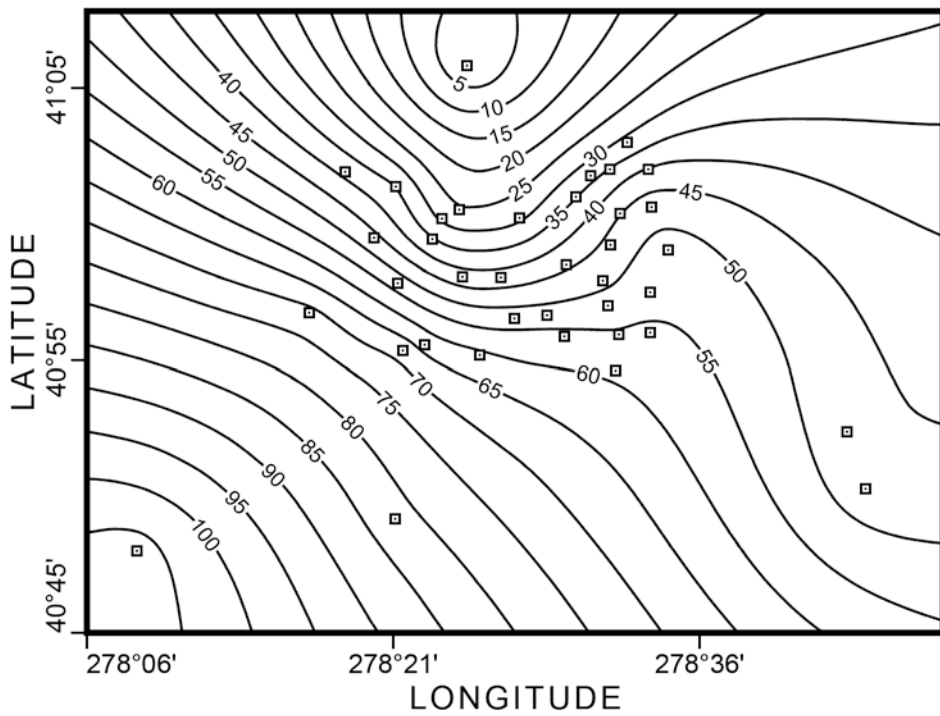


Figure 12: Geoidal heights computed by adjustment solution 3 given in cm

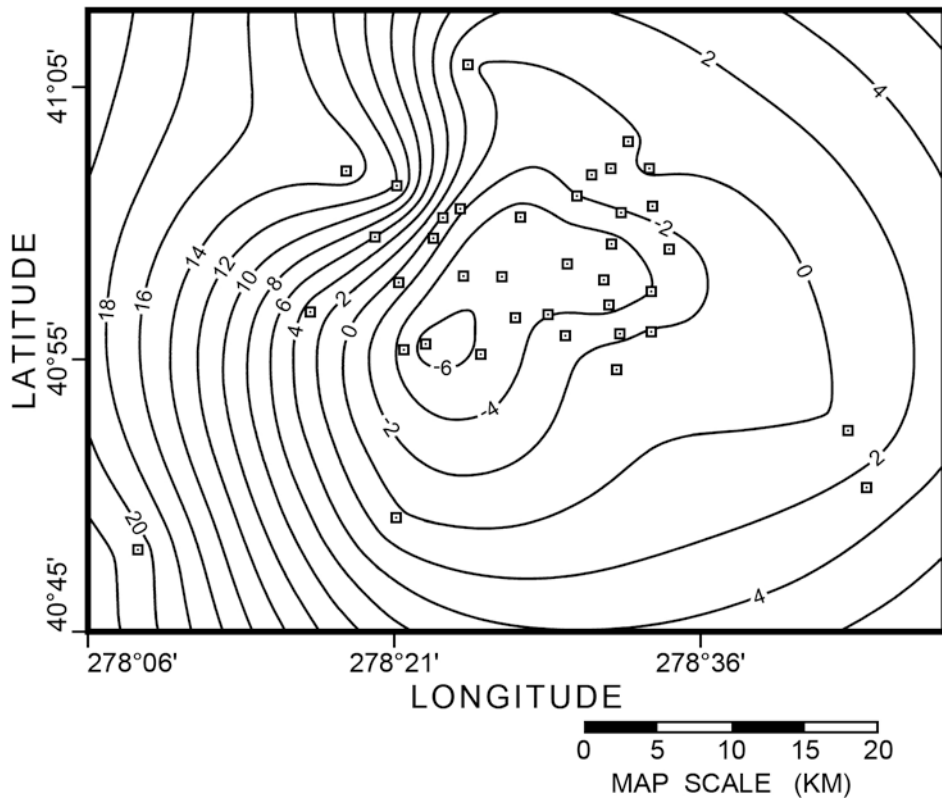


Figure 13: Geoid height differences between solutions 2 and 3 given in cm

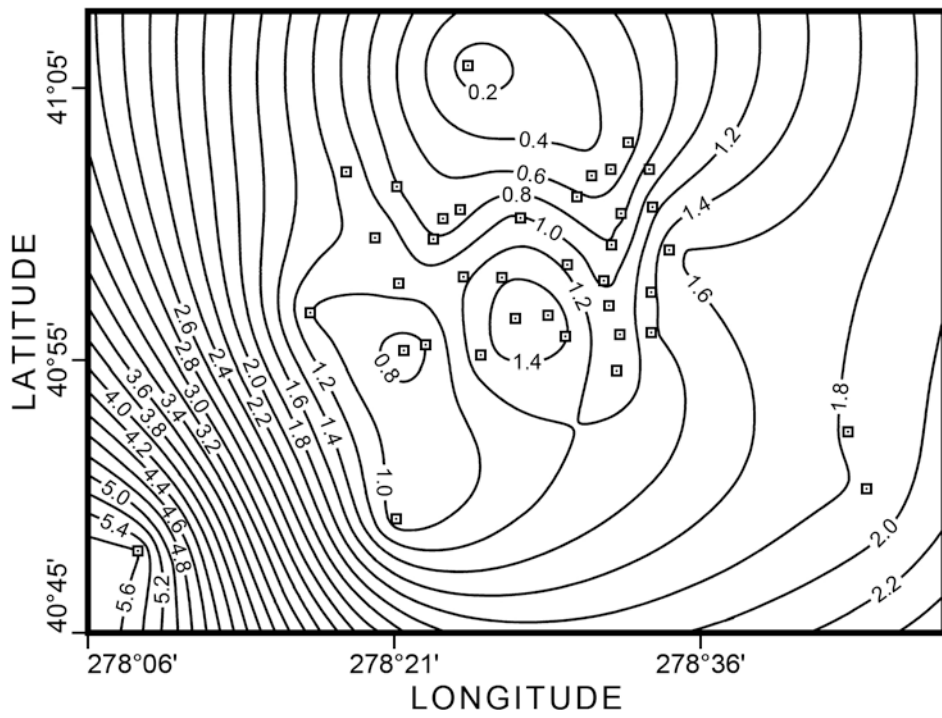


Figure 14: Height standard errors given in cm

5. APPLIED SOFTWARE PRODUCTS

The described computations were done using software developed at the Institute of Astronomical and Physical Geodesy of the University FAF Munich.

The program system OPERA which was developed in 1981 was completely revised and main parts were rewritten. The new version 2.0 is a high sophisticated program which is much faster than the old version, more operational and user-friendly. A lot of new features were added to the new program system like the integration of GPS baseline component vectors, geoidal and orthometric heights and the use of topographic information for smoothing gravity field data etc. It allows a split up of the ellipsoidal into geoidal and orthometric height as described in chapter 4.

The new program is working in an ellipsoidal coordinate system and allows the computation of 1D, 2D and 3D integrated and conventional adjustments. It is written in machine independent FORTRAN 77 and contains a comfortable pre- and postprocessor. Many program features are running in two modes (interactive or in batch). For example, the empirical covariance function and the adaption of an analytic covariance function can be computed under interactive control. The program makes use of a bit structured information storage in order to save memory and special sorting techniques are incorporated to allow the user to mix information in different ways.

Several processing modes are possible

- pure geometrical adjustment (1D, 2D, 3D),
- integrated geodesy adjustment (1D, 2D, 3D),
- prediction, filtering and interpolation.

The program allows the combined or separate determination of coordinates and gravity field dependent quantities like geoidal heights, gravity disturbing potential, gravity disturbances, deflections of the vertical and orthometric heights.

6. CONCLUSIONS

The estimated location errors caused by neglecting geoidal heights at fixed network point demonstrates the necessity to take these quantities into account for high-precise point positioning with GPS-baseline component vector.

The considered concept of solution applying the integrated model approach shows how to combine classical geodetic measurements with dynamic observations and GPS-baseline component vectors. The integrated model provides the combination of high-precise geometric information derived from GPS-interferometry with dynamic information like potential differences derived from spirit levelling. This is superior to the use of orthometric heights, which are derived using hypothetical reduction methods. Integrated model adjustment leads therefore to both, the determination of ellipsoidal heights and orthometric heights of network points with cm-accuracy.

The numerical results demonstrate the efficiency of the integrated approach adjusting three-dimensional geodetic networks.

Future investigations with our software package in areas with a more dense gravity set and with spirit levelling measurements will show the superiority of the integrated approach in deriving horizontal and vertical point positions without any usage of hypothetical reductions.

ACKNOWLEDGEMENT

The research on operational solutions of integrated geodesy adjustment models is supported by a grant of the German Research Foundation (Deutsche Forschungsgemeinschaft).

REFERENCES

- EISSFELLER, B., H. LANDAU, G. HEIN, A. BOTTSE (1985): *The processing of GPS-baseline vectors in conventional geodetic networks using gravity field information and least-squares collocation*. Paper presented at the International Symposium on Geodetic Networks and Computations, Krakow, Poland, June 18-21, 1985
- ENGELIS, T., R.H. RAPP, C.C. TSCHERNING (1984): *The precise computation of geoid undulation differences with comparison to results obtained from the Global Positioning System*. Geophysical Research Letters 11-9, 821-824
- ENGELIS, T., R.H. RAPP, Y. BOCK (1985): *Measuring orthometric height differences with GPS and gravity data*. Submitted for publication in the Manuscripta Geodaetica
- HEIN, G. (1982a): *A contribution to 3D-operational geodesy. Part 1: Principle and observational equations of terrestrial type*. In Proceedings of the International Symposium on Geodetic Networks and Computations of the IAG, Munich, August 31 to September 5, 1981, Deutsche Geodätische Kommission, Reihe B, Nr. 258/VII, 31-64, 1982
- HEIN, G. (1982b): *A contribution to 3D-operational geodesy. Part 2: Principles of solution*. In Proceedings of the International Symposium on Geodetic Networks and Computations of the IAG, Munich, 1981, Deutsche Geodätische Kommission, Reihe B, Nr. 258/VII, 65-85, 1982
- HEIN, G. (1982c): *The geoid as part of integrated geodesy*. Presented at Symposium No. 4b of the General Meeting of the International Association of Geodesy, Tokyo, Japan, May 7-20, 1982
- HEIN, G., H. LANDAU (1983): *A contribution to 3D-operational geodesy. Part 3: OPERA - A multi-purpose program for operational adjustment of geodetic observations of terrestrial type*. Deutsche Geodätische Kommission, Reihe B, Nr. 264, 1983
- HEIN G. (1985): *Orthometric Height Determination Using GPS Observations and the Integrated Geodesy Adjustment Model*. NOAA Technical Report NOS 110 NGS 32, Rockville, MD
- LANDAU, H. (1985): *Dreidimensionale Punktbestimmung im deutschen Hauptdreiecksnetz mit Hilfe von GPS-Basislinienkomponenten*. Unpublished internal report, Institute of Astronomical and Physical Geodesy, University FAF Munich
- LANDAU, H., G. HEIN, B. EISSFELLER (1985): *A stepwise approach for the integrated geodesy adjustment model*. Paper presented at the International Symposium on Geodetic Networks and Computations, Krakow, Poland, June 18-21, 1985
- LELGEMANN, D., D. EHLERT, D. HAUCK (1981): *Eine astro-gravimetrische Berechnung des Quasigeoids für die Bundesrepublik Deutschland*. Deutsche Geodätische Kommission, Reihe B, Nr. 260, Frankfurt/Main
- SCHWINTZER, P., C. REIGBER, R. STRAUSS (1985): *Macrometerbeobachtungen im Deutschen Hauptdreiecksnetz*. Deutsche Geodätische Kommission, Reihe B, Nr. 273

- SWIATEK, K. (1984): *Anwendung von Dopplersatellitenmessungen zur Genauigkeitsverbesserung geodätischer Netze*. Zeitschrift für Vermessungswesen 109, 65-75, 1984
- STEEVES, R.R. (1984): *Mathematical models for the use in the readjustment of the North American geodetic networks*. Unpublished manuscript, Geodetic Survey of Canada, Ottawa, Canada
- TSCHERNING, C.C., R.H. RAPP (1974): *Closed covariance expressions for gravity anomalies, geoid undulations and deflections of the vertical implied by anomaly degree variance models*. The Ohio State University, Department of Geodetic Science, Report No. 208, Columbus, Ohio
- WOLF, H. (1985): *Das Lage- und Höhenproblem in großen geodätischen Netzen bei Einbeziehung von Satellitendopplermessungen*. Zeitschrift für Vermessungswesen 110, 179-186, 1985

THE IAPG PHASE - DIFFERENCE PROCESSING PROGRAM
- MODELLING, SOFTWARE DEVELOPMENT AND RESULTS -

Herbert Landau
University FAF Munich
Institute of Astronomical and Physical Geodesy
Werner-Heisenberg-Weg 39
8014 Neubiberg
Federal Republic of Germany

ABSTRACT. This paper summarizes the work which was done at the Institute of Astronomical and Physical Geodesy in the field of phase difference processing for precise differential positioning with the Global Positioning System.

It includes the description of the applied model and presents the corresponding software product.

As an example the processing results of data collected in Hessen (FRG) are presented and discussed.

1. INTRODUCTION

GPS phase difference processing is one of the most powerful tools for establishing three-dimensional geodetic networks. Practical measurements have shown that accuracies of 1 ppm are attainable, so that the Global Positioning System becomes of interest for a lot of applications in geodetic research and practical surveying. Therefore our institute started with some research on the field of relative positioning and orbit determination for the GPS-satellite system. This research goes hand in hand with the development of specific software (HEIN and EISSFELLER, 1985).

The first experiences with phase difference processing software were made with programs which were kindly provided by Dr. Remondi (National Geodetic Survey, USA) for single- and triple difference processing.

Due to the absence of a double-difference processing program we decided to develop such a program taking advantage of the experiences made with the NGS-products.

The developments resulted in a user-friendly interactive menu-driven program system which allows the processing of all types of receiver data (Macrometer, TI 4100 etc.). Several models for atmospheric corrections, the possibility of processing dual frequency data, and an automatic cycle slip detection algorithm were incorporated into the program.

In the following the author will describe the applied model, the software product itself and present the results of processed measurements made during a Macrometer campaign in Germany in 1984.

2. THE THEORETICAL MODEL

2.1 The observables

In the following considerations we are dealing with the processing of double-differences of phase measurement data. The double-difference method uses the differences of raw phase measurements between two receivers and two satellites.

$$\psi_{D_j}^k(t_i) = \{ \bar{\psi}_2^k(t_i) - \bar{\psi}_1^k(t_i) \} - \{ \bar{\psi}_2^j(t_i) - \bar{\psi}_1^j(t_i) \} \quad (2-1)$$

where

t_i ... specifies the time epoch
 j, k ... are indices of the two satellites
and $\bar{\psi}_u^j(t_i)$... is the raw phase at epoch t_i for station u
to satellite j with $u = 1, 2$

Since in practice it is possible to track more than two satellites a reference satellite j is introduced which is usually the satellite with most of the observations.

The advantage of the double-difference method lies in the fact, that the influences of satellite and receiver clock errors drop nearly out, so that they can be modelled by simple quadratic polynomials.

2.2 The observation equation

The double difference observation is described by the relation

$$\begin{aligned} \psi_{D_j}^k(t_i) &= \\ &= \frac{f_s}{c} \cdot \{ \rho_2^k(t_i) - \rho_1^k(t_i) \} + \\ &+ \frac{f_s}{c} \cdot \{ \dot{\rho}_2^k(t_i) - \dot{\rho}_1^k(t_i) \} \cdot \{ a_0 + a_1(t_i - t_1) + a_2(t_i - t_1)^2 \} - \\ &- \frac{f_s}{2c} \cdot \{ \ddot{\rho}_2^k(t_i) - \ddot{\rho}_1^k(t_i) \} \cdot \{ b_0 + b_1(t_i - t_1) + b_2(t_i - t_1)^2 \} + \\ &+ f_s \cdot (1 + \alpha) \cdot \{ T_2^k(t_i) - T_1^k(t_i) \} + \\ &+ f_s \cdot \{ I_2^k(t_i) - I_1^k(t_i) \} - \end{aligned}$$

$$\begin{aligned}
& - \frac{f_s}{c} \cdot \{ \rho_2^j(t_i) - \rho_1^j(t_i) \} - \\
& - \frac{f_s}{c} \cdot \{ \dot{\rho}_2^j(t_i) - \dot{\rho}_1^j(t_i) \} \cdot \{ a_0 + a_1(t_i - t_1) + a_2(t_i - t_1)^2 \} + \\
& + \frac{f_s}{2c} \cdot \{ \rho_2^j(t_i) - \rho_1^j(t_i) \} \cdot \{ b_0 + b_1(t_i - t_1) + b_2(t_i - t_1)^2 \} - \\
& - f_s \cdot (1 + \alpha) \cdot \{ T_2^j(t_i) - T_1^j(t_i) \} - \\
& - f_s \cdot \{ I_2^j(t_i) - I_1^j(t_i) \} + \\
& + m_j^k
\end{aligned} \tag{2-2}$$

The unknowns can be classified in the following way

- a. The integer unknown m_j^k

It can be shown that the number of integer unknowns is $(l-1)$ where l is the number of observed satellites in the measurement data set.

- b. Tropospheric scale factor

Although this unknown parameter has no physical meaning, there is a widespread belief, that the insertion of such a scale factor results in an accuracy improvement (REMONDI, 1984). The corresponding coefficient of the design matrix results from the partial derivative

$$\frac{\partial \psi_{D_j}^k}{\partial \alpha} = f_s \cdot \{ T_2^k(t_i) - T_1^k(t_i) - T_2^j(t_i) + T_1^j(t_i) \} \tag{2-3}$$

The tropospheric delay T and the ionospheric delay I can be computed by special atmospheric models.

- c. Polynomial coefficients for the approximation of the common receiver time offset $\xi(t_i)$ and the time difference $\delta(t_i)$.

The receiver errors are described by

$$\xi(t_i) = a_0 + a_1(t_i - t_1) + a_2(t_i - t_1)^2 \tag{2-4}$$

$$\text{and } \delta(t_i) = b_0 + b_1(t_i - t_1) + b_2(t_i - t_1)^2 \tag{2-5}$$

The design matrix coefficients are given by

$$\frac{\partial \psi_{D_j}^k}{\partial a_n} = \frac{f_s}{c} \cdot \{ \dot{\rho}_2^k(t_i) - \dot{\rho}_1^k(t_i) - \dot{\rho}_2^j(t_i) + \dot{\rho}_1^j(t_i) \} \cdot (t_i - t_1)^n \quad (2-6)$$

$$\frac{\partial \psi_{D_j}^k}{\partial b_n} = \frac{f_s}{2c} \cdot \{ \dot{\rho}_2^k(t_i) - \dot{\rho}_1^k(t_i) - \dot{\rho}_2^j(t_i) + \dot{\rho}_1^j(t_i) \} \cdot (t_i - t_1)^n \quad (2-7)$$

with $n = 0, 1, 2$

The receiver time errors are defined by

$$\xi(t_i) = a_0 + a_1(t_i - t_1) + a_2(t_i - t_1)^2 \quad (2-8)$$

and

$$\delta(t_i) = b_0 + b_1(t_i - t_1) + b_2(t_i - t_1)^2 \quad (2-9)$$

- d. The coordinate unknowns of receiver stations are derived from the quantities $\rho(t_i)$ and $\dot{\rho}(t_i)$ which represent range and range rate between receiver and satellite location.

The partial derivatives are given by the relation

$$\begin{aligned} \frac{\partial \psi_{D_j}^k}{\partial \underline{x}} &= \frac{f_s}{c} \cdot \rho_2^k(t_i) + \\ &+ \frac{f_s}{c} \cdot \frac{\partial \dot{\rho}_2^k(t_i)}{\partial \underline{x}} \cdot \xi(t_i) - \frac{f_s}{2c} \cdot \frac{\partial \dot{\rho}_2^k(t_i)}{\partial \underline{x}} \cdot \delta(t_i) - \\ &- \frac{f_s}{c} \cdot \frac{\partial \dot{\rho}_2^j(t_i)}{\partial \underline{x}} \cdot \xi(t_i) - \\ &- \frac{f_s}{c} \cdot \frac{\partial \dot{\rho}_2^j(t_i)}{\partial \underline{x}} \cdot \delta(t_i) \end{aligned} \quad (2-10)$$

where \underline{x} is the vector of coordinate unknowns.

The partial derivatives of range and range rate are defined by the relations

$$\frac{\partial \rho(t_i)}{\partial \underline{x}} = - \frac{\underline{x}_s - \underline{x}}{\rho(t_i)} \quad (2-11)$$

$$\frac{\partial \hat{\rho}(t_i)}{\partial \underline{x}} = \frac{\underline{x}_s - \underline{x}}{\rho^2(t_i)} \cdot \hat{\rho}(t_i) - \frac{\underline{x}_s}{\rho(t_i)} \quad (2-12)$$

2.3 Atmospheric correction models

2.3.1 Tropospheric correction

Two different models of tropospheric propagation delay correction are implemented in the program. The first one was developed by GOAD and GOODMAN (1974) whereas the second is a very simple model published by BLACK (1978). Both algorithms are using surface measurements of temperature, air pressure, and relative humidity for the prediction of the current troposphere state. The different models were incorporated in order to check the accuracy of the models and their influence on baseline determination.

2.3.1 Ionospheric correction

Since C/A-Code receivers are single frequency receivers they are not able to correct for ionospheric influences as described in chapter 2.4. Therefore the program uses a special ionospheric correction model which takes advantage of the GPS-navigation data. Since ionospheric effects are very difficult to model and the applied algorithm is very easy, the correction has only a relative accuracy of 50%. Nevertheless the use of this information seems to be superior to neglecting ionospheric effects. For a detailed description of the approach the reader is referred to LANDAU, EISSFELLER (1986), KLOBUCHAR.

2.4 The processing of dual frequency data

The ionospheric effect on the signal transmission is in very good approximation inversely proportional to the square of the signal frequency (KLOBUCHAR et al., 1980). The time delay is given by the relation

$$I = \frac{A}{f^2} \quad (2-13)$$

where A ... is a scale factor depending on the current electron density in the ionosphere
and f ... is the frequency of the transmitted signal.

Considering the phase observable ψ the application of (2-12) results in

$$\Delta\psi = f \cdot I = \frac{A}{f} \quad (2-14)$$

The satellites are transmitting signals on two frequencies, which are multiplies of 10.23 (MHz).

$$L_1 : f_1 = 154 \cdot 10.23 \text{ (MHz)} = 1575.42 \text{ (MHz)}$$

$$L_2 : f_2 = 120 \cdot 10.23 \text{ (MHz)} = 1227.60 \text{ (MHz)}$$

Both frequencies are in phase at the time they are transmitted by the satellites. P-Code receivers are able to take advantage of the frequency dependent behaviour by use of the two frequencies (L_1, L_2).

Let us consider the "raw" phase measurement, neglecting receiver oscillator drift and tropospheric effects.

$$\bar{\Psi}(t_i) = \phi_S(t_i) - \phi_R(t_i) - \frac{f}{c} \cdot \rho(t_i) + \frac{A}{f} + m \quad (2-15)$$

Then the term $\frac{A}{f}$ represents the phase shift due to ionospheric effects.

Relation (2-15) can be written for each frequency.

$$L_1 : \bar{\Psi}(t_i) = \{\phi_S(t_i) - \phi_R(t_i)\} - \frac{f_1}{c} \cdot \rho(t_i) + \frac{A}{f_1} + m_1 \quad (2-16)$$

Since both, the L_1 and L_2 phase are based on the same rate of 10.23 MHz and, consequently, are fully synchronized, the following equation holds:

$$\{\phi_S(t_i) - \phi_R(t_i)\}_{L_2} = \frac{f_2}{f_1} \cdot \{\phi_S(t_i) - \phi_R(t_i)\} \quad (2-17)$$

Insertion of (2-17) in (2-16) yields

$$L_2 : \bar{\Psi}(t_i) = \frac{f_2}{f_1} \cdot \{\phi_S(t_i) - \phi_R(t_i)\} - \frac{f_2}{c} \cdot \rho(t_i) + \frac{A}{f_2} + m_2 \quad (2-18)$$

To eliminate the ionospheric effect we can use a linear combination of equations (2-16) and (2-18)

$$\bar{\Psi}(t_i) = \alpha_1 \cdot \bar{\Psi}_{L_1}(t_i) + \alpha_2 \cdot \bar{\Psi}_{L_2}(t_i) \quad (2-19)$$

with

$$\alpha_1 = \frac{f_1^2}{(f_1^2 - f_2^2)} \quad \text{and} \quad \alpha_2 = \frac{-f_1 \cdot f_2}{(f_1^2 - f_2^2)} \quad (2-20)$$

Thus we get the final observation

$$\begin{aligned} \bar{\Psi}(t_i) = \{ \phi_S(t_i) - \phi_R(t_i) \} - \frac{f_1}{c} \cdot \rho(t_i) + \\ + \alpha_1 \cdot m_1 + \alpha_2 \cdot m_2 \end{aligned} \quad (2-21)$$

By combination of the corresponding observables of the two frequencies considering (2-21) a good elimination of the ionospheric effect may be possible. The accuracy of this elimination is of the order of 2 - 3 meters. Since the differenced observations are linear combinations of quantities of type (2-21) too, the approach can be applied to all kind of processing techniques.

In practice the two frequencies are processed separately, as different cycle slips can appear in the two data sets. Afterwards the linear combination is processed, which is corrected for ionospheric influences.

2.5 The correlated nature of the observables

Since double difference observables are correlated, we have to introduce a non-diagonal weight matrix for each epoch. Each submatrix contains a 2 on the diagonal, and the non-diagonal elements are equal to 1. The submatrices together build a banded weight matrix which has to be taken into account in the adjustment process (see REMONDI, 1984, p. 122-123).

3. THE DEVELOPED SOFTWARE PRODUCT

The developed double difference processing program is a menu-driven interactive oriented program written in FORTRAN 77 and is installed on a VAX-computer. The main emphasis was put on user-friendly aspects as well as fast performance of calculations.

3.1 Program structure

The program is controlled by use of several menus providing a lot of processing features. They are described in detail in chapter 3.2. Input control is done by a special positioning file holding information about approximate station coordinates, antenna heights, file names for measurement, and orbit data, etc. The output is directed to the terminal screen and in addition to a journal file recording all user operations and program results. An example of such a journal file is given in the appendix.

3.2 Program features

In the following I like to discuss shortly the main features of the program by describing the different menu tables.

3.2.1 Main menu

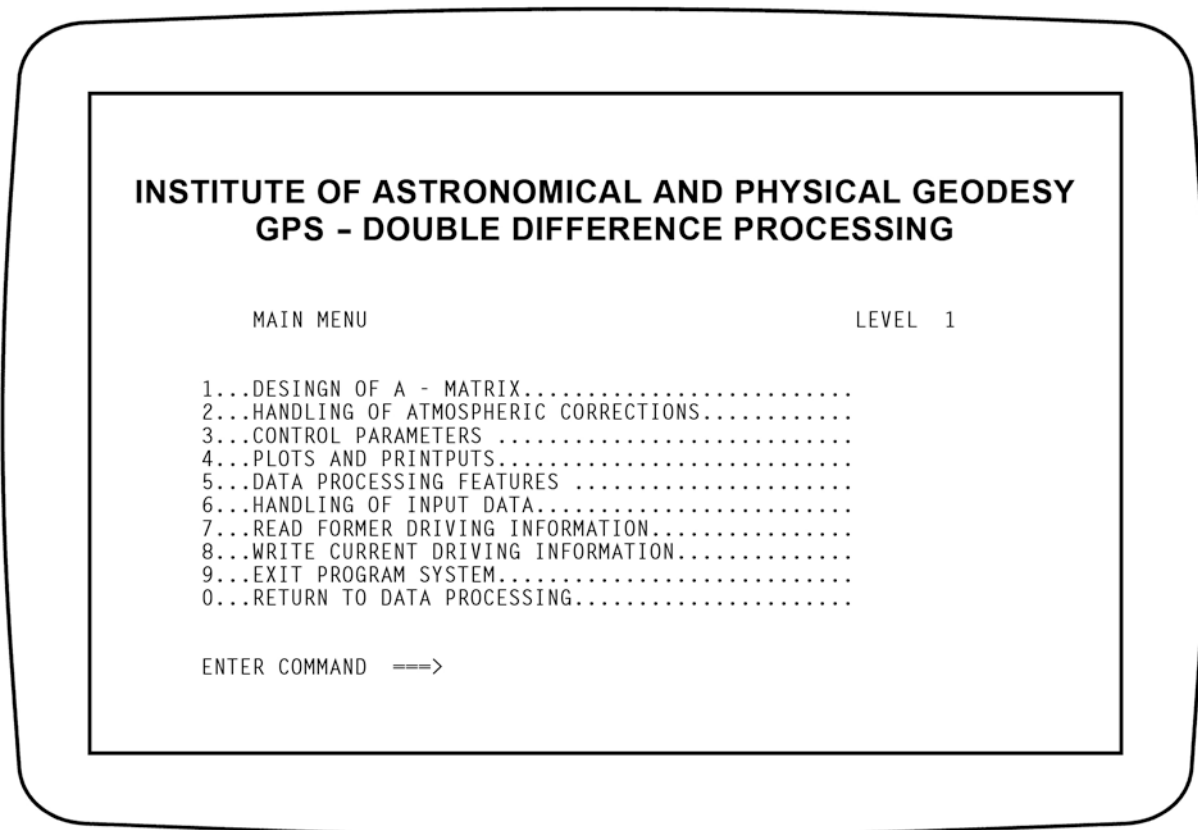


Fig. 1: Main menu

By choosing the number between 1 and 6 the user exits the main menu, and the program displays the chosen sub-menu. After finishing the data processing the operator may exit the program by pressing 9. Typing 0 results in a return to the data processing algorithm for the calculation of a new iteration with control parameters defined by the menus.

Number 6 and 7 may be chosen to read or write the current control parameters. In that case the whole necessary processing information will be transferred to or from a disk file. This is extremely useful if somebody wants to process a larger number of baseline having the same control parameters without having to define parameters each time.

3.2.2 Design of A - matrix

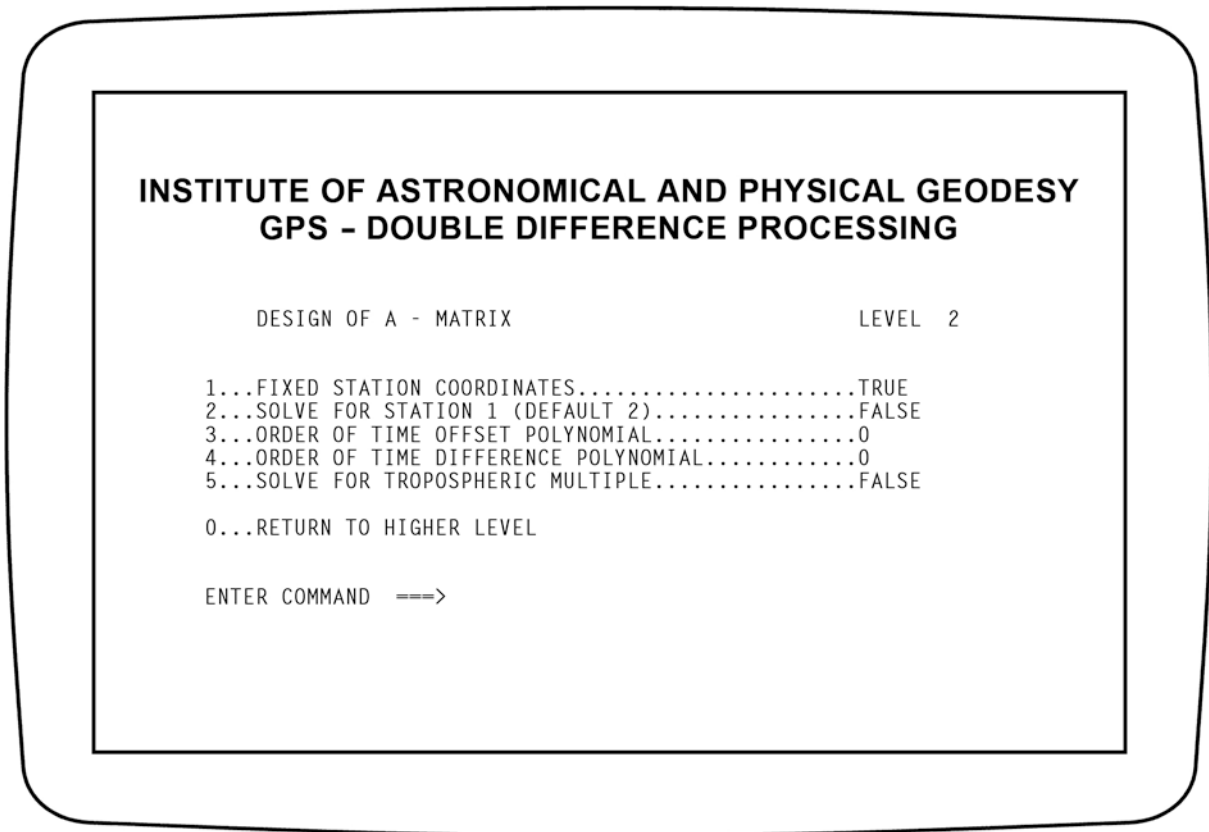


Fig. 2: Menu level 2 (Design of A - matrix)

- 1 ... monitors the fixing of station coordinates. Information records followed by "true" or "false" are always statements which can be true or false. Press 1 to switch from "true" to "false" or vice versa.
- 2 ... determines the "solve for" station. If the statement is set to true the program will solve for station 1 and if it is false it solves for station 2.
- 3 + 4 ... define the order of the time offset (time difference) polynomial.
- 5 ... activates the tropospheric scale unknown determination as discussed in chapter 2.2.

3.2.3 Handling of atmospheric corrections

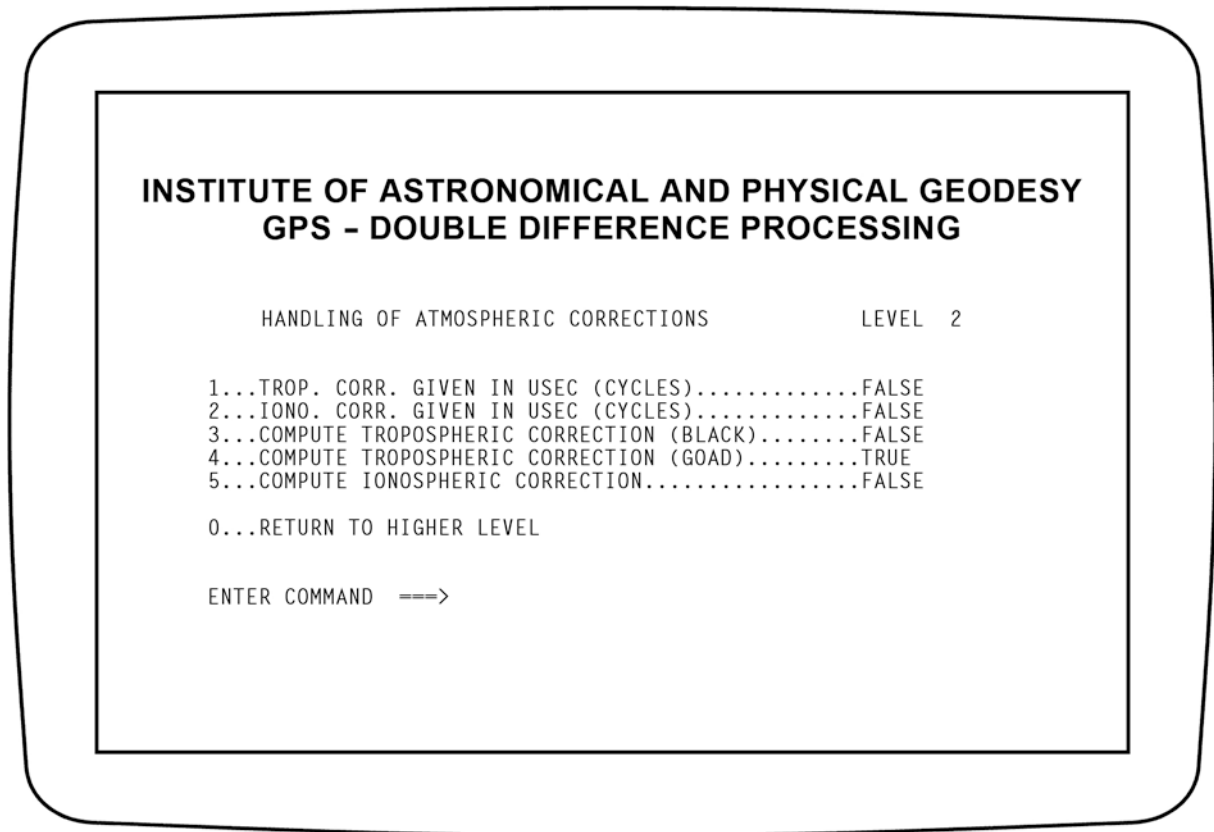


Fig. 3: Menu level 2 (Handling of atmospheric corrections)

- 1 + 2 ... control the units of given atmospheric corrections.
- 3 + 4 ... inform the program about internal computation of tropospheric correction inquiries. The Black (3) or the Goad/Goodman (4) model may be used alternatively.
- 5 ... instructs the program to correct for ionospheric influences using the Klobuchar approach.

3.2.4 Data processing features

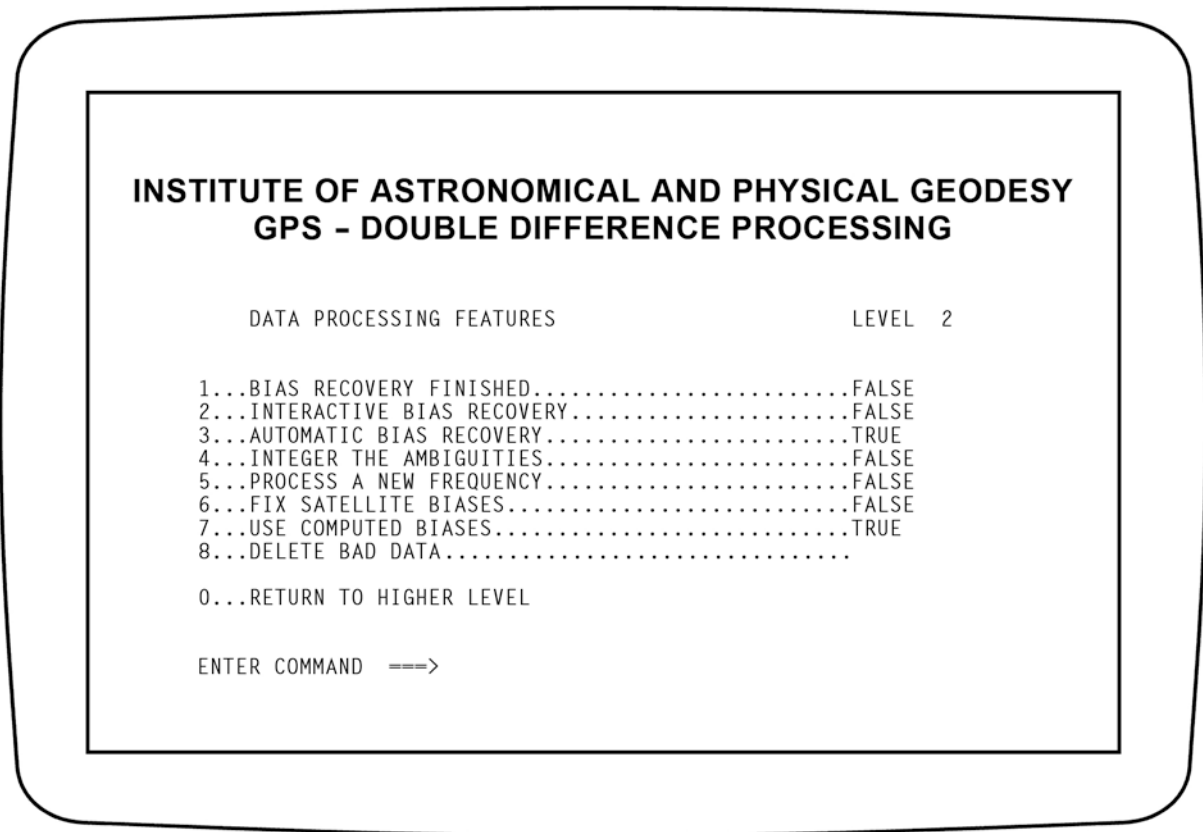


Fig. 4: Menu level 2 (Data processing features)

- 1 ... informs the program, that the bias recovery and cycle slip detection are finished and no further bias recovery is necessary.
- 2 + 3 ... choose either an interactive (user-controlled) bias recovery (2) or an automatic (program-controlled) cycle slip detection.
- 4 ... fixes the estimated ambiguities to integer values.
- 5 ... instructs the program to process a new frequency in case of dual-frequency measurements.
- 6 + 7 ... the satellite ambiguities may be fixed to pregiven values (6), otherwise the computed satellite biases are used.
- 8 ... jumps to the data deletion menu to delete outliers in the measurements.

3.2.5 Handling of input data

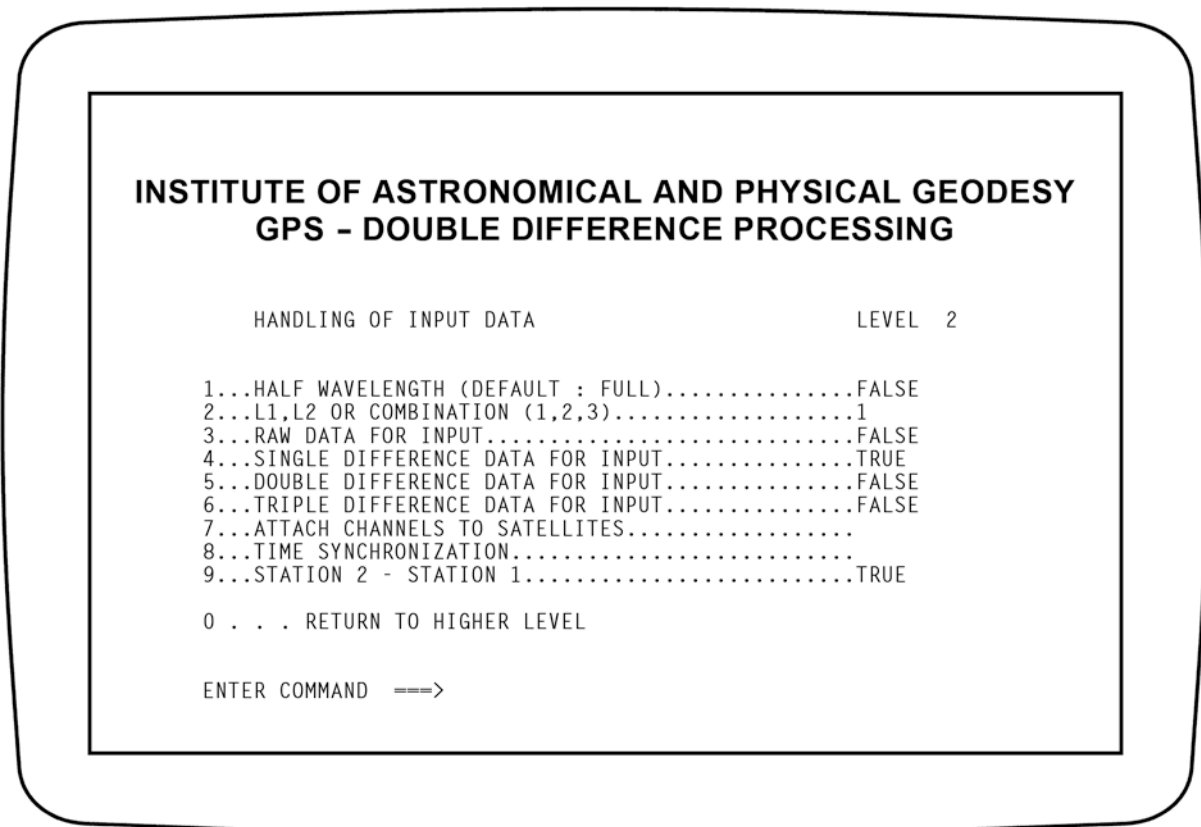


Fig. 5: Menu level 2 (Handling of input data)

- 1 ... informs the program about the type of measurement data. Half wave-length data derived from Macrometer measurements, for example, or full wave length data measured with code-receivers like the TI 4100.
- 2 ... monitors the processing of dual-frequency data. Enter 1 for L_1 -band processing, 2 for L_2 -band processing or 3 for a combination of both frequencies.
- 3 to 6 .. specify the type of measurement data to be used during processing.
- 7 ... attaches satellite numbers to the observation channels. This is not necessary if the channel numbers are identical with satellite numbers.
- 8 ... jumps to the time synchronization menu. It allows the synchronization of measurement data and orbit data. Results of clock comparison can be used for receiver synchronization.
- 9 ... informs the program about the type of measurement data used during processing in case of phase difference observation

data (single, double, triple). The differences may have been computed by differencing raw phase observables of station 2 minus station 1 or vice versa.

4. PROCESSING OF REAL DATA

4.1 Description of observed data set

In the following I would like to describe the processing of real observation data with the developed software product. It was done with data kindly provided by the Hessian Department of Surveys ("Landesvermessungsamt Hessen") and collected during a Macrometer campaign in November 1984. The data set consists of raw phase observational data at each of the stations shown in figure 6. Furthermore one state vector for each considered satellite was available. Please note, that no information about antenna heights, weather data and time synchronization was available during the computation process. An unrealistic assumption about the atmosphere during the measurement period along with an unsymmetrical distribution of satellites above the horizon (Fig. 7) could lead to the rotation of the resulting baseline components. For that reason a comparison with results obtained by a U.S. commercial firm might be difficult.

4.2 Prediction of satellite orbits

Starting with the given state vectors for each satellite we predicted the satellite position in an inertial reference frame by applying a Krogh - Shampine - Gordon fixed-step integrator and a specific force modelling described in LANDAU, HAGMAIER (1986). The satellite positions were computed for time intervals of 180 seconds. It can be assumed, that the satellite positions are accurate to approximately 50 meters.

4.3 Processing description and results

Due to difficulties in modelling atmospheric corrections caused by missing weather measurement data and unknown antenna heights, the author decided to restrict the processing to the triangle "Hausberg, Hupp, Bauernheim" observed on the 320th day of 1984 during 2:00 and 5:40 UTC time (see table 3 and figure 8). The atmospheric corrections were computed by use of a normal atmosphere. The antenna heights were put equal to zero. The baseline "Bauernheim - Hausberg" was computed by two different programs. First the author applied the single difference program received from the National Geodetic Survey. Afterwards the same baseline was processed with the developed double difference program. Another check was made by calculating a triangle and computing the vector closure. The results will be given below.

Table 1 shows the results of single and double difference processing for a single baseline. We can see that the differences in the baseline components are up to about 3 cm for the x-component, and the baseline length differs by only 4 mm. The accuracy estimates are slightly smaller for the single difference processing. Nevertheless the results look very promising for both processing types. (A detailed double difference processing output is given in the appendix.)

	SINGLE DIFFERENCES [m]	DOUBLE DIFFERENCES [m]	DIFF. [cm]
Δx	-4499.124	-4499.092	-3.2
Δy	-15105.124	-15105.124	0.0
Δz	5993.447	5993.459	-1.2
Length	16862.037	16862.033	0.4
$m_{\Delta x}(Q_{xy})$	± 0.8 cm (-0.64)	± 2.0 cm (-0.41)	
$m_{\Delta y}(Q_{xz})$	± 0.3 cm (+0.23)	± 0.5 cm (+0.71)	
$m_{\Delta z}(Q_{yz})$	± 0.3 cm (+0.44)	± 0.6 cm (+0.14)	

Table 1: Results of processing baseline "Bauernheim - Hausberg"

In order to check the double difference program a triangle with 3 baselines was processed and the vector closure was computed. The results are given in table 2.

Baseline	Δx [m] Δy [m] Δz [m]	$m_{\Delta x}$ [cm] $m_{\Delta y}$ [cm] $m_{\Delta z}$ [cm]	$Q_{\Delta x \Delta y}$ $Q_{\Delta x \Delta z}$ $Q_{\Delta y \Delta z}$
Bauernheim - Hausberg	-4499.092 -15105.124 5993.459	± 2.0 ± 0.5 ± 0.6	-0.41 0.71 0.14
Hausberg - Hupp	-10730.816 24707.399 5380.541	± 4.5 ± 1.4 ± 1.4	-0.54 0.67 0.09
Hupp - Bauernheim	15229.888 -9602.285 -11374.020	± 4.3 ± 1.3 ± 1.2	-0.55 0.64 0.12
Vector closure	-0.020 -0.010 -0.020		

Table 2: Results of double difference processing in triangle "Bauernheim-Hausberg-Hupp" and vector closure

It shows that the vector closure for the considered baseline is less than or equal to 2 cm. The processing model and the software can therefore be assumed to be correct, since vector closures of that magnitude are below the baseline component standard errors.

5. SUMMARY AND PROSPECTS

The mathematical frame for the double-difference processing with a new program system has been given along with a detailed description of the software product itself. The results of some test computations were presented in order to show the efficiency of the programmed algorithm.

Due to the lack of information, no direct comparison of our results with U.S. commercial firm's results was possible. The author intends to do more research in processing the data as soon as more information about time synchronization, weather data and antenna heights is available. The ability of processing single and triple differences will be incorporated into the program system.

6. REFERENCES

- Black, H.D. (1978): *An easily implemented algorithm for the tropospheric range correction*. Journal of Geophysical Research, Vol. 83, April 1978
- Goad, C.C., Lt. L. Goodman (1974): *A modified Hopfield tropospheric refraction model*. Presented at the Annual Fall Meeting of the American Geophysical Union in San Francisco, December 1974
- Hein, G.W., B. Eissfeller (1985): *Integrated modelling of GPS-orbits and multi-baseline components*. In Proc. of the First International Symposium on Precise Positioning with the Global Positioning System, April 15-19, 1985, p. 263-272
- Klobuchar, J.A., H. Soicher, J.A. Pearson (1980): *A preliminary evaluation of the two-frequency ionospheric correction for the NAVSTAR-Global Positioning System*. In AGARD-CP-284: Propagation effects in space/earth paths
- Klobuchar, J.A.: *Ionospheric time delay corrections for advanced satellite ranging systems*. AGARD-CP-209
- Landau, H., B. Eissfeller (1986): *Optimization of GPS-satellite selection for high precision differential positioning*. In GPS Research at the Institute of Astronomical and Physical Geodesy, Report No. 19, University FAF Munich, p. 65-105
- Landau, H., D. Hagmaier (1986): *Analysis of the required force modelling for NAVSTAR/GPS satellites*. In GPS Research at the Institute of Astronomical and Physical Geodesy, Report No. 19, University FAF Munich, p. 193-208
- Remondi, B. (1984): *Using the Global Positioning System (GPS) phase observable for relative geodesy: modelling, processing and results*. Ph.D. Dissertation, University for Space Research, The University of Texas in Austin

APPENDIX

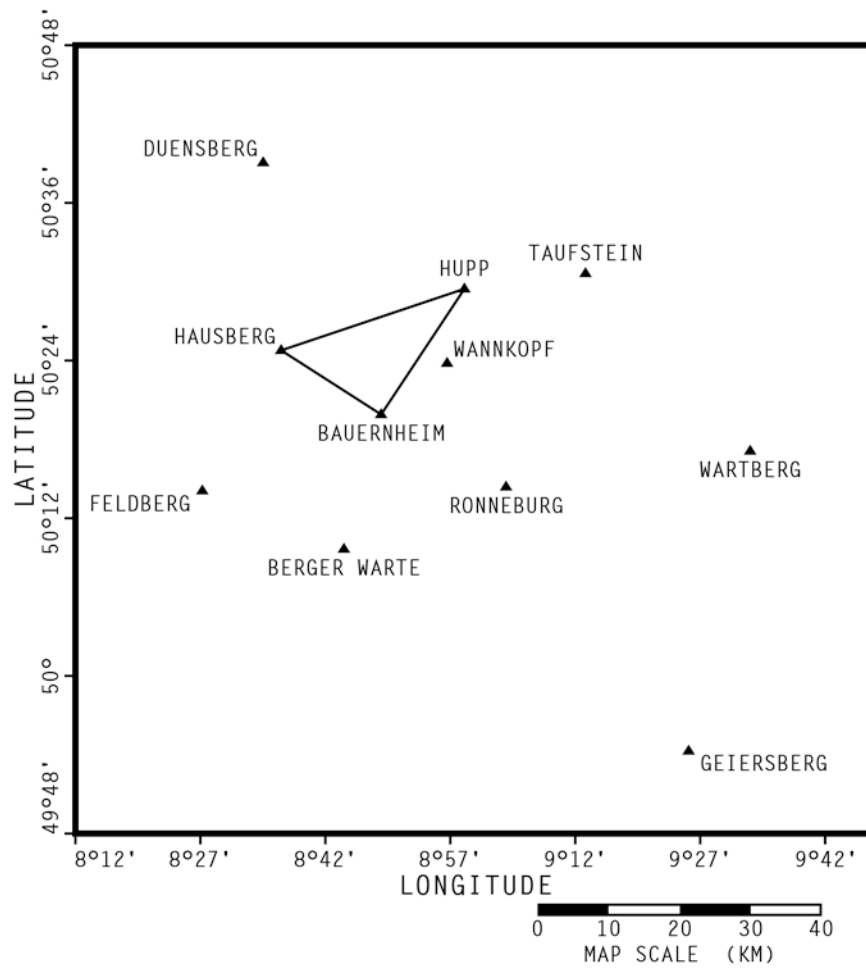


Fig. 6: Stations with GPS phase measurements

SATELLITE PASSES OF THE NAVSTAR-GPS SYSTEM

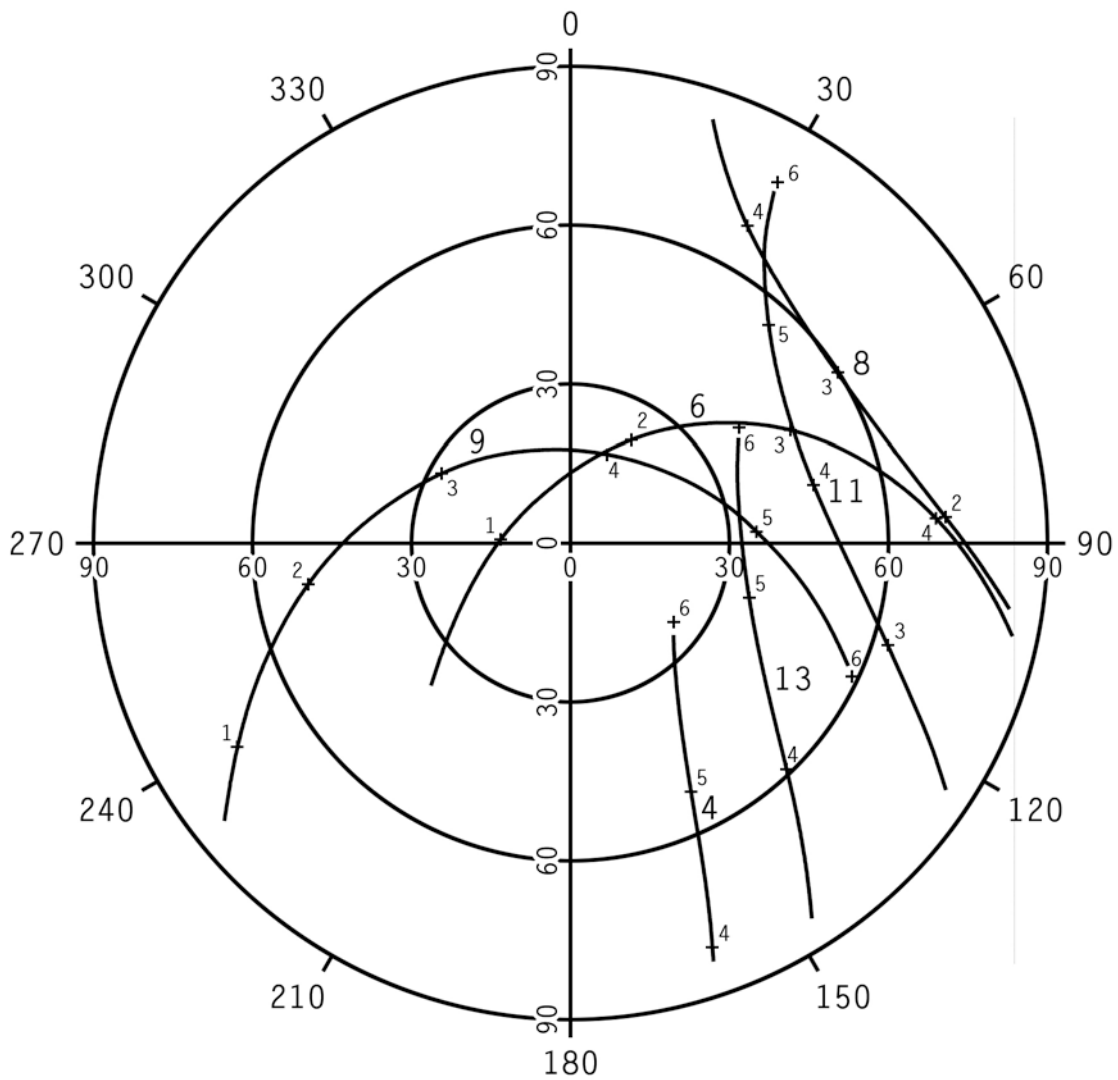
STATION : RONNEBURG

DATE : 15.11.84

Latitude : 50.240 degrees

Longitude : 9.068 degrees

Height : 236 meter



INSTITUTE OF ASTRONOMICAL AND PHYSICAL GEODESY
UNIVERSITY FAF , MUNICH

Fig. 7: Satellite passes

SATELLITE PASSES OF THE NAVSTAR-GPS SYSTEM

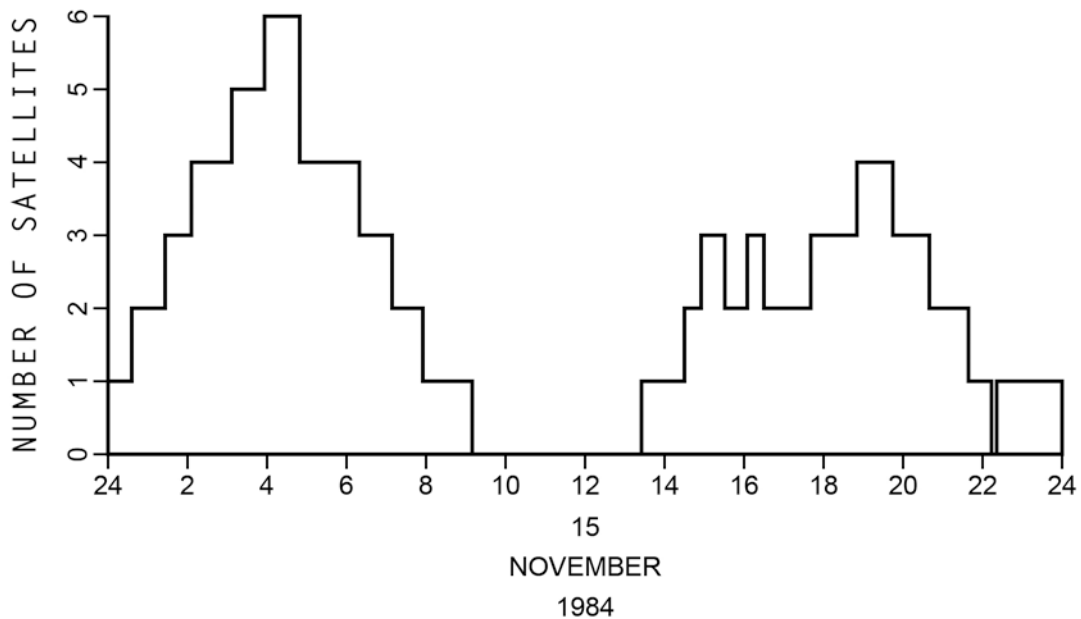
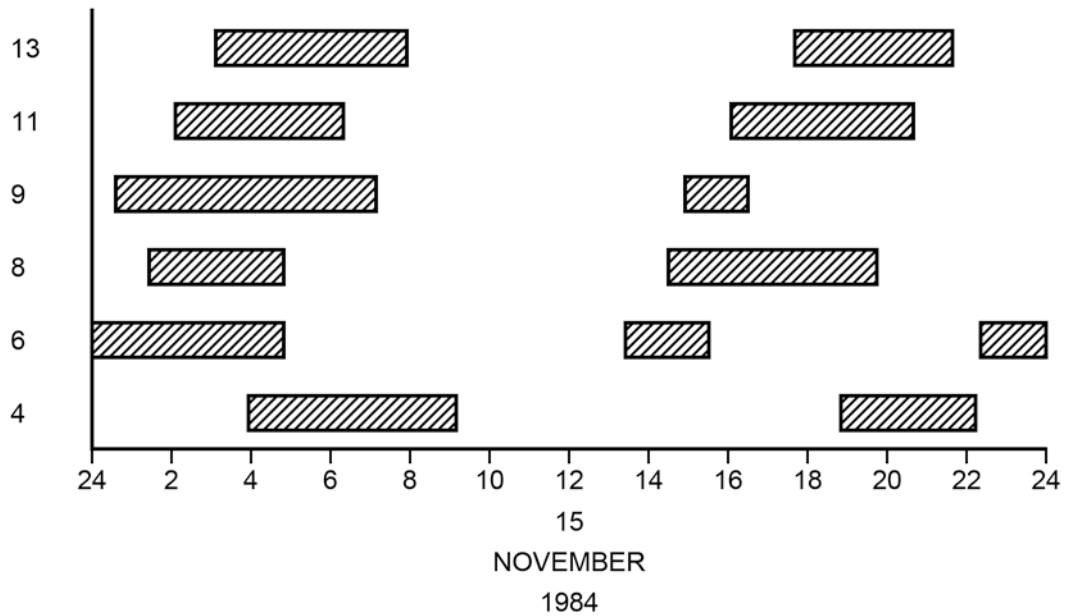
STATION : RONNEBURG

DATE : 15.11.84

Latitude : 50.240 degrees

Longitude : 9.068 degrees

Height : 236 meter



INSTITUTE OF ASTRONOMICAL AND PHYSICAL GEODESY
UNIVERSITY FAF , MUNICH

Fig. 8: Satellite visibility

VISIBILITY OF GPS SPACECRAFT ON NOVEMBER 15, 1984

STATION NAME : RONNEBURG
 LATITUDE : 50.24 DEGREES
 LONGITUDE : 9.07 DEGREES
 HEIGHT : 236.95 METER

SV NO	4		6		8		9		11		13	
HH MM	EL	AZ	EL	AZ	EL	AZ	EL	AZ	EL	AZ	EL	AZ
0:10			57	229								
0:20			62	234								
0:30			66	241			6	231				
0:40			71	250			10	234				
0:50			75	264			14	236				
1:00			78	283			18	240				
1:10			79	310			22	243				
1:20			78	338	6	98	26	246				
1:30			76	0	10	95	30	250				
1:40			73	15	13	91	34	254				
1:50			69	26	17	88	38	258				
2:00			65	34	20	84	41	263	5	122		
2:10			61	40	22	80	45	268	9	120		
2:20			57	46	25	75	49	273	13	118		
2:30			52	51	27	70	53	279	17	115		
2:40			48	56	28	65	57	286	21	112		
2:50			45	60	29	60	60	294	25	109		
3:00			41	64	30	54	63	302	29	105	6	147
3:10			37	69	29	49	66	313	32	101	10	145
3:20			33	72	28	44	69	325	35	96	14	143
3:30			29	76	27	39	71	340	38	91	19	141
3:40			26	80	25	34	72	356	40	86	24	139
3:50	6	160	22	84	22	31	72	13	42	79	28	137
4:00	11	159	19	87	19	27	70	30	42	73	33	134
4:10	15	159	15	91	16	24	69	44	42	66	37	131
4:20	20	158	12	94	13	22	66	56	42	60	42	127
4:30	25	157	8	98	9	20	63	66	40	54	46	123
4:40	30	155	5	101	5	18	60	75	38	48	50	117
4:50	35	154					56	82	35	44	53	110
5:00	40	152					52	89	32	40	55	102
5:10	45	150					48	94	29	37	57	93
5:20	50	148					45	100	25	34	57	83
5:30	55	144					41	104	21	32	57	74
5:40	59	138					37	109	17	31	55	65
5:50	63	131					33	113	13	30	52	58
6:00	67	121					29	116	9	29	49	52
6:10	69	106					25	120	5	29	45	48
6:20	69	93					21	123			41	44
6:30	68	78					17	126			37	42
6:40	66	66					13	129			33	41
6:50	63	58					9	132			28	40
7:00	59	52					5	134			24	39
7:10	54	48									20	39
7:20	50	45									16	40
7:30	45	44									11	40
7:40	40	43									7	41
7:50	36	43										
8:00	31	43										
8:10	27	44										
8:20	23	45										
8:30	18	47										
8:40	14	48										
8:50	10	50										
9:00	6	52										
9:10												
9:20												
9:30												
9:40												
9:50												
10:00												
10:10												
10:20												
10:30												
10:40												
10:50												
11:00												
11:10												

Table 3: Visibility table

SV NO	4		6		8		9		11		13	
HH MM	EL	AZ										
11:20												
11:30												
11:40												
11:50												
12:00												
12:10												
12:20												
12:30												
12:40												
12:50												
13:00												
13:10												
13:20			5	2								
13:30			7	359								
13:40			9	355								
13:50			11	351								
14:00			12	347								
14:10			13	342								
14:20			13	338								
14:30			13	334	8	309						
14:40			12	329	12	311						
14:50			11	325	16	312	5	20				
15:00			9	321	20	314	7	16				
15:10			7	317	25	315	8	12				
15:20			5	313	29	316	9	8				
15:30					34	316	10	4				
15:40					38	316	10	359				
15:50					43	316	9	355				
16:00					47	315	8	351	5	322		
16:10					52	312	7	347	9	323		
16:20					56	309	5	343	13	323		
16:30					60	304			17	323		
16:40					64	296			22	323		
16:50					67	286			26	322		
17:00					68	272			30	321		
17:10					68	258			34	319		
17:20					67	244			38	316		
17:30					64	233			42	313		
17:40					60	225			45	308	7	333
17:50					56	219			48	302	11	332
18:00					51	214			50	296	15	331
18:10					46	211			52	288	19	329
18:20					41	209			52	280	22	327
18:30					36	207			52	271	26	324
18:40					31	205			50	263	29	321
18:50	7	340			26	204			48	256	32	317
19:00	11	339			21	203			45	249	34	312
19:10	14	336			17	202			41	244	36	307
19:20	18	334			12	201			37	239	37	301
19:30	21	330			7	200			33	236	37	295
19:40	23	327							29	232	37	289
19:50	25	322							24	229	36	283
20:00	27	318							20	227	34	277
20:10	28	313							15	225	32	272
20:20	29	307							11	223	30	267
20:30	29	302							7	220	27	263
20:40	28	297									23	259
20:50	27	291									20	256
21:00	25	286									16	252
21:10	23	282									12	249
21:20	20	277									8	247
21:30	17	274									5	244
21:40	14	270										
21:50	10	266										
22:00	7	263										
22:10												
22:20			7	201								
22:30			12	202								
22:40			16	204								
22:50			24	206								
23:00			26	208								
23:10			30	210								
23:20			35	212								
23:30			40	215								
23:40			45	218								
23:50			49	222								
24:00			54	226								

Visibility table (Continued)

UNIVERSITY OF THE FEDERAL ARMED FORCES IN MUNICH
INSTITUTE OF ASTRONOMICAL AND PHYSICAL GEODESY

GPS PHASE DIFFERENCE ADJUSTMENT PROGRAM
DOUBLE DIFFERENCE PROCESSING

PROJECT : MACROMETER MEASUREMENTS IN HESSEN (FRG) NOV. 1984
DATE : 20-DEC-85

INPUT DATA :

POSITION FILE NAME..... : L0519D320.POS
SINGLE DIFFERENCE DATA FILE NAME..... : L0519D320.SNG
EPHEMERIS DATA FILE NAME..... : HES.EPH

STATION 1 : BAUERNHEIM

LATITUDE (D,M,S) : 50 19 49.9001
LONGITUDE (D,M,S) : 8 48 54.3778
ELL. HEIGHT (M) : 218.138
ANT. HEIGHT (M) : 0.000
MSL HEIGHT (M) : 218.138

STATION 2 : HAUSBERG

LATITUDE (D,M,S) : 50 24 41.5027
LONGITUDE (D,M,S) : 8 36 53.3882
ELL. HEIGHT (M) : 537.491
ANT. HEIGHT (M) : 0.000
MSL HEIGHT (M) : 537.491

APPROXIMATE BASELINE VECTOR :

DX = -4499.543 DY = -15105.0412 DZ = 5993.137 L = 16861.965 (M)

Output of double difference processing program

UNIVERSITY OF THE FEDERAL ARMED FORCES IN MUNICH
INSTITUTE OF ASTRONOMICAL AND PHYSICAL GEODESY

GPS PHASE DIFFERENCE ADJUSTMENT PROGRAM
DOUBLE DIFFERENCE PROCESSING

PROJECT : MACROMETER MEASUREMENTS IN HESSEN (FRG) NOV. 1984
DATE : 20-DEC-85

CHOSEN DRIVING PARAMETERS :

SOLVE FOR STATION 2
TROPOSPHERIC CORRECTION GIVEN IN [CYCLES]
USE COMPUTED BIASES
MULTIPLE OF RMS..... : 0.30000000D+10 cycles
ELEVATION CUTOFF ANGLE..... : 15 degrees
BIAS RECOVERY BY PROGRAMMED ALGORITHM
L1-BAND PROCESSING
WORKING WITH THE HALF WAVELENGTH
TIME DIFFERENCE MEASUREMENT DATA - ORBIT DATA : 0 SECONDS

NUMBER OF OBSERVATIONS :

SATELLITE	SD-OBSERVATIONS
4	13
6	28
8	21
9	59
11	44
13	25

CHOSEN REFERENCE SATELLITE : 9

Output of double difference processing program (Continued)

UNIVERSITY OF THE FEDERAL ARMED FORCES IN MUNICH
 INSTITUTE OF ASTRONOMICAL AND PHYSICAL GEODESY

GPS PHASE DIFFERENCE ADJUSTMENT PROGRAM
 DOUBLE DIFFERENCE PROCESSING

PROJECT : MACROMETER MEASUREMENTS IN HESSEN (FRG) NOV. 1984
 DATE : 20-DEC-85

PROCESSING RESULTS OF 1. ITERATION :

ROOT MEAN SQUARE ERROR 0.163

UNKNOWN PARAMETER	UNITS	CORRECTION	ESTIM. VALUE	STD.ERR.
DELTA-X	METER	0.4523	-4499.0908	0.0199
DELTA-Y	METER	-0.0829	-15105.1243	0.0052
DELTA-Z	METER	0.3231	5993.4600	0.0063
AMBIGUITY 4	CYCLES	-226853.673	-226853.673	0.111
AMBIGUITY 6	CYCLES	-79030.960	-79030.960	0.117
AMBIGUITY 8	CYCLES	-194827.679	-194827.679	0.195
AMBIGUITY 11	CYCLES	-243270.922	-243270.922	0.083
AMBIGUITY 13	CYCLES	-242183.051	-242183.051	0.072

LENGTH OF BASELINE : 16862.0331 METER

CORRELATION COEFFICIENTS :

QXY: -0.4137 QXZ: 0.7058 QYZ: 0.1423

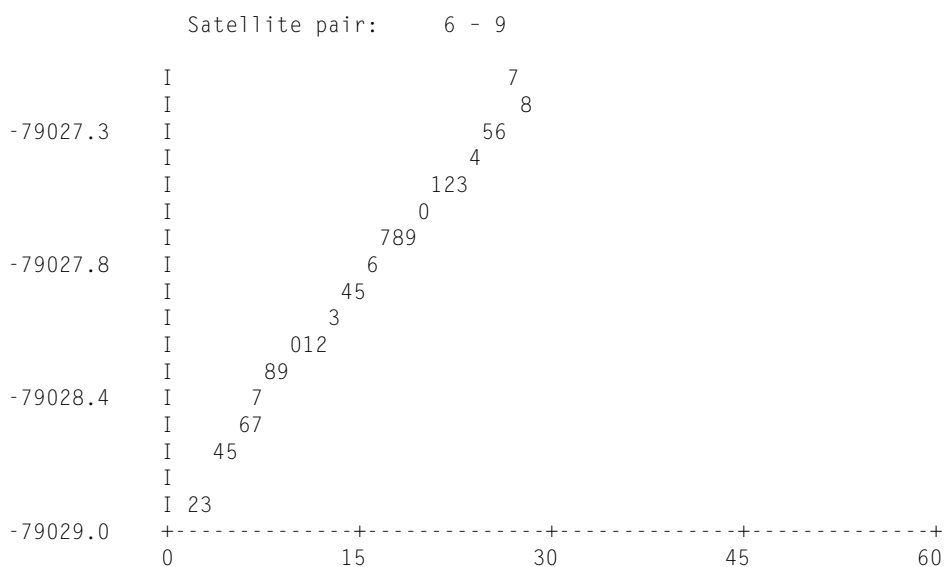
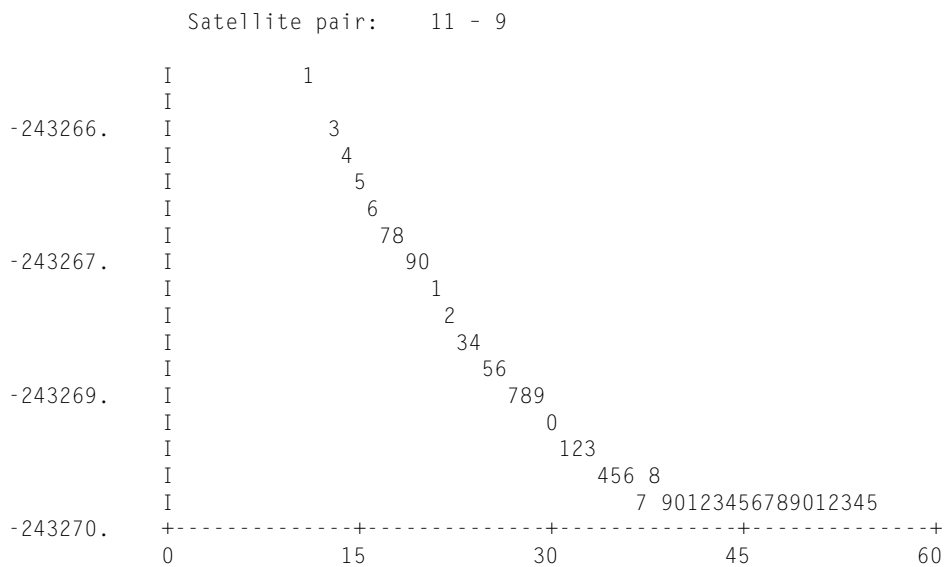
	LATITUDE	LONGITUDE	ELL. HEIGHT
BAUERNHEIM	50 19 49.9001	8 48 54.3778	218.138
HAUSBERG	50 24 41.4985	8 36 53.3806	538.017

Output of double difference processing program

UNIVERSITY OF THE FEDERAL ARMED FORCES IN MUNICH
 INSTITUTE OF ASTRONOMICAL AND PHYSICAL GEODESY

GPS PHASE DIFFERENCE ADJUSTMENT PROGRAM
 DOUBLE DIFFERENCE PROCESSING

PROJECT : MACROMETER MEASUREMENTS IN HESSEN (FRG) NOV. 1984
 DATE : 20-DEC-85

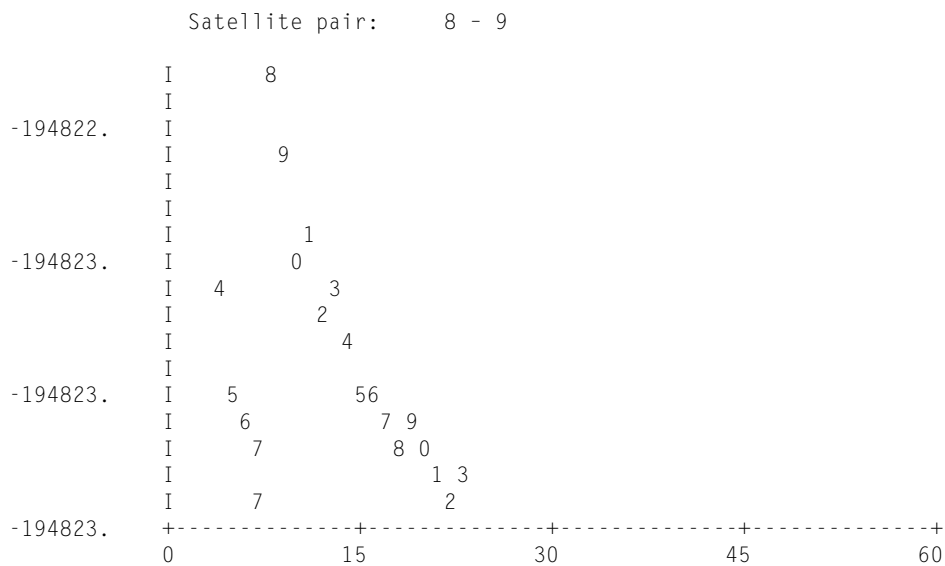
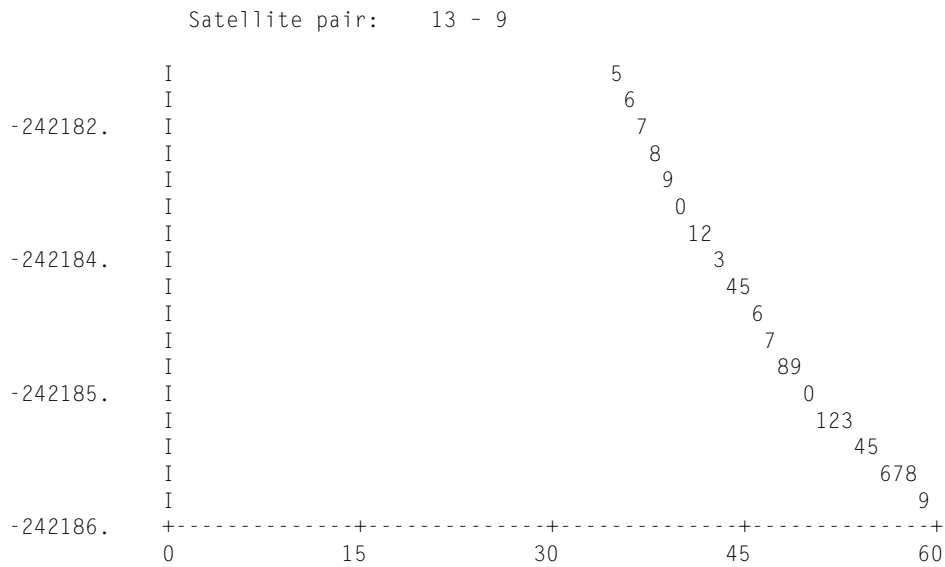


Output of double difference processing program

UNIVERSITY OF THE FEDERAL ARMED FORCES IN MUNICH
 INSTITUTE OF ASTRONOMICAL AND PHYSICAL GEODESY

GPS PHASE DIFFERENCE ADJUSTMENT PROGRAM
 DOUBLE DIFFERENCE PROCESSING

PROJECT : MACROMETER MEASUREMENTS IN HESSEN (FRG) NOV. 1984
 DATE : 20-DEC-85

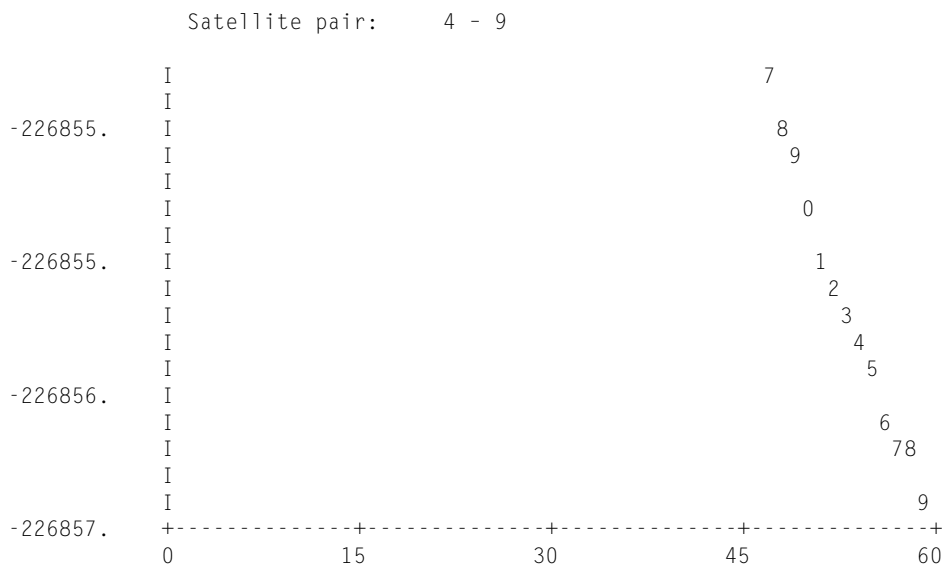


Output of double difference processing program

UNIVERSITY OF THE FEDERAL ARMED FORCES IN MUNICH
INSTITUTE OF ASTRONOMICAL AND PHYSICAL GEODESY

GPS PHASE DIFFERENCE ADJUSTMENT PROGRAM
DOUBLE DIFFERENCE PROCESSING

PROJECT : MACROMETER MEASUREMENTS IN HESSEN (FRG) NOV. 1984
DATE : 20-DEC-85



Output of double difference processing program

UNIVERSITY OF THE FEDERAL ARMED FORCES IN MUNICH
INSTITUTE OF ASTRONOMICAL AND PHYSICAL GEODESY

GPS PHASE DIFFERENCE ADJUSTMENT PROGRAM
DOUBLE DIFFERENCE PROCESSING

PROJECT : MACROMETER MEASUREMENTS IN HESSEN (FRG) NOV. 1984
DATE : 20-DEC-85

CHOSEN DRIVING PARAMETERS :

SOLVE FOR STATION 2
TROPOSPHERIC CORRECTION GIVEN IN [CYCLES]
USE COMPUTED BIASES
MULTIPLE OF RMS..... : 0.30000000D+10 cycles
ELEVATION CUTOFF ANGLE..... : 15 degrees
BIAS RECOVERY BY PROGRAMMED ALGORITHM
L1-BAND PROCESSING
WORKING WITH THE HALF WAVELENGTH
TIME DIFFERENCE MEASUREMENT DATA - ORBIT DATA : 0 SECONDS

NUMBER OF OBSERVATIONS :

SATELLITE	SD-OBSERVATIONS
4	13
6	28
8	21
9	59
11	44
13	25

CHOSEN REFERENCE SATELLITE : 9

Output of double difference processing program (Continued)

UNIVERSITY OF THE FEDERAL ARMED FORCES IN MUNICH
 INSTITUTE OF ASTRONOMICAL AND PHYSICAL GEODESY

GPS PHASE DIFFERENCE ADJUSTMENT PROGRAM
 DOUBLE DIFFERENCE PROCESSING

PROJECT : MACROMETER MEASUREMENTS IN HESSEN (FRG) NOV. 1984
 DATE : 20-DEC-85

PROCESSING RESULTS OF 1. ITERATION :

ROOT MEAN SQUARE ERROR 0.163

UNKNOWN PARAMETER	UNITS	CORRECTION	ESTIM. VALUE	STD.ERR.
DELTA-X	METER	0.0000	-4499.0908	0.0199
DELTA-Y	METER	-0.0000	-15105.1243	0.0052
DELTA-Z	METER	0.0000	5993.4600	0.0063
AMBIGUITY 4	CYCLES	0.000	-226853.673	0.111
AMBIGUITY 6	CYCLES	0.000	-79030.960	0.117
AMBIGUITY 8	CYCLES	0.000	-194827.679	0.195
AMBIGUITY 11	CYCLES	0.000	-243270.922	0.083
AMBIGUITY 13	CYCLES	0.000	-242183.051	0.072

LENGTH OF BASELINE : 16862.0331 METER

CORRELATION COEFFICIENTS :

QXY: -0.4137 QXZ: 0.7058 QYZ: 0.1423

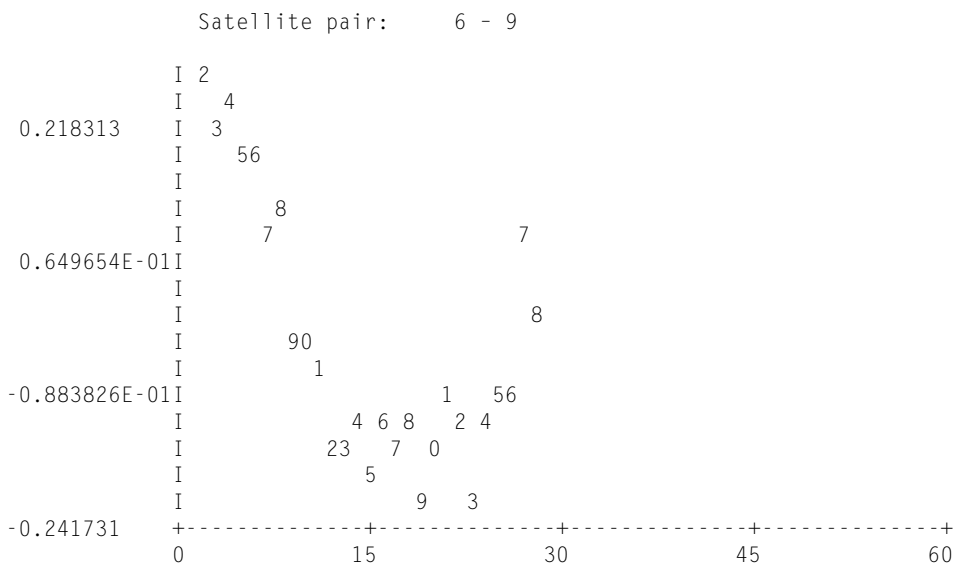
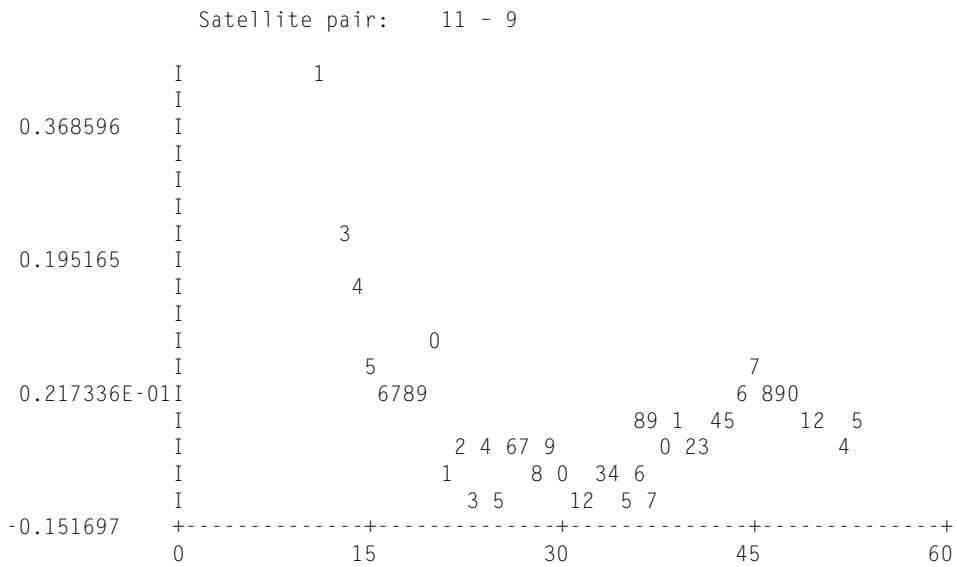
	LATITUDE	LONGITUDE	ELL. HEIGHT
BAUERNHEIM	50 19 49.9001	8 48 54.3778	218.138
HAUSBERG	50 24 41.4985	8 36 53.3806	538.017

Output of double difference processing program

UNIVERSITY OF THE FEDERAL ARMED FORCES IN MUNICH
 INSTITUTE OF ASTRONOMICAL AND PHYSICAL GEODESY

GPS PHASE DIFFERENCE ADJUSTMENT PROGRAM
 DOUBLE DIFFERENCE PROCESSING

PROJECT : MACROMETER MEASUREMENTS IN HESSEN (FRG) NOV. 1984
 DATE : 20-DEC-85

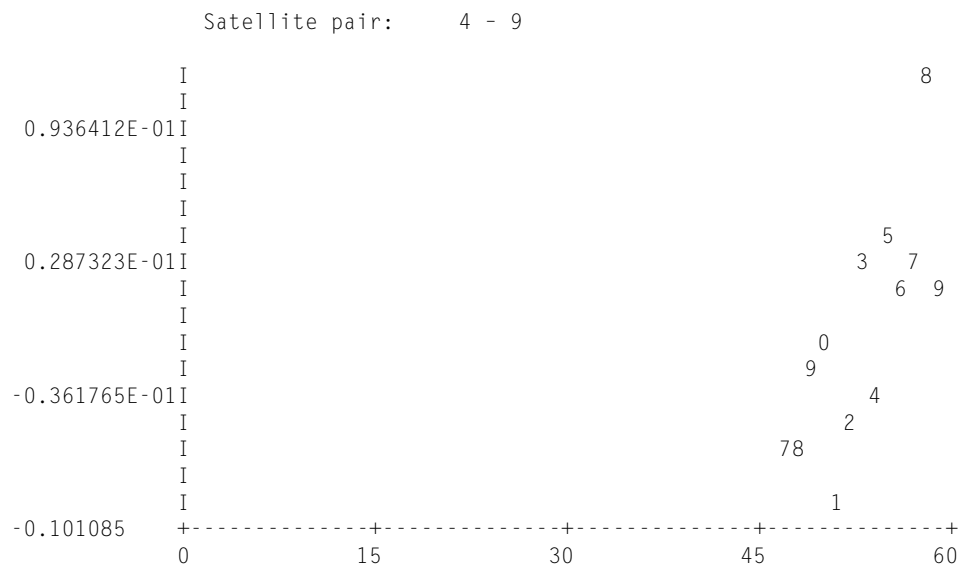


Output of double difference processing program

UNIVERSITY OF THE FEDERAL ARMED FORCES IN MUNICH
 INSTITUTE OF ASTRONOMICAL AND PHYSICAL GEODESY

GPS PHASE DIFFERENCE ADJUSTMENT PROGRAM
 DOUBLE DIFFERENCE PROCESSING

PROJECT : MACROMETER MEASUREMENTS IN HESSEN (FRG) NOV. 1984
 DATE : 20-DEC-85



Output of double difference processing program

ANALYSIS OF THE REQUIRED FORCE-MODELLING
FOR NAVSTAR / GPS SATELLITES

Herbert Landau and Dirk Hagmaier
Institute of Astronomical and Physical Geodesy
University FAF Munich
Werner-Heisenberg-Weg 39
D-8014 Neubiberg, F.R. Germany

ABSTRACT. For precise baseline determination using carrier phase measurements to GPS satellites a high-precise orbit is necessary. To achieve a positioning accuracy of 0.1 ppm (± 1 cm for a 100 km baseline) we need an orbit accuracy of 2 m. The paper describes the necessary force-modelling for an orbit integration up to 6 days. The different gravitational forces caused by earth, moon, sun and planets together with the non-gravitational forces like solar radiation pressure and air drag are discussed in detail.

1. INTRODUCTION

Geodetic positioning is more and more influenced by the NAVSTAR / GPS satellite system. Although the system is still in a setup state, accuracies of 1 ppm were achieved already using carrier phase measurements. Precise ephemeris data were an essential assumption for receiving such excellent results. The accuracies of 1 ppm were obtained by use of precise orbit data computed by the U.S. Defense Mapping Agency or an U.S. commercial firm. An error of ± 50 m can be assumed for this data (REMONDI 1984). This data can only be accessed by "authorized" users. The U.S. army even plans to deteriorate the quality of broadcast messages which give information about orbital elements of satellites. Furthermore the tracking network currently in use by the U.S. institutions is not very profitable for precise positioning in Europe. Several institutions intend to determine satellite orbits representative for the area they are interested in (NAKIBOGLU et al. (1985) for Canada, STOLZ et al. (1984) for Australia, LARDEN and BENDER (DMA) for the whole world) in order to get the highest obtainable accuracy. Studying the literature we find estimates varying between ± 20 cm and 20 m for the highest obtainable orbit accuracy.

Our institute works on the field of modelling and processing for a combined determination of station locations and satellite positions using GPS measurements (HEIN and EISSFELLER 1985). In preparation of that work we

analyzed the different forces acting on a GPS satellite with respect to the required accuracy.

2. ACCURACY REQUIREMENTS AND LIMITATIONS

The accuracy which can be obtained from GPS-carrier phase difference processing essentially depends on the accuracy of the satellite orbit. The following rule-of-thumb is a useful tool for describing the influence of the satellite orbit error on the baseline length.

$$\frac{db}{b} = \frac{dr}{\rho} \quad (2-1)$$

where b is the baseline length,
 ρ is the receiver satellite distance,
 dr is the orbit error,
and db is the error of the baseline length b .

With $\rho = 20\,000$ km we get

$\frac{db}{b}$ [ppm]	dr [m]
5	100
1	20
0.5	10
0.1	2

Table 1: Baseline accuracy

Note that for an orbit error of 20 m and a baseline length of 100 km the baseline can be estimated with an accuracy of 10 cm. To achieve a baseline accuracy of 0.1 ppm an orbit accuracy of 2 m is necessary.

Other limiting factors concerning positioning accuracy are the atmospheric effects on the propagation of the GPS signals. In the present paper we want to restrict ourselves to the force model analysis, but it should be mentioned that atmospheric propagation delays can cause errors of up to 60 m in the measured receiver-satellite range. In differential positioning the error depends mainly on the baseline length. Concerning that field of work we want to refer to LANDAU and EISSFELLER (1985).

3. PRELIMINARY CONSIDERATIONS

3.1 The reference system

The following considerations about the motion of the satellite and perturbing forces are only valid in an inertial reference frame. Therefore we will describe all effects in the instantaneous system at epoch t_0 . We use the 1950.0 reference date for locating spacecrafts and planets. The origin of the system lies in the geocenter and the x-axis points to the true equinox at $t = t_0$. The z-axis is parallel to the true rotation axis at $t = t_0$ and the y-axis is perpendicular to both.

3.2 The Kepler ellipse

In the case that no perturbing forces act on the satellite it flies on a perfect Kepler ellipse. The position of the satellite can then be described by Kepler's six orbital elements a , e , ω , i , Ω , M ,

where a is the semimajor axis of the ellipse
 e is the eccentricity
 ω is the argument of the perigee
 i is the inclination angle
 Ω is the right ascension of the ascending node
 v is the true anomaly.

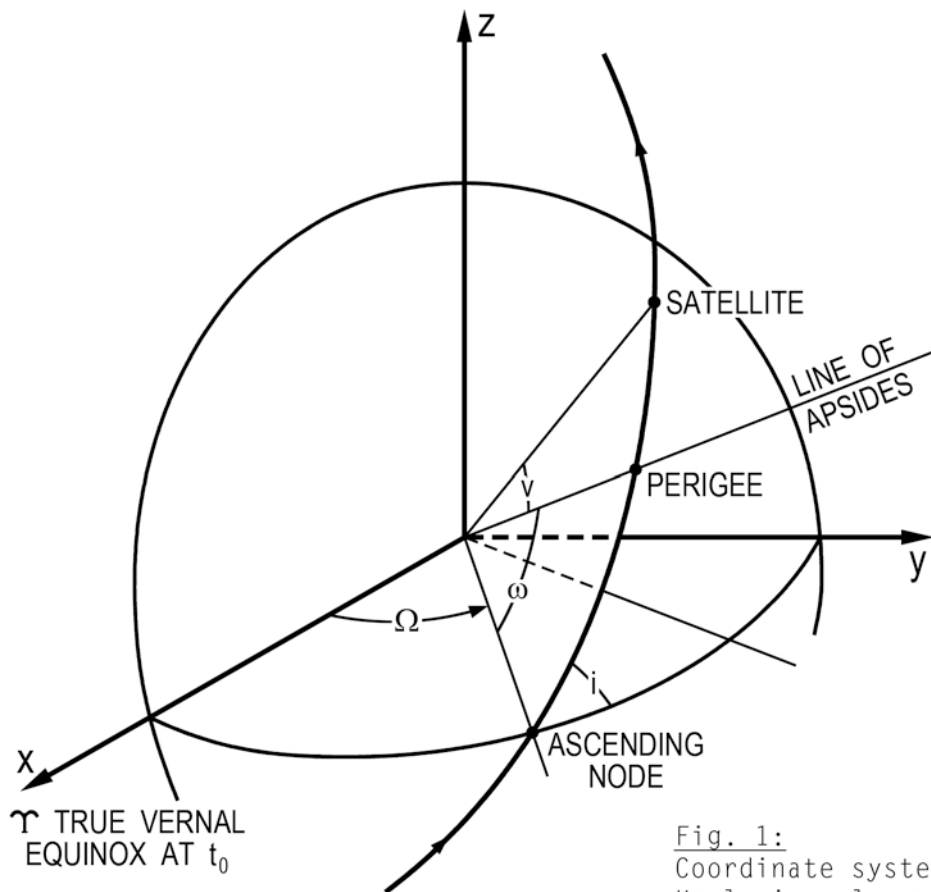


Fig. 1:
Coordinate system and
Keplerian elements

The relations between the true anomaly v , the mean anomaly M and the eccentric anomaly E are described by the equations

$$\cos v = \frac{\cos E - e}{1 - e \cos E} \quad (3-1)$$

and

$$M = E - e \sin E . \quad (3-2)$$

Those different types of anomalies will be used in the following

4. THE FORCES ACTING ON THE SPACECRAFT

In reality a lot of forces act on the satellite causing perturbations of the perfect elliptical orbit. Together they form the acceleration vector $\underline{\ddot{r}}_s$.

Its components are:

- $\underline{\ddot{r}}_{cb}$ the central body acceleration
 - $\underline{\ddot{r}}_{ns}$ acceleration caused by the non-sphericity of the body
 - $\underline{\ddot{r}}_p$ gravitational attraction by moon, sun and other planets
 - $\underline{\ddot{r}}_d$ acceleration due to air drag
 - $\underline{\ddot{r}}_{sr}$ acceleration due to solar radiation pressure
 - $\underline{\ddot{r}}_{te}$ acceleration due to earth tides (indirect effect)
- and $\underline{\ddot{r}}_{oc}$ acceleration due to ocean tides

The satellite's equation of motion can be described by the relation

$$\underline{\ddot{r}} = f(\underline{r}, \underline{\dot{r}}, \underline{p}) \quad (4-1)$$

where \underline{r} is the position vector of the satellite

$\underline{\dot{r}}$ is the velocity vector

and \underline{p} is the vector of dynamical parameters.

The vector \underline{p} is given by the relation

$$\underline{p} = \underline{p}(\underline{r}(t_0), \underline{\dot{r}}(t_0), \underline{p}') \quad (4-2)$$

where $\underline{r}(t_0)$ and $\underline{\dot{r}}(t_0)$ define position and velocity at starting epoch. The vector \underline{p}' consists of constant parameters for modelling air drag, spherical harmonic coefficients etc.

The prediction of the orbit was carried out by applying a predictor-corrector multistep algorithm for the numerical integration of the equation of motion (CAPELLARI et al. 1976).

The influence of different accelerations on the satellite position was estimated by the following procedure:

We first computed the orbit under consideration of all possible forces over a period of 6 days and used these data as "correct" values. Then we neglected the various accelerations one after the other and compared the positions with the "correct" ones. The coordinate errors were transformed into an orbital plane system splitting the difference in an along-track component pointing into the direction of satellite motion, a radial component and a cross-component perpendicular to both. These transformed differences are given in the figures in the appendix.

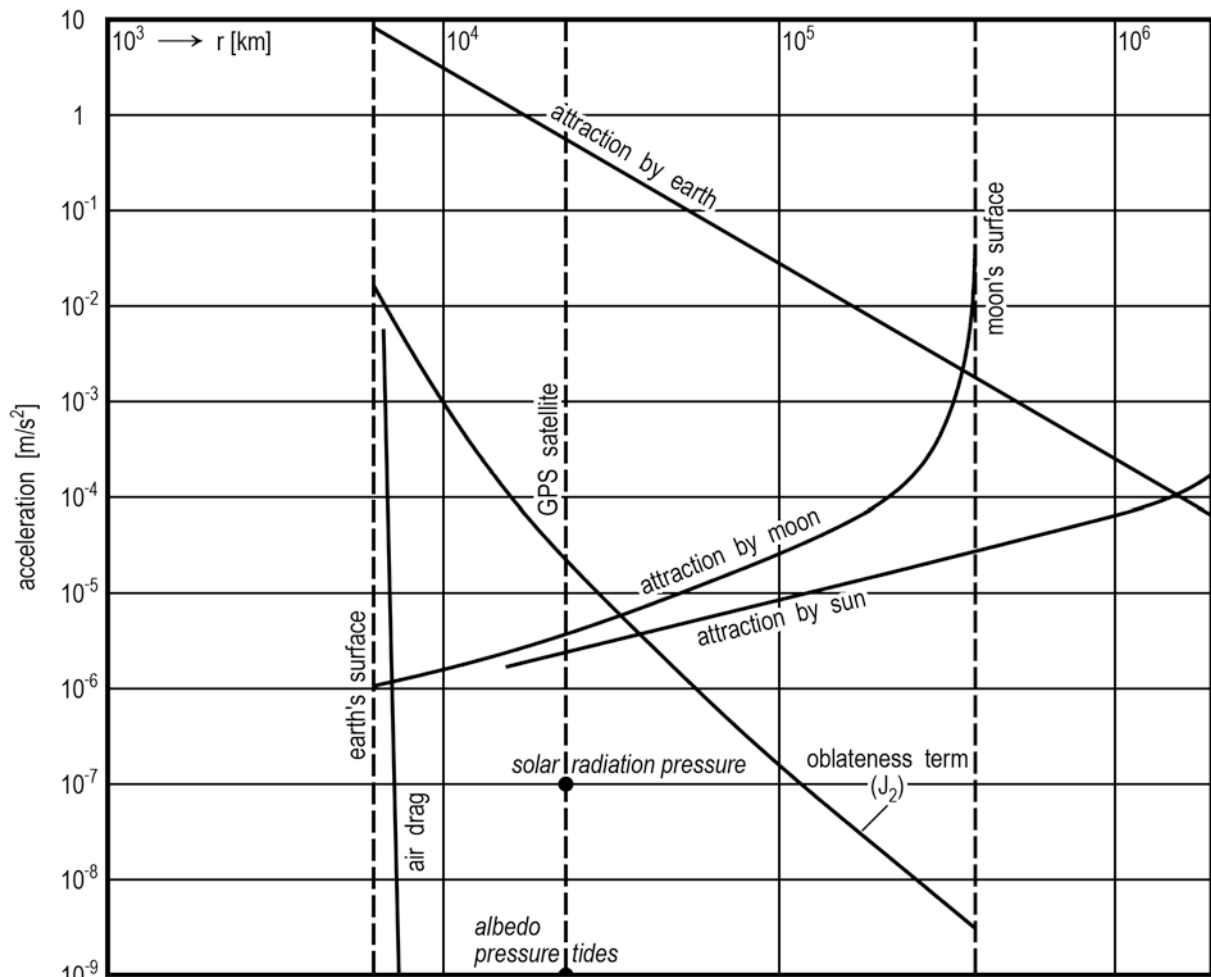


Fig. 2: Magnitudes of forces acting on a satellite

4.1 The gravity field of the earth

In the earth's exterior the Laplace differential equation is valid. Thus, the gravity potential can be represented by a spherical harmonic expansion

$$V = \frac{Gm}{r} \left[1 + \sum_{n=2}^{\infty} \left(\frac{a_E}{r} \right)^n \sum_{m=0}^n (C_{nm} \cos m\lambda + S_{nm} \sin m\lambda) P_{nm}(\sin \varphi) \right] \quad (4-3)$$

where a_E is the semimajor axis of the earth, r is the satellite-geo-center distance and φ , λ are latitude and longitude. Gm is the gravitational constant multiplied by the earth mass.

Consideration of the centrifugal potential leads to the definition of the gravitational potential W ,

$$W = V + \phi = V + \frac{1}{2} \omega_R^2 (x^2 + y^2) \quad (4-4)$$

where ω_R is the angular velocity of the earth.

The gravity acceleration is given by the gradient of the spherical harmonic expansion. The central body acceleration is defined by the main part of equation (4-3)

$$\bar{V} = \frac{Gm}{r} . \quad (4-5)$$

Additional gravitational forces due to the non-sphericity are acting on the satellite

$$\frac{\partial}{\partial x} (V - \bar{V}) , \quad \frac{\partial}{\partial y} (V - \bar{V}) , \quad \frac{\partial}{\partial z} (V - \bar{V}) . \quad (4-6)$$

They cause perturbations of the perfect elliptical orbit.

According to ARNOLD (1970) the influence of the gravity disturbing potential can be described by Lagrange perturbation equations ($R = (V - \bar{V})$).

$$\dot{a} = \frac{2}{\mu a} \cdot \frac{\partial R}{\partial M} \quad (4-7a)$$

$$\dot{e} = \frac{1 - e^2}{\mu a^2 e} \cdot \frac{\partial R}{\partial M} - \frac{\sqrt{1 - e^2}}{\mu a^2 e} \cdot \frac{\partial R}{\partial \omega} \quad (4-7b)$$

$$\dot{\omega} = - \frac{\cos i}{\mu a^2 \sqrt{1 - e^2} \sin i} \cdot \frac{\partial R}{\partial i} + \frac{\sqrt{1 - e^2}}{\mu a^2 e} \cdot \frac{\partial R}{\partial e} \quad (4-7c)$$

$$\dot{i} = \frac{\cos i}{\mu a^2 \sqrt{1 - e^2} \sin i} \cdot \frac{\partial R}{\partial \omega} - \frac{1}{\mu a^2 \sqrt{1 - e^2} \sin i} \cdot \frac{\partial R}{\partial \Omega} \quad (4-7d)$$

$$\dot{\Omega} = \frac{1}{\mu a^2 \sqrt{1 - e^2} \sin i} \cdot \frac{\partial R}{\partial i} \quad (4-7e)$$

$$\dot{M} = \mu - \frac{1 - e^2}{\mu a^2 e} \cdot \frac{\partial R}{\partial e} - \frac{2}{\mu a} \cdot \frac{\partial R}{\partial a} \quad (4-7f)$$

$$\text{with } \mu = \sqrt{\frac{Gm}{a^3}} \quad (4-8)$$

For numerical perturbation computations the equations have to be integrated with respect to time.

The different coefficients of the spherical harmonic expansion cause secular, long- and shortperiodic effects.

The zonal coefficients ($m = 0$) cause secular effects. The largest effect is caused by the C_{20} term. It leads to a rotation of the apside line (ω, M) and the ascending node (Ω). From the perturbation equations we get the following variations (ARNOLD 1970)

$$\delta\omega = C_{20} \frac{3\mu a_E^2}{4(1-e^2)^2 a^2} (1 - 5 \cos^2 i) \cdot t \quad (4-9)$$

$$\delta\Omega = C_{20} \frac{3\mu a_E^2}{2(1-e^2)^2 a^2} \cos i \cdot t \quad (4-10)$$

$$\delta M = C_{20} \frac{3\mu a_E^2}{4(1-e^2)^{3/2} a^2} (1 - 3 \cos^2 i) \cdot t \quad (4-11)$$

where μ is the angular velocity of the satellite's motion around the earth.

The acceleration due to the C_{20} term acting on the GPS satellite is about $5 \cdot 10^{-5} \text{ m/s}^2$ (see figure 2).

The orbital elements a , e and i are not affected by secular perturbations. A neglect of the C_{20} term causes an error of up to 10 000 m in the along-track component after an integration of 2 days. A consideration of coefficients up to degree and order 8 seems to be sufficient for integration spans of a few days. The error of neglecting higher order influences during a period of 6 days causes errors smaller than 10 cm (see figure 3).

4.2 Attraction by additional bodies

The gravitational central body force acting on a satellite can be easily modelled by the relation

$$\ddot{\underline{x}}_p = -G m_p \cdot \left[\frac{\underline{x} - \underline{x}_p}{|\underline{x} - \underline{x}_p|^3} + \frac{\underline{x}_p}{|\underline{x}_p|^3} \right] \quad (4-12)$$

where G is the gravitational constant
 m_p is the mass of the body
 \underline{x}_p is the position vector of the celestial body
in the inertial reference frame
 \underline{x} is the position vector of the satellite

The mass of satellite is very small, so that we can assume that the satellite does not have any significant acceleration on the earth or other planets.

The gravitational accelerations of sun and moon cause secular variations of the argument of perigee (ω) and the right ascension of the ascending node (Ω).

KOZAI (1959) gives the following relations for the variations caused by the moon

$$\frac{d\omega}{dt} = \frac{3}{4} \frac{\omega_M^2}{\mu} m_M \frac{1}{\sqrt{1-e^2}} \left(2 - \frac{5}{2} \sin^2 i + \frac{1}{2} e^2 \right) \left(1 - \frac{3}{2} \sin^2 i_M \right) \quad (4-13)$$

$$\frac{d\Omega}{dt} = \frac{3}{4} \frac{\omega_M^2}{\mu} m_M \frac{\cos i}{\sqrt{1-e^2}} \left(1 + \frac{3}{2} e^2 \right) \left(1 - \frac{3}{2} \sin^2 i_M \right) \quad (4-14)$$

where ω_M is the angular velocity of the moon's motion around the earth
 m_M is the mass of the moon in units of the earth mass.

The equations for the sun's perturbation are very similar. We only have to insert the corresponding values for m_M , ω_M and i_M . The influence of the moon is described in figure 4 and the influence of the sun in figure 5. Note that the influence in radial direction is very small in comparison to the secular variation in the along-track and the periodic variation in the cross-track component.

The influence of the gravitational forces of the planets Mercury, Venus, Mars, Jupiter, Saturn, Uranus, Neptune and Pluto causes orbit perturbations which are described in figure 6. After an integration period of 6 days the influence is smaller than 30 cm in all three components.

4.3 Acceleration due to earth tides

The attraction by third bodies causes a deformation of the earth's surface. This deformation leads to a variation of the potential. According to MELCHIOR (1983) the tidal potential is given in first-order approximation by the relation

$$W_2 = \frac{G m_p}{d^3} R_E^2 P_2(\cos z) \quad (4-15)$$

where m_p is the mass of the disturbing body
 d is the distance from the geocenter to the planet
 R_E is the mean earth radius
 P_2 is the Legendre polynomial of order 2
and z is the geocentric zenith distance of the spacecraft.

The potential caused by the non-rigidity of the earth is defined as

$$V_{te} = \left(\frac{R_E}{r} \right)^3 \cdot k_2 \cdot W_2 \quad (4-16)$$

where r is the distance between the geocenter and the satellite and k_2 is the Love number of second degree. The indirect effect of sun and moon on the earth's gravity potential causes an acceleration of about 10^{-9}m/s^2 on a GPS-spacecraft (see fig. 2). The effect on satellite positions is described in figure 7.

The acceleration due to ocean tides is a quarter of magnitude smaller than the earth tide effects. The modelling of that acceleration is rather complex, because it is influenced by coastline geometry etc. We used a Schwiderski model for computing the influence of ocean tide on GPS-spacecraft positioning. The perturbations due to these effects are given in figure 8.

4.4 Solar radiation pressure

The acceleration due to solar radiation pressure is the most difficult one to model. Usually the force can be described in a first approximation by the relation

$$\ddot{\underline{x}}_{sr} = \nu \cdot P_s \cdot C_r \cdot \frac{A}{m} \cdot a_s^2 \cdot \frac{(\underline{x} - \underline{x}_s)}{|\underline{x} - \underline{x}_s|^3} \quad (4-17)$$

where ν is the eclipse factor (0 or 1), depending on whether the satellite is in the earth's shadow or not
 P_s is the solar pressure in N/m^2
 C_r is the reflectivity constant
 A is the effective cross-sectional surface of the satellite
 m is the mass
 a_s is the semimajor axis of the earth's orbit around the sun
 \underline{x} is the position vector of the satellite
and \underline{x}_s is the position vector of the sun.

The equation describes the direct effect of the solar radiation pressure only in direction of the sun-satellite connection line. The magnitude of the acceleration for a GPS-spacecraft is about $1 \cdot 10^{-7} \text{m/s}^2$ (see fig. 2). Neglecting of this force causes errors of up to 400 m after two day integration and of 1000 m after six day integration intervals (see fig. 9). The reflection of the sunbeams on the clouds and the earth itself causes a second radiation pressure term which is only 1% of the direct effect for GPS satellites ($1 \cdot 10^{-9} \text{m/s}^2$) (RIZOS and STOLZ 1985).

There are many uncertainties in the modelling of solar radiation forces

due to changes in the solar constant, the different reflectivity constants of the different materials, the determination of the effective area A, etc.

Refinements of the solar radiation force models lead to the consideration of a y-biased acceleration along the solar panel beam (FLIEGEL et al. 1985). Several effects can cause such an acceleration, like misalignments in the solar panels (they are not perfectly perpendicular to the line between sun and satellite) and thermal radiation due to ventilation of the spacecraft. The effect of structural misalignments is given by FLIEGEL et al. (1985)

$$y = r \cdot P_s \cdot \frac{A}{m} \cdot (2d_1 + d_2 + d_3) \quad (4-18)$$

where r is the reflectivity of the solar panel

d_1 is the misalignment angle of the solar sensor

d_2 is the angle of one solar panel with respect to the other

d_3 is the yaw altitude control bias.

The magnitude of the y-bias acceleration is about $0.5 \cdot 10^{-9} \text{m/s}^2$. Neglection may cause an error of 2500 m after 14 day integration period.

The motion of the satellite and therefore the variation of the effective area A can be neglected since the solar panels are oriented by stepping motors for presenting the maximum surface to the sun.

Due to difficulties in modelling the solar radiation pressure causes the largest orbit errors. It might be difficult to model the effect with an accuracy better than 1 m for an integration period of several days.

5. CONCLUSIONS

We analyzed the behaviour and the magnitude of forces acting on a GPS satellite and found that

- an approximation of the earth's gravity field up to degree and order 8 is sufficient for modelling the perturbations due to the non-sphericity of the earth. Neglection of higher degree harmonics causes an error smaller than 5 cm.
- a consideration of gravitational forces due to third bodies is necessary for sun and moon. The influence of planets can be neglected when extrapolating over periods of a few days.
- solar radiation pressure plays a major role in the force model analysis. It causes orbit errors of hundred of meters after few revolutions. More than any other force the radiation pressure influences the radial component of the satellite's orbit (see fig. 9). An exact determination of this influence is absolute necessary for the computation of high precise orbits.
- the forces due to the indirect tidal effect of the solid earth causes after few revolutions an orbit error of more than 1 m and needs to be considered.

- ocean tides, gravitational forces of planets, albedo pressure and polar motion cause maximum orbital errors of 20 cm. Considering these influences by themselves they seem to be negligible. But note that the sum of them can cause orbit errors of about 1 m. Therefore we must consider these influences if we intend to determine satellite orbits with an accuracy below 1 m.
- the influence of air drag on GPS satellites can be neglected due to the high altitude of the satellites.

Because uncertainties in the modelling of the solar radiation pressure, we believe that an orbit determination with an accuracy of better than 1 m is at the moment hypothetical.

REFERENCES

- ARNOLD, K. (1970): *Methoden der Satellitengeodäsie*. Akademie Verlag, Berlin
- CAPELLARI, J.O., C.E. VELEZ, A.J. FUCHS (1976): *Mathematical Theory of the Goddard Trajectory Determination System*. Doc. X-582-76-77, Goddard Space Flight Center, Greenbelt, Md.
- FLIEGEL, H.F., W.A. FEESE, W.G. LAYTON (1985): *The GPS radiation force model*. In Proceedings of the First International Symposium on Precise Positioning with the Global Positioning System, April 15-19, 1985
- HEIN, G.W., B. EISSFELLER (1985): *Integrated modelling of GPS-orbits and multi-baseline components*. In Proceedings of the First International Symposium on Precise Positioning with the Global Positioning System, April 15-19, 1985, Vol. I, p. 263-272
- KOZAI, Y. (1959): *On the effects of sun and moon upon the motion of a close earth satellite*. SAO Special Report No. 22
- LANDAU, H., B. EISSFELLER (1986): *Optimization of GPS Satellite Selection for High Precision Differential Positioning*. In GPS Research 1985 at the Institute of Astronomical and Physical Geodesy, Report No. 19, University FAF Munich, p. 65-105
- LARDEN, D.R., P.L. BENDER (1982): *Preliminary study of GPS orbit determination accuracy achievable from worldwide tracking data*. In Proceedings of the Third International Geodetic Symposium on Satellite Doppler Positioning, February 8-12, 1982, Vol. 1
- MELCHIOR, P. (1983): *The Tides of the Planet Earth*. Pergamon Press
- NAKIBOGLU, S.M., E.J. KRAKIWSKY, K.P. SCHWARZ, B. BUFFET, B. WANLESS (1985): *A multi-station, multi-pass approach to Global Positioning System improvement and precise positioning*. Contract Report No. OST83-00340, submitted to Geodetic Survey of Canada, Department of Energy, Mines and Resources
- REMONDI, B. (1984): *Using the Global Positioning System (GPS) phase observable for relative geodesy: Modelling, processing and results*. Ph.D. Dissertation, University for Space Research, The University of Texas in Austin

- RIZOS, C., A. STOLZ (1985): *Force modelling for GPS satellite orbits*. In Proceedings of the First International Symposium on Precise Positioning with the Global Positioning System, April 15-19, 1985
- STOLZ, A., E.G. MASTERS, C. RIZOS (1984): *Determination of GPS satellite orbits for geodesy in Australia*. Aust. J. Geod. Photo. Surv. No. 40, June 1984

A P P E N D I X

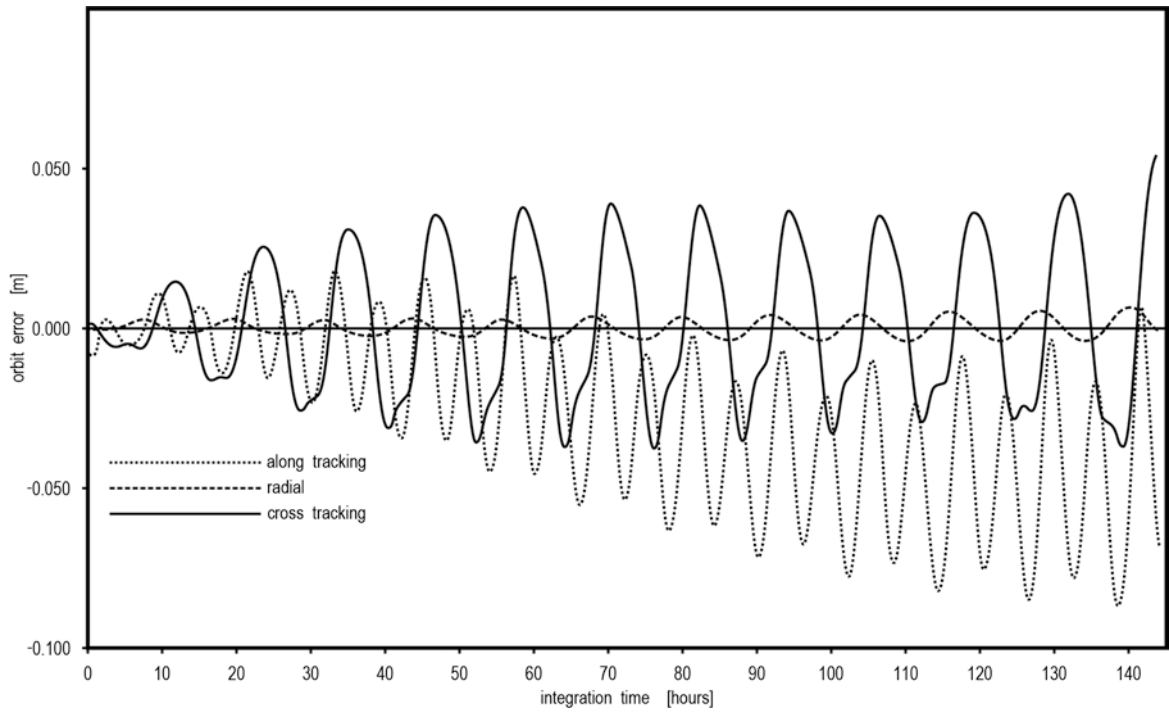


Fig. 3: Influence of spherical harmonics of degree and order greater than 8 on satellite's position

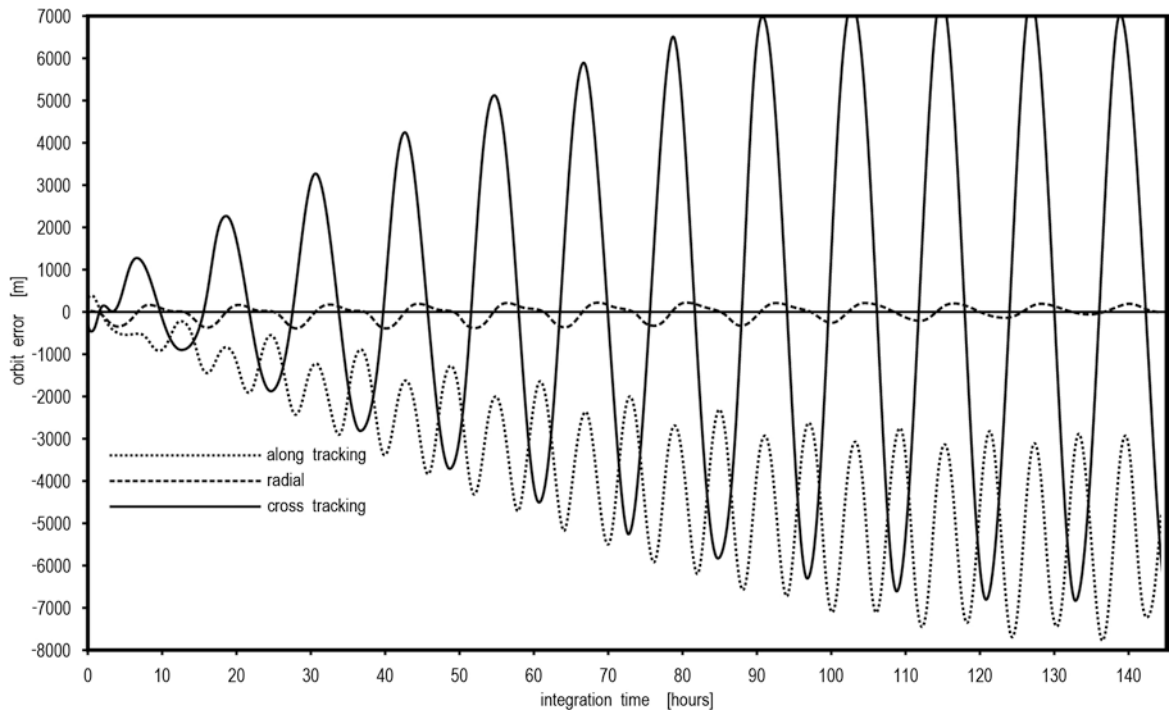


Fig. 4: Influence of the gravitational force by the moon

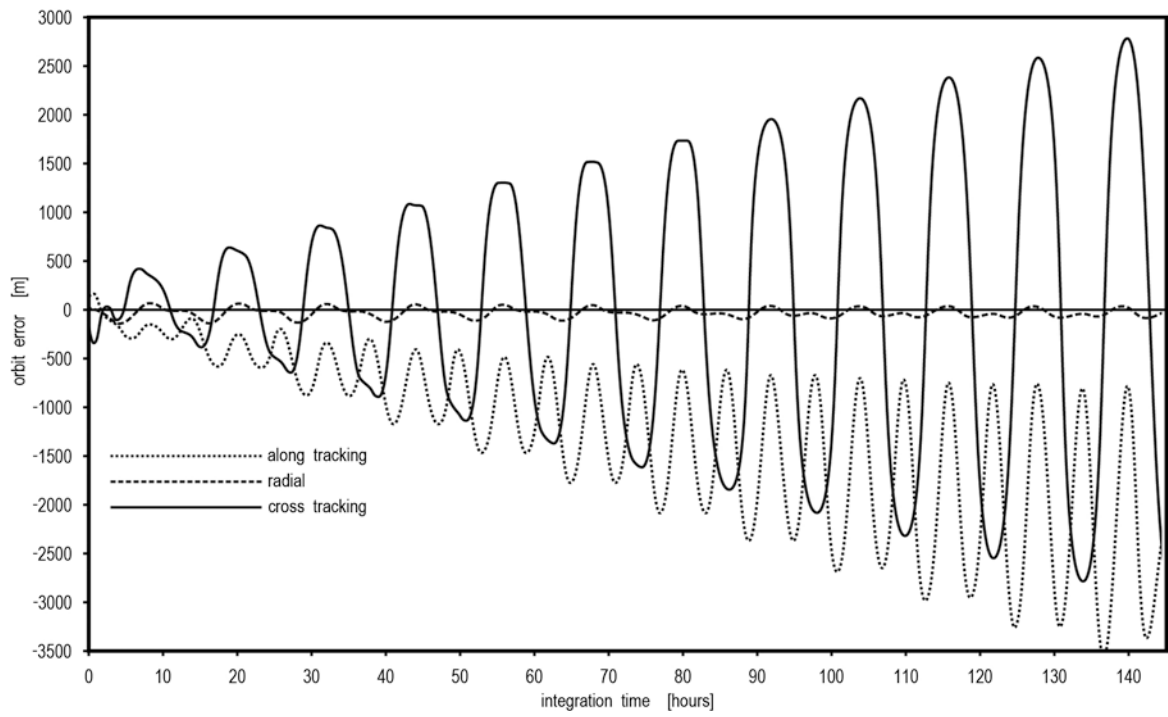


Fig. 5: Influence of the sun's gravitational force on satellite's position

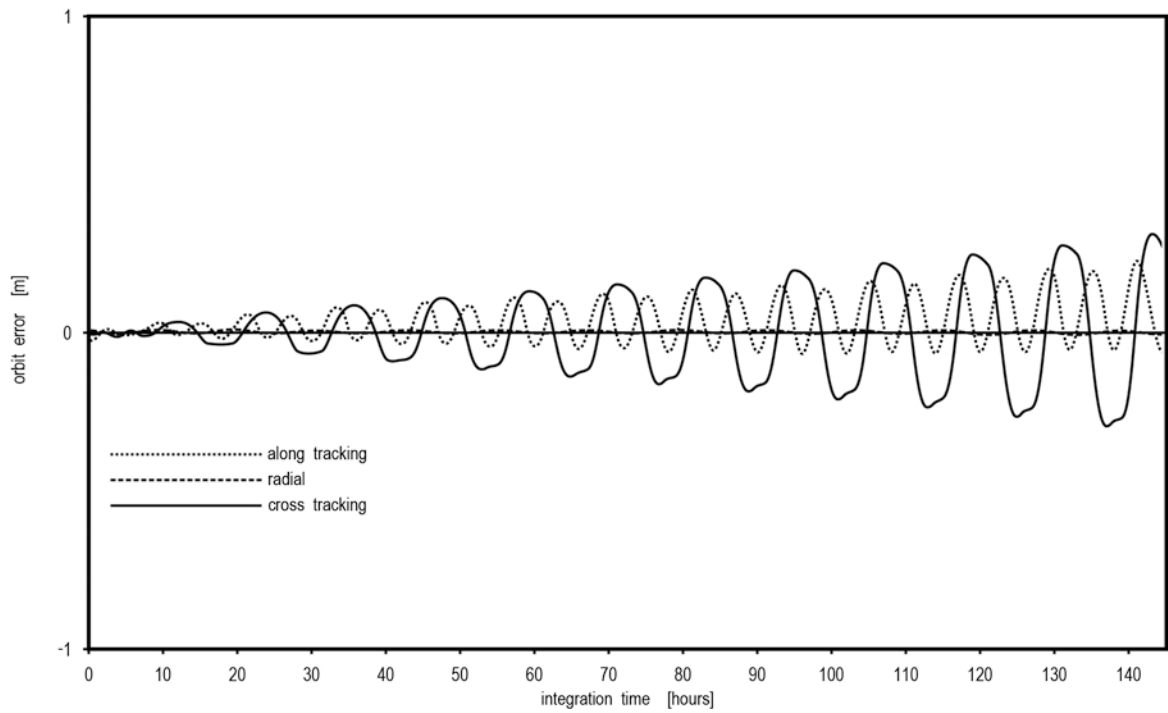


Fig. 6: Influence of the planets

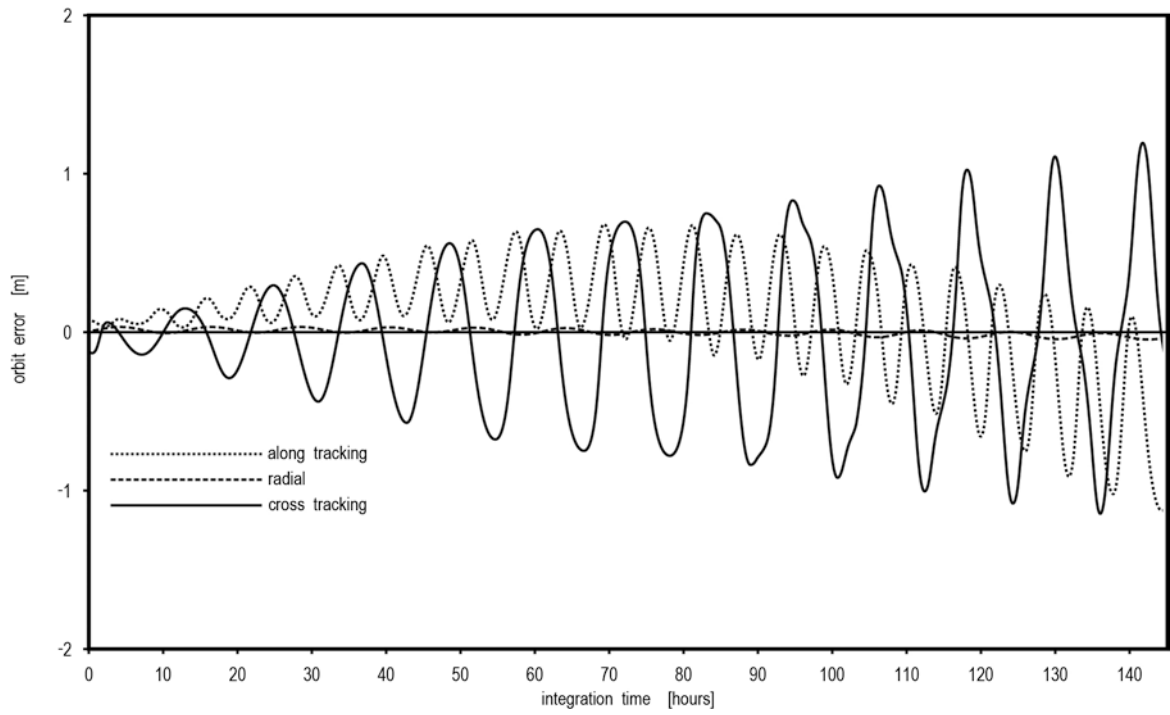


Fig. 7: Influence of solid earth tides

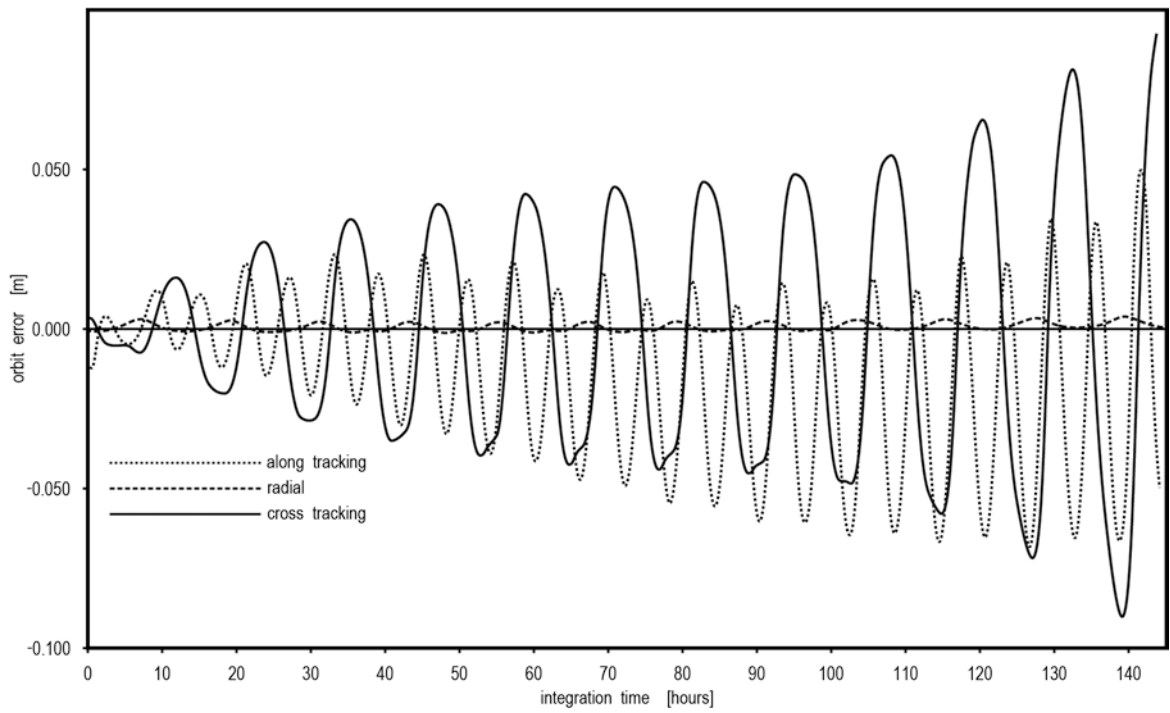


Fig. 8: Influence of ocean tides

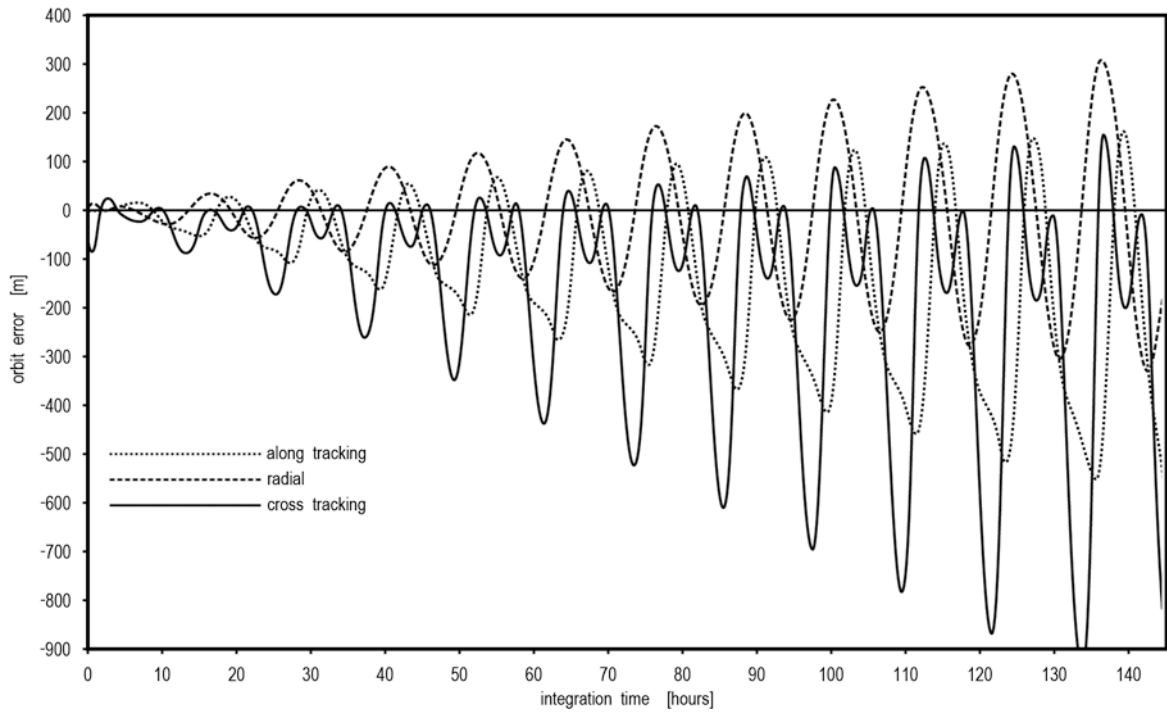


Fig. 9: Influence of solar radiation pressure

SCHRIFTENREIHE

des Wissenschaftlichen Studienganges Vermessungswesen an der HSBwM

Bisher erschienene Hefte :

- Nr. 1/78 A. Schödlbauer:
Curriculum für den wissenschaftlichen Studiengang Vermessungswesen der Hochschule der Bundeswehr München;
53 Seiten, DM 10.--
- Nr. 2/78 A. Chrzanowski and E. Dorrer (Eds.):
Proceedings "Standards and Specifications for Integrated Surveying and Mapping Systems", Workshop held in Munich,
1-2 June 1977;
181 Seiten, DM 20.--
- Nr. 3/78 W. Caspary und A. Geiger:
Untersuchungen zur Leistungsfähigkeit elektronischer Neigungsmesser;
62 Seiten, DM 10.--
- Nr. 4/79 E. Baumann, W. Caspary, H. Dupraz, W. Niemeier, H. Pelzer, E. Kuntz, G. Schmitt, W. Welsch:
Seminar über Deformationsanalysen;
106 Seiten, DM 15.--
- Nr. 5/81 K. Torlegård:
Accuracy Improvement in Close Range Photogrammetry;
68 Seiten, DM 10.--
- Nr. 6/82 W. Caspary und W. Welsch (Herausgeber):
Beiträge zur großräumigen Neutrassierung;
268 Seiten, DM 20.--
- Nr. 7/82 K. Borre and W.M. Welsch (Editors):
Proceedings "Survey Control Networks",
Meeting of FIG-Study Group 5B, Aalborg, 7 - 9 July 1982;
428 Seiten, DM 35.--
- Nr. 8/82 A. Geiger:
Entwicklung und Erprobung eines Präzisionsneigungstisches zur Kalibrierung geodätischer Instrumente;
124 Seiten, DM 10.--
- Nr. 9/83 W. Welsch (Herausgeber):
Deformationsanalysen '83;
336 Seiten, DM 25.--
- Nr. 10/84 W. Caspary, A. Schödlbauer und W. Welsch (Herausgeber):
Beiträge aus dem Institut für Geodäsie;
241 Seiten, DM 20.--

SCHRIFTENREIHE

des Wissenschaftlichen Studienganges Vermessungswesen an der HSBwM

- Nr. 11/84 W. Caspary und H. Heister (Herausgeber):
Elektrooptische Präzisionsstreckenmessung;
268 Seiten, DM 20.--
- Nr. 12/84 P. Schwintzer:
Analyse geodätisch gemessener Punktlageänderungen
mit gemischten Modellen;
155 Seiten, DM 15.--
- Nr. 13/84 G. Oberholzer:
Landespflege in der Flurbereinigung;
80 Seiten, DM 10.--
- Nr. 14/84 G. Neukum mit Beiträgen von G. Neugebauer:
Fernerkundung der Planeten und kartographische Ergebnisse;
100 Seiten, DM 25.--
- Nr. 15/84 A. Schödlbauer und W. Welsch (Herausgeber):
Satelliten-Doppler-Messungen,
Beiträge zum Geodätischen Seminar 24./25. September 1984;
394 Seiten, DM 30.--
- Nr. 16/85 M.K. Szacherska, W.M. Welsch:
Geodetic Education in Europe;
230 Seiten, DM 20.--
- Nr. 17/85 B. Eissfeller, G.W. Hein:
A Contribution to 3d-Operational Geodesy.
Part 4: The Observation Equations of Satellite Geodesy in
the Model of Integrated Geodesy;
(in Vorbereitung)
- Nr. 18/85 G. Oberholzer:
Landespflege in der Flurbereinigung, Teil II;
114 Seiten, DM 12.--
- Nr. 19/86 H. Landau, B. Eissfeller and G.W. Hein:
GPS Research 1985 at the Institute of Astronomical
and Physical Geodesy;
210 Seiten, DM 20.--
- Nr. 20/85 W. Welsch and L.A. Lapine (Editors):
Proceedings "Inertial, Doppler and GPS Measurements for
National and Engineering Surveys"
Joint Meeting of Study Groups 5B and 5C, July 1-3, 1985;
2 Bände, 630 Seiten, DM 50.--

